Application of graphene based composites in agriculture

This thesis is submitted in fulfilment of the requirement for the degree of

Doctor of Philosophy
Chemical Engineering

By **Shervin Kabiri**

July 2018

School of Chemical Engineering

Faculty of Engineering, Computer, and Mathematical Science

The University of Adelaide

ABSTRACT

The main challenge faced by agricultural research is to produce high quantity and quality food to feed a constantly growing world population. Fertilizers are an essential component of productive agricultural systems, but their efficiency of use is low due to losses to the atmosphere, soil and waters, which consequently can cause environmental damage. In addition, reaction of nutrients with soil components reduces their availability to plants and thus they may accumulate in soil. Nutrients may also be leached from soil and end up in rivers, lakes and the ocean. Improving fertilizer use efficiency is therefore a global goal and new engineering approaches are needed to design more effective nutrient delivery systems to crops which minimize losses to the environment. Recent strategies to address these problems are based on designing slow-release fertilizers using porous materials or polymer-coating of conventional fertilizers, which have seen some success but are severely limited by their cost.

Graphene (GN) and its derivatives may offer a path-way to develop more efficient fertilizers due to the outstanding physicochemical properties of GN. During the relatively short time since the discovery of GN in 2004, its unique properties have attracted great interest in multiple fields including chemistry, physics, materials science, biology and engineering. The two dimensional structure of GN, in addition to its high surface area, makes this material very attractive for the delivery of drugs or genetic material and there is also potential for application as a nutrient carrier in agriculture. Despite being one atom thick, GN is the strongest material ever tested and its unique mechanical properties made it a favourable candidate to be used as a reinforcement material to enhance the toughness of different composites and therefore a potential application to enhance the mechanical properties of fertilizer granules. Therefore, considering the excellent properties of GN-based materials, including a two-dimensional (2D) structure, a high specific surface area, a tailorable surface chemistry and a high mechanical strength, this thesis examined the potential for use of GN-based materials to improve the

nutrient delivery to crops, to enhance fertiliser use efficiency as well as the mechanical properties of granular fertilizers. The following four concepts were developed and explored in this thesis:

The first part of the thesis focuses on the development of a new carrier platform for delivery of plant nutrients based on graphene oxide (GO) sheets. To prove this concept, the micronutrients zinc (Zn) and copper (Cu) were loaded onto GO sheets. The GO sheets provided a high loading capacity for Zn and Cu (14% and 10% by weight, respectively) with slow release properties. The GO-based fertilizers displayed a biphasic release behaviour with a portion of the micronutrients released quickly, and a portion having a slow release behaviour. This was likely due to 2D structure of GO as well as the tight coordination of nutrients with oxygen functional groups of the GO sheets. A visualization method was used to assess the release and diffusion of Cu and Zn in soil from these GO-based fertilizers and demonstrated the advantages of GO carriers compared to commercial fertilizers. A pot trial demonstrated that Zn and Cu uptake by wheat was higher when using GO-based fertilizers compared to commercial zinc or copper salts. This is the first report on the agronomic performance of GO-based slow-release fertilizers and demonstrated their capability to be used as a generic platform for micronutrient delivery.

In the second part of this thesis, different formulations of GO-based micronutrient fertilizers were assessed for their ability to supply micronutrients to wheat, compared with commercial fertilizers. Both granular versus fluid forms of fertilizer, and fertilizer placement (banded versus mixed), were investigated in this study. Fluid (suspension) forms of the GO-based fertilizers were more effective than the granular forms, and the GO-based formulations were more effective than equivalent fluid and granular commercial zinc sulphate products.

The third part of this thesis utilized GN and GO as hardening agents to enhance the physical properties of granular monoammonium phosphate (MAP) fertilizers. Co-granulation of 0.5%

w/w GN sheets in MAP granules (MAP-GN) significantly enhanced the mechanical strength of MAP granules while inclusion of the same amounts of GO sheets (MAP-GO) improved the strength to a lesser extent (18 times improvement versus 8 times). The abrasion of MAP-GN was 70% less than the unamended MAP granules, while the impact resistance of MAP-GN was 75% greater than unamended MAP. The inclusion of GN not only improved the physical properties of granules but also slightly slowed the release of phosphorus to soil. The advantages of GN and GO sheets in improving the physical properties of MAP granules were explained by their high specific area and high mechanical properties in addition to their 2D geometry. These results indicate the potential for GN/GO additives to improve the physical properties of granular fertilizers.

The fourth and final part of this thesis investigated the concentration dependence of GN addition to fertilizer (MAP and diammonium phosphate (DAP)) granules in improving fertilizer physical quality. The optimum concentration of GN for MAP and DAP were 0.5 w% and 0.05w%, respectively and adding greater amounts of GN decreased the crushing strength rather than increasing it. It was also observed that the improved crushing strength of GN-amended granules depended on the initial hardness of fertilizers - the crushing strength of softer granules such as MAP was enhanced almost 15 fold, while harder granules such as DAP had much smaller improvements in crushing strength. Furthermore, this work investigated whether GN made by different methods, and therefore having different properties (level of deoxygenation, specific surface area (SSA) and sheet size), had similar effects on the physical quality of fertilizers. Graphene with a higher degree of deoxygenation and SSA, and lower particle size, was more effective in improving the crushing strength of MAP. However, there was little effect of GN properties on DAP granules amended with GN, likely due to the higher initial crushing strength of DAP.

DECLARATION

I certify that this work contains no material which has been accepted for the award of any other degree or diploma in my name, in any university or other tertiary institution and, to the best of my knowledge and belief, contains no material previously published or written by another person, except where due reference has been made in the text. In addition, I certify that no part of this work will, in the future, be used in a submission in my name, for any other degree or diploma in any university or other tertiary institution without the prior approval of the University of Adelaide and where applicable, any partner institution responsible for the joint-award of this degree.

I acknowledge that copyright of published works contained within this thesis resides with the copyright holder(s) of those works.

I also give permission for the digital version of my thesis to be made available on the web, via the University's digital research repository, the Library Search and also through web search engines, unless permission has been granted by the University to restrict access for a period of time.

SHERVIN KABIRI Date: 01.07.2018

PREFACE

This thesis is submitted as a “thesis by publication” in accordance with “Specifications for Thesis 2013” of The University of Adelaide. The PhD research spanning 3.5 years generated 5 peer-reviewed journal articles: 2 published as first author and 3 is submitted in 2018. Also working in other projects created 10 publications, (2 as first author and 8 as co-author). This PhD research resulted in one provisional patents. The research chapters included in this thesis were published or submitted as research articles in highly esteemed journals in the field. The list of publications is provided in the following pages.

LIST OF PUBLICATIONS ARISING FROM THIS THESIS

Peer-reviewed journal articles

Published Articles

1. **Shervin Kabiri**, Roslyn Baird, Diana N.H. Ivan Andelkovic, Mike J. McLaughlin and Dusan Losic, "Co-granulation of Low Rates of Graphene and Graphene Oxide with Macronutrient Fertilizers Remarkably Improves their Physical Properties", *Journal of ACS Sustainable Chemistry &Engineering*. **2018**, 6, 1299-1309.
2. **Shervin Kabiri**, Fien Degryse, Diana N.H. Tran, Rodrigo C. da Silva, Mike J. McLaughlin and Dusan Losic, "Graphene Oxide: A New Carrier for Slow Release of Plant Micronutrients", *Journal of ACS Applied. Materials & Interfaces* **2017**, 9, 43325-43335.

Submitted Articles

1. **Shervin Kabiri**, Rodrigo C. da Silva , Fien Degryse , Diana N.H. Tran, Mike J. McLaughlin, Dusan Losic, "Suspension micronutrient fertilizers manufactured using zinc-loaded graphene oxide- are more efficient than granular forms in both banded and mixed applications" submitted to Journal of *ACS Environmental science and technology,* (2018).
2. **Shervin Kabiri**, Diana N.H. Tran, Roslyn Baird, Mike J. McLaughlin, Dusan Losic, "Revealing the dependence of concentration and physicochemical properties of graphene on the crushing strength of co-granulated fertilizers" submitted to *Carbon,* (2018).
3. **Shervin Kabiri**, Diana N.H. Tran, Mike J. McLaughlin, Dusan Losic, "Graphene materials for efficient and sustainable agriculture: current progress and perspectives" submitted to *Chemical Society Reviews,* (2018).

Patents

1. Graphene for fertilizer applications, Australian Provisional Patent Application No: 2016905131. PCT/AU2017/051362

List of contributing journal publications during this PhD

1. Ivan B. Andelkovic, **Shervin Kabiri**, Ehsan Tavakkoli, Jason K. Kirby, Mike J. McLaughlin, Dusan Losic "Graphene oxide-Fe(III) composite containing phosphate -A novel slow release fertilizer for improved agriculture management" *Journal of Cleaner Production* **2018**, 185, 97-104.

2. Md J. Nine, **Shervin Kabiri**, Tran Thanh Tung, Diana N.H. Tran, Dusan Losic "Electrostatic powder coatings of pristine graphene: A new approach for coating of granular and fibril substrates", *Journal of Applied Surface Science* **2018** , 441, 187-193.
3. R. Karunagaran, C. Coghlan, T.T. Tung, **S. Kabiri**, D. Tran, C. Doonan, D. Losic "Study of iron oxide nanoparticle phases in graphene aerogels for oxygen reduction reaction" *New Journal of Chemistry* **2017**, 41, 15180 – 15186.
4. Md J. Nine, Diana N. H. Tran, Tran Thanh Tung, **Shervin Kabiri**, Dusan Losic, "Graphene borate as an efficient fire retardant for cellulosic materials with multiple and synergetic modes of action", *Journal of ACS Applied Materials & Interfaces* **2017**, 9 ,10160–10168.
5. Faisal Alotaibi, Tran T. Tung, Md J. Nine, **S. Kabiri**, Mahmoud Moussa, Diana N. H. Tran, Dusan Losic, "Scanning Atmospheric Plasma for Ultrafast Reduction of Graphene Oxide and Preparation of Broad Range of Highly Conductive Graphene Films", *Carbon* **2017**,127,113-121.
6. Pravin Patil , Madhuprasad , Mahesh P. Bhat , Manasa G. Gatti , **Shervin Kabiri** , Tariq Altalhi, Ho-Young Jung, Dusan Losic, Mahaveer Kurkuri "Chemodosimeter functionalized diatomaceous earth particles for visual detection and removal of trace mercury ions from water" *Chemical Engineering Journal*, **2017**, 327, 725-733.
7. **Shervin Kabiri**, Ngoc Hoa-Diana Tran, Martin A.Cole, Dusan Losic, "Functionalized three-dimensional (3D) graphene composite for high efficiency removal of mercury" *Journal of Environment Science.: Water Research and Technology.*, **2016**, 2, 390-402.
8. Ngoc Hoa-Diana Tran, **Shervin Kabiri**, Ting Rui Sim, Dusan Losic, "Selective adsorption of oil–water mixtures using polydimethylsiloxane (PDMS)–graphene sponges" , *Journal of Environmental Science: Water Research and technology* **2015**, 1, 298-305
9. Ivan Andelkovic, Ngoc Hoa-Diana Tran, **Shervin Kabiri**, Sara Azari, Marijana Markovic, Dusan Losic, "Graphene , Aerogels Decorated with α-FeOOH Nanoparticles for Efficient Adsorption of Arsenic from Contaminated Waters" *Journal of ACS Applied Materials & Interfaces* **2015**, 7, 9758-9766.

10. **Shervin Kabiri**, Ngoc Hoa-Diana Tran, Sara Azari, Dusan Losic, "Graphene-Diatom silica nanoparticles for efficient removal of mercury ions from water" *Journal of ACS Applied Materials & Interfaces* **2015**, 7, 11815-11823.

Conference Poster Presentations

1. **S. Kabiri,** D. Tran and D. Losic "Graphene 3 dimensional aerogel composites for efficient removal of mercury" Chemeca, Adelaide, Australia, September 2016.
2. S. Maher, **S. Kabiri**, J. Qin, K. Gulaty, A. ElMekawy, K. Kaur, L.Marques, G. Atkins, D. Findlay, A. Evdokiou and D. Losic " 3D printed Titanium Implants with Nano-Engineered Surface Titania Nanotubes for Localized Drug Delivery" Chemeca, Adelaide, Australia, September 2016
3. S. Maher, A. Santos, **S. Kabiri**, T. Kumeria, P. Forward, M. Lambert, D. Losic " Engineering of Magnetically Targeted pH-Sensitive Micro-Capsules with Multifunctional Cargo Using Droplet-based Microfluidic" Chemeca, Adelaide, Australia, September 2016.
4. Colin River, **Shervin Kabiri**, Roslyn Baird, Ashleigh Broadbent, Rodrigo C. da Silva, Fien Degryse, Bogumila Tomczak and Mike. J. McLaughlin "Coating contact angel as a predictor of fertilizer stability in high humid condition" New Zealand Society of Soil Science and Soil Science Australia joint Conference, Queenstown, New Zealand, December 2016.
5. R. Karunagaran, C. Coghlan, T.T. Tung, **S. Kabiri**, D. Tran, C. Doonan, D. Losic "Study of iron oxide nanoparticle phases in graphene aerogels for oxygen reduction reaction" Research Day - Centre for Energy Technology, Adelaide, November 2016.
6. Colin Rivers, **Shervin Kabiri**, Roslyn Baird, Ashleigh Broadbent, Rodrigo C. da Silva, Fien Degryse, Bogumila Tomczak and Mike. J. McLaughlin "Coating contact angel as a predictor of fertilizer stability in high humid condition" New Zealand Society of Soil Science and Soil Science Australia joint Conference, Queenstown, New Zealand, December 2016.

ACKNOWLEDGMENT

Firstly, I would like to express my sincere gratitude to my supervisors Prof. Dusan Losic, Prof. Mike.J. McLaughlin and Dr. Diana Tran for the continuous support of my Ph.D study and related research, for their patience, motivation, and immense knowledge. Their guidance helped me in all the time of research and writing of this thesis. I could not have imagined having better advisors and mentor for my Ph.D study.

My special thanks also go to Dr.Fien Degryse, Dr. Ivan Andelkovic, Roslyn Baird and Dr, Rodrigo C.da Silvia for their generosity, sharing their expertise knowledge as well as comments on my work. A special thanks to Dr.Md Julker Nine, Dr. Ramesh Karunagaran, Dr Mahdieh Nemati, Supriya Lath and Emma Knight for their support and for motivating me whenever I found myself hopeless. Special thanks to my fellow friends at the University of Adelaide and all around the world who supported me and encouraged me to strive towards my goal.

My grateful thanks go to Bogumila Tomczak, Colin Rivers and Ashleigh Broadbent for their technical support at the School of Agriculture, Food and Wine of the University of Adelaide. I thank the School of Chemical Engineering staff, analytical lab manager, workshop technical staff and administration team at the University of Adelaide for their individual help.

I would also like to acknowledge the Australian Government and the University of Adelaide for an APA scholarship to financial support me during my PhD study. The support of the Australian Research Council (ARC DP 150101760) is also gratefully acknowledged.

Nothing would have been possible without the support and endless love of my dear husband Mahdi. I am so grateful for his endless support for the last 3.5 years to help me to accomplish my dream of becoming a scientist. I sincerely thank Mahdi and my daughter Mahya for sacrificing their valuable family time for my PhD. Last but not least, special thanks to my mother, my father and my sisters and brother for their unconditional love and support.

TABLE OF CONTENTS

Chapter 1

Introduction

1.1. Background

In the first half of this century, global demand for food is expected to grow by 53% on top of the present level to satisfy the needs of around 9 billion people on earth.[1] The population growth will most likely occur in developing countries, those already with limited ability to feed their rising population.[2] Meanwhile, the world's arable land area diminishes due to the industrialization, urbanization, and desertification and land degradation.[3] Furthermore, due to rapid global warming and emissions of greenhouse gases owing to the consumption of hydrocarbon fuels, fossil fuels need to be replaced by renewable sources such as biofuels.[4] Due to these reasons, crop yields per unit area need to continuously increase by applying more fertilizers and enhancing fertilizer use efficiency.

Fertilizers containing plant macro- and micro-nutrients are required to replace nutrients removed by harvested crops.[5] While crop yields have improved remarkably through the use of fertilizers, concerns have been raised regarding losses of fertilizer nutrients to the atmosphere and to waterways. For example, a large portion of (30% -70%) of applied N fertilizer is lost depending on application method and soil conditions, which leads to major environmental and health problems and lost production for farmers.[1,6]

In this framework, nanotechnology and engineering of novel nanomaterials offers a possible pathway to develop new generation fertilizers that are more effective.[7] The advantages of nanomaterials are their high surface area to volume ratio, tailored surface functionalization, high loading capability, and their small size that assist with their potential mobility through soil pores.[8] Furthermore, nanoscale fertilizers may enhance the agronomic efficiency of fertilizers due to their specific chemical properties.[8] Recently, several studies have investigated the application of nanoscale fertlizers,[9, 10] but most have been limited to the investigation of the interaction of nanomaterials with plants under laboratory conditions.[11, 12] Despite the potential for the use of nanomaterials in agriculture, a major limitation is their high cost and concerns for environmental safety.[13] Therefore, for nanomaterials to become widely adopted in agriculture, there is a need to develop inexpensive and environmentally safe materials that can be used for different purposes in agriculture.

Increasing demand for food and fuel and the resultant intensification of agriculture will increase the volumes of fertilizers manufactured and transported globally, which raises the challenge of maintaining fertilizer quality.[1] Solid fertilizers mostly in the form of granular products should have appropriate mechanical strength to resist fracturing and the creation of dust during handling and storage processes.[14] However, many fertilizers have poor physical quality.[15, 16] Airborne dust is undesirable due to health and safety risks for those exposed during the manufacturing of fertilizers or their application on the farm. It also leads to loss of nutrient.[16] Many different technologies are used by fertilizer manufacturers to control or reduce dust generation by using hardening agents, but most of these materials suffer from low efficiency, high cost, contamination concerns, and potential environmental and occupational health concerns.[16, 17] Therefore, there is a need for new materials to address the limitations of currently used fertilizers in terms of improved agronomic performance, reduced losses to the environment, multiple modes of action and acceptable costs.

Graphene (GN), a 21st century material, has the potential to address these limitations due to its unique physicochemical properties, notably the exceptionally high surface area, electron and thermal mobility and mechanical strength.[18-20] Since its discovery in 2004, it has attracted tremendous interest in all fields of technology, from electronic systems to biomedical devices.[19, 21] It is also recognized as a biocompatible material and hence has attracted considerable biomedical interest for the development of nanocarriers for drug and gene delivery, and cancer therapy.[21-24] The exceptional mechanical property of GN-based materials has also triggered efforts to use them as reinforcement materials to enhance the mechanical properties of different composites.[25-28] Therefore, the unique properties of GN-based materials are the background to this Ph.D. thesis to utilize those properties in agricultural science and enhance fertilizer use efficiency and physical quality as summarized in Figure 1.

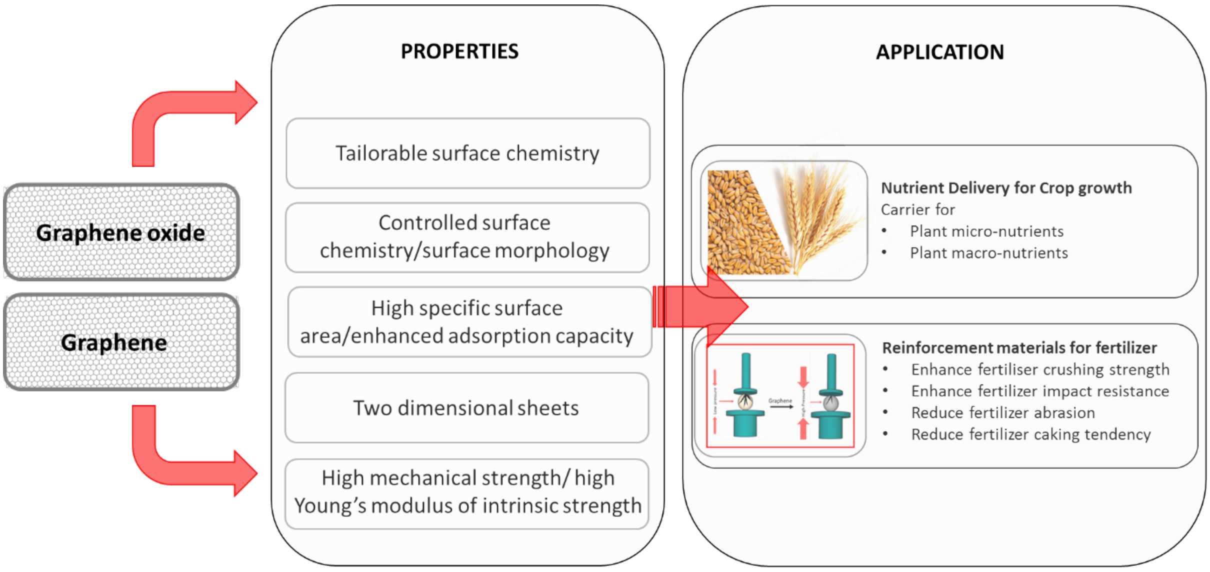

Figure 1. Graphene-based material applications in agriculture proposed in this thesis.

This Ph.D. is one of the first studies to examine the use of GN-based materials as fertilizers. I hypothesised that the two dimensional structure of GN-based materials and their high specific surface area, in addition to their tailorable surface chemistry, could make them a potential candidate for carrying different plant micro- or macro-nutrients. Furthermore, considering the high mechanical strength of GN.[27, 29] I hypothesised that GN-based materials could be applied as hardening agents for existing commercial fertilizers to address the long-standing problems caused by their fragility and physical losses related to low crushing strength, susceptibility to abrasion and low impact resistance.

1.1. Research aims and objectives

The major aims of this thesis was to investigate the application of GN and its derivatives, such as graphene oxide (GO) and graphene composites, as nutrient carriers or hardening agents to enhance fertilizer use efficiency and mechanical strength. In this context, the first approach (aim 1) was to synthesise GO-based carriers for delivery of micronutrients. Aim 2 explored the efficiency of GO-based fertilizers for enhancing crop yield and nutrient uptake. Aim 3 explored the effect of GN-based materials on the physical properties of granular fertilizers. The final approach (Aims 4) investigated the effect of GN concentration and physicochemical properties on the crushing strength of granular fertilizers.

- **Aim 1**: To synthesise GO-based carriers for delivery of micronutrient (Chapter 3).
    - Objective 1: To demonstrate the concept that GO sheets can be used as a platform for loading and carrying plant micronutrients such as zinc and copper.
    - Objective 2: To investigate the cumulative release of GO-based fertilizers in water and their release pattern and diffusion in soil.
    - Objective 3: To explore whether GO-based fertilizers can act as slow-release fertilizers.
- **Aim 2**: To explore the efficiency of GO-based fertilizers in enhancing plant dry mass and nutrient uptake and compare their performance with commercial fertilizers (Chapter 4).
    - Objective 1: To explore the effect of fertilizer method of application for example banded versus mixing on plant dry mass and nutrient uptake.
    - Objective 2: To investigate the effect of fertilizer form for example using fluid or granular form on their efficiency in improvement of plant nutrient uptake and yield.
- **Aim 3**: To demonstrate a new concept of utilizing low rates of GN and GO as additives to enhance the physical properties of commercial fertilizer granules. (Chapter 5).
    - Objective 1: To explore the effect of small content of GN or GO additives on enhancement of the physical properties of congratulated phosphorus based fertilizer by their examining crushing strength, abrasion, impact resistance and caking tendency.

- Objective 2: To reveal whether GN-based additives as hardening agents can affect the release of nutrients in the soil while simultaneously enhancing their physical properties

- **Aim 4**: To investigate the fundamental aspects of the influence of GN additives on improving the mechanical properties of fertilizers. (Chapter 6).
  - Objective 1: To explore the effect of GN concentration on crushing strength of fertilizers and to find the optimum concentration of GN which crushing strength decreases beyond that concentration
  - Objective 2: To investigate the effect of GN different properties including its deoxygenation degree due to different reduction methods, specific surface area, particle size and surface functionalization on the crushing strength of granular fertilizers.

1.2. Thesis outline

This thesis is the outcome of research studies during my Ph.D. program which is presented in the form of journal publications. The chapters in this thesis are arranged in the form of journal publications in the following sequence;

- **Chapter 1**: This chapter introduces the significance of the research project and thesis, and outlines the key contributions to the field of research.
- **Chapter 2**: This chapter reviews the literature covering recent advances in the application of GN-based materials in different fields including environmental science, pesticides and organic pollutant removal, biosensors, gene delivery, protective coatings and reinforcement materials and correlates them to their potential applications in agriculture. This chapter also reviews the recent progress in application of GN-based materials in agriculture and provides the research problem and gaps, in addition to future perspectives in the application of GN-based materials in agriculture. Outcomes are one review paper submitted to the

journal of RSC Chemical Reviews. Note this paper reviews some of the findings of subsequent chapters.

- **Chapter 3**: This chapter addresses Aim 1. It investigates the application of GO as a carrier for the plant micronutrients Zn and Cu The content of Chapter 3 was published as a research article and is also included in an Australian provisional patent application.
- **Chapter4**: This chapter investigates the efficiency of different Zn-GO-based fertilizer formulations on wheat plant growth and nutrient uptake and compares their efficiency with commercial Zn fertilizers in a Zn-deficient soil. The content of this chapter is submitted to a peer-reviewed journal (ACS Environmental Science and Technology) for publication.
- **Chapter 5**: This chapter focuses on the effect of GN and GO as hardening agents to enhance the physical properties of fertilizer granules of mono ammonium phosphate (MAP). Different physical properties of fertilizers including the crushing strength, abrasion, impact resistance and caking tendency were measured after co-granulating low rates of GN (or GO) with MAP. The content of this chapter was published as a research article and is protected by an Australian provisional patent application.
- **Chapter 6**: This chapter provides a more detailed examination of the effect of GN concentration on the crushing strength of two different fertilizers, MAP and diammonium phosphate (DAP), with different initial hardness. This chapter also investigated the effect of GN production method, specific surface area and sheet size on the crushing strength of MAP and DAP granules. The content of this chapter is ready to be submitted to a peer-reviewed journal for publication.
- **Chapter 7**: This chapter presents the conclusions and perspectives for future work on the application of GN-based materials in agriculture.

References:

1. Albadarin, A. B.; Lewis, T. D.; Walker, G. M. Granulated polyhalite fertilizer caking propensity. *Powder Technology* 2017, 308, 193-199.
2. Rengel, Z. *Nutrient use in crop production*. The Howorth Press: USA, 1998; Vol. 2.
3. Shaviv, A. Advances in controlled-release fertilizers. *Advances in Agronomy* 2001, 71, 1-49.
4. Gelfand, I.; Sahajpal, R.; Zhang, X.; Izaurralde, R. C.; Gross, K. L.; Robertson, G. P. Sustainable bioenergy production from marginal lands in the US midwest. *Nature* 2013, 493, 514-517
5. Das, G. H. T. A review on controlled release advanced glassy feertilizer. In *Global Journal of Sicence Frontier research:B chemistry*, 44 ed.; 2014; Vol. 14, pp. 32-44.
6. Chien S.H, P. L. I., Cantarella H. Chapter 8, Recent developments of fertilizer production and use to improve nutrient efficiency and minimize environmental impacts. Donald LS, ed. Advances in Agronomy: Academic Press 2009, pp. 267-322.
7. Kashyap, P. L.; Xiang, X.; Heiden, P. Chitosan nanoparticle based delivery systems for sustainable agriculture. *International Journal of Biological Macromolecules* 2015, 77, 36-51.
8. Raliya, R.; Saharan, V.; Dimkpa, C.; Biswas, P. Nanofertilizer for precision and sustainable agriculture: current state and future perspectives. *Journal of Agricultural and Food Chemistry* 2017.
9. Giroto, A. S.; Guimarães, G. G. F.; Foschini, M.; Ribeiro, C. Role of slow-release nanocomposite fertilizers on nitrogen and phosphate availability in soil. *Scientific Reports* 2017, 7, 46032.
10. Kottegoda, N.; Sandaruwan, C.; Priyadarshana, G.; Siriwardhana, A.; Rathnayake, U. A.; Berugoda Arachchige, D. M.; Kumarasinghe, A. R.; Dahanayake, D.; Karunaratne, V.; Amaratunga, G. A. J. Urea-Hydroxyapatite nanohybrids for slow release of nitrogen. *ACS Nano* 2017, 11, 1214-1221.
11. Dev, A.; Srivastava, A. K.; Karmakar, S. Uptake and toxicity of nanomaterials in plants. In *Nanoscience in Food and Agriculture 5*, Ranjan, S.; Dasgupta, N.; Lichtfouse, E., Eds. Springer International Publishing: Cham, 2017; pp. 169-204.
12. Zaytseva, O.; Neumann, G. Carbon nanomaterials: production, impact on plant development, agricultural and environmental applications. *Chemical and Biological Technologies in Agriculture* 2016, 3, 17.
13. Gogos, A.; Knauer, K.; Bucheli, T. D. Nanomaterials in plant protection and fertilization: Current State, Foreseen Applications, and Research Priorities. *Journal of Agricultural and Food Chemistry* 2012, 60, 9781-9792.
14. Matejovic, I. Determination of carbon and nitrogen in samples of various soils by the dry combustion. *Communications in Soil Science and Plant Analysis* 1997, 28, 1499-1511.
15. Hignett, T. P. Physical and chemical properties of fertilizers and methods for their determination. In *Fertilizer Manual*, Hignett, T. P., Ed. Springer Netherlands: Dordrecht, 1985; pp 284-316.
16. Rehberg, B. E.; Hall, W. L. Fertilizer compositions and method of making such compositions. U.S. Patent US 5238480 A: 1993.
17. Kucera P, Sawyer WG. Fertilizer composition incorporating fibrous material for enhanced particle integrity. U.S. Patent US20120285211A1, 2015.
18. Geim, A. K. Graphene: Status and prospects. *Science* 2009, 324, 1530-1534.
19. Geim, A. K.; Novoselov, K. S. The rise of graphene. *Nature Materials* 2007, 6, 183-191.
20. Perreault, F.; Fonseca de Faria, A.; Elimelech, M. Environmental applications of graphene-based nanomaterials. *Chemical Society Reviews* 2015, 44, 5861-5896.
21. Zhang, Y.; Nayak, T. R.; Hong, H.; Cai, W. Graphene: A versatile nanoplatform for biomedical applications. *Nanoscale* 2012, 4, 3833-3842.
22. Zhao, H.; Ding, R.; Zhao, X.; Li, Y.; Qu, L.; Pei, H.; Yildirimer, L.; Wu, Z.; Zhang, W. Graphene-based nanomaterials for drug and/or gene delivery, bioimaging, and tissue engineering. *Drug Discovery Today* 2017, 22, 1302-1317.
23. Gonçalves, G.; Vila, M.; Portolés, M.-T.; Vallet-Regi, M.; Gracio, J.; Marques, P. A. A. P. Nano-Graphene oxide: A potential multifunctional platform for cancer therapy. *Advanced Healthcare Materials* 2013, 2, 1072-1090.

24. Liu, J.; Cui, L.; Losic, D. Graphene and graphene oxide as new nanocarriers for drug delivery applications. *Acta Biomaterialia* 2013, 9, 9243-9257.
25. Gholampour, A.; Valizadeh Kiamahalleh, M.; Tran, D. N. H.; Ozbakkaloglu, T.; Losic, D. From graphene oxide to reduced graphene oxide: Impact on the physiochemical and mechanical properties of graphene–cement composites. *ACS Applied Materials & Interfaces* 2017, 9, 43275-43286.
26. Gholampour, A.; Kiamahalleh, M. V.; Tran, D. H.; Ozbakkaloglu, T.; Losic, D. Revealing the dependence of the physiochemical and mechanical properties of cement composites on graphene oxide concentration. *RSC Advances* 2017, 7, 55148-55156.
27. Kim, H.; Abdala, A. A.; Macosko, C. W. Graphene/Polymer nanocomposites. *Macromolecules* 2010, 43, 6515-6530.
28. Li, Z.; Guo, Q.; Li, Z.; Fan, G.; Xiong, D.-B.; Su, Y.; Zhang, J.; Zhang, D. Enhanced mechanical properties of graphene (reduced graphene oxide)/aluminum composites with a bioinspired nanolaminated structure. *Nano Letters* 2015, 15, 8077-8083.
29. Lee, C.; Wei, X.; Kysar, J. W.; Hone, J. Measurement of the elastic properties and intrinsic strength of monolayer graphene. *Science* 2008, 321, 385-388.

Chapter 2

Graphene materials for efficient and sustainable agriculture: Current progress and perspectives

This section is included in the thesis as it appears as a manuscript submitted by **Shervin Kabiri,** Diana N.H. Tran, Mike J. McLaughlin and Dusan Losic, "Graphene materials for efficient and sustainable agriculture: current progress and perspectives", to the journal ***Chemical Society Reviews***, (2018).

Statement of Authorship

Title of Paper	Graphene materials for efficient and sustainable agriculture: current progress and perspectives
Publication Status	☐ Published ☐ Accepted for Publication ☑ Submitted for Publication ☐ Unpublished and Unsubmitted w ork w ritten in manuscript style
Publication Details	Chemical Society review

Principal Author

Name of Principal Author (Candidate)	Shervin Kabiri		
Contribution to the Paper	Performing the literature review and writing the manuscript		
Overall percentage (%)	80		
Certification:	This paper reports on original research I conducted during the period of my Higher Degree by Research candidature and is not subject to any obligations or contractual agreements with a third party that would constrain its inclusion in this thesis. I am the primary author of this paper.		
Signature		Date	22/06/2018

Co-Author Contributions

By signing the Statement of Authorship, each author certifies that:

i. the candidate's stated contribution to the publication is accurate (as detailed above);

ii. permission is granted for the candidate in include the publication in the thesis; and

iii. the sum of all co-author contributions is equal to 100% less the candidate's stated contribution.

Name of Co-Author	Diana N.H. Tran		
Contribution to the Paper	I acted as the secondary supervisor for Shervin Kabiri and helped her to design and improve the final drafts of the manuscript for submission. I give consent for Shervin Kabiri to present this paper for examination towards the Doctorate of philosophy.		
Signature		Date	22/06/2018

Name of Co-Author	Mike J. McLaughlin		
Contribution to the Paper	I acted as the secondary supervisor for Shervin Kabiri and aided in design and evaluation of manuscript for submission. I give consent for Shervin Kabiri to present this paper for examination towards the Doctorate of philosophy.		
Signature		Date	22/06/218

Name of Co-Author	Dusan Losic		
Contribution to the Paper	I acted as the primary supervisor for Shervin Kabiri and aided in design and evaluation of manuscript for submission. I give consent for Shervin Kabiri to present this paper for examination towards the Doctorate of philosophy.		
Signature		Date	22/06/218

Graphene materials for efficient and sustainable agriculture: current progress and perspectives

Shervin Kabiri [ǂ], *Diana N.H. Tran*[ǂ], *Mike J. McLaughlin*[*‡] *and Dusan Losic*[* ǂ]

[ǂ] School of Chemical Engineering, Engineering North Building, The University of Adelaide, Adelaide, SA 5005, Australia

[‡] Fertilizer Technology Research Centre, School of Agriculture, Food and Wine, The University of Adelaide, Waite Campus, PMB1, Glen Osmond, SA 5064, Australia

Abstract:

The unique physicochemical properties of graphene (GN) and GN-based materials, particularly their two-dimensional (2D) structure, remarkable high specific surface area, electron mobility, barrier properties and mechanical strength have led to the development of many new products and technologies to address challenging problems across broad sectors including agriculture. Despite the great progress in the area of material science, biomedicine, energy and environmental science, the application of GN-based materials in agriculture science is still at an early stage. This review paper describes the current stage of exploration and future perspective of the application of GN-based materials in the agriculture. In this review, we have also focused on some unique properties of GN-based materials and assess their suitability in agriculture science. It also highlights the challenges needed to be overcome and addresses the fundamental questions regarding the safe and efficient deployment of GN-based materials in agriculture.

1. Introduction

The world's population is increasing at a high rate and will reach 9.8 million by 2050, hence to continue to provide sufficient food for this growing population will be one of mankind's greatest challenges. Global food production must increase by 70–100% within the next 30 years to meet the future needs of the world's ever-growing population.[1,2] One of the major challenges faced by the agricultural sector to achieve these expectations is to significantly increase food production without degrading the soil-health and agro-ecosystem quality.[1,2] In addition, sustainability of agricultural production is threatened by many factors including the deterioration of soil health, the significant adverse effects of climate change, increased aquatic and terrestrial environmental pollution, and pesticide resistance in insects and pathogens.[1,3,4] Furthermore, the area of the world's arable land has diminished due to extensive industrialization, urbanization, and desertification and land degradation from heavy flooding and climate change.[5] Data collected by the Food and Agriculture Organization of the United Nations (FAO) indicated that the diminution and degradation of soil and water create serious challenges in regard to the production of sufficient agricultural crops to meet the demand of an ever growing population.[6] Therefore, there is an urgent need to change the manner in which crops are irrigated, increase the efficiency of pesticides, reduce pollution and generally make agriculture more environmentally friendly by finding a rapid and precise way to detect pathogens and pests, as well as an effective system for targeted pesticide delivery. Along with the above issues, fertilizers also play a key role in the long-term sustainability of food production and more efficient use of fertilizers needs to be achieved to prevent serious concerns regarding environmental, health, and energy and resource conservation.

It has been identified that fertilizers are one of the key elements that can help the agricultural sector to meet its food production goal. Commercial fertilizers are responsible for 40 to 60% of the world food production.[7] In the last few decades, the main goal of applying fertilizers in agriculture was focused on delivering the required nutrients to increase or sustain optimal crop yield. Although crop production improved remarkably as a combined result of fertilizer management and pest control, efficient nutrient use and recovery still remain low.[8, 9] Nitrogen is the most widely applied plant nutrient and is the most important chemical input for crop production from an economic viewpoint.[10] Unfortunately, 30-70% of applied nitrogen (N) fertilizer is lost to the atmosphere or leached, depending on the application method and soil conditions, which leads to major environmental and health problems, and financial difficulty for farmers.[8, 9] The main adverse environmental effects associated with N-based fertilizers are related to nitrate leaching into ground water, and emission of greenhouse gases (particularly nitrous oxide (N_2O)) and ammonia (NH_3) volatilization.[8, 9] In contrast, other fertilizer nutrients such as phosphorus (P), potassium (K), zinc (Zn), and copper (Cu) etc. can be strongly bound, or "fixed", in soil due to the complexation and formation of strong electrostatic or chemical bonds with other elements or soil components such as organic matter, iron and aluminium oxides, carbonates and oxides, and become less available to be taken up by plants.[11,12] Ultimately the fixed nutrients in soil can be washed away with sediments due to runoff, where they can create serious aquatic system pollution.[13] Furthermore, nearly 85% of the world's total mined P resources are used by farmers as fertilizer and ultimately reserves of P are finite, meaning that availability and quality will decline, and cost will increase.[14] Although some strategies, such as growing crops hydroponically have been developed, this system of production costs approximately 10 times more than conventional crops.[15, 16] To ensure that the proper use of fertilizer is beneficial for crop production and to reduce the detrimental environmental aspects associated with fertiliser use, it is necessary to develop new and sustainable strategies that result in improved crop production. This can be achieved by advancing fertilizer performance and improving the method of application. One of the most promising strategies in this aspect is the development of advanced and efficient fertilizers that have a release of nutrients in synchrony with plant demand.[17]

Slow- or controlled-release fertilizers (SRFs or CRFs) could provide significant advantages in terms of minimising losses to the environment and maximising uptake by the crop – this could reduce amounts of fertilizer required, reduce costs and save on labour as only a single application would be required for each growing season.[5] S/CRFs also decrease the risks of seedling toxicity suffered by some highly soluble fertilizer formulations. Current SRFs often have the disadvantage of high cost due to the expensive coating technologies used. Some of the coating materials are non-biodegradable and add extra pollutants to the soil, making these types of fertilizers not environmentally friendly. Furthermore, in some cases their release pattern is not compatible with plant demand in field applications.[5] Therefore, the development of new and advanced materials for S/CRFs is needed to contribute, not only to enhance fertilizer use efficiency, but also reduce adverse environmental effects and agriculture production costs associated with their application.[17] For this reason it is timely to consider the use of multifunctional new materials in agriculture. Not only it can improve nutrient delivery to plants but can also be used successfully to deliver other substances including pesticides, herbicides, fungicides, and plant hormones or genetic materials to improve crop yield and protection.

In this regard, nanotechnology and nanomaterials aimed to minimize nutrient losses and increase crop yield by optimizing nutrient management are now considered a key approach to modernize agriculture in the 21st century .[18, 19] Nanotechnology is a promising strategy and a novel tool to manage molecular biotic and abiotic stresses of plants, detect plant disease rapidly and improve plants nutrient and pesticide absorption.[15,20] In agriculture, nanotechnology has opened up many new opportunities including sensing nutrients, pesticides and contamination, postharvest processing of agricultural products for shelf life improvement, smart or targeted delivery of nanoscale nutrients, pesticides and biomolecules to effectively control plant disease and improve their growth, water purification and nutrient recovery.[15, 21] Among the number of nanomaterials explored to date, graphene (GN) is a very attractive nanomaterial for these applications due to its outstanding properties and unique 2D structure.

Graphene has created a great deal of interest in various research fields and commercial industry after its discovery in 2004 .[22, 23] As a material with a thickness of a single atom, GN simultaneously exhibits high level of electrical conductivity ranging from 10 000 $cm^2V^{-1} s^{-1}$ to

50 000 cm^2V^{-1} s^{-1} at room temperature, thermal conductivity above 3000 W m^{-1} K^{-1}, and outstanding mechanical strength (measure Young's modulus of 1 TPa and intrinsic strength of 130 GPa), which makes this material exceptionally suitable for a wide range of applications.[24-27] Such versatility, combined with other unique properties including impermeability to gases and water molecules, a tailorable surface chemistry, antibacterial properties, thermal stability and most importantly a high specific surface area, have rendered GN and GN-based materials attractive as technological tools.[28-31] A wide range of applications of GN-based materials are demonstrated, from nanocarriers for drug delivery, new generation of biosensors, probes for cell and biological images, pollutant removal from aquatic ecosystems, protective coatings and reinforcement materials for different media.[23,25-27,32-37] It is not surprising that GN-based materials are considered as an excellent solution to address many problems in agriculture.

In this review we aim to present the main properties of GN-based materials relevant to their applications in different sections of agriculture ranging from nutrient and pesticide delivery, gene delivery, biosensors, protective coatings and reinforcement materials in order to assess the possibilities offered by these novel carbon-based materials. This review will specifically describe the current application of GN-based materials in agriculture, in particular as a fertilizer platform (micro- and macro-nutrients) for delivery of balanced and sustained nutrition, pesticide and herbicide delivery for crop protection and weed eradication, reinforcement materials for enhancement of physical properties of fertilizer granules and as a barrier coating to slow down nutrient release. The current applications of GN in agriculture presented in this review are summarised in Figure 1. The mass production of GN-based materials, their supply to the market and related problems is also discussed. The review also introduces some possible applications of GN-based materials in different areas of agricultural science which have not yet been explored, but where there is potential. Finally, the current status of research related to the impact of GN-based materials to plant growth and soil heath is summarized.

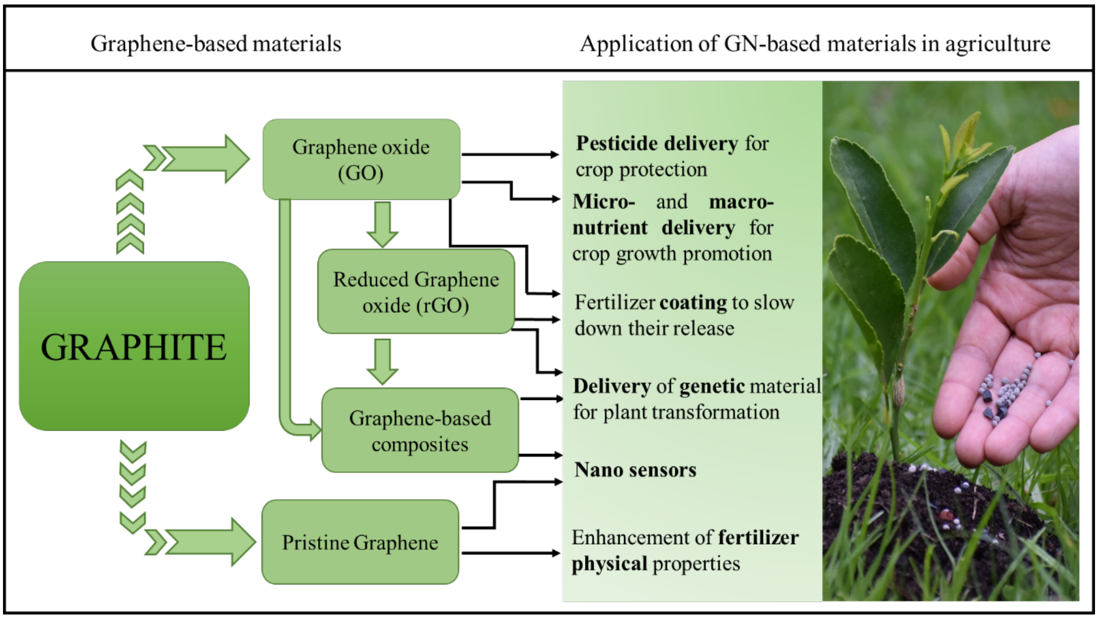

Figure 1. Schematic diagram of different graphene-based materials production and their application in agriculture.

2. Graphene-based materials: concepts, laboratory and industrial production methods

Graphene-based materials including pristine GN, graphene oxide (GO), reduced graphene oxide (rGO), graphene quantum dots (GNQDs) and GN/GO-based composites can be obtained by using either graphite as the starting material or by the synthetic process from carbon precursors where many different production methods are used.[38,39] The major differences between GN materials produced by different methods is their surface chemistry, number of layers and size of sheets as indicated in Figure 2.[40] Different GN-based materials and their laboratory or industrial methods of preparation summarized in following sections.

2.1. Pristine graphene

Arguably the most intensively researched material since its discovery is pristine GN due to its extraordinary physical properties. It is the basic structural element of graphite, strongly pi-pi stacked together to form the lamellar structure with an interlayer distance of

0.335 nm between the GN sheets.[41] Graphene in its pristine form exhibits outstanding properties, such as excellent conductivity for both electricity and heat, and is the strongest material ever measured. A large specific surface area of 2600 m^2/g has been predicted for GN and its carbon atoms arranged in the 2D pristine sheets are so tightly packed that not even helium atoms can pass through.[42] A single layer of pristine GN can be produced by micromechanical exfoliation of graphite using an adhesive tape. This simple method generates a high quality GN ideal for research purposes but is labour-intensive and not scalable for large production.[24, 43] Pristine GN can also be generated by the ultrasonication of graphite in water or organic solvents. However, the drawback of this approach is a relatively low-yield.[44, 45] The most common approach to produce scalable and high quality GN is to directly synthesize GN by thermal decomposition of silicon carbide (SiC[13]) or epitaxial growth of GN on transition metals through chemical vapour deposition using hydrocarbons or alcohols.[46-50] However, regardless of which method is used, pristine GN is not soluble in polar solvents and tends to aggregate in aqueous solution. Therefore, the first requirement for handling GN for further practical purposes is to chemically functionalize its surface which in turn will modify its chemical, structural and electronic properties.[42]

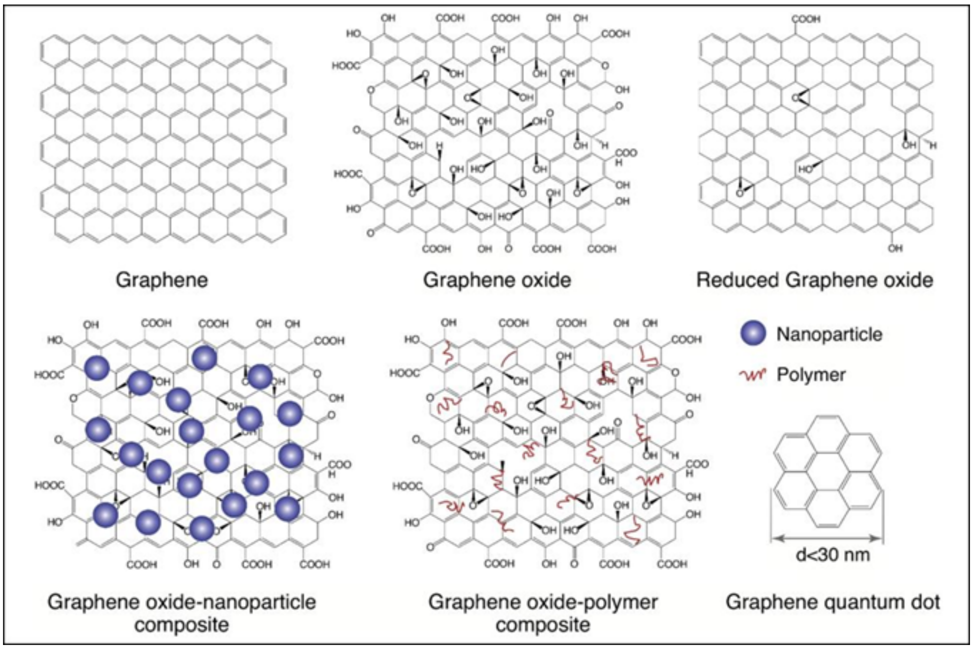

Figure 2. Schematic of different graphene-based materials with potential use in agriculture. Adapted with permission from.[40]

2.2. Graphene oxide

Another popular approach to prepare GN-based materials is to use graphene oxide (GO), which is the oxidized form of graphite. Graphene oxide usually consists of single, bi- or multi-layer GN sheets with a high density of oxygen functional groups in the carbon lattice. It can be synthesised at low cost, commonly using the Hummers method or derivatives thereof, which involves using concentrated acid with oxidizing agents such as potassium permanganate ($KMnO_4$).[51] Graphene oxide sheets contain different types of oxygen functional groups- mostly epoxy and hydroxyl groups on their basal plane, and carbonyl, phenol, carboxyl and lactone at the edges of their sheet.[38,52,53] The hydroxyl and epoxy groups on the surface of GO sheets are likely to form hydrogen bonds and weak interactions with other groups, while carbonyl and hydroxyl related to the carboxylic acid groups are responsible for the negative surface charge and stable dispersion of GO in all polar solvents.[54] The stable dispersion of GO in polar solvents combined with its high specific surface area and high density of oxygen functional groups makes it an ideal platform for a wide variety of chemical functionalization. Therefore, GO is widely considered as the starting material to synthesise novel GN-based materials.[38,51] Although the presence of different oxygen functional groups on the surface and edge of GO increases its stability in polar solutions as well as its chemical reactivity, its mechanical, electrical and thermal properties decrease due to the disrupted sp^2 strudcture.[55-58]

2.3.Reduced graphene oxide

If the goal is to produce GN from non-mechanical methods, the GO dispersion needs to be somehow chemically or hydrothermally reduced, resulting in a GN suspension.[59,60] Chemical reduction of GO is a very fast method for GN production and is solution-processable (graphene can be made in a solvent such as water or an organic solvent).[61] The most widely used reducing agent, although toxic and dangerous, is hydrazine that typically forms hydrazone with the carbonyl groups of GO.[62] In order to avoid the generation of toxic chemicals, environmentally-friendly chemicals such as L-aspartic acid, L-ascorbic acid and D-glucose have been proposed, which provide a clean way to deoxygenate the GO.[60,63-65] However, chemical reduction of GO always alters its chemical structure forming carbon vacancies and clustered pentagonal, or heptagonal carbon structures, or residual oxygen content, which displays partial restoration of the mechanical and electrical properties of pristine GN.[25,66,67] Another method to produce GN with less defects using non-toxic chemicals is the hydrothermal reduction of GO in an aquatic environment under sub- or supercritical pressure and varying temperature.[68] Usually, the hydrothermally reduced GN holds a minimum level of defects and the π-network conjugates quickly, however GN aggregates strongly and re-dispersion in water *via* ultrasonication and pH adjustment is not as comparable with chemically reduced GN.[60] In addition to the chemical and hydrothermal reduction of GO, thermal annealing, photoelectron or ultraviolet (UV) reduction, plasma and microwave-assisted reduction are popular techniques, depending on the final application.[38,59,60,69]

2.4.Graphene quantume dots

Graphene quantum dots (GNQDs) are another type of GN-based material with a lateral size of less than 30 nm consisting of one, or up to ten layers of GN and can be fabricated using both bottom-up and top-down approaches. The bottom-up route includes solution chemistry including the synthesis of aromatic compounds as GN moieties with a certain number of conjugated carbon atoms, which includes oxidative condensation reactions, pyrolysis, cage opening and nitration reactions.[70-74] Preparing GNQDs with the top-down method involves hydrothermal cutting, electron beam lithography, electrochemical oxidation and chemical exfoliation.[75-78] Graphene quantum dots show intense intrinsic photoluminescence and high stability, due to the strong quantum confinement and edge effects, and these properties can be further tuned by changing their size, shape defects and surface chemistry.[79-84] GNQDs have many advantages, such as low toxicity and excellent biocompatibility compared with conventional semiconductor quantum dots containing cadmium or other heavy metals, which suffer from high toxicity induced by the heavy metal.[85] Therefore, GNQDs have been diversely developed in biological applications including biosensors, cellular imaging, drug delivery and photodynamic therapy.[86, 87]

2.5. Graphene or graphene oxide composites

The rich oxygenated moieties of the GO sheets are a versatile platform to undergo covalent functionalization to prepare different GO composites, where attachment of new moieties can be carried out by different reaction routes including acylation reactions, epoxy ring opening reactions, isocyanate/esterification reactions and diazotization.[88] Amine modification of carboxylic groups presented at the edges of GO (or rGO) sheets are usually prepared using active reagents such as thionyl chloride ($SOCl_2$),[89-92] 1-ethyl-3-(3-(dimethylamino)propyl)-carbodiimide (EDC)/*N*-hydroxysulfosuccinimide (NHS),[93,94] and *N*,*N*-dicyclohexylcarbodiimide (DCC),[95,96] and amine-terminated organic molecules. Other amine-terminated molecules such as DNA,[97] polyethylene glycol (PEG)[93] and polyethyleneimine (PEI)[98] have also been effectively embedded on GO sheets *via* an amidation reaction. The amine terminated organic molecules grafted onto rGO can alter its water stability and the resulted composite materials exhibit exceptional biocompatibility in biological media, a property that can subsequently be used for delivery and DNA detection.[26] Epoxy groups on the surface of GO sheets are expected to undergo ring-opening reactions and form amide or ester bonds (depending on the nucleophilic reagents, e.g. R-NH_2 or R-OH) upon nucleophilic attack at an α-carbon.[99,100] Previously executed examples of this type of reaction include poly(allylamine) forming an amide bond with GO through a ring-opening reaction,[99] while poly(vinyl alcohol) has been grafted onto GO sheets by an ester bond.[100] Silanes, such as 3-

aminopropyltriethoxysilane (APTES) and ionic liquids such as 1-(3-aminopropyl)-3-methylimidazolium bromide terminated with an amine group have been attached to GO sheets *via* the epoxy ring-opening reaction.[101,102] GO sheets have also been functionalized with isocyanate compounds *via* amides or carbamate esters bonds by esterification reactions, which subsequently remove the surface hydroxyls and edge carboxyl groups of GO sheets making it less hydrophilic and more compatible with polar aprotic solvents.[41,88,103]

Besides covalent functionalization of GN-based materials, non-covalent functionalization of GN can take place *via* hydrophilic interaction, electrostatic binding and π-π stacking to attach polymers or biomolecules.[34,88] Materials like Tween, Pluronic F127 (PF 127) and PEGylated phospholipid have attached to rGO *via* a hydrophilic interaction for different biomedical applications.[104-106] Positively charged polymers like polyethyleneimine (PEI) and chitosan have been grafted onto negatively charged GO sheets *via* electrostatic interactions for gene and drug delivery purposes that potentially could be implemented in gene delivery in agriculture.[107,108] Natural biomolecules such as proteins, gelatine and DNA can also be immobilized on the surface of GN by π-π binding between those molecules and the GN plane.[109-111] Immobilizing DNA on GN sheets has been widely used to develop GN-based DNA sensors.[112-115]

Finally, GN has been explored for 'hard' functionalization with foreign inorganic materials, (e.g. metallic and metal oxide nanoparticles including gold (Au), silver (Ag), palladium (Pd), platinum (Pt), nickel (Ni), Cu, Zn, titanium dioxide (TiO_2), zinc oxide (ZnO), manganese oxide (MnO_2), cobalt oxide (Co_3O_4) and iron oxides and oxyhydroxides (Fe_3O_4 and αFeOOH) to enhance the properties of the inorganic materials or to combine the properties of two entities for different applications including catalysis, water remediation, electrochemical sensors, and biomedicine.[34,88,116-121] The high surface area of GO and rGO occupied by the negatively charged oxygenated groups provide abundant nucleation sites for metal nanoparticle growth to produce GN-metal nanoparticle (NP) composites. To date, a large number of strategies have been developed to interface inorganic nanomaterials with GN either by *in situ* nucleation and growth of inorganic materials or physical grafting and covalent attachment on GN sheets.[88]As a result of the variety of active functional groups (-OH, -COOH, epoxy) on GO and the presence of surface pi (π) electrons on both GN/GO, these materials can be widely functionalized with different organic compounds, metal ions, metal/metal oxide NPs and polymers to prepare GN/GO composites for different applications.[23,27,34,88,122] Different modification strategies, including covalent and non-covalent approaches, can be designed to engineer functional GN/GO composites depending on their specific applications in agriculture.[34,88]

2.6. Industrial production methods of graphene and its derivatives

The promising results of GN-based materials at a laboratory scale for different research fields has triggered interest in the mass and industrial production of GN and its derivatives for application in different industries.[123] Many companies and their industrial enterprises have started to prepare GN on a scale of tons, GN film and other GN-related materials, which is a necessary requirement for industrial or agricultural applications. Different production methods for mass production of GN-based materials have been developed depending on the application targeted and hence the specific properties required. The target application and hence specific quality, the industrial scalability of a specific product, and the stability and controllability of manufacturing also affects the production method utilized.[123] The four main scalable production techniques for bulk production of GN used in industry are (i) the exfoliation of graphite directly in a liquid phase, (ii) electrochemical exfoliation of graphite in dilute acid, (iii) oxidation of graphite to GO and reduction of GO to rGO and (iv) chemical vapour disposition (CVD).

Table 1. Common industrial methods used for bulk production of GN-based materials by different companies.

Production method	Company	Ref
Direct exfoliation of graphite in liquid	GN solution, GN powder and GN nameplates	[124-128]
Electrochemical exfoliation of graphite	GN solution and composites	[129]
Oxidation of graphite to GO and reduction of GO to rGO	GO solution, GO powder, rGO solution and rGO powder	[130-132]
Chemical vapour deposition	GN film and GN foam film	[131,133-135]

Direct liquid phase exfoliation of graphite is one of the methods used for large scale production of pristine GN because of the low price and abundance of graphite. The key factor in liquid exfoliation of graphite is to overcome van der Waals interaction between GN layers while preserving the size of GN sheets.[123] First Graphene Ltd. has recently developed an environmentally friendly and safe electrochemical exfoliation method of converting ultra-high grade graphite into a low cost and high quality GN, in bulk quantities.[129] The company stated that with a GN production capacity of 2 tons per year, the GN they produce can be used for development of applications in modern materials, energy storage devices, coatings and polymers (Figure 3 A). The oxidation of graphite to GO following Brodie and Hummers methods and subsequent reduction of GO with various reducing agents or burning off the oxygen thermally with microwave or plasma as discussed earlier are potential alternative approaches used by industry for large scale production of GN and its derivatives (Figure 3B).[60,62,69,136]

The large scale production of GN-based materials with these techniques has the advantage that products made from GO could be custom-built or matched with end-user requirements. However, standardization of any GN product is difficult due to the inconsistencies in the starting raw material. Hence, the physical and chemical properties of products from different companies vary widely, due to the different techniques used for production.[123] Although, the mass production and applications of GN-based materials have emerged onto the market, and some great advantages of GN materials for commercial application have become obvious, these materials still suffer from problems such as bulk characterization and application need a very close communication with GN-based material production due to the dependence of the structure and properties of produced GN to their method of preparation.

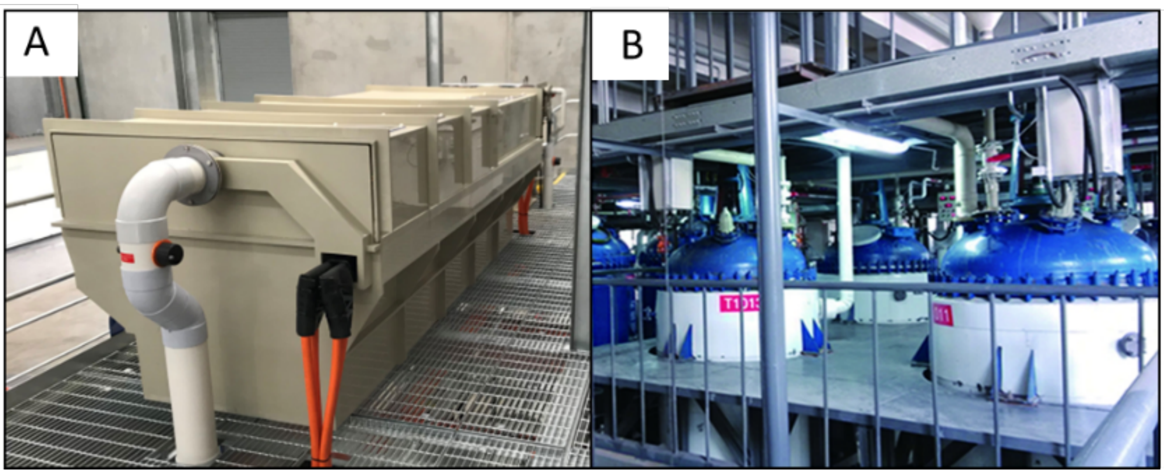

Figure 3. A) Graphene powder production line in The First Graphene Ltd. With electrochemical exfoliation method and B) Graphene powder production line in The Sixth Element Materials Technology Co. Ltd with oxidation of GO and reduction to rGO. All photos are used with permission of copyright.

3. Properties and applications of graphene-based materials

The high specific surface area of GN-based materials makes them ideal candidates for loading of different plant nutrients or interacting with different chemical compounds and biological species. In terms of GN, existence of the large density of delocalized π electrons on its planar surface makes it suitable for non-covalent functionalization with organic molecules.[137] Furthermore, the conjugated basal plane of GN facilitates the reaction with some pesticides and herbicides or other biomolecules containing aromatic structures via π-π stacking for the targeted delivery of chemicals, or fabricating biosensors.[138-140] Graphene is also characterized by its hydrophobicity which enables it to adsorb many hydrophobic organic molecules or polymers *via* van der Waals interaction.[141] In addition to the above non-covalent interactions, the presence of abundant oxygen or other functional groups in GO and other GN/GO composites provides more opportunity to immobilize inorganic materials or biomolecules through covalent bonds. Oxygen-containing groups, mainly carboxylic and hydroxyl, of GO can complex with different metal ions or participate in ionic interaction or hydrogen bonding with analogue parts of biomolecules, which can be used for plant nutrient or pesticide delivery or gene delivery applications.[23,25,40,142]

In addition to their high specific surface area and reactivity, GN and GO have remarkable barrier properties attributed to their physical structure. The nuclei of carbon atoms with a measured C-C bond length of 0.14 nm form a hexagonal GN lattice with a diameter of 0.25 nm for the individual hexagonal pores.[143] The pore diameter can further decrease to 0.06 nm if the van der Waals radii (0.11 nm) of the carbon atoms are considered. With such small geometric pores, the GN lattice represents minimum permeability for molecules, even small ones such as helium.[28] Therefore, the impermeable 2D structure of GN-based materials with barrier properties to reactive gases or water can be used as a barrier coating for fertilizers, to reduce hygroscopicity and structural degradation which can decrease the moisture adsorption and consequent cracking of fertilizers. Furthermore, GN has demonstrated a potential application for wear and scratch resistance coatings because of its mechanical robustness as a monolayer of GN film can withstand high pressure differences - up to 6 atm.[27,28] The strong covalent bonds of C-C atoms formed by sp^2 hybridization in the close-packed crystal structure of GN is responsible for its incredible mechanical strength, which makes it a potential candidate to be used as an anti-abrasion coating for fertilizers. Along with the properties of pristine GN, GO sheets can maintain a relatively large interlayer distance due to the oxygen-containing functional groups decorated asymmetrically on each plane. Between stacked GO sheets a network of nanocapillaries forms through which water is allowed to permeate smoothly allowing GO to be an efficient film barrier coating for fertilizers to decrease water penetration and slow down the release of nutrients.[144,145]

The mechanical properties of GN-based materials have also inspired researchers to incorporate GN-based materials in different matrices such as cement, metal matrix, ceramic and polymers to enhance their mechanical strength.[36,37,146-150] Both GN/GO can enhance the mechanical properties of reinforced matrices due to their high mechanical strength and high surface area of their planar sheets.[151] Consequently, GN-based materials can be used to enhance the physical quality of fertilizer granules to solve a long lasting problem related to their fragility.[152]

Graphene, which is a single layer of carbon atoms packed into a two-dimensional (2D) honeycomb lattice, has been extensively studied in terms of its properties, especially for its electronic and thermal properties because of its π-π bonds on both sides of the GN plane. The high electron mobility in GN ranges from 10 000 cm^2V^{-1} s^{-1} to 50 000 cm^2V^{-1} s^{-1} at room temperature and it can sustain current densities up to six orders of magnitude higher than copper.[24,55,153] A thermal conductivity of 5000 W/m/K has been reported for GN sheets.[24] The electronic properties of layered GN components are extremely useful for agriculture applications. Both GN and rGO have excellent electrical conductivity related to their sp^2 hybridized structure, which can be applied for sensing purposes to detect environmental pollutants, such as toxic gases and heavy metals, as well as biomolecules, including nucleic acid, hormones and microbial toxins.[154-160]

4. Application of GN-based materials as a chemical delivery system

Graphene-based materials have been explored broadly in medicine, either as a nanocarrier for drug and/or gene delivery or bioimaging .[26,40] As plant nutrients, pesticides and genes are in the form of metallic or non-metallic ions, organic molecules or biomolecules, the adsorption or attaching ability of different GN-based materials towards those materials can lead to their application as a loading platform. Hence, GN-based materials can be tailored as a delivery vehicle to carry and deliver plant micro or macronutrients, pesticides and genes as described in Figure 4.[26,140,142,161,162] However, the application of GN-based materials as a carrier of biologically-useful materials in agriculture is in the early stages of investigation and the commercial application of this potential has yet to be realised.

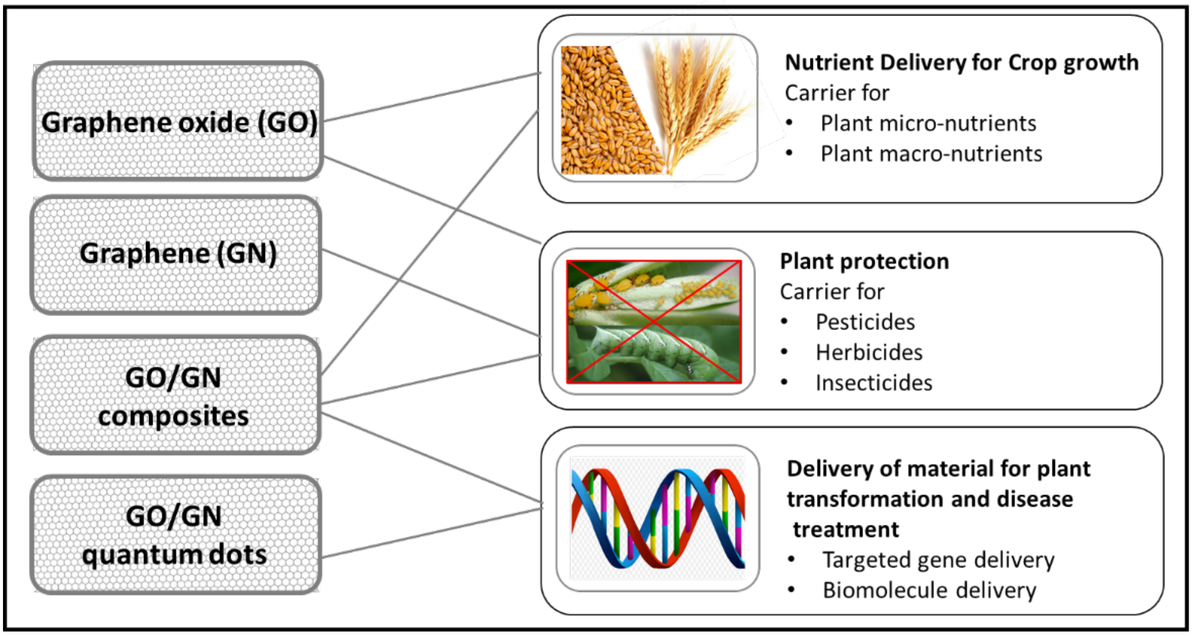

Figure 4. Potential application of graphene-based materials as a delivery platform in agriculture.

4.1.Nutrient delivery for plant balanced and sustained crop nutrition

One of the main goals of applying fertilizers is to deliver plant micro-nutrients (boron (B), iron (Fe), molybdenum (Mo), Cu, Zn and manganese (Mn)) and macro-nutrients (N, P, K, magnesium (Mg), sulphur (S) and calcium (Ca)) to either increase crop yield or sustain their optimal yield.[9,152] Conventional fertilizer application methods are either a soil application as a granular, suspension or liquid product, or as a soluble or suspension foliar (sprayed over leaves) application. As noted earlier, some nutrients such as B and N are easily leached from soils, while others, such as Cu, P or Zn, are strongly sorbed by soil. These reactions reduce the capture of nutrients by crops, and lead both to inefficient use of nutrients and potentially serious environmental issues.[163] Slow- or controlled-release fertilizers are employed to supply the plant's demand of nutrients in a slower and sustainable manner, hence avoiding temporal overdose and overcoming the environmental drawbacks of highly soluble fertilizers.[142,164] Graphene-based materials have demonstrated the ability to sorb both metallic and non-metallic species from aqueous solutions[23,25] which highlights their potential application to adsorb, carry and deliver plant nutrients.

With these principles in mind, a preliminary study conducted by our laboratories demonstrated for the first time the use of GO sheets as a carrier and platform for plant miro-nutrients Cu and Zn.[142] Both micronutrient fertilizers consisted of GO loaded with micronutrients (Zn-GO and Cu-GO) prepared in the form of solid pellets providing a slow- and sustained release of Cu and Zn to soil and aqueous solutions (Figure 5 A -G). The significant difference in the release pattern of the micronutrients from GO-based carriers compared with conventional fertilizer was explained by the tight coordination and complexation of metal ions with the oxygen functional groups on the GO surface and edges (Figure 5H).[25,165] Another factor that affected the release pattern of these GO- based fertilizers was related to the 2D structure of GO sheets as they tend to fold and aggregate during the nutrient loading process due to the reduction in electrostatic repulsion of the GO sheets.[166, 167] Therefore, to release the nutrients from the GO material, first the chemical bonding of the metallic ions and oxygen-containing groups on the surface of the GO sheet must be broken and then water molecules have to penetrate through the interconnected channels formed between the rolled or agglomerated GO sheets to release the nutrients, which is a time consuming process and results in a slower release of nutrients (Figure 5I).[142] An additional feature of GO is the residual acidity in the material, which can enhance the availability of both P and micronutrients in alkaline soils. Hence, plant dry mass and nutrient uptake was enhanced compared to commercial fertilizer materials in a highly calcareous soil. The results of this study suggest that GO can be applied as a new platform to load and carry plant cationic micro- or macro- nutrients such as Ca, Co, Cu, Fe, K, Mg, Mn and Zn.

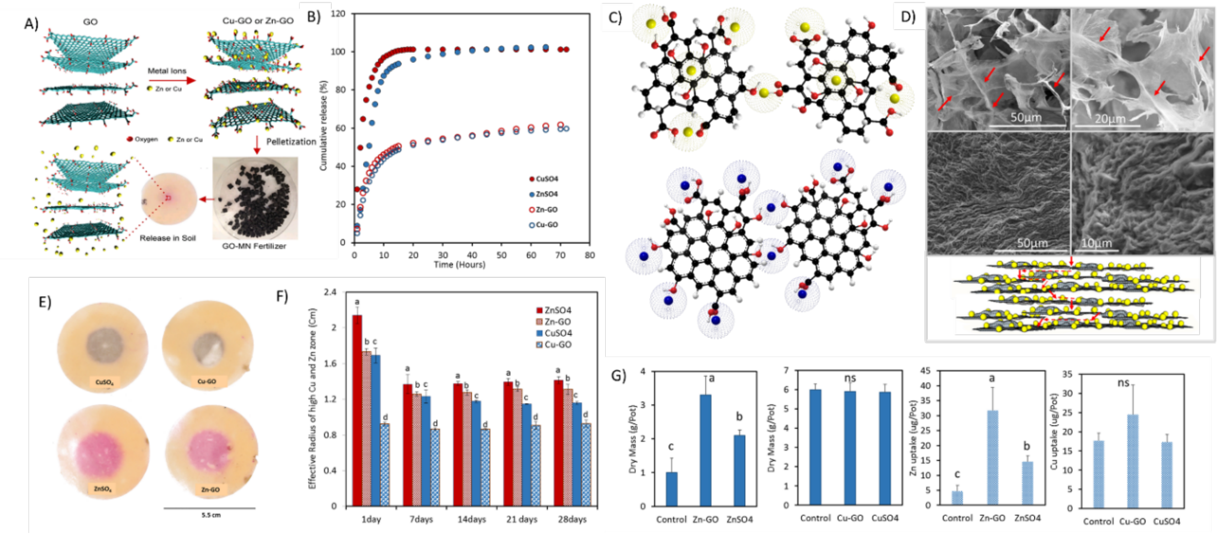

Figure 5. (A)Schematic showing preparation process of GO-based fertilizers, (B) kinetic release study of Zn from Zn-GO and $ZnSO_4$, and Cu from Cu-GO and $CuSO_4$ from the columns, (C) bonding of Zn or Cu to GO sheets, SEM images of (C) rolled Zn and Cu-loaded GO sheets, rolled and wrinkled GO sheets, and low-resolution and high-resolution SEM images of Zn/Cu-loaded GO sheets stacked on top of each other, and schematic of water penetration through the stacked structure of fertilizers granules, (E and F) photos of visualization test and their results and (G) results of plant dry mass and nutrient uptake with GO-based fertilizers compared to commercial fertilizers . Adapted with permission from.[142]

Although GO has shown promising results in the adsorption of metallic ions, the adsorption capacity can be further enhanced by surface functionalization of GO or anchoring nanoparticles on the surface. Graphene-based composites containing inorganic materials, such as magnetic or non-magnetic NPs can adsorb different metallic or non-metallic ions.[118-120,168-170] GN-based composites have shown a higher adsorption capacity towards metallic ions because the immobilization of NPs on the GN sheets prevents sheet agglomeration, thus reducing any losses in surface area and adsorption capacity.[169,171] The high affinity of GN-based composites containing NPs may be attributed to the combined effect of the metallic ion complexation with both NPs and the active sites of GN itself.[119,169,170] The immobilization of NPs on the surface of GN sheets can also enhance the surface area of the final composite, improving the number of binding sites for the ions.[170,172] In addition, grafting organic compounds such as ethylenediamine triacetic acid (EDTA), poly acrylamide (PAM), (3-mercaptopropyl) trimethoxysilane (MPTMS) and chitosan can enhance the adsorption capacity of GO-based materials.[173-176] Therefore, there is a potential for GN/GO composites to be used as a nutrient delivery platform for a wide range of nutrient ions and organic molecules, however there is still considerable scope for further investigations in this area.

The loading of anionic nutrients (B, Mo, Se, P, S) on GO is challenging as both the carrier and nutrient are negatively charged. Hence, GN/GO composites that have a positive surface charge are more favourable for loading. Figure 6 represents the main strategies for adsorption of metal and non-metal ions on GN-based materials, which can be consequently be used to load different plant nutrients on GN-based materials.

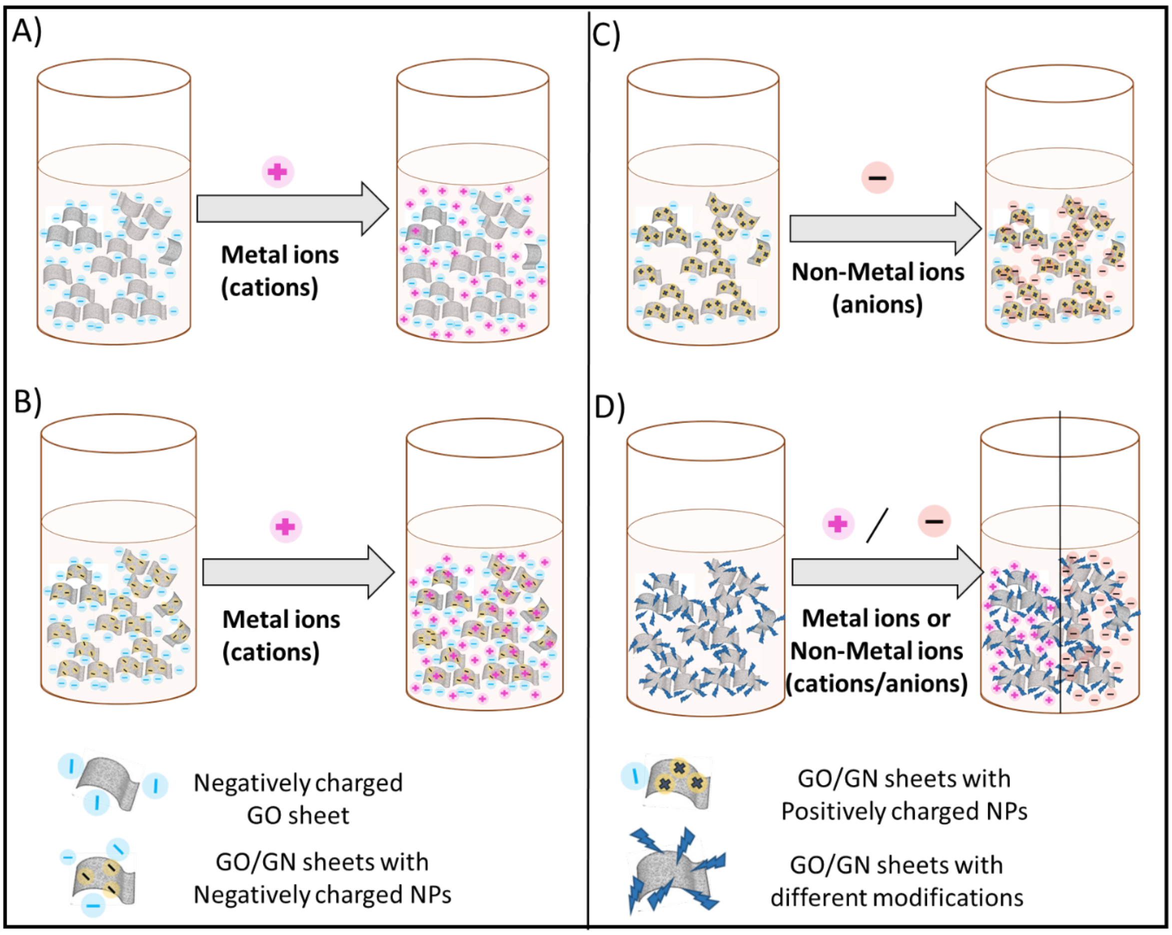

Figure 6. Main strategies to adsorb plant different nutrients on GN-based materials. a) The adsorption of positively charged or cationic nutrients such as Ca, Cu, Fe, Mg, Mn and Zn (metal ions) on negatively charged and non-modified GO sheets, with the mechanism of adsorption based on electrostatic interaction of negatively charged GO sheets and cations, b) the adsorption of cations and negatively charged nanoparticles (NPs) anchored on GN or GO sheets (GN/GO –NPs composites), with the mechanism of adsorption based on electrostatic interaction of negatively charged NPs on GN/GO sheets and cations or chemical bonding between GN/GO-NPs sheets and cations c) the adsorption of anions and positively charged nanoparticles (NPs) anchored on GN or GO sheets (GN/GO –NPs composites), with the mechanism of adsorption based on electrostatic interaction of positively charged NPs on GN/GO sheets and anions or chemical bonding between GN/GO-NPs sheets and anions and d) the adsorption of cations or anions on different functional groups on the surface of GN/GO sheets, mechanisms dependent on the functional groups.

An example of the use of GN-based composites for nutrient delivery is provided by Andelkovic et al. who developed GO-Fe composites as potential P fertilizers .[161] A schematic diagram of the proposed concept is presented in Figure 7A. The loading process of PO_4^- was conducted in two stages, the first stage was based on attachment of Fe^{+3} ions with carboxylic groups present at the edges of GO sheets to form a GO-Fe composite. The second stage was attachment of phosphate ions onto the positively charged GO-Fe composite. The amount of P loaded onto the GO-Fe composite was 48 mg g^{-1} and the release pattern of P from the final product was very slow compared to commercial monoammonuim phosphate (MAP) fertilizer in both water and soil (Figure 7B and C), which could provide useful slow release properties in soils prone to P leaching or surface runoff. However, one disadvantage of the GO-Fe-P composite was its relatively low P content (~5%) compared to commercial P fertilizers, which usually contain 10 to 20% P and this poses limitations for commercial use due to increased transport and application costs. Similar results were reported by others regarding the limitations in loading of P onto carriers such as layered double hydroxides.[177, 178] Therefore, future work needs to focus on increasing the P loading to minimize transport and feeding costs. In this context, Andelkovic et al. increased the loading of P to 15% on a GO-Fe composite, which is comparable to the P percentage of commercial products. The enhancement in the loading capacity of P was simply achieved by increasing the initial concentration of GO from 0.1 mg/ml to 10 mg/ml during the attachment of Fe^{+3} ions which enabled the interaction of Fe^{+3} ions with alkoxide and hydroxyl functional groups present in the basal plane of GO and intercalation of Fe^{+3} ions on aggregated GO sheets. The GN-Fe-P composites contained similar content of P as commercial products but release was slower than commercial MAP.

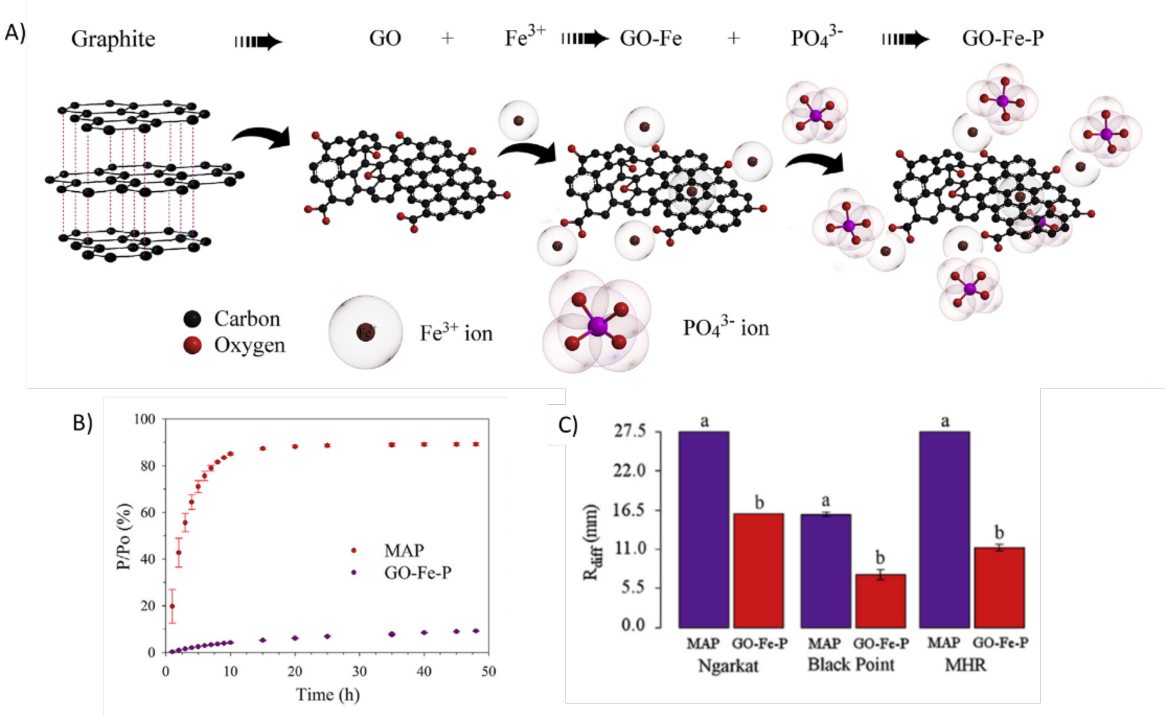

Figure 7. (A) Schematic diagram of the synthesis procedure of the GO-Fe-P composite, kinetics of P release from MAP granules and GO-Fe-P pellets in columns: (B) solution concentrations of P released over time and (C) radius of visualization at 56 d after addition of MAP or GO-Fe-P granules to the soil. Adapted with permission from.[161]

4.2.GN-based materials as pesticide carriers

The indiscriminate use of pesticides along with complications in controlling pests have been the subjects of intense debate and discussion in agriculture over the last few decades.[1] Pesticides including insecticides, herbicides and fungicides are commonly used in the form of powders, suspensions and emulsions and regularly do not guarantee targeted delivery of compounds, which leads to serious environmental issues due to degradation, volatilization and leaching to the biosphere.[179,180] Recently, novel pesticide formulations with prolonged and better control of drug release are appearing and slow-release formulations which significantly decrease the amount of leached pesticide and surface migration have been the focus of research into pesticide delivery systems.[181] There are several reports of encapsulating different agrochemicals by polymeric NPs for slow-release purposes.[182] Wang and co-workers applied nanosized inorganic particles such as TiO_2, SiO_2, Fe_2O_3 or Al_2O_3 as a vehicle for pesticide delivery to increase the bioactivity and reduce environmental drawbacks.[183] However, a pesticide nanocarrier is expected to efficiently bind to both the pesticide and to the plant so that it can release the active ingredient successfully and be able to gradually reduce the volume of pesticide used.[140]

Recent studies have shown the efficiency of GN-based materials in adsorbing different pesticides from the environment showing their potential to be used for pesticide delivery.[184, 185] Graphene oxide and rGO have been applied for the adsorption of different pesticides such as malathion (ML), endosulfan (ES) and chlopyrifos (CP) from aquatic environments.[185] They have representative strong adsorption capacity of 1200, 1100, and 800 mg g^{-1} for CP, ES and ML, respectively, higher than any material investigated previously. The observed removal capacity of GN-based materials toward those pesticides was related to the formed electrostatic interactions between GN and the pesticide species and subsequent precipitation in aqueous solution. High specificity of GN-based materials to sorb pesticide species with their insensitivity to pH change, in addition to their antibacterial properties, makes them very attractive for pesticide removal compared to other carbon-based materials.[185] Liu and co-workers developed GN-composites made of GN-coated silica for the removal of eleven organo-phosphate pesticides with a removal efficiencies of more than 95% for nine of them.[186] The new composite materials performed greater than silica, graphite, C18 silica, activated carbon and rGO. The adsorption mechanism was based on the π-bonding network between the benzene rings of GN and electron-donating atoms such as N, S and P within the pesticide formulation and hydrogen bonding, in addition to π-π and hydrophobic interactions.[186] Therefore, GN-based materials, owing to their high specific surface area and tailorable surface chemistry have the potential to adsorb and carry pesticides at levels much higher than observed with other carbon-based materials.

At present there are two reports available regarding the application of GN-based materials as a delivery matrix for pesticides in agriculture. A recent study by Sharma and co-workers revealed the targeted pesticide delivery of nano-sticker copper selenate NPs anchored on GO sheets (GO@Cu_{2-x}-Se).[140] The advanced GO@Cu_{2-x}-Se pesticide carrier was able to release the active ingredient due to a pH change in the insect gut and to hydrophobic carriers in the hemolymph environment. They supposed that the combination of GO and $Cu_{2-x}Se$ may also help pesticide delivery due to photothermal stimulation, while Cu and Se are plant micronutrient. These same researchers also performed biological studies on cauliflower plants infested with *Pieris rapae* to estimate the feasibility to deliver the pesticide chlorpyrifos with an enhancement of >35% of larval mortality. Furthermore, they estimated that for a 1 ha cauliflower crop, 2.5 g of GO@Cu_{2-x}-Se may be sufficient for successful treatment, showing that smaller quantities can cover a larger crop surface area (Figure 8 A-C).[140] Tong and co-workers described the use of polydopamine (PDA)-coated GO sheets for controlled release and pesticide-loss control to solve the low-utilization and wash-off problems of water soluble pesticides.[162] The results demonstrated that PDA-GO had a high pesticide (hymexazol) loading capacity with pH-dependent and (near infra-red) NIR-laser-dependent release property (Figure 8 D-F). The adhesion-performance investigation of PDA-GO loaded hymexazol revealed that hymexazol persistence was much higher after successive rainfall compared to hymexazol by itself (Figure 8 G). The bioactivity experiments conducted against *Fusarium oxysporum f. sp. cucumebrium* Owen showed an inhibition activity similar to that of hymexazol solution.[162] There is therefore an obvious opportunity for the application of GN-based materials in pesticide delivery.[140]

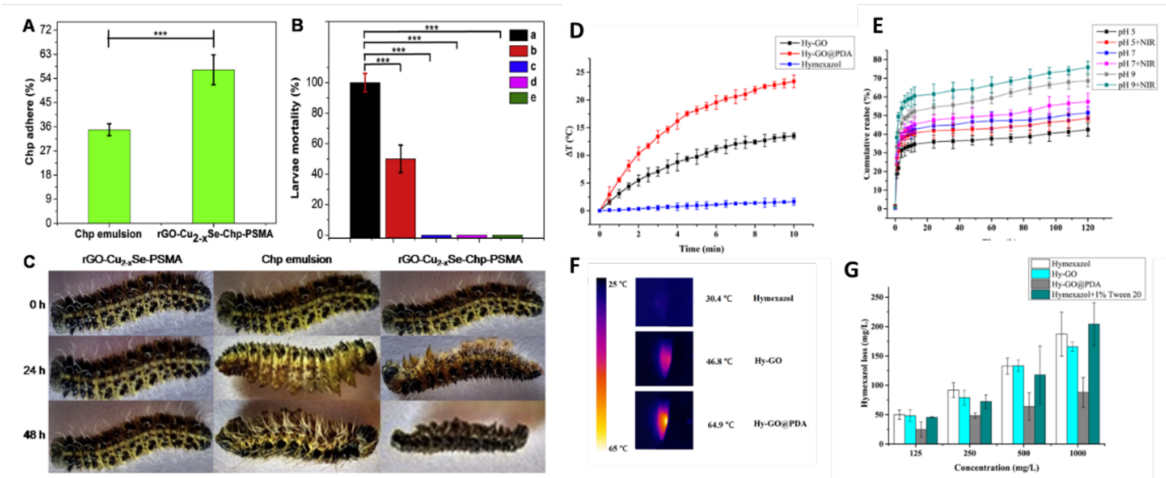

Figure 8. Efficiency of rGO-Cu$_{2-x}$Se-chp-PSMA in resistance to runoff and pest mortality in comparison to chlorpyrifos emulsion. A) percent chlorpyrifos adhered on leaf, sprayed in the form of rGO-Cu$_{2-x}$Se-chp-PSMA and chlorpyrifos emulsion. B) mortality of the pest (percentage) after 72 h of the leaf being sprayed with 10 μg of chlorpyrifos in the treatment forms followed by simulated rain washing (material toxicity is negated by maintaining material control), a) rGO-Cu$_{2-x}$Se-chp-PSMA, b) Chp emulsion, c) rGO-Cu$_{2-x}$Se-PSMA, d) Cu$_{2-x}$Se, e) GO, C) photograph of *P. rapae* larvae before and after (24 and 48 h) feeding the respective treatments, D) temperature-variation curves of the aqueous dispersions of hymexazol, Hy-GO, and Hy-GO@PDA exposed to an 808 nm laser, E) temperature-variation curves of the Hy-GO@PDA dispersion at different concentrations, F) IR thermal images of the hymexazol, Hy-GO, and Hy-GO@PDA solutions under continuous NIR-laser irradiation and G) amount of hymexazol loss in the hymexazol solution, Hy-GO solution, Hy-GO@PDA solution, and hymexazol solution with 1% Tween 20. Adapted with permission from.[140,162]

Due to the fungicidal properties of carbon-based materials, GN and it derivatives are also promising materials for the development of novel fungicides. It was found that anti-microbial activity of GO was the highest toward *P. aeruginosa* compared to rGO under similar conditions.[187] The antibacterial property of both GO and rGO was dose-dependent and related to the generation of reactive oxygen species, leading to cell death. Different studies have revealed that the anti-microbial property of GN-based materials was due to damage to cell membranes and disruption of lipid membranes through the extraction of phospholipids,[188] electron transport[189] and increased production of reactive oxygen species.[190,191] The anti-bacterial effect of GN-based materials has been reviewed by others in detail.[192]

While the majority of published research has reported the anti-microbial property of GN-based materials, some bacterial species were found to live in the presence of GN materials with no inhibition of bacterial growth.[193] *E. coli* bacteria were able to grow faster and develop denser biofilms when attached to GO sheets compared to cultures prepared without it, indicating that GO enhanced bacterial proliferation.[194] Also, other gram-negative bacteria have been more resistant to cell membrane damage compared to gram-positive bacteria by graphene sheets, which is due to the presence of the outer membrane layer in the structure of gram-negative organisms.[195] It has been stated that the possible contaminants retained from the GO preparation or application of high GO concentrations might be responsible for antibacterial effect of GO observed in previous reports.[194]

4.3.GN-based materials with potential application for delivery of genetic material for plant transformation

Gene therapy is a method that treats a genetic disease by using genes, and this method has resulted in considerable research.[40] Common methods of gene transfer in plants are *Agrobacterium*-mediated transformation,[196] electroporation, polyethylene glycol-mediated gene transfer, bombardment-mediated gene delivery[197] etc., all of which are expensive and labour intensive, as well as causes significant perturbation to cell growth (0.01-20%) and efficency.[1] Different nanomaterials have shown improvement of gene delivery due to their significant advantages in comparison to conventional and traditional gene delivery strategies. Nanomaterials are applicable to both monocotyledonous and dicotyledonous plants as they can overcome transgenic silencing (refers to the molecular process preventing the expression of a specific genes) by modifying the DNA copies. In addition, NPs can act as a multifunctional system for the delivery of plant genes as their surface can be easily functionalized to enhance their efficiency to carry multiple genes without involving traditional methods that require complex carriers.[1] GN-based materials have been used as an appropriate candidate for gene delivery due to their high loading capacity, tailorable surface chemistry and increased gene transfection. [40]

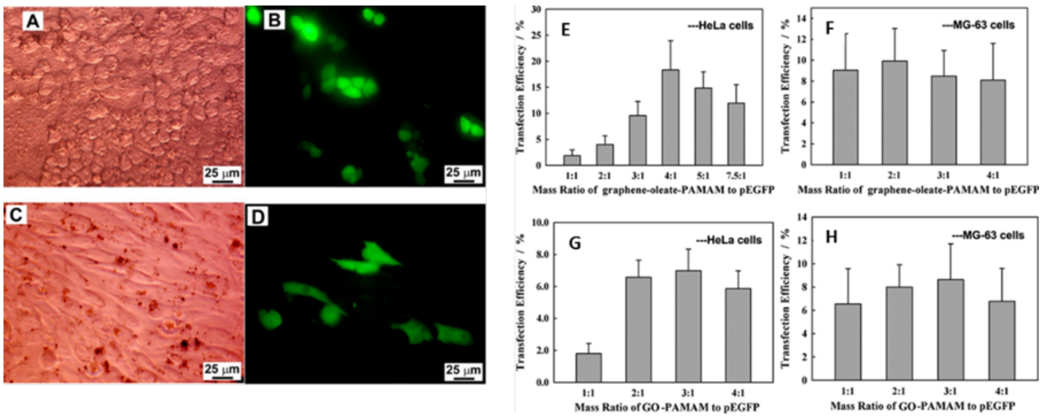

Figure 9. Bright-field (A,C) and fluorescence (B,D) images of HeLa (A,B), MG-63 (C,D) cells successfully transfected with GFP gene by using the graphene-oleate-PAMAM hybrids, and GFP transfection efficiency of graphene-oleate-PAMAM (E,F) GO-PAMAM (G,H) to HeLa, and (E,G) MG-63 (F,H) cells at different mass ratio Adapted with permission.[200]

To date, GN-based materials have been extensively used as gene transformers, and to decrease their toxicity towards different cells and to obtain a positively charged surface for proper electrostatic interaction with anionic oligonucleotides different surface modifications were employed using polymers such as chitosan[198], polyethyleneimine (PEI)[199] and polyamidoamine (PAMAM).[200] PAMAM functionalized GN with oleic acid had good biocompatibility and improved gene transfection efficiency, up to 13 times than ultrasonicated GN (Figure 9 A-H)[200] PEI-functionalized GO has been used for siRNA (short interfering RNA) and gene delivery showing significantly low toxicity with high transfection efficiency.[107,201] Targeted delivery of DNA with chitosan-functionalized GO and a high loading capacity of 4 mmol/g to human hepatic carcinoma cells was successful in less than 0.5 h and no obvious cytotoxicity was observed even at a concentration of 100 mg/m.[202] Further details and examples regarding the application of GN-based materials in gene delivery to human cells can be found in other review papers.[26,40] GN-based materials have also been applied for gene therapy and intramolecular protein vaccine delivery.[203, 204] Some reports are available for DNA-delivery to plant cells using different nanomaterials such as ZnO, silica and chitosan nanoparticles, indicating that new nutrient delivery systems can be developed by using different nanomaterials, therefore, GN-based materials with nanometre size can by exploited for this purpose.[1]

5. GN-based materials as coatings to slow down the release of nutrients

A coating can be defined as a layered cover for the surface of a bulk material to achieve specific properties. The major goal of the surface and bulk material coating is to protect against corrosion, fouling, mechanical abrasion, microorganisms and environmental damage.[27] The combination of the unique 2D structure and chemical properties of GN-based materials makes them an excellent platform for different types of coatings. A wide variety of coating methods can be applied by using GN–based materials. This includes CVD,[205,206] electrophoretic deposition,[207,208] powder spray including electrostatic powder coating and plasma spray coating,[27,209] solution spray,[210] dip coating,[211] spin coating[212] and brushing[213] to coat different surfaces. The application of GN-based materials for protective coatings has been reviewed extensively elsewhere,[27] thus only a selection of some of these applications will be briefly explained here.

Graphene-based materials have been used as a barrier coating to protect different substrates against corrosion due to their impermeable 2D structure, which provides a barrier to reactive gases, liquids, acids and salts.[214] Pioneering work on the use of one layer of GN as a corrosive barrier applied by CVD was reported by Chen and co-workers to protect copper surfaces from corrosion.[205] Despite having good corrosion barrier properties in the short term, CVD-grown GN showed an existence of wrinkled sheets and some defects arising from the synthesis and transfer process, allowed oxidation of the metal which was later solved by depositing multi layers of GN on the surface.[27] Other facile routes such as electrochemical deposition (ED) were also used. In one case, a layer-by-layer deposition of a polymer-GN was used to protect different surfaces.[215,216] The GN-polymer coating showed >94.3% corrosion resistance in a silane environment using an ED deposition method. Wang and co-workers reported GN as flame retardant additive to a polymer matrix which showed a delay in the oxidation of the material.[217] In addition to the barrier coating, GN-based materials have been extensively used as wear and scratch resistance, antifouling, pollutant adsorption and antiseptic coating for many different purposes, the details of which have been discussed in other reports.[27]

To improve fertilizer efficiency and protect the environment, there has been increasing research towards developing new technologies to cover common fertilizers with physical barriers that can control or slow down their release of nutrients.[38, 218] Past efforts developing slow- or controlled-released fertilizers focused on employing polymers or inorganic materials such as sulphur and other minerals as coatings. However, most of these coating techniques utilize organic solvents or hazardous monomers, which not only increase the cost of production, but also led to further environmental issues.[38] One early study on GN-based materials as a barrier coating for fertilizer granules was reported by Zhang et al. where the encapsulation of potassium nitrate (KNO_3) pellets by a rGO barrier film was shown to delay nutrient release.[218] Dip coating of pellets in the GO solution and the subsequent heating to 90 °C provided a film of rGO due to the reduction of GO with K ions. Furthermore, K ions acted as a ‘‘glue” and soldered adjacent GN sheets making a shell around the pellets to create a shell and prevent the fast release of nutrients. Unfortunately, most thermally reduced GO materials are particularly brittle and suffer from structural defects which results in surplus water permeation.[214] Therefore, in a recently published study, a film of an environmentally friendly polymer and GO membrane was used to coat KNO_3 granules in a sandwich-like structure (Figure 10 A and B).[145] The existence of the GO membrane provided a longer diffusion path for the hydrated K^+ and NO_3^- and hence a slower diffusion rate for hydrated K^+ due to the cation-π interactions between K^+ and GO. As a result, the nutrient release of the film-coated KNO_3 fertilizer was prolonged. The release duration for using only the pure polymer as a coating was 24 days while it was extended to 26, 29, 34 and 38 days for a polymer/GO composite films when the amounts of GO in the coating were 0.18%, 0.72%, 1.43% and 2.86%, respectively (Figure 10 C).[145] Hence, GN-based materials offer great opportunities to improve the slow-release characteristics of fertilizers, particularly if both GN or GO can be produced in large scale, with green methods, at reasonably low cost.[218]

The use of pristine GN as coating material is often limited due to its poor dispersability in water and organic solvents.[42] A dispersant-free coating approach was considered on urea granules utilising a rotary drum and the electrostatic deposition of pristine GN which occurs due to the solid lubricity property of GN and the interlayer electrostatic interaction of GN sheets. [209] The GN coating was used to enhance the mechanical properties of the urea granules and not for nutrient release purposes. The results showed that a thin layer (~2.4 µm) of pristine GN coating (Figure D-L) minimized the moisture-induced caking tendency of commercial urea granules and exhibited better moisture rejection ability at a relative humidity (RH) of 85%, two times higher than uncoated urea in addition to an improvement in their anti-abrasive properties (Figure M and N).

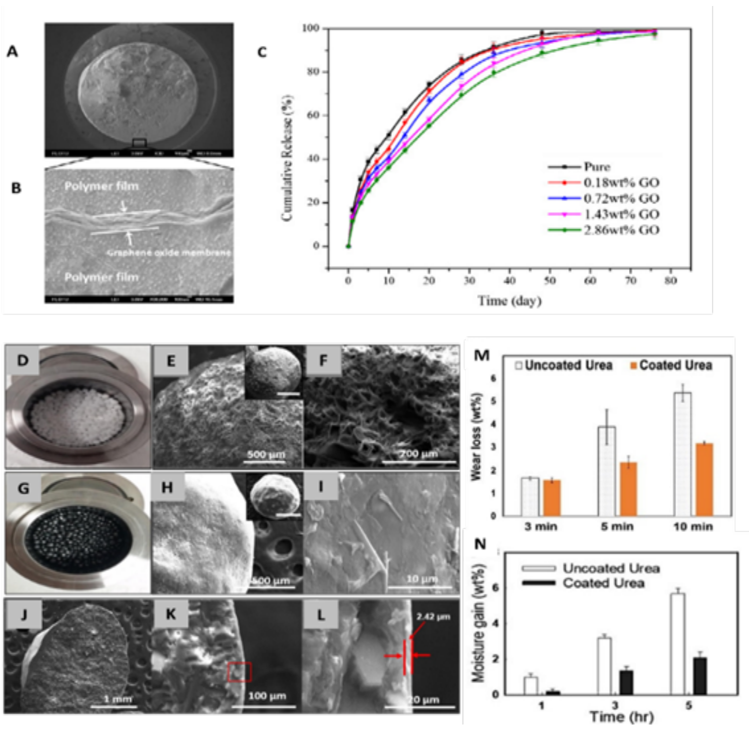

Figure 10. (A and B) Cross-sectional morphology of the polymer composite film coated on KNO_3 granules with spraying 1.75% GO and (C) cumulative release curves of KNO_3 granules coated with polymer composites containing different % of GO, (D-F) photo and SEM images of urea fertilizer, (G-L) photo and SEM images of urea fertilizer coated with pristine graphene, (M) wear loss and (N) moisture adsorption of coated and uncoated urea. Adapted with permission. [145,209]

6. GN-based materials as reinforcement to enhance fertilizer physical properties

Reinforcement materials contain distinctive physical and chemical properties. They can be particles, layered materials, fibres or clusters embedded in a wide variety of polymers, metal matrices, cement or other composites.[219-221] However, most micron-sized traditional reinforcement materials require high loadings to enhance the mechanical properties of the final product, which increases the price and leads to heavier composites, especially in the case of polymers. Furthermore, the lack of interfacial interaction between the filler and frame material are other drawbacks of traditional reinforcement materials, which results in a failure of the final product due to weak interfacial adhesion.[222] Recently, many studies have focused on newly produced nanomaterials, especially carbon nanotubes (CNTs), GN and GO sheets, as reinforcement materials for different composites.[147, 221, 223, 224] Although CNTs are considered to be excellent reinforcement materials due to their high aspect ratio, high tensile strength and conductivity etc., they suffer from high agglomeration and insufficient dispersion in the composite matrix due to their lack of surface chemistry, and cost-intensive instruments are needed to synthesis them.[223,225] GN-based materials have been extensively used as reinforcement materials to enhance the mechanical properties of different composites, including cement and polymers due to its high Young's modulus of 1 TPa and yield strength of 130 GPa.[56, 226] In addition, 2D GN sheets are flexible with a very high theoretical specific surface area (2630 m^2/g) that enhances the interfacial interaction between them and the added composites, which makes them a favourable candidate to be used as a replacement for traditional reinforcements.[221, 226, 227]

One of the critical parameters in market selection of any fertilizer apart from its nutrient content is its physical quality.[228, 229] Therefore, fertilizer granules are required to have sufficient mechanical hardness to withstand routine handling in transport and spreading.[230] The hardness of fertilizer granules can be characterized by measuring crushing strength, abrasion and impact resistance.[152] Also granular fertilizers should have appropriate mechanical strength to resist significant fracturing and creation of excessive dust during the handling and storage process to meet the needs of the market.[231] However, most fertilizers produced by different techniques such as granulation, prilling or compaction suffer from having irregular protrusions on their surface which finally leads to substantial quantities of dust being created during their handling and spreading in the farm.[229, 232] This airborne dust leads to negative environmental effects and increased costs for both fertilizer producers and users due to the loss of nutrients.[152] To overcome these considerable drawbacks, different hardening additives such as calcium oxide, calcium hydroxide, cement and fly ash have been used to improve the physical properties of granular fertilizers and reduce their propensity for dust generation.[233,234] For example, formaldehyde or low concentrations of lignosulfonate have been used to supress dust generation from urea fertilizers.[233, 235, 236] Gelling-type clays, such as attapulgite or sepiolite, and binders such as melamine have also been utilized to increase the hardness of urea fertilizers.[152]

In one recent study by the authors, different percentages of GN and GO ranging from 0.05 to 0.5 wt % were co-granulated with monoammonium phosphate (MAP).[152] Scanning electron microscopy characterization showed the inclusion of GN/GO sheets in MAP granules (Figure 11A). The results of this study showed that co-granulation with 0.5% w/w GN sheets (MAP-GN) significantly enhanced the mechanical strength of MAP granules (~18 times improvement) while inclusion of the same amounts of GO sheets (MAP-GO) improved the strength to a lesser extent (~8 times improvement) (Figure 11B). Graphene also increased the resistance to abrasion of the MAP granules (>70%) and improved impact resistance (>75%). Interestingly, heating MAP-GO after granulation enhanced the physical properties of MAP-GO in comparison to granules dried under ambient temperatures. The inclusion of GN in MAP granules not only enhanced the physical properties of granules but decreased slightly release of P in soil (Figure 11C). The advantages of GN and GO sheets compared with current additives in enhancing the physical properties of MAP granules were explained by their high specific area, advanced mechanical properties and their 2D geometry. These results confirm the potential of GN/GO additives to enhance the physical properties of MAP granules that could be translated to other fertilizers and applied by industry.

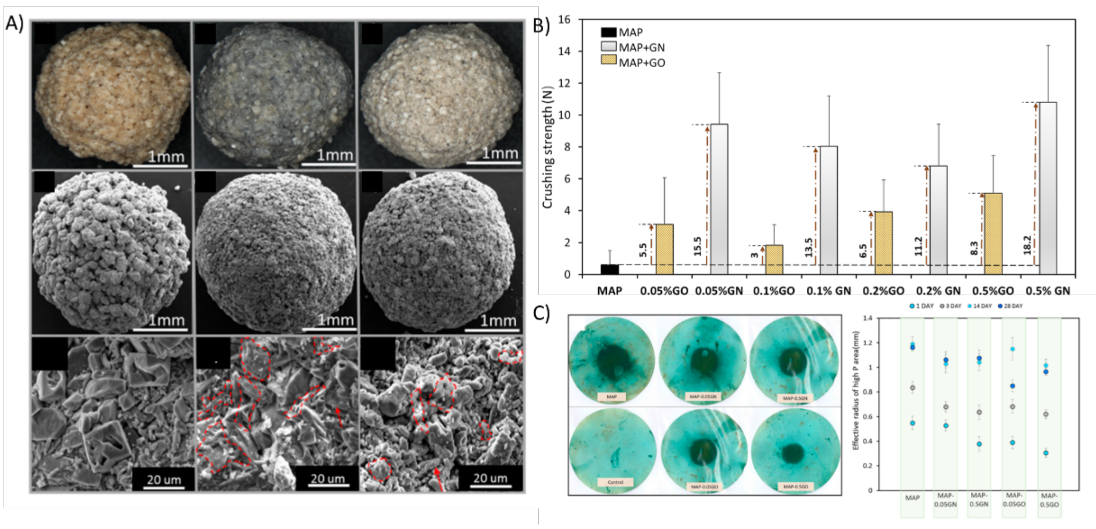

Figure 11. (A) Crushing strength of monoammonium phosphate (MAP) (control) and MAP with different concentrations (0.05 to 0.5%) of graphene (GN) and graphene oxide (GO), (B-K) low and high resolution SEM images of top surface of MAP and MAP with GN from 0.05 to 0.5%. Adapted with permission from [152]

Another study by the authors investigated the influence of (GN) concentration on the crushing strength of two fertilizers – MAP and diammonium phosphate (DAP) to find an optimum concentration for GN-based additives in fertilizer granules. Furthermore, the effect of different GN physiochemical properties such as method of preparation, particle size, specific surface area and surface functionalization on the crushing strength on both fertilizer granules was investigated. The results showed considerable concentration dependence, with optimum concentrations of 0.5% GN for MAP and 0.05% for DAP, increasing the crushing strength of MAP and DAP granules by 1680 % and 67.3%, respectively. Beyond this point their crushing strength was decreased. Furthermore, GN samples with a higher degree of reduction and higher specific surface area were more effective than others on enhancing the crushing strength of granules. Furthermore, GN samples functionalized with iron nanoparticles enhanced the physical properties of co-granulated fertilizers.

7. GN-based sensors for applications in agriculture

In the past few years, there has been a huge improvement in the production and structure of sensors and biosensors due to the incorporation of various nanomaterials such as nanowires based on metal oxides, semiconductors made of silicon, indium or gallium, quantum dots based on different cadmium derivatives, CNTs and different metal nanoparticles due to their conductivity and relative biocompatibility. Carbon-based nanomaterials such as CNTs and GN and its derivatives have dominated scientific interest in fabrication of sensors and biosensors due to their unique properties.[237, 238] Development of novel technologies based on CNTs which can be successfully used for rapid, high sensitivity and easy sensing of targeted chemicals are well documented in different studies.[238, 239] The atomic thickness of GN and its extremely high specific surface area makes it very sensitive to changes in local environmental conditions due to the direct interaction of all carbon atoms with analytes, a property that is very important in the fabrication of improved electrochemical sensors and biosensors.[240, 241] The main advantages of GN over CNTs in applications for sensing and biosensing approaches are its low production cost from graphite and the fact that it does not contain any metal impurities like CNTs, which often restricts that material's electrochemistry.[241] In addition, the tailorable surface chemistry, easy attachment of the biomolecules by π-π stacking and hydrophobic interaction, solution-processing ability, biocompatibility and lower noise ratio are advantages of GN-based material over other materials.[237] In the last few years a large number of GN-based material sensors have been applied in different areas such as clinical analysis, medical diagnostics, environmental monitoring and food sensing. The majority of sensors used for these applications are operated based on the transduction principle, but some optical and piezo-electric sensors have also been produced.[237] The analytical performance of sensors has been evaluated based on sensitivity and selectivity, detection limit, and repeatability and reproducibly, which are essential to validate an analytical method and ensure the quality of results.[242]

In agricultural science, online and accurate sensing opens up opportunities for sensing in many different areas including *in situ* analysis of pollutants such as the presence of metal ions, pesticide and herbicide residue in crops and in the environment (soil and water), detection and identification of infectious diseases in crops, and online measurements of important food processing parameters such as bacteriological contamination and food safety control. The analysis of heavy metal ions and pesticide residues in the environment is important due to the high toxicity and serious risk to human health of many metals and pesticides.[243] Heavy metal ions including cadmium (Cd), lead (Pb) and Zn have been detected by sensors based on functionalized GN.[244-246] A GN-based sensor was used to detect Cd in water, which represented the working efficiency at a Cd concentration level of 0.25 µg/l.[247] A sensitive and disposable sensing platform for trace analysis of Cd and Pb was also developed using a GN-modified composite film with a detection limit of 0.042 and 0.089 µg/l for Cd and Pb, respectively.[244] Graphene oxide based electrochemical sensors were used to detect Hg with gold-nanostructured sensors with a detection limit of 1.9 µg/l which is lower than the current WHO guidelines (6 µg/l) and GO-ionic liquid/gold NPs composites with a detection limit of 0.006 µg/L.[237,248,249] The GO-ionic liquid/gold NPs composite sensor was reusable with relative standard deviation of 2.6% by immersing it in a solution of nitric acid (HNO_3), potassium chloride (KCl) and EDTA.[249] A carbon dot-labelled oligodeoxyribonucleotide and GO fluorescence biosensor was also applied for Hg detection with a higher limit of detection than other electrochemical sensors reported so far. The feasibility of the sensor for detection of Hg was also examined by determining Hg in standard citrus leaf samples, which demonstrated an agreement between the results obtained by the reference method and the sensor.[250]

Organophosphate pesticides (OPs) cause neurotoxicity due to their ability to inhibit cholinesterase and long term exposure can lead to disruption of the endocrine systems in organisms. Unfortunately, many pesticides used in agriculture can transform into much more toxic products due to physical, chemical and biological processes.[251,252] A photoelectrochemical nanocomposite biosensor was applied to detect OPs using CdSe/ZnS quantum dots and GN deposited on a ITO-coated glass electrode, showing high sensitivity towards OPs, good reproducibility and ideal stability.[253] The efficiency of the sensor was mainly attributed to the ability of GN in efficient separation of the photogenerated carriers and consequent hindering of the recombination of electrons and holes in the QDs.[253] The photoelectrochemical sensors also performed a rapid, sensitive and selective detection of 4-aminophenol with a low detection limit of 2.3×10^{-8} M and excellent reproducibility.[254] Another electrochemical sensor was fabricated by immobilization of acetylcholinesterase on NiO NPs/carboxylic GN/Nafion-modified glass carbon electrodes for the detection of methyl parathion, chlorpyrifos, and carbofuran pesticides.[255] The biosensor showed acceptable stability after a month storage period, retaining 91% of its initial electrochemical response and recoveries in the range of 93.0–105.2% were observed after applying it to real samples such as tap and lake water.[255]

Recently, flexible microscale sensors made of GN-NPs was fabricated using a versatile, simple and inexpensive method by drop-casting GN film onto a pre-patterned polydimethylsiloxane (PDMS) surface containing negative features and subsequent transfer of this pattern onto a target tape.[256] This method was effective for producing GN-based nanomaterial micro-patterns on different types of adhesive tape. The GN-based sensor was used to estimate the required time for water to move from the plant roots to the upper and lower leaves by monitoring water vapour escaping from the leaves and changes in the local humidity (RH) level of the leaf surface (Figure 12 A-D). The structured RH sensors made on polyimide tape were installed on the back surface of the fourth and ninth leaf of two-month old maize plants (labelled B73) and another type of plant with a mixed genetic stock. The sensing mechanism was based on changes in the electrical resistance of GN in different moisture environments. A resistance increment was observed for the lower and upper sensors of B73 at 55 and 13 min, respectively after irrigation. Similarly, a resistance increment was reported at 82 and 110 min for the lower and upper sensors respectively for the mixed genetic stock. This pioneering research indicates there is a huge advantage of using on-leaf tape sensor technology to allow selection of plants with desirable water transport characteristics or improved tolerance to water stress, which is a major objective of crop breeding.[256]

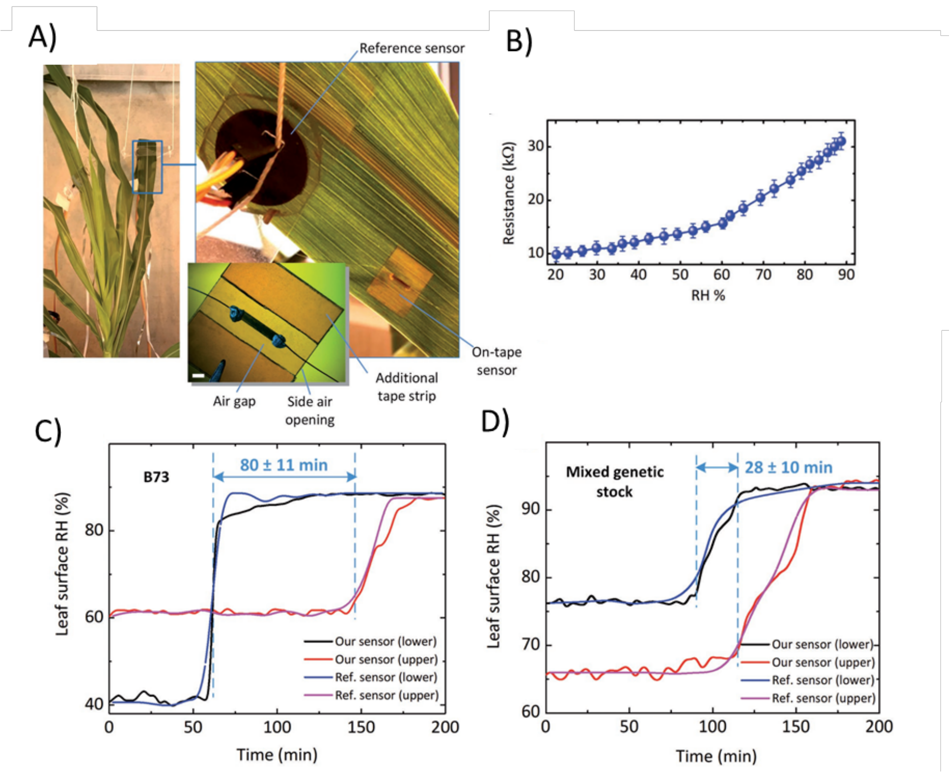

Figure 12. A) A photo of the GN-based RH sensor and a commercial RH sensor placed at the back of the maize leaf, B) resistance of the graphene sensor as a function of RH, and real-time monitoring of the RH level on the leaf surface after plant irrigation at two maize plants: C) B73 and D) a mixed genetic stock. Adapted with permission.[256]

Graphene-based materials can also be used for real time sensing of toxic gases for remote sensing of plant diseases by placing them onto local insects or plants similar to CNT-graphite sensors.[257] Furthermore, applying sensors to different locations can give a full picture of the spatial distribution of disease severity at a field-scale, which can assist detection of hot spots and allow for targeted treatment application, which will significantly reduce the adverse environmental and economic effects of agrochemicals.[164] The first attempt to apply GN-based materials as gas sensors was reported by Schedin et al.,[155] who applied pristine GN obtained from the mechanical cleavage of graphite. The pristine GN was supported on a Si wafer using a lithography method. High sensitivity of the prepared sensor for detection of individual NO_2 molecules was related to the high specific surface area of pristine GN combined with its greater carrier mobility and low intrinsic electric noise.[155] Indeed, this work by Schedin et al.[25] was motivation and a catalyst for further research regarding the electrochemical potential of GN-based materials for sensing applications.[25] Additional information regarding the application of GN-based materials sensors for gas detection are summarized in Table 2.

Table 2. Summary of different types of GN-based sensors used for sensing gases.

Gas detected	Sensor type or fabrication	Sensing material	Detection limit	Ref
NO_2	Electron-beam lithography	Pristine GN	Single NO_2 molecules	155
CO, O_2 and NO_2	GN deposited on sensor chip	Pristine GN film and ribbons	Signals of 3 and 35 for 100 ppm of CO and NO_2 , respectively	258
NO_2	Casting rGO on gold electrodes by lithography using Si wafers	rGO	at 100 ppm NO_2 sensitivity of 1.56	259
NH_3 and NO_2	gold electrodes prepared by lithography	rGO-SnO_2 nanocomposites	1 ppm for NO_2	260
NH_3 ,CH_4 and H_2	gold electrodes prepared by lithography	CVD grown GN	very sensitive to NH_3 in the mixture of NH_3 and CH_4 regardless of the excess of CH_4 in the mixture	261

H_2	gold electrodes prepared by lithography	GN-PANI	sensitivity of16.57% toward 1% of H_2 gas,	262
NH_3	GN deposited on electrode by syringe	rGO-PANI		263
NH_3 , NO_2 and DNT	Single layer rGO deposited on the gold electrode	rGO		264
NH_3	Piezoelectric sensor	GO		265
CH_4	Optical sensor	rGO-CNT-PMMA		266

LOD, PANI, PMMA: poly (methylmethacrylate): CNT: carbon nanotube;

8. Toxicity of GN based materials to plant life

From the rapid expansion in the production of GN-based materials and nanomaterials, it is essential to study the potential risk associated with the exposure of these materials in different environments to ensure safe application.[27] Gaining knowledge about nanomaterial and plant interactions is not only important for ecological risk assessment but may also promote their application in agriculture.[164] Phytotoxicology of engineered nanomaterials is quite a new field of research and the potential toxicity of NPs, especially GN-based materials on plants, has not yet been widely investigated.[164] There is some controversy over the toxic potential of GN-based materials with reports suggesting there are potential safety issues related to their use.

A large number of *in vitro* and *in vivo* toxicity assessment of GN-based materials against bacteria, mammalian cells, and animal models are found to adversely affect growth and/or function depending on the dose, exposure time and morphology (shape and composition), etc., but surface modifications can significantly reduce toxicity.[267] Most findings have suggested designing GN-based materials with low toxicity for biomedical applications.[26, 268] On the other hand, progressive studies have reported the application of GN-based materials in drug delivery, gene delivery, cancer therapy, and as scaffolds for cell culture.[26] To this date, GN and GO have not revealed significant *in vitro* toxicity to a number of human cell lines, including Raji, HCT-116, Hela-A549, OVCAR-3, U87MG, MDA-MB-435 and MCF-7, even by exposing them to high doses up to 100 mg/ml. However, the dose and size of GN-based materials should be considered as the toxicity of GN is highly dose- and size-dependent.[267]

The interaction of CNTs with plants has been studied in more depth than GN-based materials. The physiological changes due to the interaction with CNTs mostly involve changes of gene expression, [269,270] DNA damage [271,272] and increased formation of reactive oxygen speciose (ROS).[273,274] However, the response of the plant to CNTs appears to be variable depending on the plant species, [275, 276] and stages of plant ontogenesis and variety.[277-279] Similar to CNTs, uptake into seeds and seedlings, plant growth stimulation at low concentrations and growth inhibition at high concentrations has been also demonstrated for graphene. However, there are few studies on the toxic effects of different GN-based materials on plants and, similarly to what has been reported for human and animal species, controversy on whether or not these materials are actually safe or not.

The effect of GN on the germination and growth of rice seeds was investigated in a study where seeds were treated with different concentrations of GN.[280] Germination rate was obviously delayed with the increase of GN concentration up to 200 mg/l and the growth of radical and plumula was inhibited, in addition to the changes in the morphology of the rice seeds. However, after treating with 5 mg/l of GN for 16 days, promising effects on adventitious root number, and fresh weight of root and sprout were observed, pointing out that a low concentration of GN improved some plant growth indices. Another study investigated the phytotoxicity of GN and its effect on root and shoot growth, biomass, shape, cell death, and reactive oxygen species (ROS) of cabbage, tomato, red spinach, and lettuce by incubating seedlings in a GN concentration from 500 to 2000 mg/l for a time period of 20 days (Figure 13 A-F).[281] The results showed significant inhibition of plant growth and biomass production with a reduction in the number and size of leaves with a concentration dependent manner. Root growth inhibition was found at 2000 mg/l concentration at different ranges (~18 to 78%) depending on the plant species. Treatments of seeds with GN at concentrations above 500 mg/l led to the production of ROS that further led to necrosis, loss of plasma membrane integrity, and eventual cell death. However, lettuce did not exhibit similar toxicity to GN at similar treatment concentrations indicating the phytotoxicity of GN was dependent on plant species. Furthermore, the results highlight the effect of concentration and exposure time on the phytotoxicity of GN towards plants. Exposure of plants in hydroponic culture however is very different to exposure in soil, where in soil GN or GO are likely to heterocoagulate, similar to CNTs, with soil colloids which would vastly reduce potential toxicity.[282]

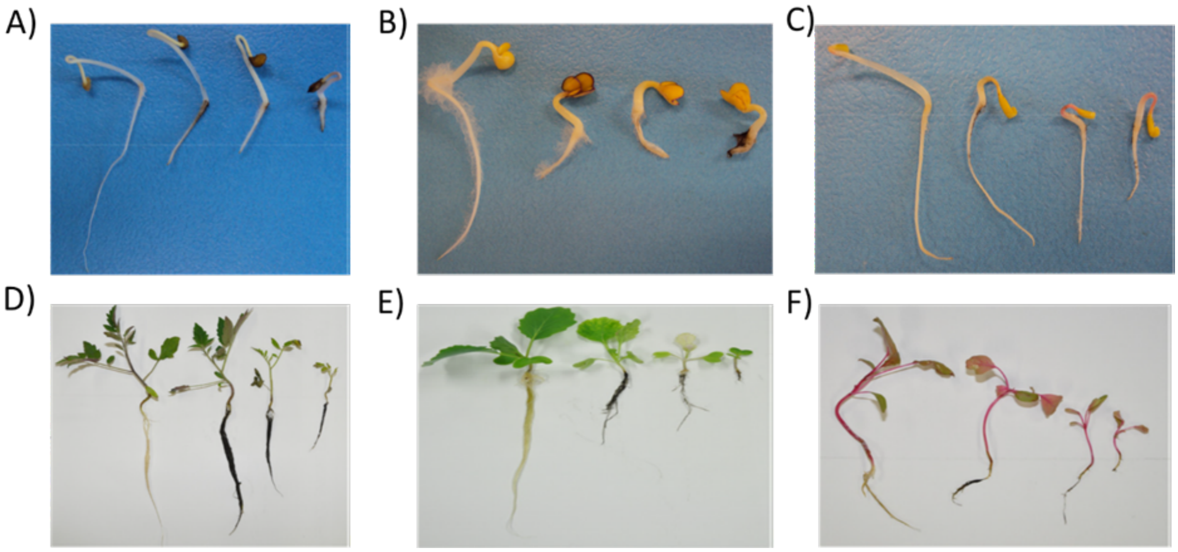

Figure 13. Effect of GN on cotyledons and root systems of (A-C) tomato, cabbage, and red spinach seeds, respectively, and effect of GN on growth and development of (D-F) cabbage, tomato, and red spinach seedlings which were hydroponically grown in Hoagland media for 20 days with and without graphene, respectively. Adapted with permission.[281]

The toxicity of several carbon nanomaterials (activated carbon, GN, single- and multi-walled carbon nanotubes) at a concentration of 50 μg/ml was investigated using germination of tomato seedlings in a growth medium containing mixed Murashige and Skoog (MS).[283] Graphene induced the lowest activation of stress related to the *LeAqp2* gene compared to the all other carbon-based material that were tested. The results of photothermal and photoacoustic imaging showed no effect of GN on plant growth rate due to the inability of GN to penetrate the plant tissue. In another study, hydrated GN ribbons (HGR) promoted aged seed germination by 15%, root differentiation between 52 and 59%, and enhanced resistance to oxidative stress compared to GN and GO.[284] Further to this , GN has been shown to have a positive effect on the germination of tomato seeds and seedling in a study conducted by Zhang et al.[285] Analytical results indicated there was penetration of GN into the seed husk which resulted in faster germination and higher germination rates because it facilitates water uptake. However, during the seedling growth period, GN adversely affected seedling biomass accumulation, suggesting that GN plays a complicated role in affecting the initial stage of seed germination and subsequent seedling growth. A very detailed study on the effect of different concentrations of GO inducing the oxidative stress of faba bean seedlings was conducted by Anjum et al.[286,287] They showed that seeds treated with GO at low and high concentrations of 100, 200 and 1600 mg/l decreased the antioxidative glutathione metabolism and increased the amount of ROS. However, by applying moderate concentrations of GO (400 and 800 mg/l) the glutathione pool was enhanced and the formation of ROS was reduced due to improved seed water content.

1. Advantages and disadvantages of GN-based materials for soil application

The extensive use of GN-based materials in different fields and their application in agriculture could cause their release and subsequent build-up in the soil, therefore, the interaction of GN-based materials with the different components of soil needs to be addressed. Addition of GN-based materials may cause some changes in the microbial community, composition and structure of soil. Chung et al. conducted a study on the effect of GO on different soil enzymes including xylosidase, 1,4-β-n-acetyl glucosaminidase, and phosphatase in a 59-day soil incubation experiment.[288] Soil amended with up to 1 mg GO per g lowered the activity of enzymes by 50% compared to control soils but the microbial biomass was not affected. Overall they showed that although the soil enzyme activity can be reduced the short term by applying GO into soils, enzyme activity can recover over time.[288] Additionally, indirect toxicity of GO has been reported in wheat (*T. aestivum*) in As-polluted soil due to the inducing phytotoxicity of arsenic (As).[289] The mechanical damage of the cell wall and plasma membrane by GO led to an increase in As uptake, which consequently caused toxicity and changes in metabolism. In contrast, GO applied to contaminated soil with Cd caused some positive changes as indicated by greater dehydrogenase activity, increased RA (the number of sequences affiliated with phylum divided by the total sequence number per sample) of some dominant bacterial phyla and decreased bioavailability of Cd.[290]

In a recent study, GO changed the bacterial community in a soil while also causing changes in soil properties.[291] Bacterial communities in soil amended with GO became richer and more diverse compared to unamended soil. Furthermore, the structure of soil bacterial communities was changed by adding GO, including selective enrichment of some nitrogen-fixing and dissimilatory iron-reducing bacterial genes. Graphene oxide has also been found to aid water transport through soil, promoting the germination of plants.[292] It was found that GO can collect existing water in soil due to the oxygen-containing functional groups on its structure that could then transport the water to the seeds and promote their germination. It is proposed that the strong interaction of GO and soil grains can stabilize residual GO sheets in soil and prevent their dispersion and uptake by plants, as no GO was detected on the surface or inside the plant cells.

Additionally, different studies have investigated degradation of carbon-based materials such as single- and multi-wall CNTs in the presence of a wide variety of catalytic peroxidase enzymes such as myeloperoxidase (MPO), horseradish peroxidase (HRP), and lignin peroxidase (LiP) which exist naturally in the body and in the environment.[293] A recent study demonstrated the degradation of GO in the presence of low concentration of HRP (~40 μm) with emphasis on the effect of surface functionalization of the carbon nanomaterials and pre-treatment requirement, such as exposure to strong acids prior to enzymatic degradation (Figure 14).[294] Computational docking studies indicated that HRP preferred to bind with the basal plane of both GO and rGO rather than their edges. Another study conducted by Xing and co-workers showed degradation of few-layer pristine GN with hydrogen peroxide (H_2O_2) at physiologically and environmentally relevant concentrations of H_2O_2 (1–0.001 M). [293] Lawani and co-workers[295] investigated the interactions of nanoribbons of GO and rGO with lignin peroxidase (LiP), a ligninolytic enzyme released from white rot fungus. Both GO and rGO nanoribons treated with LiP had complete or partial degradation within 96 h in the presence of veratyl alcohol (VA) or H_2O_2. This study proposed that VA may be an essential factor for degradation of rGO nanoribbons via LiP treatment. However both studies suggested that the wide presence of white rot fungi and LiP, and thereby H_2O_2, in nature could lead to efficient degradation of any GN-based material contamination present in the environment. [295]

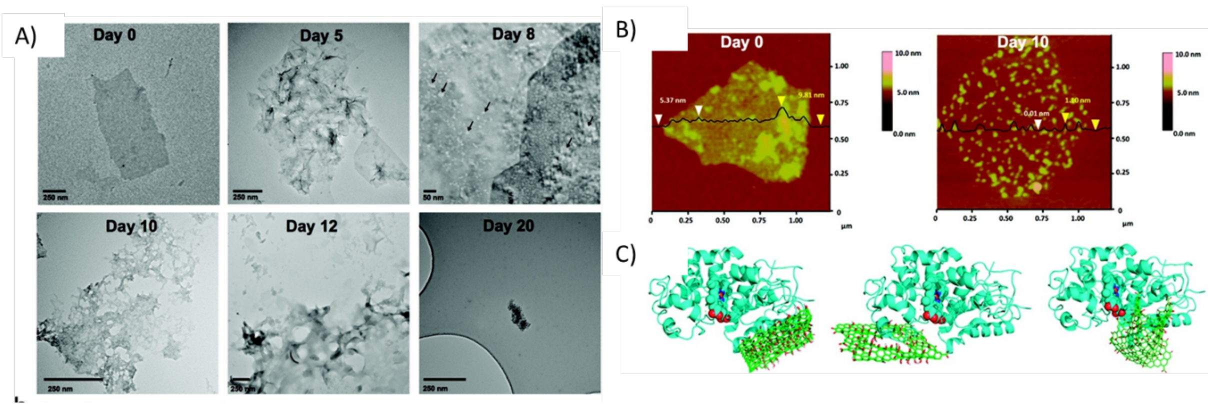

Figure 14. (A) TEM micrographs of GO after incubation with HRP and H_2O_2. Arrows indicate hole formation in the basal plane of GO at day 8. (B) atomic force microscopy (AFM) images with section analysis of graphene oxide with HRP at day 0 (left) and GO with holes at day 10 (right). (c) binding poses of HRP on (from left to right) GO, porous GO, and a small sheet of GO calculated using molecular docking studies. Adapted with permission.[294]

Conclusions and perspectives

This present review demonstrates that the application of GN-based materials in many sectors of agriculture is still in its early, but rapidly blooming, stage. Inspiring and promising research has already been achieved with regard to the delivery of plant nutrients and pesticides, which is expected to improve delivery control and reduce input rates. However, questions still remain regarding the resultant effect of GN-related materials on the environment and its fate within biological cycles. The benefits of GN-based materials will be further recognized, if they can be used to efficiently transport and deliver chemicals such as fungicides, herbicides and insecticides, or other substances such as plant hormones, elicitors and nucleic acids into localized areas and targeted sites of the plant tissue. This could consequently reveal insight into plant life cycles at a physiological, biochemical and genetic level, ultimately assessing to make sustainable agriculture a reality. In addition, there is already a platform to improve their application for real time sensing of toxic gases, including the remote sensing of plant diseases by placing GN-based sensors onto insects or plants. This type of technology can give a full picture of the spatial distribution of disease severity at a field scale which can help to detect hot spots and apply targeted treatment, as a significant contribution in reducing the adverse effects of agrochemicals. There is a need to conduct further, more comprehensive, studies on the effect of GN-based materials as a hardening agent to enhance the physical properties of different fertilizers using new production methods, then extend these to other methods of fertilizer preparation including compaction or prilling. Finally, it may be possible to apply GN-based materials loaded with nutrients or pesticides as a hardening agent to enhance their physical properties while improving fertilizer performance.

Interest in the application of GN-based materials in agriculture is increasing, however the major concerns regarding the application of GN-based materials in agriculture include their lack of scale, high cost and low quantity. Most production methods are not scalable to the large quantities needed for fertilizer production and although costs are falling, they are still expensive materials compared to other materials used in agriculture. Most bulk methods for production of GN also have inherent limitations on the quality of the GN produced, which limits their application in the market, but it can be manipulated to a degree by many production methods and it is important to remember there is no need for high quality GN in agriculture.

Other challenges need to be addressed for their application in agriculture include: (1) designing novel GN-based materials for controlled release and enhanced nutrient and pesticides uptake rates; (2) characterizing and understanding the structure of different GN-based materials for a detailed picture of the interactions and fate of these materials in the environment; (3) optimisation of GN-based materials properties and use, in particular exposure concentration and time, size, surface charge, surface chemistry and agglomeration/aggregation for their successful application in different agricultural areas; (4) developing GN-based materials with dual effects that can act as both fertilizers and pesticides carriers, which provide sustained release and stability for plant protection management; (5) optimizing GN-based materials dose–response, and other factors to expand their application as hardening agents for a wide range of fertilizers; (6) understanding human and environmental exposure to GN-based materials through nutritional uptake or food chain contamination and the effect of exposure concentration, surface chemistry and their toxicity towards, plants, soil and water; and (7) developing common strategies to test laboratory-scale GN-based materials in real farm applications for broader technology validation and translation. Overall it can be concluded that GN-based materials have a promising future in agriculture, by adding value to crop productivity and improving agricultural practices in a sustainable and achievable way.

References:

1. Kashyap, P. L.; Xiang, X.; Heiden, P. Chitosan nanoparticle based delivery systems for sustainable agriculture. *International Journal of Biological Macromolecules* 2015, 77, 36-51.
2. Tilman, D.; Cassman, K. G.; Matson, P. A.; Naylor, R.; Polasky, S. Agricultural sustainability and intensive production practices. *Nature* 2002, 418, 671-677.
3. Foley, J. A.; DeFries, R.; Asner, G. P.; Barford, C.; Bonan, G.; Carpenter, S. R.; Chapin, F. S.; Coe, M. T.; Daily, G. C.; Gibbs, H. K.; Helkowski, J. H.; Holloway, T.; Howard, E. A.; Kucharik, C. J.; Monfreda, C.; Patz, J. A.; Prentice, I. C.; Ramankutty, N.; Snyder, P. K. Global consequences of land use. *Science* 2005, 309, 570-574.
4. Foley, J. A.; Ramankutty, N.; Brauman, K. A.; Cassidy, E. S.; Gerber, J. S.; Johnston, M.; Mueller, N. D.; O'Connell, C.; Ray, D. K.; West, P. C.; Balzer, C.; Bennett, E. M.; Carpenter, S. R.; Hill, J.; Monfreda, C.; Polasky, S.; Rockström, J.; Sheehan, J.; Siebert, S.; Tilman, D.; Zaks, D. P. M. Solutions for a cultivated planet. *Nature* 2011, 478, 337-342.
5. Azeem, B.; KuShaari, K.; Man, Z. B.; Basit, A.; Thanh, T. H. Review on materials & methods to produce controlled release coated urea fertilizer. *Journal of Controlled Release* 2014, 181, 11-21.
6. (UN), U. n. *World population projected to reach 9.7 billion by 2050*; UN: New York, 2015.

7. T.L.Roberts. The role of fertilizers in growing the worlds food. *Better Crops* 2009, 93.
8. Shaviv, A. Advances in controlled-release fertilizers. In *Advances in Agronomy*, Academic Press: 2001; Vol. Volume 71, pp 1-49.
9. Chien, S. H.; Prochnow, L. I.; Cantarella, H. Chapter 8 Recent developments of fertilizer production and use to improve nutrient efficiency and minimize environmental impacts. In *Advances in Agronomy*, Academic Press: 2009; Vol. Volume 102, pp 267-322.
10. González, M. E.; Cea, M.; Medina, J.; González, A.; Diez, M. C.; Cartes, P.; Monreal, C.; Navia, R. Evaluation of biodegradable polymers as encapsulating agents for the development of a urea controlled-release fertilizer using biochar as support material. *Science of The Total Environment* 2015, 505, 446-453.
11. Degryse, F.; Smolders, E.; Parker, D. R. Partitioning of metals (Cd, Co, Cu, Ni, Pb, Zn) in soils: Concepts, methodologies, prediction and applications – A review. *European Journal of Soil Science* 2009, 60, 590-612.
12. Hettiarachchi, G. M.; Lombi, E.; McLaughlin, M. J.; Chittleborough, D.; Self, P. Density changes around phosphorus granules and fluid bands in a calcareous soil. *Soil Science Society of America Journal* 2006, 70, 960-966.
13. Carpenter, S. R.; Caraco, N. F.; Correll, D. L.; Howarth, R. W.; Sharpley, A. N.; Smith, V. H. Nonpoint pollution of surface waters with phosphorus and nitrogen. *Ecological Applications* 1998, 8, 559-568.
14. Massachusetts Institute of Technology (MIT). Fighting peak phosphorus; http://web.mit.edu/12.000/www/m2016/finalwebsite/solutions/phosphorus.html (accessed March 2017) .
15. Raliya, R.; Saharan, V.; Dimkpa, C.; Biswas, P. Nanofertilizer for precision and sustainable agriculture: Current state and future perspectives. *Journal of Agricultural and Food Chemistry* 2017, 66, 6487-6503.
16. Pimentel, D. W., A. World population agriculture and malnutrition *World Watch* 2004, 3.
17. Wang, X.; Lu, S.; Gao, C.; Xu, X.; Wei, Y.; Bai, X.; Feng, C.; Gao, N.; Liu, M.; Wu, L. Biomass-based multifunctional fertilizer system featuring controlled-release nutrient, water-retention and amelioration of soil. *RSC Advances* 2014, 4, 18382-18390.
18. Sharon, M. C., A.; Kumar, R. Nanotechnology in agricultural diseases and food safety. *Journal of Phytology* 2010, 2, 9.
19. Srilatha.B. Nanothechnology in agriculture. *Nanomedicien and Nnaotechnology* 2011, 2, 2-7.
20. Kashyap, P. L.; Xiang, X.; Heiden, P. Chitosan nanoparticle based delivery systems for sustainable agriculture. *International Journal of Biological Macromolecules* 2015, 77, 36-51.
21. Gogos, A.; Knauer, K.; Bucheli, T. D. Nanomaterials in plant protection and fertilization: Current state, Foreseen applications, and research priorities. *Journal of Agricultural and Food Chemistry* 2012, 60, 9781-9792.
22. Novoselov, K. S.; Geim, A. K.; Morozov, S. V.; Jiang, D.; Zhang, Y.; Dubonos, S. V.; Grigorieva, I. V.; Firsov, A. A. Electric field effect in atomically thin carbon films. *Science* 2004, 306, 666-669.
23. Kemp, K. C.; Seema, H.; Saleh, M.; Le, N. H.; Mahesh, K.; Chandra, V.; Kim, K. S. Environmental applications using graphene composites: Water remediation and gas adsorption. *Nanoscale* 2013, 5, 3149-3171.
24. Geim, A. K. Graphene: Status and prospects. *Science* 2009, 324, 1530-1534.
25. Perreault, F.; Fonseca de Faria, A.; Elimelech, M. Environmental applications of graphene-based nanomaterials. *Chemical Society Reviews* 2015, 44, 5861-5896.
26. Liu, J.; Cui, L.; Losic, D. Graphene and graphene oxide as new nanocarriers for drug delivery applications. *Acta Biomaterialia* 2013, 9, 9243-9257.
27. Nine, M. J.; Cole, M. A.; Tran, D. N. H.; Losic, D. Graphene: A multipurpose material for protective coatings. *Journal of Materials Chemistry A* 2015, 3, 12580-12602.
28. Bunch, J. S.; Verbridge, S. S.; Alden, J. S.; van der Zande, A. M.; Parpia, J. M.; Craighead, H. G.; McEuen, P. L. Impermeable atomic membranes from graphene sheets. *Nano Letters* 2008, 8, 2458-2462.

29. Tu, Y.; Lv, M.; Xiu, P.; Huynh, T.; Zhang, M.; Castelli, M.; Liu, Z.; Huang, Q.; Fan, C.; Fang, H.; Zhou, R. Destructive extraction of phospholipids from Escherichia coli membranes by graphene nanosheets. *Nature Nanotechnology* 2013, 8, 594-601.
30. Yung Ho, K.; Sangchul, L.; Woojin, P.; Gunho, J.; Minhyeok, C.; Jong-Hoon, L.; Hyunung, Y.; Takhee, L.; Kwanghee, L. Thermal stability of multilayer graphene films synthesized by chemical vapor deposition and stained by metallic impurities. *Nanotechnology* 2012, 23, 075702.
31. Chen, G.; Weng, W.; Wu, D.; Wu, C.; Lu, J.; Wang, P.; Chen, X. Preparation and characterization of graphite nanosheets from ultrasonic powdering technique. *Carbon* 2004, 42, 753-759.
32. Feng, L.; Wu, L.; Qu, X. New horizons for diagnostics and therapeutic applications of graphene and graphene oxide. *Advanced Materials* 2013, 25, 168-186.
33. Wang, Y.; Li, Z.; Wang, J.; Li, J.; Lin, Y. Graphene and graphene oxide: Biofunctionalization and applications in biotechnology. *Trends in Biotechnology* 2011, 29, 205-212.
34. Yang, K.; Feng, L.; Shi, X.; Liu, Z. Nano-graphene in biomedicine: Theranostic applications. *Chemical Society Reviews* 2013, 42, 530-547.
35. Gonçalves, G.; Vila, M.; Portolés, M.-T.; Vallet-Regi, M.; Gracio, J.; Marques, P. A. A. P. Nano-Graphene oxide: A potential multifunctional platform for cancer therapy. *Advanced Healthcare Materials* 2013, 2, 1072-1090.
36. Lu, Z.; Hou, D.; Meng, L.; Sun, G.; Lu, C.; Li, Z. Mechanism of cement paste reinforced by graphene oxide/carbon nanotubes composites with enhanced mechanical properties. *RSC Advances* 2015, 5, 100598-100605.
37. Gholampour, A.; Valizadeh Kiamahalleh, M.; Tran, D. N. H.; Ozbakkaloglu, T.; Losic, D. From graphene oxide to reduced graphene oxide: Impact on the physiochemical and mechanical properties of graphene–cement composites. *ACS Applied Materials & Interfaces* 2017, 9, 43275-43286.
38. Compton, O. C.; Nguyen, S. T. Graphene oxide, highly reduced graphene oxide, and graphene: Versatile building blocks for carbon-based materials. *Small* 2010, 6, 711-723.
39. Yoo, J. M.; Kang, J. H.; Hong, B. H. Graphene-based nanomaterials for versatile imaging studies. *Chemical Society Reviews* 2015, 44, 4835-4852.
40. Zhao, H.; Ding, R.; Zhao, X.; Li, Y.; Qu, L.; Pei, H.; Yildirimer, L.; Wu, Z.; Zhang, W. Graphene-based nanomaterials for drug and/or gene delivery, bioimaging, and tissue engineering. *Drug Discovery Today* 2017, 22, 1302-1317.
41. Hontoria-Lucas, C.; López-Peinado, A. J.; López-González, J. d. D.; Rojas-Cervantes, M. L.; Martín-Aranda, R. M. Study of oxygen-containing groups in a series of graphite oxides: Physical and chemical characterization. *Carbon* 1995, 33, 1585-1592.
42. Rodriguez-Perez, L.; Herranz, M. a. A.; Martin, N. The chemistry of pristine graphene. *Chemical Communications* 2013, 49, 3721-3735.
43. Geim, A. K.; Novoselov, K. S. The rise of graphene. *Nature Materials* 2007, 6, 183-191.
44. Zhu, Y.; Murali, S.; Cai, W.; Li, X.; Suk, J. W.; Potts, J. R.; Ruoff, R. S. Graphene and graphene oxide: Synthesis, properties, and applications. *Advanced Materials* 2010, 22, 3906-3924.
45. Hernandez, Y.; Nicolosi, V.; Lotya, M.; Blighe, F. M.; Sun, Z.; De, S.; McGovern, I. T.; Holland, B.; Byrne, M.; Gun'Ko, Y. K.; Boland, J. J.; Niraj, P.; Duesberg, G.; Krishnamurthy, S.; Goodhue, R.; Hutchison, J.; Scardaci, V.; Ferrari, A. C.; Coleman, J. N. High-yield production of graphene by liquid-phase exfoliation of graphite. *Nature Nanotechnology* 2008, 3, 563-568.
46. Li, X.; Cai, W.; An, J.; Kim, S.; Nah, J.; Yang, D.; Piner, R.; Velamakanni, A.; Jung, I.; Tutuc, E.; Banerjee, S. K.; Colombo, L.; Ruoff, R. S. Large-area synthesis of high-quality and uniform graphene films on copper foils. *Science* 2009, 324, 1312-1314.
47. Kwon, S.-Y.; Ciobanu, C. V.; Petrova, V.; Shenoy, V. B.; Bareño, J.; Gambin, V.; Petrov, I.; Kodambaka, S. Growth of semiconducting graphene on palladium. *Nano Letters* 2009, 9, 3985-3990.
48. Alpha, T. N. D.; Johann, C.; Tim, N. P.; Carsten, B.; Thomas, M. Structure of epitaxial graphene on Ir(111). *New Journal of Physics* 2008, 10, 043033.
49. Kim, K. S.; Zhao, Y.; Jang, H.; Lee, S. Y.; Kim, J. M.; Kim, K. S.; Ahn, J.-H.; Kim, P.; Choi, J.-Y.; Hong, B. H. Large-scale pattern growth of graphene films for stretchable transparent electrodes. *Nature* 2009, 457, 706.

50. Guermoune, A.; Chari, T.; Popescu, F.; Sabri, S. S.; Guillemette, J.; Skulason, H. S.; Szkopek, T.; Siaj, M. Chemical vapor deposition synthesis of graphene on copper with methanol, ethanol, and propanol precursors. *Carbon* 2011, 49, 4204-4210.
51. Dreyer, D. R.; Park, S.; Bielawski, C. W.; Ruoff, R. S. The chemistry of graphene oxide. *Chemical Society Reviews* 2010, 39, 228-240.
52. Chen, D.; Feng, H.; Li, J. Graphene oxide: Preparation, functionalization, and electrochemical applications. *Chemical Reviews* 2012, 112, 6027-6053.
53. Lerf, A.; He, H.; Forster, M.; Klinowski, J. Structure of graphite oxide revisited. *The Journal of Physical Chemistry B* 1998, 102, 4477-4482.
54. Paredes, J. I.; Villar-Rodil, S.; Martínez-Alonso, A.; Tascón, J. M. D. Graphene oxide dispersions in organic solvents. *Langmuir* 2008, 24, 10560-10564.
55. Sreeprasad, T. S.; Berry, V. How do the electrical properties of graphene change with its functionalization? *Small* 2013, 9, 341-350.
56. Lee, C.; Wei, X.; Kysar, J. W.; Hone, J. Measurement of the elastic properties and intrinsic strength of monolayer graphene. *Science* 2008, 321, 385-388.
57. Suk, J. W.; Piner, R. D.; An, J.; Ruoff, R. S. Mechanical properties of monolayer graphene oxide. *ACS Nano* 2010, 4, 6557-6564.
58. Gómez-Navarro, C.; Burghard, M.; Kern, K. Elastic properties of chemically derived single graphene sheets. *Nano Letters* 2008, 8, 2045-2049.
59. Chua, C. K.; Pumera, M. Chemical reduction of graphene oxide: A synthetic chemistry viewpoint. *Chemical Society Reviews* 2014, 43, 291-312.
60. Pei, S.; Cheng, H.-M. The reduction of graphene oxide. *Carbon* 2012, 50, 3210-3228.
61. Wang, Y.; Shi, Z.; Yin, J. Facile synthesis of soluble graphene via a green reduction of graphene oxide in tea solution and its biocomposites. *ACS Applied Materials & Interfaces* 2011, 3, 1127-1133.
62. Stankovich, S.; Dikin, D. A.; Piner, R. D.; Kohlhaas, K. A.; Kleinhammes, A.; Jia, Y.; Wu, Y.; Nguyen, S. T.; Ruoff, R. S. Synthesis of graphene-based nanosheets via chemical reduction of exfoliated graphite oxide. *Carbon* 2007, 45, 1558-1565.
63. Tran, D. N. H.; Kabiri, S.; Losic, D. A green approach for the reduction of graphene oxide nanosheets using non-aromatic amino acids. *Carbon* 2014, 76, 193-202.
64. Fernández-Merino, M. J.; Guardia, L.; Paredes, J. I.; Villar-Rodil, S.; Solís-Fernández, P.; Martínez-Alonso, A.; Tascón, J. M. D. Vitamin C is an ideal substitute for hydrazine in the reduction of graphene oxide suspensions. *The Journal of Physical Chemistry C* 2010, 114, 6426-6432.
65. Zhu, C.; Guo, S.; Fang, Y.; Dong, S. Reducing sugar: new functional molecules for the green synthesis of graphene nanosheets. *ACS Nano* 2010, 4, 2429-2437.
66. Gómez-Navarro, C.; Meyer, J. C.; Sundaram, R. S.; Chuvilin, A.; Kurasch, S.; Burghard, M.; Kern, K.; Kaiser, U. Atomic structure of reduced graphene oxide. *Nano Letters* 2010, 10, 1144-1148.
67. Bagri, A.; Mattevi, C.; Acik, M.; Chabal, Y. J.; Chhowalla, M.; Shenoy, V. B. Structural evolution during the reduction of chemically derived graphene oxide. *Nature Chemistry* 2010, 2, 581.
68. Zhou, Y.; Bao, Q.; Tang, L. A. L.; Zhong, Y.; Loh, K. P. Hydrothermal dehydration for the "Green" reduction of exfoliated graphene oxide to graphene and demonstration of tunable optical limiting properties. *Chemistry of Materials* 2009, 21, 2950-2956.
69. Alotaibi, F.; Tung, T. T.; Nine, M. J.; Kabiri, S.; Moussa, M.; Tran, D. N. H.; Losic, D. Scanning atmospheric plasma for ultrafast reduction of graphene oxide and fabrication of highly conductive graphene films and patterns. *Carbon* 2018, 127, 113-121.
70. Yan, X.; Cui, X.; Li, L.-s. Synthesis of large, stable colloidal graphene quantum dots with tunable size. *Journal of the American Chemical Society* 2010, 132, 5944-5945.
71. Tang, L.; Ji, R.; Cao, X.; Lin, J.; Jiang, H.; Li, X.; Teng, K. S.; Luk, C. M.; Zeng, S.; Hao, J.; Lau, S. P. Deep ultraviolet photoluminescence of water-soluble self-passivated graphene quantum dots. *ACS Nano* 2012, 6, 5102-5110.
72. Liu, R.; Wu, D.; Feng, X.; Müllen, K. Bottom-up fabrication of photoluminescent graphene quantum dots with uniform morphology. *Journal of the American Chemical Society* 2011, 133, 15221-15223.
73. Lu, J.-J.; Cai, Y.-J.; Ding, J. Curcumin induces DNA damage and caffeine-insensitive cell cycle arrest in colorectal carcinoma HCT116 cells. *Molecular and Cellular Biochemistry* 2011, 354, 247-252.

74. Wang, L.; Wang, Y.; Xu, T.; Liao, H.; Yao, C.; Liu, Y.; Li, Z.; Chen, Z.; Pan, D.; Sun, L.; Wu, M. Gram-scale synthesis of single-crystalline graphene quantum dots with superior optical properties. *Nature Communications* 2014, 5, 5357.
75. Pan, D.; Zhang, J.; Li, Z.; Wu, M. Hydrothermal route for cutting graphene sheets into blue-luminescent graphene quantum dots. *Advanced Materials* 2010, 22, 734-738.
76. Ponomarenko, L. A.; Schedin, F.; Katsnelson, M. I.; Yang, R.; Hill, E. W.; Novoselov, K. S.; Geim, A. K. Chaotic dirac billiard in graphene quantum dots. *Science* 2008, 320, 356-358.
77. Favaro, M.; Ferrighi, L.; Fazio, G.; Colazzo, L.; Di Valentin, C.; Durante, C.; Sedona, F.; Gennaro, A.; Agnoli, S.; Granozzi, G. Single and multiple doping in graphene quantum dots: Unraveling the origin of selectivity in the oxygen reduction reaction. *ACS Catalysis* 2015, 5, 129-144.
78. Peng, J.; Gao, W.; Gupta, B. K.; Liu, Z.; Romero-Aburto, R.; Ge, L.; Song, L.; Alemany, L. B.; Zhan, X.; Gao, G.; Vithayathil, S. A.; Kaipparettu, B. A.; Marti, A. A.; Hayashi, T.; Zhu, J.-J.; Ajayan, P. M. Graphene quantum dots derived from carbon fibers. *Nano Letters* 2012, 12, 844-849.
79. Guo, C. X.; Yang, H. B.; Sheng, Z. M.; Lu, Z. S.; Song, Q. L.; Li, C. M. Layered graphene/quantum dots for photovoltaic devices. *Angewandte Chemie International Edition* 2010, 49, 3014-3017.
80. Girit, Ç. Ö.; Meyer, J. C.; Erni, R.; Rossell, M. D.; Kisielowski, C.; Yang, L.; Park, C.-H.; Crommie, M. F.; Cohen, M. L.; Louie, S. G.; Zettl, A. Graphene at the edge: Stability and dynamics. *Science* 2009, 323, 1705-1708.
81. Gupta, V.; Chaudhary, N.; Srivastava, R.; Sharma, G. D.; Bhardwaj, R.; Chand, S. Luminscent graphene quantum dots for organic photovoltaic devices. *Journal of the American Chemical Society* 2011, 133, 9960-9963.
82. Shtein, M.; Pri-Bar, I.; Varenik, M.; Regev, O. Characterization of graphene-nanoplatelets structure via thermogravimetry. *Analytical Chemistry* 2015, 87, 4076-4080.
83. Li, L.; Wu, G.; Yang, G.; Peng, J.; Zhao, J.; Zhu, J.-J. Focusing on luminescent graphene quantum dots: current status and future perspectives. *Nanoscale* 2013, 5, 4015-4039.
84. Buzaglo, M.; Shtein, M.; Regev, O. Graphene quantum dots produced by microfluidization. *Chemistry of Materials* 2016, 28, 21-24.
85. Yang, S.-T.; Cao, L.; Luo, P. G.; Lu, F.; Wang, X.; Wang, H.; Meziani, M. J.; Liu, Y.; Qi, G.; Sun, Y.-P. Carbon dots for optical imaging in vivo. *Journal of the American Chemical Society* 2009, 131, 11308-11309.
86. Ran, X.; Sun, H.; Pu, F.; Ren, J.; Qu, X. Ag Nanoparticle-decorated graphene quantum dots for label-free, rapid and sensitive detection of Ag+ and biothiols. *Chemical Communications* 2013, 49, 1079-1081.
87. Sun, H.; Ji, H.; Ju, E.; Guan, Y.; Ren, J.; Qu, X. Synthesis of fluorinated and nonfluorinated graphene quantum dots through a new top-down strategy for long-time cellular imaging. *Chemistry – A European Journal* 2015, 21, 3791-3797.
88. Gong, X.; Liu, G.; Li, Y.; Yu, D. Y. W.; Teoh, W. Y. Functionalized-graphene composites: fabrication and applications in sustainable energy and environment. *Chemistry of Materials* 2016, 28, 8082-8118.
89. Niyogi, S.; Bekyarova, E.; Itkis, M. E.; McWilliams, J. L.; Hamon, M. A.; Haddon, R. C. Solution properties of graphite and graphene. *Journal of the American Chemical Society* 2006, 128, 7720-7721.
90. Xu, Y.; Liu, Z.; Zhang, X.; Wang, Y.; Tian, J.; Huang, Y.; Ma, Y.; Zhang, X.; Chen, Y. A graphene hybrid material covalently functionalized with porphyrin: Synthesis and optical limiting property. *Advanced Materials* 2009, 21, 1275-1279.
91. Liu, Z.-B.; Xu, Y.-F.; Zhang, X.-Y.; Zhang, X.-L.; Chen, Y.-S.; Tian, J.-G. Porphyrin and fullerene covalently functionalized graphene hybrid materials with large nonlinear optical properties. *The Journal of Physical Chemistry B* 2009, 113, 9681-9686.
92. Zhang, X.; Huang, Y.; Wang, Y.; Ma, Y.; Liu, Z.; Chen, Y. Synthesis and characterization of a graphene–C60 hybrid material. *Carbon* 2009, 47, 334-337.
93. Liu, Z.; Robinson, J. T.; Sun, X.; Dai, H. PEGylated nanographene oxide for delivery of water-insoluble cancer drugs. *Journal of the American Chemical Society* 2008, 130, 10876-10877.

94. Zhang, K.; Li, H.; Xu, X.; Yu, H. Facile and efficient synthesis of nitrogen-functionalized graphene oxide as a copper adsorbent and its application. *Industrial & Engineering Chemistry Research* 2016, 55, 2328-2335.
95. Veca, L. M.; Lu, F.; Meziani, M. J.; Cao, L.; Zhang, P.; Qi, G.; Qu, L.; Shrestha, M.; Sun, Y.-P. Polymer functionalization and solubilization of carbon nanosheets. *Chemical Communications* 2009, 2565-2567.
96. Jang, S.-Y.; Kim, Y.-G.; Kim, D. Y.; Kim, H.-G.; Jo, S. M. Electrodynamically sprayed thin films of aqueous dispersible graphene nanosheets: highly efficient cathodes for dye-sensitized solar cells. *ACS Applied Materials & Interfaces* 2012, 4, 3500-3507.
97. Mohanty, N.; Berry, V. Graphene-based single-bacterium resolution biodevice and DNA transistor: Interfacing graphene derivatives with nanoscale and microscale biocomponents. *Nano Letters* 2008, 8, 4469-4476.
98. Park, W. B.; Bandyopadhyay, P.; Nguyen, T. T.; Kuila, T.; Kim, N. H.; Lee, J. H. Effect of high molecular weight polyethyleneimine functionalized graphene oxide coated polyethylene terephthalate film on the hydrogen gas barrier properties. *Composites Part B: Engineering* 2016, 106, 316-323.
99. Park, S.; Dikin, D. A.; Nguyen, S. T.; Ruoff, R. S. Graphene oxide sheets chemically cross-linked by polyallylamine. *The Journal of Physical Chemistry C* 2009, 113, 15801-15804.
100. Salavagione, H. J.; Gómez, M. A.; Martínez, G. Polymeric modification of graphene through esterification of graphite oxide and poly(vinyl alcohol). *Macromolecules* 2009, 42, 6331-6334.
101. Yang, H.; Li, F.; Shan, C.; Han, D.; Zhang, Q.; Niu, L.; Ivaska, A. Covalent functionalization of chemically converted graphene sheets via silane and its reinforcement. *Journal of Materials Chemistry* 2009, 19, 4632-4638.
102. Yang, H.; Shan, C.; Li, F.; Han, D.; Zhang, Q.; Niu, L. Covalent functionalization of polydisperse chemically-converted graphene sheets with amine-terminated ionic liquid. *Chemical Communications* 2009, 3880-3882.
103. Blagbrough, I. S.; Mackenzie, N. E.; Ortiz, C.; Scott, A. I. The condensation reaction between isocyanates and carboxylic acids. A practical synthesis of substituted amides and anilides. *Tetrahedron Letters* 1986, 27, 1251-1254.
104. Park, S.; Mohanty, N.; Suk, J. W.; Nagaraja, A.; An, J.; Piner, R. D.; Cai, W.; Dreyer, D. R.; Berry, V.; Ruoff, R. S. Biocompatible, robust free-standing paper composed of a Tween/graphene composite. *Advanced Materials* 2010, 22, 1736-1740.
105. Hu, H.; Yu, J.; Li, Y.; Zhao, J.; Dong, H. Engineering of a novel pluronic F127/graphene nanohybrid for pH responsive drug delivery. *Journal of Biomedical Materials Research Part A* 2012, 100A, 141-148.
106. Robinson, J. T.; Tabakman, S. M.; Liang, Y.; Wang, H.; Sanchez Casalongue, H.; Vinh, D.; Dai, H. Ultrasmall reduced graphene oxide with high near-infrared absorbance for photothermal therapy. *Journal of the American Chemical Society* 2011, 133, 6825-6831.
107. Feng, L.; Zhang, S.; Liu, Z. Graphene based gene transfection. *Nanoscale* 2011, 3, 1252-1257.
108. Depan, D.; Shah, J.; Misra, R. D. K. Controlled release of drug from folate-decorated and graphene mediated drug delivery system: Synthesis, loading efficiency, and drug release response. *Materials Science and Engineering: C* 2011, 31, 1305-1312.
109. Hu, W.; Peng, C.; Lv, M.; Li, X.; Zhang, Y.; Chen, N.; Fan, C.; Huang, Q. Protein corona-mediated mitigation of cytotoxicity of graphene oxide. *ACS Nano* 2011, 5, 3693-3700.
110. Liu, K.; Zhang, J.-J.; Cheng, F.-F.; Zheng, T.-T.; Wang, C.; Zhu, J.-J. Green and facile synthesis of highly biocompatible graphene nanosheets and its application for cellular imaging and drug delivery. *Journal of Materials Chemistry* 2011, 21, 12034-12040.
111. Liu, J.; Li, Y.; Li, Y.; Li, J.; Deng, Z. Noncovalent DNA decorations of graphene oxide and reduced graphene oxide toward water-soluble metal-carbon hybrid nanostructures via self-assembly. *Journal of Materials Chemistry* 2010, 20, 900-906.
112. He, S.; Song, B.; Li, D.; Zhu, C.; Qi, W.; Wen, Y.; Wang, L.; Song, S.; Fang, H.; Fan, C. A graphene nanoprobe for rapid, sensitive, and multicolor fluorescent DNA analysis. *Advanced Functional Materials* 2010, 20, 453-459.
113. Dubuisson, E.; Yang, Z.; Loh, K. P. Optimizing label-free DNA electrical detection on graphene platform. *Analytical Chemistry* 2011, 83, 2452-2460.

114. Yin, Z.; He, Q.; Huang, X.; Zhang, J.; Wu, S.; Chen, P.; Lu, G.; Chen, P.; Zhang, Q.; Yan, Q.; Zhang, H. Real-time DNA detection using Pt nanoparticle-decorated reduced graphene oxide field-effect transistors. *Nanoscale* 2012, 4, 293-297.
115. He, Q.; Sudibya, H. G.; Yin, Z.; Wu, S.; Li, H.; Boey, F.; Huang, W.; Chen, P.; Zhang, H. Centimeter-long and large-scale micropatterns of reduced graphene oxide films: Fabrication and sensing applications. *ACS Nano* 2010, 4, 3201-3208.
116. Shen, J.; Shi, M.; Li, N.; Yan, B.; Ma, H.; Hu, Y.; Ye, M. Facile synthesis and application of Ag-chemically converted graphene nanocomposite. *Nano Research* 2010, 3, 339-349.
117. Huang, X.; Yin, Z.; Wu, S.; Qi, X.; He, Q.; Zhang, Q.; Yan, Q.; Boey, F.; Zhang, H. Graphene-based materials: synthesis, characterization, properties, and applications. *Small* 2011, 7, 1876-1902.
118. Andjelkovic, I.; Tran, D. N. H.; Kabiri, S.; Azari, S.; Markovic, M.; Losic, D. Graphene aerogels decorated with α-FeOOH nanoparticles for efficient adsorption of arsenic from contaminated waters. *ACS Applied Materials & Interfaces* 2015, 7, 9758-9766.
119. Kabiri, S.; Tran, D. N. H.; Azari, S.; Losic, D. Graphene-diatom silica aerogels for efficient removal of mercury ions from water. *ACS Applied Materials & Interfaces* 2015, 7, 11815-11823.
120. Tran, D. N. H.; Kabiri, S.; Wang, L.; Losic, D. Engineered graphene-nanoparticle aerogel composites for efficient removal of phosphate from water. *Journal of Materials Chemistry A* 2015, 3, 6844-6852.
121. Murphy, C. J.; Sau, T. K.; Gole, A. M.; Orendorff, C. J.; Gao, J.; Gou, L.; Hunyadi, S. E.; Li, T. Anisotropic metal nanoparticles: Synthesis, assembly, and optical applications. *The Journal of Physical Chemistry B* 2005, 109, 13857-13870.
122. Yu, X.; Zhang, W.; Zhang, P.; Su, Z. Fabrication technologies and sensing applications of graphene-based composite films: Advances and challenges. *Biosensors and Bioelectronics* 2017, 89, 72-84.
123. Zhu, Y.; Ji, H.; Cheng, H.-M.; Ruoff, R. S. Mass production and industrial applications of graphene materials. *National Science Review* 2018, 5, 90-101.
124. http://www.appliedgraphenematerials.com/.
125. http://www.nbmorsh.com/h-index.html.
126. http://www.superc.com.cn/en/index.aspx.
127. http://www.hxnano.com/english/index.aspx.
128. http://www.carbonene.cn/.
129. https://www.firstgraphite.com.au/.
130. http://www.c6th.com.
131. http://www.bgtmaterials.com/.
132. https://www.graphenea.com/.
133. http://fuxitech.gotoip3.com/.
134. http://www.cz2dcarbon.com/en/.
135. http://www.graphenesquare.com/.
136. Zhu, Y.; Stoller, M. D.; Cai, W.; Velamakanni, A.; Piner, R. D.; Chen, D.; Ruoff, R. S. Exfoliation of graphite oxide in propylene carbonate and thermal reduction of the resulting graphene oxide platelets. *ACS Nano* 2010, 4, 1227-1233.
137. Loh, K. P.; Bao, Q.; Ang, P. K.; Yang, J. The chemistry of graphene. *Journal of Materials Chemistry* 2010, 20, 2277-2289.
138. Viswanathan, S.; Narayanan, T. N.; Aran, K.; Fink, K. D.; Paredes, J.; Ajayan, P. M.; Filipek, S.; Miszta, P.; Tekin, H. C.; Inci, F.; Demirci, U.; Li, P.; Bolotin, K. I.; Liepmann, D.; Renugopalakrishanan, V. Graphene-protein field effect biosensors: Glucose sensing. *Materials Today* 2015, 18, 513-522.
139. Yan, L.; Chang, Y. N.; Zhao, L.; Gu, Z.; Liu, X.; Tian, G.; Zhou, L.; Ren, W.; Jin, S.; Yin, W.; Chang, H.; Xing, G.; Gao, X.; Zhao, Y. The use of polyethylenimine-modified graphene oxide as a nanocarrier for transferring hydrophobic nanocrystals into water to produce water-dispersible hybrids for use in drug delivery. *Carbon* 2013, 57, 120-129.
140. Sharma, S.; Singh, S.; Ganguli, A. K.; Shanmugam, V. Anti-drift nano-stickers made of graphene oxide for targeted pesticide delivery and crop pest control. *Carbon* 2017, 115, 781-790.

141. Georgakilas, V.; Tiwari, J. N.; Kemp, K. C.; Perman, J. A.; Bourlinos, A. B.; Kim, K. S.; Zboril, R. Noncovalent functionalization of graphene and graphene oxide for energy materials, biosensing, catalytic, and biomedical applications. *Chemical Reviews* 2016, 116, 5464-5519.
142. Kabiri, S.; Degryse, F.; Tran, D. N. H.; da Silva, R. C.; McLaughlin, M. J.; Losic, D. Graphene oxide: A new carrier for slow release of plant micronutrients. *ACS Applied Materials & Interfaces* 2017, 9, 43325-43335.
143. Gass, M. H.; Bangert, U.; Bleloch, A. L.; Wang, P.; Nair, R. R.; Geim, A. K. Free-standing graphene at atomic resolution. *Nature Nanotechnology* 2008, 3, 676-681.
144. Sun, P.; Zhu, M.; Wang, K.; Zhong, M.; Wei, J.; Wu, D.; Xu, Z.; Zhu, H. Selective ion penetration of graphene oxide membranes. *ACS Nano* 2013, 7, 428-437.
145. An, D.; Liu, B.; Yang, L.; Wang, T.-J.; Kan, C. Fabrication of graphene oxide/polymer latex composite film coated on KNO_3 fertilizer to extend its release duration. *Chemical Engineering Journal* 2017, 311, 318-325.
146. Pan, Z.; He, L.; Qiu, L.; Korayem, A. H.; Li, G.; Zhu, J. W.; Collins, F.; Li, D.; Duan, W. H.; Wang, M. C. Mechanical properties and microstructure of a graphene oxide–cement composite. *Cement and Concrete Composites* 2015, 58, 140-147.
147. Hwang, J.; Yoon, T.; Jin, S. H.; Lee, J.; Kim, T.-S.; Hong, S. H.; Jeon, S. Enhanced mechanical properties of graphene/copper nanocomposites using a molecular-level mixing process. *Advanced Materials* 2013, 25, 6724-6729.
148. Li, M.-X.; Xie, J.; Li, Y.-D.; Xu, H.-H. Reduced graphene oxide dispersed in copper matrix composites: Facile preparation and enhanced mechanical properties. *physica status solidi (a)* 2015, 212, 2154-2161.
149. Wang, H.; Xie, G.; Ying, Z.; Tong, Y.; Zeng, Y. Enhanced mechanical properties of multi-layer graphene filled poly(vinyl chloride) composite films. *Journal of Materials Science and Technology* 2015, 31, 340-344.
150. Barun, D.; Prasad, K. E.; Ramamurty, U.; Rao, C. N. R. Nano-indentation studies on polymer matrix composites reinforced by few-layer graphene. *Nanotechnology* 2009, 20, 125705.
151. Rafiee, M. A.; Rafiee, J.; Wang, Z.; Song, H.; Yu, Z.-Z.; Koratkar, N. Enhanced mechanical properties of nanocomposites at low graphene content. *ACS Nano* 2009, 3, 3884-3890.
152. Kabiri, S.; Baird, R.; Tran, D. N. H.; Andelkovic, I.; McLaughlin, M. J.; Losic, D. Cogranulation of low rates of graphene and graphene oxide with macronutrient fertilizers remarkably improves their physical properties. *ACS Sustainable Chemistry & Engineering* 2018, 6, 1299-1309.
153. Bolotin, K. I.; Sikes, K. J.; Jiang, Z.; Klima, M.; Fudenberg, G.; Hone, J.; Kim, P.; Stormer, H. L. Ultrahigh electron mobility in suspended graphene. *Solid State Communications* 2008, 146, 351-355.
154. Pumera, M. Graphene-based nanomaterials and their electrochemistry. *Chemical Society Reviews* 2010, 39, 4146-4157.
155. Schedin, F.; Geim, A. K.; Morozov, S. V.; Hill, E. W.; Blake, P.; Katsnelson, M. I.; Novoselov, K. S. Detection of individual gas molecules adsorbed on graphene. *Nature Materials* 2007, 6, 652.
156. Stankovich, S.; Dikin, D. A.; Dommett, G. H. B.; Kohlhaas, K. M.; Zimney, E. J.; Stach, E. A.; Piner, R. D.; Nguyen, S. T.; Ruoff, R. S. Graphene-based composite materials. *Nature* 2006, 442, 282.
157. Liu, Y.; Dong, X.; Chen, P. Biological and chemical sensors based on graphene materials. *Chemical Society Reviews* 2012, 41, 2283-2307.
158. Zhou, M.; Zhai, Y.; Dong, S. Electrochemical sensing and biosensing platform based on chemically reduced graphene oxide. *Analytical Chemistry* 2009, 81, 5603-5613.
159. Wang, Y.; Li, Y.; Tang, L.; Lu, J.; Li, J. Application of graphene-modified electrode for selective detection of dopamine. *Electrochemistry Communications* 2009, 11, 889-892.
160. Eissa, S.; Ng, A.; Siaj, M.; Tavares, A. C.; Zourob, M. Selection and identification of DNA aptamers against okadaic acid for biosensing application. *Analytical Chemistry* 2013, 85, 11794-11801.
161. Andelkovic, I. B.; Kabiri, S.; Tavakkoli, E.; Kirby, J. K.; McLaughlin, M. J.; Losic, D. Graphene oxide-Fe(III) composite containing phosphate – A novel slow release fertilizer for improved agriculture management. *Journal of Cleaner Production* 2018, 185, 97-104.
162. Tong, Y.; Shao, L.; Li, X.; Lu, J.; Sun, H.; Xiang, S.; Zhang, Z.; Wu, Y.; Wu, X. Adhesive and stimulus-responsive polydopamine-coated graphene oxide system for pesticide-loss control. *Journal of Agricultural and Food Chemistry* 2018.

163. Corradini, E.; de Moura, M. R.; Mattoso, L. H. C. A preliminary study of the incorparation of NPK fertilizer into chitosan nanoparticles. *Express Polymer Letters* 2010, 4, 509-515.
164. Zaytseva, O.; Neumann, G. Carbon nanomaterials: production, impact on plant development, agricultural and environmental applications. *Chemical and Biological Technologies in Agriculture* 2016, 3, 17.
165. Sitko, R.; Zawisza, B.; Malicka, E. Graphene as a new sorbent in analytical chemistry. *TrAC Trends in Analytical Chemistry* 2013, 51, 33-43.
166. Yang, S.-T.; Chang, Y.; Wang, H.; Liu, G.; Chen, S.; Wang, Y.; Liu, Y.; Cao, A. Folding/aggregation of graphene oxide and its application in Cu^{2+} removal. *Journal of Colloid and Interface Science* 2010, 351, 122-127.
167. Peng, W.; Li, H.; Liu, Y.; Song, S. Comparison of Pb(II) adsorption onto graphene oxide prepared from natural graphites: Diagramming the Pb(II) adsorption sites. *Applied Surface Science* 2016, 364, 620-627.
168. Gollavelli, G.; Chang, C.-C.; Ling, Y.-C. Facile synthesis of smart magnetic graphene for safe drinking water: heavy metal removal and disinfection control. *ACS Sustainable Chemistry & Engineering* 2013, 1, 462-472.
169. Cong, H.-P.; Ren, X.-C.; Wang, P.; Yu, S.-H. Macroscopic multifunctional graphene-based hydrogels and aerogels by a metal ion induced self-assembly process. *ACS Nano* 2012, 6, 2693-2703.
170. Zhu, J.; Wei, S.; Gu, H.; Rapole, S. B.; Wang, Q.; Luo, Z.; Haldolaarachchige, N.; Young, D. P.; Guo, Z. One-pot synthesis of magnetic graphene nanocomposites decorated with core@double-shell nanoparticles for Fast chromium removal. *Environmental Science & Technology* 2012, 46, 977-985.
171. Chandra, V.; Park, J.; Chun, Y.; Lee, J. W.; Hwang, I.-C.; Kim, K. S. Water-dispersible magnetite-reduced graphene oxide composites for arsenic removal. *ACS Nano* 2010, 4, 3979-3986.
172. Jabeen, H.; Chandra, V.; Jung, S.; Lee, J. W.; Kim, K. S.; Kim, S. B. Enhanced Cr(vi) removal using iron nanoparticle decorated graphene. *Nanoscale* 2011, 3, 3583-3585.
173. Kabiri, S.; Tran, D. N. H.; Cole, M. A.; Losic, D. Functionalized three-dimensional (3D) graphene composite for high efficiency removal of mercury. *Environmental Science: Water Research & Technology* 2016, 2, 390-402.
174. Madadrang, C. J.; Kim, H. Y.; Gao, G.; Wang, N.; Zhu, J.; Feng, H.; Gorring, M.; Kasner, M. L.; Hou, S. Adsorption behavior of EDTA-graphene oxide for Pb (II) removal. *ACS Applied Materials & Interfaces* 2012, 4, 1186-1193.
175. Yang, Y.; Xie, Y.; Pang, L.; Li, M.; Song, X.; Wen, J.; Zhao, H. Preparation of reduced graphene oxide/poly(acrylamide) nanocomposite and Its adsorption of Pb(II) and methylene blue. *Langmuir* 2013, 29, 10727-10736.
176. Liu, L.; Li, C.; Bao, C.; Jia, Q.; Xiao, P.; Liu, X.; Zhang, Q. Preparation and characterization of chitosan/graphene oxide composites for the adsorption of Au(III) and Pd(II). *Talanta* 2012, 93, 350-357.
177. Everaert, M.; Warrinnier, R.; Baken, S.; Gustafsson, J.-P.; De Vos, D.; Smolders, E. Phosphate-exchanged Mg–Al layered double hydroxides: a new slow release phosphate fertilizer. *ACS Sustainable Chemistry & Engineering* 2016, 4, 4280-4287.
178. Wang, X.; Lü, S.; Gao, C.; Feng, C.; Xu, X.; Bai, X.; Gao, N.; Yang, J.; Liu, M.; Wu, L. Recovery of ammonium and phosphate from wastewater by wheat straw-based amphoteric adsorbent and reusing as a multifunctional slow-release compound fertilizer. *ACS Sustainable Chemistry and Engineering* 2016, 4, 2068-2079.
179. Gerstl, Z.; Nasser, A.; Mingelgrin, U. Controlled release of pesticides into soils from clay - polymer formulations. *Journal of Agricultural and Food Chemistry* 1998, 46, 3797-3802.
180. Xu, X.; Bai, B.; Wang, H.; Suo, Y. A near-infrared and temperature-responsive pesticide release platform through core–shell polydopamine@PNIPAm nanocomposites. *ACS Applied Materials & Interfaces* 2017, 9, 6424-6432.
181. Chen, J.; Wang, W.; Xu, Y.; Zhang, X. Slow-release formulation of a new biological pesticide, pyoluteorin, with mesoporous silica. *Journal of Agricultural and Food Chemistry* 2011, 59, 307-311.
182. Zheng, H.; Shang, Q. Water suspension acetamiprid nano capsule preparation and its reparing method. . *Chem. Abs.* 2005, 143, 213751.
183. Wang, X.; Wang, Y.; Xiong, X.; Li, T.; Liang, J.; Chen, J. Aqueous nano insecticide suspension and its preparation process. *Chem Abs* 2004, 142.

184. Agarwal, S.; Sadeghi, N.; Tyagi, I.; Gupta, V. K.; Fakhri, A. Adsorption of toxic carbamate pesticide oxamyl from liquid phase by newly synthesized and characterized graphene quantum dots nanomaterials. *Journal of Colloid and Interface Science* 2016, 478, 430-438.
185. Maliyekkal, S. M.; Sreeprasad, T. S.; Krishnan, D.; Kouser, S.; Mishra, A. K.; Waghmare, U. V.; Pradeep, T. Graphene: a reusable substrate for unprecedented adsorption of pesticides. *Small* 2013, 9, 273-283.
186. Liu, X.; Zhang, H.; Ma, Y.; Wu, X.; Meng, L.; Guo, Y.; Yu, G.; Liu, Y. Graphene-coated silica as a highly efficient sorbent for residual organophosphorus pesticides in water. *Journal of Materials Chemistry A* 2013, 1, 1875-1884.
187. Gurunathan, S.; Han, J. W.; Dayem, A. A.; Eppakayala, V.; Kim, J.-H. Oxidative stress-mediated antibacterial activity of graphene oxide and reduced graphene oxide in Pseudomonas aeruginosa. *International Journal of Nanomedicine* 2012, 7, 5901-5914.
188. Chen, J.; Peng, H.; Wang, X.; Shao, F.; Yuan, Z.; Han, H. Graphene oxide exhibits broad-spectrum antimicrobial activity against bacterial phytopathogens and fungal conidia by intertwining and membrane perturbation. *Nanoscale* 2014, 6, 1879-1889.
189. Liu, S.; Hu, M.; Zeng, T. H.; Wu, R.; Jiang, R.; Wei, J.; Wang, L.; Kong, J.; Chen, Y. Lateral dimension-dependent antibacterial activity of graphene oxide sheets. *Langmuir* 2012, 28, 12364-12372.
190. Hui, L.; Piao, J.-G.; Auletta, J.; Hu, K.; Zhu, Y.; Meyer, T.; Liu, H.; Yang, L. Availability of the basal planes of graphene oxide determines whether it is antibacterial. *ACS Applied Materials & Interfaces* 2014, 6, 13183-13190.
191. Mangadlao, J. D.; Santos, C. M.; Felipe, M. J. L.; de Leon, A. C. C.; Rodrigues, D. F.; Advincula, R. C. On the antibacterial mechanism of graphene oxide (GO) Langmuir-Blodgett films. *Chemical Communications* 2015, 51, 2886-2889.
192. Al-Jumaili, A.; Alancherry, S.; Bazaka, K.; Jacob, M. V. Review on the antimicrobial properties of carbon nanostructures. *Materials* 2017, 10, 1066.
193. Wang, G.; Qian, F.; Saltikov, C. W.; Jiao, Y.; Li, Y. Microbial reduction of graphene oxide by Shewanella. *Nano Research* 2011, 4, 563-570.
194. Ruiz, O. N.; Fernando, K. A. S.; Wang, B.; Brown, N. A.; Luo, P. G.; McNamara, N. D.; Vangsness, M.; Sun, Y.-P.; Bunker, C. E. Graphene oxide: A nonspecific enhancer of cellular growth. *ACS Nano* 2011, 5, 8100-8107.
195. Akhavan, O.; Ghaderi, E. Toxicity of graphene and graphene oxide nanowalls against bacteria. *ACS Nano* 2010, 4, 5731-5736.
196. Cheng, M.; Lowe, B. A.; Spencer, T. M.; Ye, X.; Armstrong, C. L. Factors influencing Agrobacterium-mediated transformation of monocotyledonous species. *In Vitro Cellular & Developmental Biology - Plant* 2004, 40, 31-45.
197. Klein, T. M.; Wolf, E. D.; Wu, R.; Sanford, J. C. High-velocity microprojectiles for delivering nucleic acids into living cells. *Nature* 1987, 327, 70.
198. Hu, H.; Tang, C.; Yin, C. Folate conjugated trimethyl chitosan/graphene oxide nanocomplexes as potential carriers for drug and gene delivery. *Materials Letters* 2014, 125, 82-85.
199. Teimouri, M.; Nia, A. H.; Abnous, K.; Eshghi, H.; Ramezani, M. Graphene oxide-cationic polymer conjugates: Synthesis and application as gene delivery vectors. *Plasmid* 2016, 84-85, 51-60.
200. Liu, X.; Ma, D.; Tang, H.; Tan, L.; Xie, Q.; Zhang, Y.; Ma, M.; Yao, S. Polyamidoamine dendrimer and oleic acid-functionalized graphene as biocompatible and efficient gene delivery vectors. *ACS Applied Materials & Interfaces* 2014, 6, 8173-8183.
201. Tian, B.; Wang, C.; Zhang, S.; Feng, L.; Liu, Z. Photothermally enhanced photodynamic therapy delivered by nano-graphene oxide. *ACS Nano* 2011, 5, 7000-7009.
202. Cao, X.; Zheng, S.; Zhang, S.; Wang, Y.; Yang, X.; Duan, H.; Huang, Y.; Chen, Y. Functionalized graphene oxide with hepatocyte targeting as anti-tumor drug and gene intracellular transporters. *Journal of Nanoscience and Nanotechnology* 2015, 15, 2052-2059.
203. Shen, H.; Liu, M.; He, H.; Zhang, L.; Huang, J.; Chong, Y.; Dai, J.; Zhang, Z. PEGylated graphene oxide-mediated protein delivery for cell function regulation. *ACS Applied Materials and Interfaces* 2012, 4, 6317-6323.
204. Li, H.; Fierens, K.; Zhang, Z.; Vanparijs, N.; Schuijs, M. J.; Van Steendam, K.; Feiner Gracia, N.; De Rycke, R.; De Beer, T.; De Beuckelaer, A.; De Koker, S.; Deforce, D.; Albertazzi, L.; Grooten, J.; Lambrecht, B. N.; De Geest, B. G. Spontaneous protein adsorption on graphene oxide nanosheets

allowing efficient intracellular vaccine protein delivery. *ACS Applied Materials and Interfaces* 2016, 8, 1147-1155.
205. Chen, S.; Brown, L.; Levendorf, M.; Cai, W.; Ju, S.-Y.; Edgeworth, J.; Li, X.; Magnuson, C. W.; Velamakanni, A.; Piner, R. D.; Kang, J.; Park, J.; Ruoff, R. S. Oxidation resistance of graphene-coated Cu and Cu/Ni alloy. *ACS Nano* 2011, 5, 1321-1327.
206. Prasai, D.; Tuberquia, J. C.; Harl, R. R.; Jennings, G. K.; Bolotin, K. I. Graphene: Corrosion-inhibiting coating. *ACS Nano* 2012, 6, 1102-1108.
207. He, W.; Zhu, L.; Chen, H.; Nan, H.; Li, W.; Liu, H.; Wang, Y. Electrophoretic deposition of graphene oxide as a corrosion inhibitor for sintered NdFeB. *Applied Surface Science* 2013, 279, 416-423.
208. Singh, B. P.; Nayak, S.; Nanda, K. K.; Jena, B. K.; Bhattacharjee, S.; Besra, L. The production of a corrosion resistant graphene reinforced composite coating on copper by electrophoretic deposition. *Carbon* 2013, 61, 47-56.
209. Nine, M. J.; Kabiri, S.; Tung, T. T.; Tran, D. N. H.; Losic, D. Electrostatic powder coatings of pristine graphene: A new approach for coating of granular and fibril substrates. *Applied Surface Science* 2018, 441, 187-193.
210. Nine, M. J.; Cole, M. A.; Johnson, L.; Tran, D. N. H.; Losic, D. Robust superhydrophobic graphene-based composite coatings with self-cleaning and corrosion barrier properties. *ACS Applied Materials & Interfaces* 2015, 7, 28482-28493.
211. Li, P. F.; Zhou, H.; Cheng, X. Investigation of a hydrothermal reduced graphene oxide nano coating on Ti substrate and its nano-tribological behavior. *Surface and Coatings Technology* 2014, 254, 298-304.
212. Anandan, S.; Narasinga Rao, T.; Sathish, M.; Rangappa, D.; Honma, I.; Miyauchi, M. Superhydrophilic graphene-loaded TiO_2 thin film for self-cleaning applications. *ACS Applied Materials & Interfaces* 2013, 5, 207-212.
213. Nine, M. J.; Tran, D. N. H.; Tung, T. T.; Kabiri, S.; Losic, D. Graphene-borate as an efficient fire retardant for cellulosic materials with multiple and synergetic modes of action. *ACS Applied Materials & Interfaces* 2017, 9, 10160-10168.
214. Su, Y.; Kravets, V. G.; Wong, S. L.; Waters, J.; Geim, A. K.; Nair, R. R. Impermeable barrier films and protective coatings based on reduced graphene oxide. *Nature Communications* 2014, 5, 4843.
215. Sahu, S. C.; Samantara, A. K.; Seth, M.; Parwaiz, S.; Singh, B. P.; Rath, P. C.; Jena, B. K. A facile electrochemical approach for development of highly corrosion protective coatings using graphene nanosheets. *Electrochemistry Communications* 2013, 32, 22-26.
216. Yu, L.; Lim, Y.-S.; Han, J. H.; Kim, K.; Kim, J. Y.; Choi, S.-Y.; Shin, K. A graphene oxide oxygen barrier film deposited via a self-assembly coating method. *Synthetic Metals* 2012, 162, 710-714.
217. Wang, X.; Song, L.; Yang, H.; Lu, H.; Hu, Y. Synergistic effect of graphene on antidripping and fire resistance of intumescent flame retardant poly(butylene succinate) composites. *Industrial & Engineering Chemistry Research* 2011, 50, 5376-5383.
218. Zhang, M.; Gao, B.; Chen, J.; Li, Y.; Creamer, A. E.; Chen, H. Slow-release fertilizer encapsulated by graphene oxide films. *Chemical Engineering Journal* 2014, 255, 107-113.
219. Huang, T. C.; Yeh, J. M.; Lai, C. Y. 18 - Polymer nanocomposite coatings A2 - Gao, Fengge. In *Advances in Polymer Nanocomposites*, Woodhead Publishing: 2012; pp 605-638.
220. Dorri Moghadam, A.; Omrani, E.; Menezes, P. L.; Rohatgi, P. K. Mechanical and tribological properties of self-lubricating metal matrix nanocomposites reinforced by carbon nanotubes (CNTs) and graphene – A review. *Composites Part B: Engineering* 2015, 77, 402-420.
221. Chuah, S.; Pan, Z.; Sanjayan, J. G.; Wang, C. M.; Duan, W. H. Nano reinforced cement and concrete composites and new perspective from graphene oxide. *Construction and Building Materials* 2014, 73, 113-124.
222. Bhattacharya, M. Polymer nanocomposites—A comparison between carbon nanotubes, graphene, and clay as nanofillers. *Materials* 2016, 9, 262.
223. Mittal, G.; Dhand, V.; Rhee, K. Y.; Park, S.-J.; Lee, W. R. A review on carbon nanotubes and graphene as fillers in reinforced polymer nanocomposites. *Journal of Industrial and Engineering Chemistry* 2015, 21, 11-25.

224. Rashad, M.; Pan, F.; Tang, A.; Lu, Y.; Asif, M.; Hussain, S.; She, J.; Gou, J.; Mao, J. Effect of graphene nanoplatelets (GNPs) addition on strength and ductility of magnesium-titanium alloys. *Journal of Magnesium and Alloys* 2013, 1, 242-248.
225. Sharma, S.; Kothiyal, N. C. Comparative effects of pristine and ball-milled graphene oxide on physico-chemical characteristics of cement mortar nanocomposites. *Construction and Building Materials* 2016, 115, 256-268.
226. Kim, H.; Abdala, A. A.; Macosko, C. W. Graphene/Polymer nanocomposites. *Macromolecules* 2010, 43, 6515-6530.
227. Pazat, A.; Barrès, C.; Bruno, F.; Janin, C.; Beyou, E. Preparation and properties of elastomer composites containing "Graphene"-based fillers: A review. *Polymer Reviews* 2017, 1-41.
228. Palacios, J. J.; Fernández-Rossier, J. *Phys. Rev. B* 2008, 77, 195428.
229. Rehberg, B. E.; Hall, W. L. Fertilizer compositions and method of making such compositions. U.S. Patent US 5238480 A: 1993.
230. Walker, G. M.; Magee, T. R. A.; Holland, C. R.; Ahmad, M. N.; Fox, N.; Moffatt, N. A. Compression testing of granular NPK fertilizers. *Nutrient Cycling in Agroecosystems* 1997, 48, 231-234.
231. Matejovic, I. Determination of carbon and nitrogen in samples of various soils by the dry combustion. *Communications in Soil Science and Plant Analysis* 1997, 28, 1499-1511.
232. Hignett, T. P. Physical and chemical properties of fertilizers and methods for their determination. In *Fertilizer Manual*, Hignett, T. P., Ed. Springer Netherlands: Dordrecht, 1985; pp 284-316.
233. Aylen, P. B.; Blyth, J. C. Particulate urea with finely divided inorganic material incorporated for hardness nonfriability and anti-caking. U.S .Patent US 5782951 A: 1998.
234. Blouin, G. M. Production of high-strength, storage-stable particulate urea. US Patent 4587358: 1986.
235. Detroit, W. J. Lignosulfonate treated fertilizer particles. U.S. Patent US 4846871 A: 1989.
236. Mark Stephen, R.; Tommy, C. D. Binding agents effect on physical and chemical attributes of nitrogen-fortified poultry litter and biosolids granules. 2013, 56.
237. Justino, C. I. L.; Gomes, A. R.; Freitas, A. C.; Duarte, A. C.; Rocha-Santos, T. A. P. Graphene based sensors and biosensors. *TrAC Trends in Analytical Chemistry* 2017, 91, 53-66.
238. Zaporotskova, I. V.; Boroznina, N. P.; Parkhomenko, Y. N.; Kozhitov, L. V. Carbon nanotubes: Sensor properties. A review. *Modern Electronic Materials* 2016, 2, 95-105.
239. Gooding, J. J. Nanostructuring electrodes with carbon nanotubes: A review on electrochemistry and applications for sensing. *Electrochimica Acta* 2005, 50, 3049-3060.
240. He, Q.; Wu, S.; Yin, Z.; Zhang, H. Graphene-based electronic sensors. *Chemical Science* 2012, 3, 1764-1772.
241. Pumera, M.; Ambrosi, A.; Bonanni, A.; Chng, E. L. K.; Poh, H. L. Graphene for electrochemical sensing and biosensing. *TrAC - Trends in Analytical Chemistry* 2010, 29, 954-965.
242. Justino, C. I. L.; Rocha-Santos, T. A.; Duarte, A. C.; Rocha-Santos, T. A. Review of analytical figures of merit of sensors and biosensors in clinical applications. *TrAC Trends in Analytical Chemistry* 2010, 29, 1172-1183.
243. Velasco-Garcia, M. N.; Mottram, T. Biosensor technology addressing agricultural problems. *Biosystems Engineering* 2003, 84, 1-12.
244. Huangfu, C.; Fu, L.; Li, Y.; Li, X.; Du, H.; Ye, J. Sensitive stripping determination of cadmium(ii) and lead(ii) on disposable graphene modified screen-printed electrode. *Electroanalysis* 2013, 25, 2238-2243.
245. Chen, M.; Chao, M.; Ma, X. Poly(crystal violet)/graphene-modified electrode for the simultaneous determination of trace lead and cadmium ions in water samples. *Journal of Applied Electrochemistry* 2014, 44, 337-344.
246. Chaiyo, S.; Mehmeti, E.; Žagar, K.; Siangproh, W.; Chailapakul, O.; Kalcher, K. Electrochemical sensors for the simultaneous determination of zinc, cadmium and lead using a Nafion/ionic liquid/graphene composite modified screen-printed carbon electrode. *Analytica Chimica Acta* 2016, 918, 26-34.

247. Wu, L.; Fu, X.; Liu, H.; Li, J.; Song, Y. Comparative study of graphene nanosheet- and multiwall carbon nanotube-based electrochemical sensor for the sensitive detection of cadmium. *Analytica Chimica Acta* 2014, 851, 43-48.
248. Martín-Yerga, D.; González-García, M. B.; Costa-García, A. Use of nanohybrid materials as electrochemical transducers for mercury sensors. *Sensors and Actuators, B: Chemical* 2012, 165, 143-150.
249. Zhou, N.; Li, J.; Chen, H.; Liao, C.; Chen, L. A functional graphene oxide-ionic liquid composites-gold nanoparticle sensing platform for ultrasensitive electrochemical detection of Hg2+. *Analyst* 2013, 138, 1091-1097.
250. Cui, X.; Zhu, L.; Wu, J.; Hou, Y.; Wang, P.; Wang, Z.; Yang, M. A fluorescent biosensor based on carbon dots-labeled oligodeoxyribonucleotide and graphene oxide for mercury (II) detection. *Biosensors and Bioelectronics* 2015, 63, 506-512.
251. Li, J.; Li, N.; Ma, M.; Giesy, J. P.; Wang, Z. In vitro profiling of the endocrine disrupting potency of organochlorine pesticides. *Toxicology Letters* 2008, 183, 65-71.
252. Sinclair, C. J.; Boxall, A. B. A. Assessing the ecotoxicity of pesticide transformation products. *Environmental Science & Technology* 2003, 37, 4617-4625.
253. Li, X.; Zheng, Z.; Liu, X.; Zhao, S.; Liu, S. Nanostructured photoelectrochemical biosensor for highly sensitive detection of organophosphorous pesticides. *Biosensors and Bioelectronics* 2015, 64, 1-5.
254. Wang, R.; Yan, K.; Wang, F.; Zhang, J. A highly sensitive photoelectrochemical sensor for 4-aminophenol based on CdS-graphene nanocomposites and molecularly imprinted polypyrrole. *Electrochimica Acta* 2014, 121, 102-108.
255. Yang, L.; Wang, G.; Liu, Y.; Wang, M. Development of a biosensor based on immobilization of acetylcholinesterase on NiO nanoparticles–carboxylic graphene–nafion modified electrode for detection of pesticides. *Talanta* 2013, 113, 135-141.
256. Oren, S.; Ceylan, H.; Schnable, P. S.; Dong, L. High-resolution patterning and transferring of graphene-based nanomaterials onto tape toward roll-to-roll production of tape-based wearable sensors. *Advanced Materials Technologies* 2017, 2, 1700223-n/a.
257. Lee, K.; Park, J.; Lee, M.-S.; Kim, J.; Hyun, B. G.; Kang, D. J.; Na, K.; Lee, C. Y.; Bien, F.; Park, J.-U. In-situ synthesis of carbon nanotube–graphite electronic devices and their integrations onto surfaces of live plants and insects. *Nano Letters* 2014, 14, 2647-2654.
258. Joshi, R. K.; Gomez, H.; Alvi, F.; Kumar, A. Graphene films and ribbons for sensing of O_2, and 100 ppm of CO and NO_2 in practical conditions. *The Journal of Physical Chemistry C* 2010, 114, 6610-6613.
259. Ganhua, L.; Leonidas, E. O.; Junhong, C. Reduced graphene oxide for room-temperature gas sensors. *Nanotechnology* 2009, 20, 445502.
260. Mao, S.; Cui, S.; Lu, G.; Yu, K.; Wen, Z.; Chen, J. Tuning gas-sensing properties of reduced graphene oxide using tin oxide nanocrystals. *Journal of Materials Chemistry* 2012, 22, 11009-11013.
261. Gautam, M.; Jayatissa, A. H. Gas sensing properties of graphene synthesized by chemical vapor deposition. *Materials Science and Engineering: C* 2011, 31, 1405-1411.
262. Al-Mashat, L.; Shin, K.; Kalantar-zadeh, K.; Plessis, J. D.; Han, S. H.; Kojima, R. W.; Kaner, R. B.; Li, D.; Gou, X.; Ippolito, S. J.; Wlodarski, W. Graphene/Polyaniline nanocomposite for hydrogen sensing. *The Journal of Physical Chemistry C* 2010, 114, 16168-16173.
263. Huang, X.; Hu, N.; Gao, R.; Yu, Y.; Wang, Y.; Yang, Z.; Siu-Wai Kong, E.; Wei, H.; Zhang, Y. Reduced graphene oxide-polyaniline hybrid: Preparation, characterization and its applications for ammonia gas sensing. *Journal of Materials Chemistry* 2012, 22, 22488-22495.
264. Fowler, J. D.; Allen, M. J.; Tung, V. C.; Yang, Y.; Kaner, R. B.; Weiller, B. H. Practical chemical sensors from chemically derived graphene. *ACS Nano* 2009, 3, 301-306.
265. Li, X.; Chen, X.; Yao, Y.; Li, N.; Chen, X. High-stability quartz crystal microbalance ammonia sensor utilizing graphene oxide isolation layer. *Sensors and Actuators, B: Chemical* 2014, 196, 183-188.
266. Mishra, S. K.; Tripathi, S. N.; Choudhary, V.; Gupta, B. D. Surface plasmon resonance-based fiber optic methane gas sensor utilizing graphene-carbon nanotubes-poly(methyl methacrylate) hybrid nanocomposite. *Plasmonics* 2015, 10, 1147-1157.

267. Lalwani, G.; D'Agati, M.; Khan, A. M.; Sitharaman, B. Toxicology of graphene-based nanomaterials. *Advanced drug delivery reviews* 2016, 105, 109-144.
268. Guo, X.; Mei, N. Assessment of the toxic potential of graphene family nanomaterials. *Journal of Food and Drug Analysis* 2014, 22, 105-115.
269. Yan, S.; Zhao, L.; Li, H.; Zhang, Q.; Tan, J.; Huang, M.; He, S.; Li, L. Single-walled carbon nanotubes selectively influence maize root tissue development accompanied by the change in the related gene expression. *Journal of Hazardous Materials* 2013, 246-247, 110-118.
270. Ghosh, M.; Bhadra, S.; Adegoke, A.; Bandyopadhyay, M.; Mukherjee, A. MWCNT uptake in Allium cepa root cells induces cytotoxic and genotoxic responses and results in DNA hyper-methylation. *Mutation Research/Fundamental and Molecular Mechanisms of Mutagenesis* 2015, 774, 49-58.
271. Ghosh, M.; Chakraborty, A.; Bandyopadhyay, M.; Mukherjee, A. Multi-walled carbon nanotubes (MWCNT): Induction of DNA damage in plant and mammalian cells. *Journal of Hazardous Materials* 2011, 197, 327-336.
272. Katti, D. R.; Sharma, A.; Pradhan, S. M.; Katti, K. S. Carbon nanotube proximity influences rice DNA. *Chemical Physics* 2015, 455, 17-22.
273. Begum, P.; Fugetsu, B. Phytotoxicity of multi-walled carbon nanotubes on red spinach (Amaranthus tricolor L) and the role of ascorbic acid as an antioxidant. *Journal of Hazardous Materials* 2012, 243, 212-222.
274. Liu, Q.; Zhang, X.; Zhao, Y.; Lin, J.; Shu, C.; Wang, C.; Fang, X. Fullerene-Induced increase of glycosyl residue on living plant cell wall. *Environmental Science & Technology* 2013, 47, 7490-7498.
275. Begum, P.; Ikhtiari, R.; Fugetsu, B.; Matsuoka, M.; Akasaka, T.; Watari, F. Phytotoxicity of multi-walled carbon nanotubes assessed by selected plant species in the seedling stage. *Applied Surface Science* 2012, 262, 120-124.
276. Cañas, J. E.; Long, M.; Nations, S.; Vadan, R.; Dai, L.; Luo, M.; Ambikapathi, R.; Lee, E. H.; Olszyk, D. Effects of functionalized and nonfunctionalized single-walled carbon nanotubes on root elongation of select crop species. *Environmental Toxicology and Chemistry* 2008, 27, 1922-1931.
277. Stampoulis, D.; Sinha, S. K.; White, J. C. Assay-dependent phytotoxicity of nanoparticles to plants. *Environmental Science & Technology* 2009, 43, 9473-9479.
278. Tiwari, D. K.; Dasgupta-Schubert, N.; Villaseñor Cendejas, L. M.; Villegas, J.; Carreto Montoya, L.; Borjas García, S. E. Interfacing carbon nanotubes (CNT) with plants: Enhancement of growth, water and ionic nutrient uptake in maize (Zea mays) and implications for nanoagriculture. *Applied Nanoscience* 2014, 4, 577-591.
279. Lahiani, M. H.; Dervishi, E.; Chen, J.; Nima, Z.; Gaume, A.; Biris, A. S.; Khodakovskaya, M. V. Impact of carbon nanotube exposure to seeds of valuable crops. *ACS Applied Materials & Interfaces* 2013, 5, 7965-7973.
280. Liu, S. W., Hongmin; Li, Zhiyang; Li, Shun; Yan, Han; He, Yong; Tian, Zhihong. Effect of graphene on germinattion and seedling morphology in rice. *Jouranl of Nanoscience and Nanotechnology* 2015, 15, 17.
281. Begum, P.; Ikhtiari, R.; Fugetsu, B. Graphene phytotoxicity in the seedling stage of cabbage, tomato, red spinach, and lettuce. *Carbon* 2011, 49, 3907-3919.
282. Kasel, D.; Bradford, S. A.; Šimůnek, J.; Pütz, T.; Vereecken, H.; Klumpp, E. Limited transport of functionalized multi-walled carbon nanotubes in two natural soils. *Environmental Pollution* 2013, 180, 152-158.
283. Khodakovskaya, M. V.; De Silva, K.; Nedosekin, D. A.; Dervishi, E.; Biris, A. S.; Shashkov, E. V.; Galanzha, E. I.; Zharov, V. P. Complex genetic, photothermal, and photoacoustic analysis of nanoparticle-plant interactions. *Proceedings of the National Academy of Sciences of the United States of America* 2011, 108, 1028-1033.
284. Hu, X.; Zhou, Q. Novel hydrated graphene ribbon unexpectedly promotes aged seed germination and root differentiation. *Scientific Reports* 2014, 4, 3782.
285. Zhang, M.; Gao, B.; Chen, J.; Li, Y. Effects of graphene on seed germination and seedling growth. *Journal of Nanoparticle Research* 2015, 17, 78.

286. Anjum, N. A.; Singh, N.; Singh, M. K.; Shah, Z. A.; Duarte, A. C.; Pereira, E.; Ahmad, I. Single-bilayer graphene oxide sheet tolerance and glutathione redox system significance assessment in faba bean (Vicia faba L.). *Journal of Nanoparticle Research* 2013, 15, 1770.
287. Anjum, N. A.; Singh, N.; Singh, M. K.; Sayeed, I.; Duarte, A. C.; Pereira, E.; Ahmad, I. Single-bilayer graphene oxide sheet impacts and underlying potential mechanism assessment in germinating faba bean (Vicia faba L.). *Science of The Total Environment* 2014, 472, 834-841.
288. Chung, H.; Kim, M. J.; Ko, K.; Kim, J. H.; Kwon, H.-a.; Hong, I.; Park, N.; Lee, S.-W.; Kim, W. Effects of graphene oxides on soil enzyme activity and microbial biomass. *Science of The Total Environment* 2015, 514, 307-313.
289. Hu, X.; Kang, J.; Lu, K.; Zhou, R.; Mu, L.; Zhou, Q. Graphene oxide amplifies the phytotoxicity of arsenic in wheat. *Scientific Reports* 2014, 4, 6122.
290. Xiong, T.; Yuan, X.; Wang, H.; Leng, L.; Li, H.; Wu, Z.; Jiang, L.; Xu, R.; Zeng, G. Implication of graphene oxide in Cd-contaminated soil: A case study of bacterial communities. *Journal of Environmental Management* 2018, 205, 99-106.
291. Du, J.; Hu, X.; Zhou, Q. Graphene oxide regulates the bacterial community and exhibits property changes in soil. *RSC Advances* 2015, 5, 27009-27017.
292. He, Y.; Hu, R.; Zhong, Y.; Zhao, X.; Chen, Q.; Zhu, H. Graphene oxide as a water transporter promoting germination of plants in soil. *Nano Research* 2018, 11, 1928-1937.
293. Xing, W.; Lalwani, G.; Rusakova, I.; Sitharaman, B. Degradation of graphene by hydrogen peroxide. *Particle & Particle Systems Characterization* 2014, 31, 745-750.
294. Kotchey, G. P.; Allen, B. L.; Vedala, H.; Yanamala, N.; Kapralov, A. A.; Tyurina, Y. Y.; Klein-Seetharaman, J.; Kagan, V. E.; Star, A. The enzymatic oxidation of graphene oxide. *ACS Nano* 2011, 5, 2098-2108.
295. Lalwani, G.; Xing, W.; Sitharaman, B. Enzymatic degradation of oxidized and reduced graphene nanoribbons by lignin peroxidase. *Journal of materials chemistry. B, Materials for biology and medicine* 2014, 2, 6354-6362.

Chapter 3

Graphene oxide: A new carrier for slow release of plant micronutrient

This section is included in the thesis as it appears as a journal paper published by **Shervin Kabiri,** Fien Degryse, Diana N.H. Tran, Rodrigo C. da Silva, Mike J. McLaughlin and Dusan Losic, "Graphene Oxide: A New Carrier for Slow Release of Plant Micronutrients", ***Journal of ACS Appl . Mater Interfaces,*** 2017, 9, 43325-43335.

Statement of Authorship

Title of Paper	Graphene Oxide: a New Carrier for Slow Release of Plant Micronutrient
Publication Status	☑ Published ☐ Accepted for Publication ☐ Submitted for Publication ☐ Unpublished and Unsubmitted w ork w ritten in manuscript style
Publication Details	Journal of ACS Applied material and Interfaces, 2017

Principal Author

Name of Principal Author (Candidate)	Shervin Kabiri		
Contribution to the Paper	Under the supervision of Dusan Losic, Michael McLaughlin and Diana Tran, I developed, designed and conducted the experiments, interpreted and processed the data and wrote the manuscript for submission.		
Overall percentage (%)	85		
Certification:	This paper reports on original research I conducted during the period of my Higher Degree by Research candidature and is not subject to any obligations or contractual agreements with a third party that would constrain its inclusion in this thesis. I am the primary author of this paper.		
Signature		Date	22/06/2018

Co-Author Contributions

By signing the Statement of Authorship, each author certifies that:

i. the candidate's stated contribution to the publication is accurate (as detailed above);

ii. permission is granted for the candidate in include the publication in the thesis; and

iii. the sum of all co-author contributions is equal to 100% less the candidate's stated contribution.

Name of Co-Author	Fien Degryse		
Contribution to the Paper	I helped Shervin Kabiri (candidate) with interpreting experimental results and improving the manuscript for submission. I give consent for Shervin Kabiri to present this paper for examination towards the Doctorate of philosophy.		
Signature		Date	22/062018

Name of Co-Author	Rodrigo C. da Silva		
Contribution to the Paper	I helped Shervin Kabiri (candidate) with interpreting experimental results and improving the manuscript for submission. I give consent for Shervin Kabiri to present this paper for examination towards the Doctorate of philosophy.		
Signature		Date	22/06/218

Name of Co-Author	Diana N.H. Tran		
Contribution to the Paper	I acted as the secondary supervisor for Shervin Kabiri and helped her to design the experiments and improve the final drafts of the manuscript for submission. I give consent for Shervin Kabiri to present this paper for examination towards the Doctorate of philosophy.		
Signature		Date	22/06/2018

Name of Co-Author	Mike J. McLaughlin		
Contribution to the Paper	I acted as the secondary supervisor for Shervin Kabiri and aided in design and development of experiments and evaluation of manuscript for submission. I give consent for Shervin Kabiri to present this paper for examination towards the Doctorate of philosophy.		
Signature		Date	22/06/2018

Name of Co-Author	Dusan Losic		
Contribution to the Paper	I acted as the primary supervisor for Shervin Kabiri and aided in design and development of experiments and evaluation of manuscript for submission. I give consent for Shervin Kabiri to present this paper for examination towards the Doctorate of philosophy.		
Signature		Date	22/06/2018

ACS APPLIED MATERIALS & INTERFACES

Research Article

Cite This: ACS Appl. Mater. Interfaces 2017, 9, 43325−43335

www.acsami.org

Graphene Oxide: A New Carrier for Slow Release of Plant Micronutrients

Shervin Kabiri,[†,§] Fien Degryse,[‡] Diana N. H. Tran,[†,§] Rodrigo C. da Silva,[‡] Mike J. McLaughlin,[*,‡] and Dusan Losic[*,†,§]

[†]School of Chemical Engineering, The University of Adelaide, Engineering North Building, Adelaide, SA 5005, Australia

[‡]Fertilizer Technology Research Centre, School of Agriculture, Food and Wine, The University of Adelaide, Waite Campus, PMB1, Glen Osmond, SA 5064, Australia

[§]ARC Research Hub for Graphene Enabled Industry Transformation, The University of Adelaide, South Australia, 5005 Australia

Supporting Information

ABSTRACT: The environmental problems and low efficiency associated with conventional fertilizers provides an impetus to develop advanced fertilizers with slower release and better performances. Here, we report of development of a new carrier platform based on graphene oxide (GO) sheets that can provide a high loading of plant micronutrients with controllable slow release. To prove this concept, two micronutrients, zinc (Zn) and copper (Cu), were used to load on GO sheets and hence formulate GO-based micronutrients fertilizer. The chemical composition and successful loading of both nutrients on GO sheets were confirmed by X-ray photoelectron spectroscopy, thermogravimetric analysis, and X-ray diffraction (XRD). The prepared Zn-graphene oxide (Zn−GO) and Cu-graphene oxide (Cu−GO) fertilizers showed a biphasic dissolution behavior compared to that of commercial zinc sulfate and copper sulfate fertilizer granules, displaying desirable fast and slow micronutrient release. A visualization method and chemical analysis were used to assess the release and diffusion of Cu and Zn in soil from GO-based fertilizers compared with commercial soluble fertilizers to demonstrate the advantages of GO carriers and show their capability to be used as a generic platform for macro- and micronutrients delivery. A pot trial demonstrated that Zn and Cu uptake by wheat was higher when using GO-based fertilizers compared to that when using standard zinc or copper salts. This is the first report on the agronomic performance of GO-based slow-release fertilizer.

KEYWORDS: *graphene oxide, micronutrients, slow release, fertilizers, carrier*

■ INTRODUCTION

Plant micronutrients are only needed in small amounts but are essential for the growth and development of crops. Therefore, micronutrient fertilizers have been applied for many years to optimize plant yield.[1] Among the essential trace elements, zinc (Zn) plays a critical role in maintaining healthy root systems, in activating enzymes and detoxifying free radicals, and in preserving tolerance to plant stressors.[2] Zinc deficiency not only affects crop growth but also is critical for human health. Zinc deficiency is the fifth leading risk factor for illness and death of children in developing countries where grain is an essential component of their staple diets.[3] Copper (Cu) is also considered as one of the essential trace elements for plant growth and development. It has vital roles in the metabolism of plants and controlling fungal disease.[4] Although the plant's demand for Cu is relatively low compared with most other micronutrients, the consequence of Cu deficiency is still devastating to plants and may result in poor crop yields affecting food supplies.[5]

Most of the conventional micronutrients applied as fertilizers globally are water-soluble salts that include mainly sulfates or their chelated forms. In acidic sandy soils and high rainfall environments, soluble and chelated micronutrients may be lost by leaching and run-off, which leads to high dosage requirements, serious environmental problems, and economic costs.[6,7] Another limiting factor is the strong retention of micronutrients in soil, either through strong adsorption reactions to clays and organic matter or precipitation of insoluble compounds in the soil that dramatically reduce the efficacy of micronutrient fertilizers. One method that has been considered as a solution for these problems involves the use of slow-release fertilizers (SRFs) or controlled-release fertilizers (CRFs) that provide plant essential nutrients in a slower mode compared with traditional fertilizers. CRFs may play an

Received: July 4, 2017
Accepted: November 21, 2017
Published: November 21, 2017

DOI: 10.1021/acsami.7b07890
ACS Appl. Mater. Interfaces 2017, 9, 43325−43335

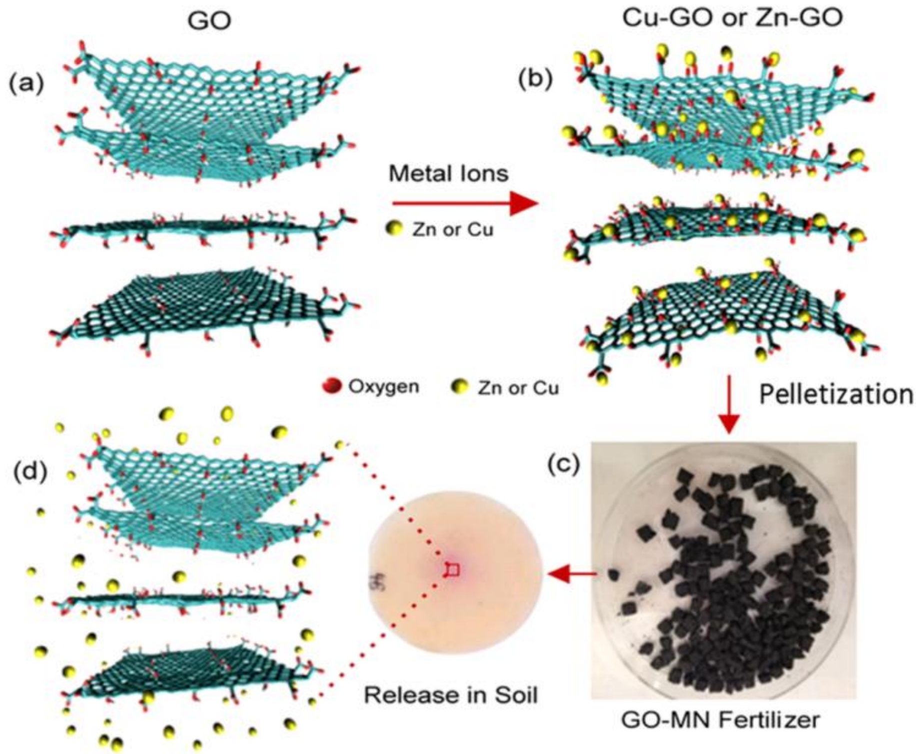

Figure 1. Schematic of the preparation and release of slow-release micronutrients graphene oxide-zinc/copper-based fertilizers. (a) GO prepared from natural graphite rocks by the acid exfoliation process with different functional groups (−OH and −COOH) used as the micronutrient carrier, (b) GO sheets loading with micronutrients, Cu or Zn metal ions attached to the oxygen functional groups on the surface and edges of the sheets, (c) photos of the prepared GO-micronutrient (GO-MN) fertilizer in form of the pellets (Cu−GO or Zn−GO), and (d) the release study in soil using prepared pellets (Cu−GO or Zn−GO) showing slow release of micronutrients from GO carriers.

important role in increasing crop efficiency due to sustained correction of mineral deficiency and reductions in the frequency of fertilization, thereby minimizing costs and reducing environmental pollution.[8] Therefore, development of CRF technologies to control the release of nutrients from soluble fertilizers has attracted tremendous attention in last two decades.[9] Currently, most research on CRF technologies is directed to regulating nitrogen (N) release from fertilizers. Very few types of controlled-release micronutrient fertilizers are commercially available, and they are generally based on insoluble oxides and their mixture with polyphosphates.[10] This concept using a short-chain polyphosphate has been explored for the slow release of Cu- and Zn-based micronutrient fertilizers.[6,11,12] Although these formulations have suitable properties for SRFs, their major drawback is the very high cost, hence making them unprofitable for broad acre farming.[13,14] The release mechanisms of the nutrients from these CRFs are based on either diffusion through their coating or slow hydrolysis. However, soil parameters such as water content, pH, ionic content, and temperature are other factors that affect nutrient release by hydrolysis or diffusion. Therefore, there is a potential mismatch between the release rates of the micronutrients to the soil and the required rate of nutrient uptake by crops.[7,15]

In the past few years, graphene has attracted enormous research interests due to its unique 2-D structure, high surface area, and remarkable structural, mechanical, thermal, optical, and electrical properties desired for many applications.[16−19] One of the most common approaches to graphene-based materials is to use of graphene oxide (GO) because of its scalable and low cost production from graphite.[20] Graphene oxide is a water-dispersible derivative of graphene showing high density of oxygen functional groups (carboxyl, hydroxyl, carbonyl, and epoxy) in the carbon lattice and is produced by chemical oxidation of graphite.[21] The presence of different oxygen functional groups on the surface and edges of GO sheets makes it a unique and easily accessible substrate for multivalent functionalization and efficient loading of molecules.[22] Since 2008, after the first report by Dai et al.[23] showing the use of GO as an efficient nanocarrier for drug delivery, enormous number of studies have been carried out to explore and apply GO carriers for widespread biomedical applications ranging from drug/gene delivery, plant biology, and biological sensing and imaging to biocompatible scaffold for cell culture.[24−28] The exciting achievements obtained on biomedical applications of graphene make these materials very attractive for nutrient delivery in agriculture and development of a novel class of slow-release fertilizers.

Beyond the biomedical application of graphene-based materials, a variety of studies have described the applications of these materials for the removal of inorganic species from aquatic environments.[20,29] Most of these studies have employed GO as adsorbent for the removal of metal ions from water due to GO's high content of oxygen functional groups available for interaction with metal ions. Furthermore, the high specific surface area (theoretical 2620 m^2 g^{-1}) of graphene-based materials make them an ideal candidate for processes involving adsorption or surface reactions.[30,31] The adsorption capacity of

DOI: 10.1021/acsami.7b07890
ACS Appl. Mater. Interfaces 2017, 9, 43325−43335

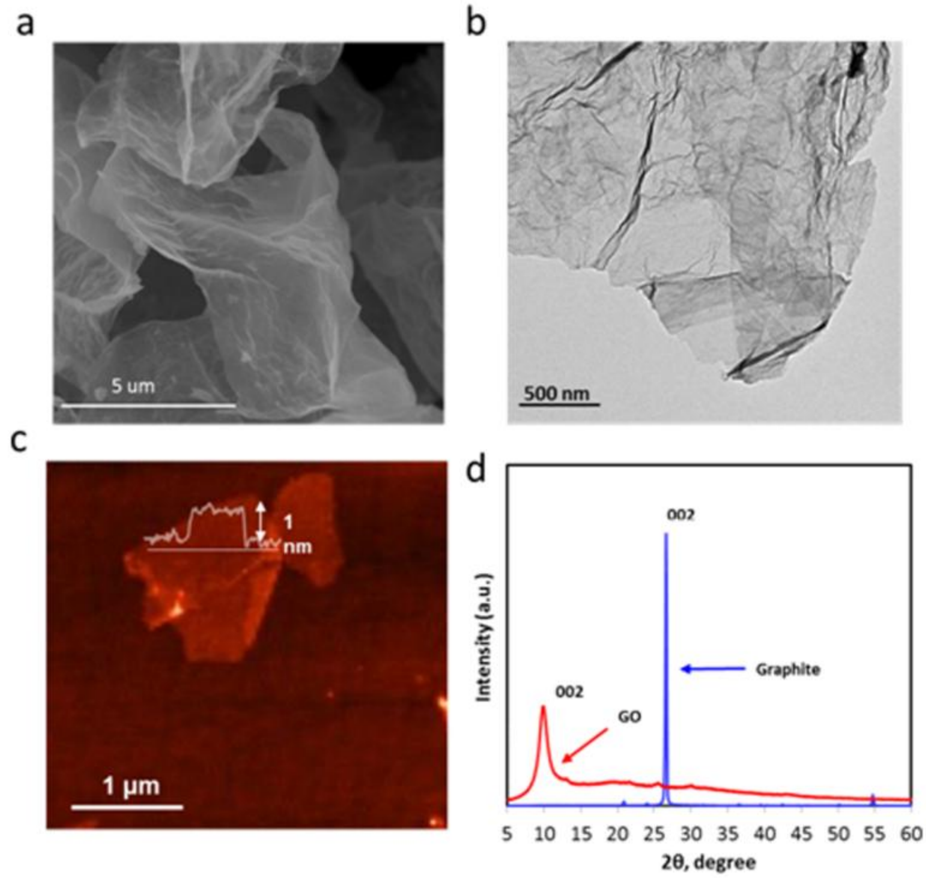

Figure 2. Characterization of graphene oxide (GO) used as micronutrient carrier: (a) SEM and (b) TEM, (c) AFM images of single GO sheets confirming a few-layer thickness, and (d) XRD pattern of graphite and graphene oxide (GO).

Cu^{2+} by GO (46 mg Cu g^{-1}) is around 10 times more than that of activated carbon.[32] The adsorptive property of GO was investigated for Cu^{2+}, Zn^{2+}, Cd^{2+}, and Pb^{2+}, where the following maximum sorption capacities were observed: 294, 354, 530, and 1119 mg g^{-1}, respectively.[33−36] Considering the high adsorption capacity of GO for metal ions and its application as carrier for loading and delivery of therapeutic molecules, it is reasonable to expect that GO could be successfully used as carrier for plant micronutrients.

Several studies have investigated the short- and long-term impact of graphene-based materials in animal or cell modules, plant, and on the environment.[24,28,37−40] These studies show that there are several factors influencing the interaction of graphene-based materials with biological cells, including the lateral size, surface structure, functionalization, charge, impurities, aggregations, and corona effects.[41−43] On the basis of these studies, by increasing the hydrophilicity or dispensability of graphene-based materials, their biocompatibility will increase.[44] Therefore, GO sheets with large numbers of hydrophilic groups on their surface and edges are more likely to be biocompatible with animal and plant cells.[24] Furthermore, different studies have highlighted the significance of an eco-friendly enzymatic degradation strategy using the peroxidase family of enzymes, such as horseradish peroxidases, myeloperoxidases, and lignin peroxidase (a ligninolytic enzyme released from white rot fungus) to degrade graphene-based materials.[45−47] Therefore, GO could be degraded efficiently on the soil due to the presence of a huge amount of white rot fungi or lignin peroxidase in nature and avoid environmental pollution.

Currently, used micronutrient fertilizers generally have fast release, which may cause considerable loss of nutrients, thus lowering their efficiency and increasing the cost of the crop production. In this work, we present a new concept to address these limitations and demonstrate the use of GO sheets as new carriers for large capacity loading of plant micronutrients and their application for advanced fertilizers with sustained and slow release. The idea is based on the unique properties of GO, having an ultra large surface area and high density of oxygen functional groups on the surface that can provide electrostatic interaction and affinity for binding and loading of metal ions used as micronutrients. Figure 1 shows the scheme of the proposed concept showing loading and release of Cu and Zn ions on GO sheets and preparation of Cu−GO and Zn−GO solid fertilizer in the form of pellets. Here, we explored the performance of these new graphene-based micronutrient fertilizers by evaluating their loading capacity and release performance in solution and soil and their availability to plants.

■ RESULTS AND DISCUSSION

The SEM and TEM image of GO used as micronutrients carrier, confirming their typical size, irregular shape, and few-layers thickness are shown in Figure 2a,b. Their thickness was more precisely determined by atomic force microscopy (AFM), showing presence of oxidized functional groups on the surface of the single GO sheet (Figure 2c).[48,49] Further characterization

DOI: 10.1021/acsami.7b07890
ACS Appl. Mater. Interfaces 2017, 9, 43325−43335

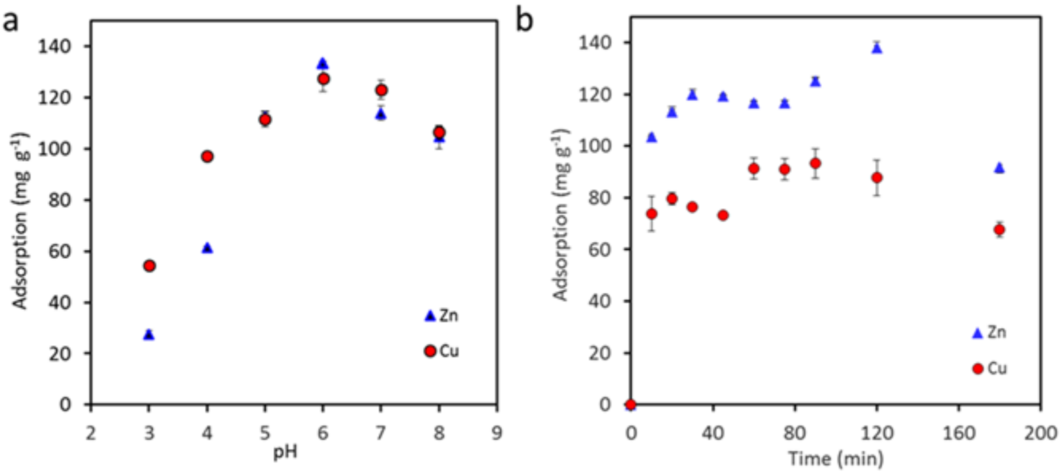

Figure 3. (a) Influence of pH on adsorption of Zn and Cu (20 mg L^{-1}) on GO sheets (5 mg) and (b) kinetic study of Zn and Cu adsorption at pH of 6 and 4.5 for Zn and Cu adsorption, respectively (with initial concentration of 20 mg L^{-1} for both Zn and Cu).

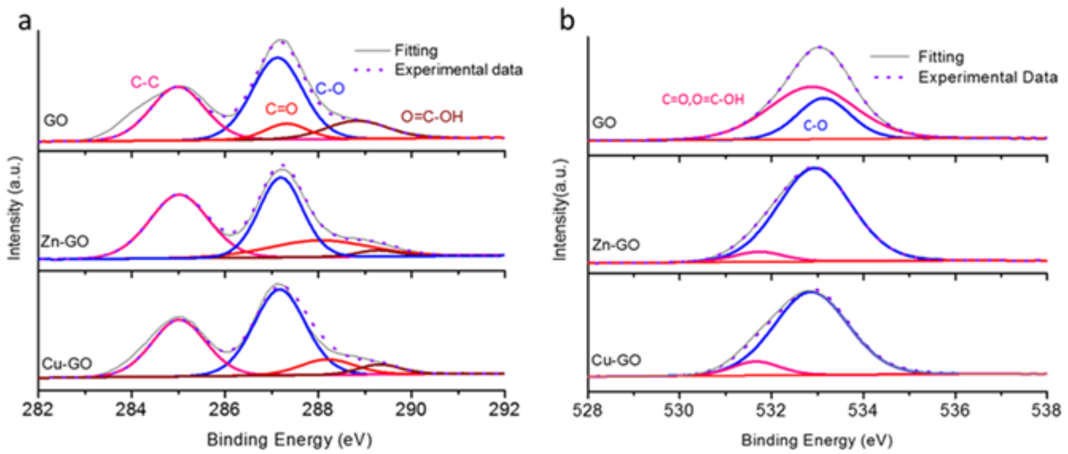

Figure 4. High-resolution XPS spectra of (a) C 1s and (b) O 1s obtained from GO sheets before and after metal-ion adsorption (Zn–GO and Cu–GO).

carried out using X-ray diffraction (XRD) spectroscopy (Figure 2d) showed a major peak 2θ for graphite at 26.6° that corresponds to an interplanar spacing of (002) hexagonal layers of carbon atoms. This intensive peak disappears in the XRD pattern of GO sheets and is replaced with a broad and weak peak at 2θ = 9.9° that is characteristic of GO.[50] Fourier transform infrared spectroscopy (FTIR) and X-ray photoelectron spectroscopy (XPS) confirmed the presence of oxygen-containing functional groups on the surface of GO, which has been discussed in detail in the Supporting Information (Figure S1, Supporting Information).

To confirm the capability of GO as a carrier for different micronutrients, a series of batch adsorption experiments were conducted in which the adsorption capacity of GO for Cu and Zn were determined. The influence of pH on the adsorption of these metal ions on GO surface was initially explored because pH affects the speciation of these metal ions as well as the surface properties of the GO sheets. This is relevant for determining the adsorption capacity of Zn and Cu on GO sheets and to prevent the precipitation of their oxide or hydroxides. Figure 3a shows the adsorption of both Cu and Zn ions increased gradually from pH 3–6 and remained constant at pH 6–7 before decreasing at pH 8. At a low concentration of Cu within the pH range of 3–7.5, Cu^{2+} is the dominant species of Cu species, whereas copper hydroxide ($Cu(OH)_2$) is predicted to be the dominant species at higher pH values up to 12.3 (Figure S2, Supporting Information).[51] Furthermore, the pH_{pzc} (point of zero charge) value of GO is 3.8–3.9, which means at pH values >3.9, GO is negatively charged and thus the electrostatic interactions of the positively charged metal ions and the negative surface of the GO sheets become stronger.[33,52] At higher pH, the formation of hydroxide complexes of copper ($CuOH^+$) in solution occurs; hence, the adsorption of Cu decreases due to the lower positive charge and electrostatic attraction of ($CuOH^+$) compared to that of Cu^{2+}.[31,51] In the case of Zn, the adsorption more sharply increases with pH from pH 3 to 6, as the predominant Zn species is Zn^{2+} in the pH range of 3–6 and the increasing negative charge on the GO sheets with increasing pH thus results in stronger adsorption. The low adsorption of Zn^{2+} on the GO sheets at pH 3 could be due to the competition between H^+ and Zn^{2+} for the same sorption sites.[31] The slight decrease of Zn adsorption at pH 7–8 can be explained by the formation of $Zn(OH)_2$ that is precipitating in the solution. Furthermore, at high pH values, the predominant Zn species is $Zn(OH)^-_3$, which is difficult to be adsorbed on negatively charged GO.[31] These results for Zn

DOI: 10.1021/acsami.7b07890
ACS Appl. Mater. Interfaces 2017, 9, 43325–43335

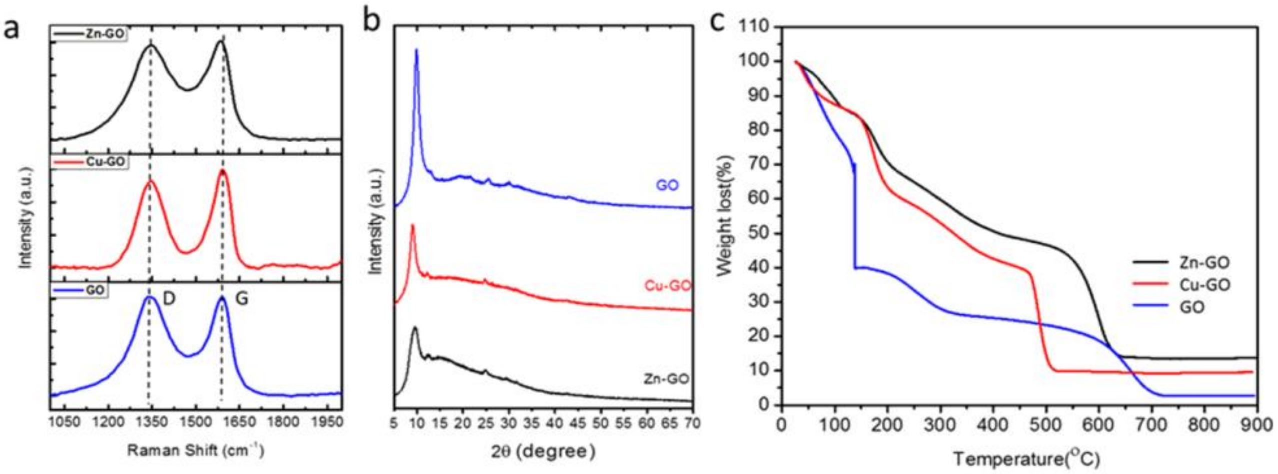

Figure 5. Comparative (a) Raman spectra, (b) XRD patterns, and (c) TGA curves of GO (control) before and Zn−GO and Cu−GO after loading of Zn and Cu ions.

and Cu adsorption on GO are in agreement with previous studies performed for different reasons (water purifications) reported in the literature.[30,31]

The kinetic rate of adsorption for these two metal ions on the GO sheets using optimized pH conditions (pH 6 for Zn and pH 4.5 for Cu) was determined and is presented in Figure 3b.[53] The results show a significant increase in adsorption of both ions at the beginning of the process (first 10 min), with slow increase after 10−20 min and reaching the maximum after 120 min. The amount of solute adsorbed per gram GO (q_e) determined from the experimental data was 137 and 93 mg g^{-1} for Zn^{2+} and Cu^{2+}, respectively. Both pseudo-first- and pseudo-second-rate adsorption kinetic models were used to study the kinetics of the sorption process (Supporting Information S3).[34,53] The experimental values of q_e were close to the calculated q_e values from the pseudo-second-order equation (133 and 73 mg g^{-1} for Zn^{2+} and Cu^{2+}, respectively). The presented pseudo-second-order kinetic models also showed higher value of correlation coefficients (R^2 values) compared to that of the pseudo-first-order models. This suggests that the sorption of Zn and Cu ions is controlled by chemical adsorption and strong attachment of these ions to the oxygen functional groups on the surface of the GO sheets (Table S3, Supporting Information).[31] The conclusion can be made that the adsorption capacity of the GO is directly related to the number of active sites that exist on the GO surface.[31,32]

To gain insight into the chemical composition of the prepared GO-based micronutrients and to investigate the nature of the chemical binding between the metal ions and GO sheets, XPS characterizations were performed. The selected survey spectra and high-resolution graphs for specific elements obtained from GO sheets before and after Zn and Cu-ion adsorption are presented in Figures 4 and S4, Supporting Information. The appearance of Zn (Zn 3s/3p) and Cu (Cu 3s) peaks in the survey spectra of Zn−GO and Cu−GO, respectively, confirm the presence of the metal ions (Zn 4.34%, Cu 6.2%) on the GO structures (Table S3, Supporting Information). High-resolution analyses of C 1s and O 1s for both Zn−GO and Cu−GO composites are presented in Figure 4a,b. Deconvolution of the C 1s spectrum for GO showed that the primary peak at 285 eV can be attributed to the sp^2-hybridized carbon of the GO sheets (Figure 4a). The peak was asymmetric due to the presence of other carbon functionalities, including sp^3/aliphatic hydrocarbon species and carbon−oxygen species, such as C−OH, C−O−C, C═O, and C−OOH.[49] The C 1s spectra of Zn−GO and Cu−GO composites is also fitted to four peaks corresponding to C═C or C−C, C−O, C═O, and O═C−O. However, the binding energies of the C═O and O═C−O peaks of Zn−GO and Cu−GO composites were slightly shifted toward higher bonding energy directions after Zn and Cu binding, which indicates the inclusion of the metal ions on the GO matrix.[31,54,55] Furthermore, the O 1s XPS spectra of GO, Zn−GO, and Cu−GO and the binding energies of oxygen in the various functional groups were allocated according to those in the literature (Figure 4b).[49,56] The O 1s spectrum of GO without metal ions is significantly different both in position, shape, and maximum intensity from the spectra for GO with adsorbed Zn and Cu ions. This result confirms the involvement of the oxygen functional groups presented on the surface of GO on the sorption of the metal ions, which is in agreement with previous studies.[31,55]

Further characterization to confirm the attachment of metal ions on the GO surface was performed using Raman, XRD, and thermogravimetric analysis (TGA) characterizations. The Raman spectrum of GO (Figure 5a) showed the characteristic D and G bands at 1341 and 1595 cm^{-1}, respectively. The Raman plots of Zn−GO and Cu−GO also contained both the G and D bands, but the occurrence of a mild blueshift of the "G band" (~9 cm^{-1}) for both Zn−GO and Cu−GO and a redshift of the "D band" (~8 cm^{-1}) for Cu−GO composites suggested that the Zn and Cu functionalization altered the structural vibrations of the Zn−GO and Cu−GO composites.[55]

The X-ray diffraction pattern of GO showed predominate peaks at $2\theta \sim 9.86°$ (Figure 5b), which can be assigned as the (001) reflection corresponding to the graphite interlayer distance. This (001) reflection was also observed for the Cu−GO and Zn−GO composites. However, this peak shifted to lower 2θ values (ca. 9.08 and 9.64° for Cu−GO and Zn−GO, respectively), which is evidence of the intercalation of the metal ions.[54] Furthermore, a significant peak broadening was observed for Cu−GO and Zn−GO compared to that of GO, which may originate from the particle (crystallite) size broadening or lattice strain broadening.[57] No diffraction

DOI: 10.1021/acsami.7b07890
ACS Appl. Mater. Interfaces 2017, 9, 43325−43335

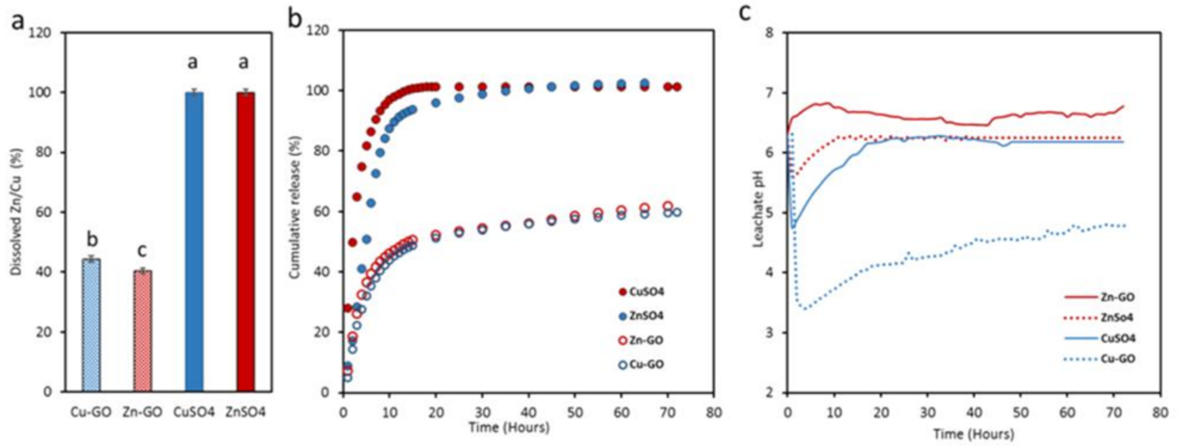

Figure 6. (a) Batch water solubility of Zn and Cu from Zn−GO, Cu−GO, $ZnSO_4$, and $CuSO_4$ fertilizers, (b) kinetic release study of Zn from Zn−GO and $ZnSO_4$, and Cu from Cu−GO and $CuSO_4$ from the columns, and (c) changes in the pH of the elutes from the columns as a function of time. Error bars represent the standard error (n = 3). Bars with different letters are significantly different at a 5% significance level.

peaks from any other impurities (such as metal oxides) were detected in the XRD data of Cu−GO and Zn−GO.

The comparative thermogravimetric (TG) graphs of the GO, Zn−GO, and Cu−GO-loaded GO carriers performed by a TG analyzer are presented in Figure 5c. GO is thermally unstable and starts to lose mass upon heating even below 100 °C. The major weight loss (∼70%) occurs at ∼300 °C, which is probably due to the pyrolysis of the liable oxygen-containing functional groups.[58] Although both Zn−GO and Cu−GO followed a similar profile as that of GO, their thermal stability increased compared to that of GO. The TG curve of GO showed a weight loss of ∼98%, whereas the TG curves of Zn−GO and Cu−GO showed lower weight losses (∼86−90%) compared to those of bare GO, confirming the presence of Zn and Cu in the GO structure.

After confirming the structure and chemical composition of the prepared Cu−GO and Zn−GO composites, in the last characterization experiment, we quantified the amount of Zn and Cu micronutrients loaded on GO sheets using standard methods by the open vessel aqua regia extraction method.[59,60] It was found that 135 mg g^{-1} of Zn and 100 mg g^{-1} of Cu were loaded on the GO sheets. These results are in agreement with those of the TGA analysis during combustion of the Zn−GO and Cu−GO composites, showing their Zn and Cu loading around 14 and 10%, respectively. Considering that our prepared GO carriers were not optimized in terms of the maximized density of active cites (oxygen groups), it is expected that the observed loading capacity of GO can be further improved if required.

To evaluate the nutrient release of Zn−GO and Cu−GO pellets (i.e., in a granular form comparable to that of commercial granular fertilizers), a series of experiments were performed to determine their water solubility, dissolution and release rate in a column perfusion method, and their release rate in soil. The water solubility results of Zn−GO and Cu−GO granules compared to those of $ZnSO_4$ and $CuSO_4$ granules are presented in Figure 6a. Results show that the Zn−GO and Cu−GO granules released only 40 and 44% of their nutrients, respectively, compared with 100% of $ZnSO_4$ and $CuSO_4$ granules under the same conditions.

Figure 6b shows the Zn- and Cu-ion release profiles compared with controls obtained by the column perfusion method. Again, a significant difference in the release rate was observed between Zn−GO and Cu−GO and $ZnSO_4$ and $CuSO_4$ granules. The release for both systems showed a biphasic behavior consisting of an initial burst release for 5 h, followed by a slow release that was monitored over 72 h. However, during this burst release only ∼30% of Zn and Cu ions were released from GO carriers compared with 75−80% released from $ZnSO_4$ and $CuSO_4$ granules. The rapid initial release of nutrients in the first 5 h is likely related to the release of physiosorbed metal salts or loosely adhered metal ions to the surface of the GO sheets. The increasing amount of sulfur (S) in the XPS survey spectra of Cu−GO and Zn−GO (2.02 and 1.69%, respectively) compared with the amount of S in the GO sheets (0.67%) confirms the physical attachment of $ZnSO_4$ and $CuSO_4$ salts during the loading process (Table S3, Supporting Information). In the case of $ZnSO_4$ and $CuSO_4$ fertilizers, almost all Zn and Cu were released within 20 h, compared with 50% from GO-based granules that showed a very slow release rate of ∼55% after 72 h.

The pH of elutes from the column experiment was evaluated for all tested samples to determine the influence of released ions on the pH of solution (Figure 6c). During the burst-phase of the release (first 5 h), the pH of the Zn−GO treatment was initially higher than that for the $ZnSO_4$ granules. Both Zn−GO and $ZnSO_4$ showed a slight increase in the pH of the leachate within the first few hours, after which the pH remained constant over time (Figure 6c). The reason for the slight increase of leachate pH during the leaching test from the column for Zn-based fertilizers could be related to proton consumption during dissolution of Zn species from the surface of the fertilizer granules.[61,62] In contrast, the pH of the initial fractions from the columns with $CuSO_4$ and Cu−GO decreased from 6.5 to 3.6 for $CuSO_4$ and 3.4 for Cu−GO within the first few hours (2 h for $CuSO_4$ and 4 h Cu−GO). However, once the dissolution of the $CuSO_4$ granules was complete, the column elutes tended toward the higher pH values that result from the percolating solution (0.01 mol L^{-1} $CaCl_2$, pH 6.5). For Cu−GO, the pH of elute did not converge to the pH of the calcium chloride ($CaCl_2$) solution because the dissolution

DOI: 10.1021/acsami.7b07890
ACS Appl. Mater. Interfaces 2017, 9, 43325−43335

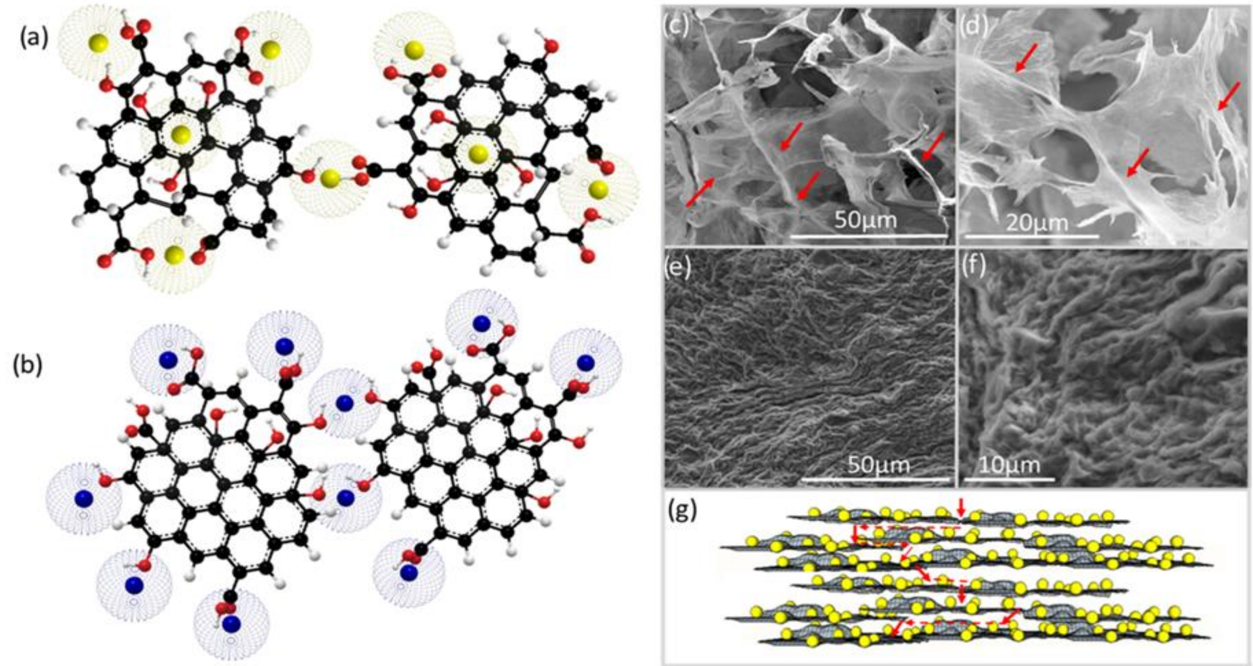

Figure 7. Schematic diagram of GO sheet interactions with (a) Zn^{2+} ions and (b) Cu^{2+} ions and SEM images of (c) rolled Zn and Cu-loaded GO sheets, (d) rolled and wrinkled GO sheets, and (e) low-resolution and (f) high-resolution SEM images of Cu-loaded GO sheets stacked on top of each other, and (g) schematic of water penetration through the stacked structure of fertilizers granules.

process continued and was not complete. The significant decrease in the eluted solution from the columns with Cu can be explained by the effect of pH on the speciation of Cu. As discussed previously, at higher pH (pH > 6), hydrolyzed Cu species are the prominent Cu species. The hydrolysis of Cu ions to soluble $Cu(OH)_2$ produces H^+ ions, which makes the leachate acidic. The pH was lower for the Cu−GO treatment than for the $CuSO_4$ treatment. This may be related to the physiosorbed acid on the GO sheets during the adsorption process of the Cu ions on the GO sheets, which was conducted under acidic conditions (pH 4.5).

This significant difference in the release pattern of the micronutrients from the GO-based carriers compared with the $ZnSO_4$ and $CuSO_4$ salts is explained by tight coordination of the metal ions and oxygen functional groups on the GO surface.[63] The metal ions can also form a strong complex of Zn^{2+} or Cu^{2+} with two adjacent carboxylate groups or an adjacent phenolic OH group and carboxylate groups at the edges of GO sheets.[63−65] In the case of Zn^{2+} and Cu^{2+}, Zn^{2+} is a d^{10} ion and its complexes possess a single ground state; Cu^{2+} is a d^9 ion, and its complexes possess a double ground state.[66] The Cu^{2+} tends to bind in a syn conformation with oxygen-containing functional groups (e.g., carboxylate groups), whereas Zn^{2+} ions are more likely to bind in a direct conformation, while they are sharing two oxygen atoms of the same carboxylic group (Figure 7a,b).[63,67] Furthermore, the GO sheets might be bridged by metal ions through the complexation with hydroxyl or carboxyl groups at the edges of GO sheets.[65] Therefore, the release of Zn and Cu will be slower compare to that of the $ZnSO_4$ and $CuSO_4$ salts due to their strong attachment to GO sheets.

Another mechanism for the slow release of nutrients from GO-based fertilizers is the low accessibility of nutrients in the GO matrix due to the trapping of loaded nutrients between GO sheets. After adding the metal ions to the GO suspension, aggregates form due to the reduction of electrostatic repulsion of the Zn- and Cu-loaded sheets.[32,64] It can be seen from SEM images of freeze-dried Zn- and Cu-loaded GO sheets (Figure 7c) that the GO sheets are folded and create a rodlike structure. They are also wrinkled (Figure 7d) and stacked against each other in the aggregates. The wrinkled and rolled GO sheets stack on top of each other more during the preparation process of Zn−GO or Cu−GO granules (Figures 7e,f). Therefore, water molecules have to penetrate through the interconnected channels formed between the rolled or agglomerated GO sheets to release Zn and Cu (Figure 7g), which is a time consuming process.

The mechanism of Zn and Cu-ion release from Zn−GO and Cu−GO carriers was described and interpreted using two kinetic models, known as the zero-order and first-order models (eqs 1 and 2).[68,69]

$$\frac{M_t}{M_\infty} = kt \tag{1}$$

$$\frac{M_t}{M_\infty} = 1 - \exp^{(-kt)} \tag{2}$$

where M_t and M_∞ represent the amount of nutrients released at time t and equilibrium, respectively, and k is a solubility rate constant. These two equations have been already used in the prediction of the controlled release of drugs and mineral components of fertilizers.[68,70,71] The predicted values calculated by the first-order model for release of nutrients from the starting fertilizers (Zn−GO and Cu−GO) satisfactorily fit the experimental data. The correlation coefficients for Zn and Cu solubility rates calculated by the first-order model were 0.92

DOI: 10.1021/acsami.7b07890
ACS Appl. Mater. Interfaces 2017, 9, 43325−43335

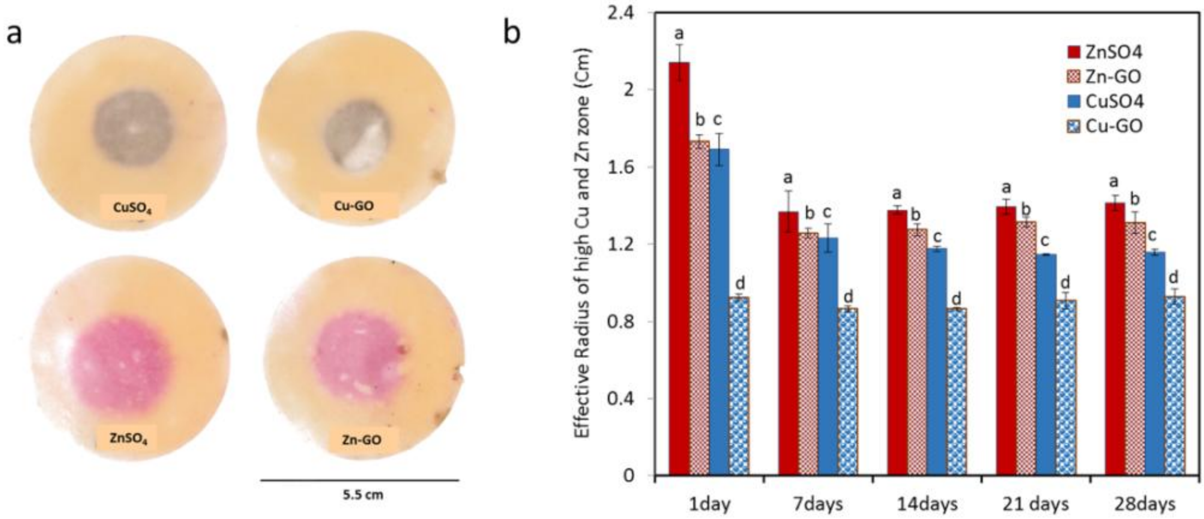

Figure 8. (a) Visualized Zn and Cu diffusion zones in an acid soil (Tumby Bay, Table S1, Supporting Information) from $CuSO_4$, Cu−GO, $ZnSO_4$, and Zn−GO fertilizer granules (containing 10 mg of nutrient) added in the center of a Petri dish filled with the soil and incubated for 28 days, and (b) radius of the high-Zn and high-Cu zone (derived as $\sqrt{A/\pi}$, with A as the area of the Zn and Cu diffusion zone) at 1, 7, 14, 21, and 28 days after the addition of Zn−GO, Cu−GO, $ZnSO_4$, and $CuSO_4$ fertilizers. Error bars represent the standard error (n = 3). Bars with different letters are significantly different (at a 5% significance level) at a given time point.

Table 1. Chemical Analysis Results on Soil Concentrically Sampled around the Fertilizer Application Sites at 28 Days after Addition of Zn and Cu Fertilizers[a]

	pH		Zn or Cu solution concentration ($\mu g\ L^{-1}$)		% of added metal (Zn or Cu)	
fertilizer	<9 mm	>9 mm	<9 mm	>9 mm	at <9 mm	at >9 mm
$ZnSO_4$	6.55(0.02)	6.42(0.08)	2067(67.5)	289(23.2)	70(0.00)	30.0(0.00)
Zn−GO	6.62(0.07)	6.33(0.02)	4199(69.8)	570(46.5)	71(0.06)	28.0(0.00)
$CuSO_4$	6.08(0.06)	6.40(0.03)	2209(85.1)	331(19.4)	68(0.02)	31.5(0.00)
Cu−GO	6.20(0.05)	6.40(0.05)	2395(179)	148(23.7)	82(0.01)	19.0(0.01)

[a]At 10 mg Zn; $ZnSO_4$ and Zn−GO, and 10 mg Cu; $CuSO_4$ and Cu−GO; pH and solution concentrations of Zn and Cu in a 1 mM $CaCl_2$ extract from different soil sections and the percentage of added Zn and Cu recovered at <9 mm from the granules were measured (standard error of three replicates between brackets).

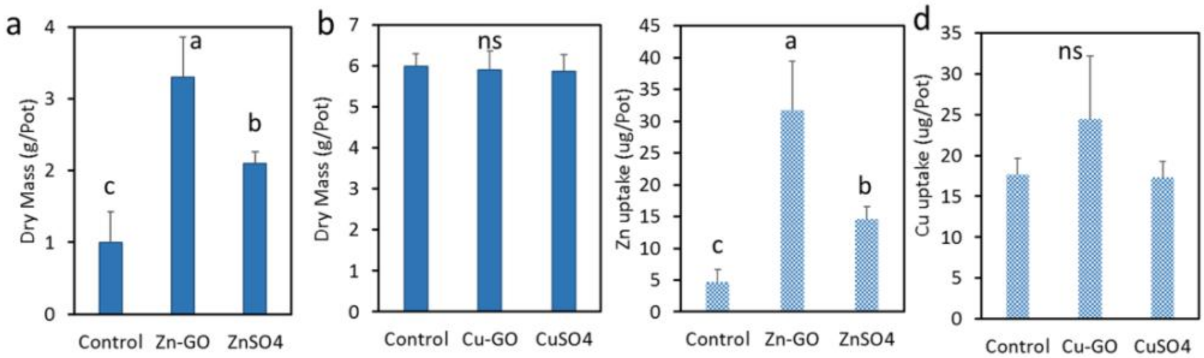

Figure 9. (a) Effect of different Zn and (b) different Cu formulations on grain yield (dry mass) of wheat and (c, d) effect of different Zn and Cu formulations on nutrient uptake by plants. Error bars represent the standard error (n = 3). Bars with different letters are significantly different at a 5% significance level, and bars with ns are not significantly different.

and 0.95 for Zn−GO and Cu−GO composites, respectively (Figure S4, Supporting Information). Furthermore, the slope of the regression line between observed and predicted values yielded a slope of 0.95 and 0.94, respectively, which shows the strength of using a first-order kinetic model to explain the release of the nutrient form GO matrix (Figure S5, Supporting Information). Conversely, the zero-order kinetic model did not describe the nutrient release well.

Furthermore, the diffusion and transport of released Zn and Cu ions from prepared Zn−GO and Cu−GO granules was examined in soil over 28 days using a visualization method.[72] This technique mimics real conditions in soil and is designed to explore the release and distribution rate of micronutrients in

DOI: 10.1021/acsami.7b07890
ACS Appl. Mater. Interfaces 2017, 9, 43325−43335

soil and their potential availability for plants. The visualized Zn- and Cu-ion distribution for all formulations from day 1 to day 28 is presented in Figure S6, Supporting Information. The visualized Zn- and Cu-ion distribution zones at 28 days after application of $ZnSO_4$, Zn−GO, $CuSO_4$, and Cu−GO fertilizers in the soil are shown in Figure 8a. The diffusion of Zn and Cu was initially greater when added as $ZnSO_4$ and $CuSO_4$ compared to that when added as Zn−GO and Cu−GO ($P < 0.05$) (Figure 8b). For all components, the radius of the diffusion zone decreased between day 1 and day 7, which can be explained by continuous sorption of Cu and Zn in soil around fertilizer granules. Within a day, diffusion transported Zn and Cu over a volume of soil that had enough adsorption capacity to strongly retain the Zn and Cu and their further movement was slower.[72] Furthermore, lower diffusion of Cu from Cu-based materials compared to Zn diffusion from Zn-based fertilizers was related to the lower mobility of Cu in the soil.[73]

Results of the chemical analysis of the soil are presented in Table 1. Concentrations of Zn and Cu in the diffusion zones in soil matched those from the visualization results. In the case of $ZnSO_4$ and Zn−GO granules, similar amounts of Zn were recovered at >9 mm from the granules, 30 and 28%, respectively. In soil with $CuSO_4$ granules, 31.5% of the fertilizer Cu was recovered at >9 mm, whereas in soil with Cu−GO granules, 19% of the fertilizer Cu was recovered in this zone.

Finally, the efficiency of Zn−GO and Cu−GO fertilizers for improving yield and Zn or Cu content of durum wheat (*Triticum durum* cv. Yallaroi) was studied. The grain dry mass was higher when the soil was fertilized with Zn−GO compared to that when the soil was fertilized with $ZnSO_4$ granules ($P < 0.05$) (Figure 9a). However, there was no difference in plant dry mass for soil treated with Cu−GO and $CuSO_4$ fertilizers ($P > 0.05$) (Figure 9b) because this soil was not Cu responsive, as evident from similar yield for the control (no Cu) and the Cu-amended treatments. Regarding nutrient uptake, plants treated with the Zn−GO fertilizer showed significantly higher nutrient uptake than those treated with Zn salts and the control ($P < 0.05$) (Figure 9c). The Cu uptake was slightly higher for the Cu−GO fertilizer than for the Cu salt and control treatments, but this difference was not significant (Figure 9d). The lower uptake in the treatments with Zn salt is likely related to fixation of Zn in this calcareous soil, e.g., due to irreversible adsorption on carbonates or precipitation as Zn hydroxides or carbonate. Compared with Zn and Cu salts, GO is able to form a stronger complex with Zn or Cu and thus Zn−GO and Cu−GO may have less interaction with the soil components, keeping these micronutrients in more available forms to be taken up by the plants.[74]

To the best of our knowledge, this is the first report on the agronomic performance of novel GO-based slow-release micronutrient fertilizers compared to traditional, fully soluble salts. This study clearly shows promise for the developed GO-based nutrient carriers with a slow-release pattern as new fertilizer materials.

■ CONCLUSIONS

In this study, we have demonstrated the use of GO sheets as a new carrier for nutrients, resulting in a slow release and sustained delivery of micronutrients such as Zn and Cu. The micronutrient fertilizers (Zn−GO and Cu−GO) prepared in the form of solid pellets showed a high nutrient loading capacity (more than 10%), which is related to the high surface area of GO and high density of oxygen binding sites on the surface and edge of GO, responsible for binding the micronutrient ions. The GO-based carrier had a biphasic nutrient release characteristic with an ability to supply micronutrients in both fast-release (ca. 40% for 5 h) and slow sustained release. This release pattern is highly desirable and advantageous for the crops where seedling establishment needs high nutrient loadings and at later stages of crops growth where a slower and sustained release of micronutrients is needed. The significant loading and desirable release performances of GO-based carriers make them favorable material for loading of any nutrient (macro, micro, and their combinations), and therefore they could be used as generic carriers for creation of a new generation of advanced SRFs. Given that the price of commercially produced GO will most likely significantly decrease in the near future, there is a strong prospect that industrial-scale production of these high-performing graphene-based fertilizers will become commercially feasible over time.

■ ASSOCIATED CONTENT

Supporting Information

The Supporting Information is available free of charge on the ACS Publications website at DOI: 10.1021/acsami.7b07890.

Experimental section including; Graphene oxide (GO) preparation, batch adsorption and pH experiments, Cu and Zn loading on graphene oxide sheets, dissolution kinetics study of Zn−GO and Cu−GO fertilizers using column perfusion, zinc and copper diffusion visualization method; (Table S1) selected physical and chemical properties of the soil used in soil diffusion study, measuring soil pH and total Zn and Cu in the soil, plant study, selected physical and chemical properties of the soil used in plant study (Table S2); characterizations and statistical analysis; Fourier transform infrared spectroscopy (FTIR) and high-resolution XPS peaks (Figure S1); thermodynamic speciation of Zn and Cu ions (Figure S2); pseudo-first-order and pseudo-second-order kinetic models (S3); kinetic parameters of the pseudo-first-order and pseudo-second-order equations for Zn^{2+} and Cu^{2+} sorption on GO (Table S3); percent elemental concentration for GO, Zn−GO, and Cu−GO composites from XPS survey scans (Table S4); XPS characteristics (Figure S4); mathematical release models (Figure S5); cumulative release of nutrients (Figure S6); visualized copper diffusion and visualized zinc diffusion (Figure S7) (PDF)

■ AUTHOR INFORMATION

Corresponding Authors

*E-mail: dusan.losic@adelaide.edu.au (D.L.).

*E-mail: michael.mclaughlin@adelaide.edu.au (M.J.M.).

ORCID

Diana N. H. Tran: 0000-0002-4023-3373

Rodrigo C. da Silva: 0000-0002-2345-3729

Dusan Losic: 0000-0002-1930-072X

Notes

The authors declare no competing financial interest.

■ ACKNOWLEDGMENTS

The authors thank the support of the Australian Research Council (ARC) funding ARC DP 150101760 and ARC IH

150100003 (Graphene Enabled Industry Transformation) for financial support to this work. The support from The University of Adelaide and the Schools of Chemical Engineering and Agriculture, Food and Wine is acknowledged.

■ REFERENCES

(1) Zhang, M.; Gao, B.; Chen, J.; Li, Y.; Creamer, A. E.; Chen, H. Slow-release fertilizer encapsulated by graphene oxide films. *Chem. Eng. J.* **2014**, *255*, 107−113.

(2) McBeath, T. M.; McLaughlin, M. J. Efficacy of zinc oxide as fertilizers. *Plant Soil* **2014**, *374*, 843−855.

(3) Zhao, A.-q.; Tian, X.-h.; Chen, Y.-l.; Li, S. Application of ZnSO4 or Zn-EDTA fertilizer to a calcareous soil: Zn diffusion in soil and its uptake by wheat plants. *J. Sci. Food Agric.* **2016**, 1484−1491.

(4) Zhu, Q.; Zhang, M.; Ma, Q. Copper-based foliar fertilizer and controlled release urea improved soil chemical properties, plant growth and yield of tomato. *Sci. Hortic.* **2012**, *143*, 109−114.

(5) Li, P.; Li, L.; Du, Y.; Hampton, M. A.; Nguyen, A. V.; Huang, L.; Rudolph, V.; Xu, Z. P. Potential foliar fertilizers with copper and zinc dual micronutrients in nanocrystal suspension. *J. Nanopart. Res.* **2014**, *16*, 1−11.

(6) Ray, S. K.; Varadachari, C.; Ghosh, K. Novel Slow-Releasing Micronutrient Fertilizers. 2. Copper Compounds. *J. Agric. Food Chem.* **1997**, *45*, 1447−1453.

(7) Bandyopadhyay, S.; Ghosh, K.; Varadachari, C. Multimicronutrient Slow-Release Fertilizer of Zinc, Iron, Manganese, and Copper. *Int. J. Chem. Eng.* **2014**, *2014*, No. 327153.

(8) Rico, M. I.; Alvarez, J. M.; Vallejo, A. Preparation of Fertilizers with Rosin and Tricalcium Phosphate Coated Zinc Chelates. Laboratory Characterization. *J. Agric. Food Chem.* **1995**, *43*, 2758−2761.

(9) Jin, S.; Yue, G.; Feng, L.; Han, Y.; Yu, X.; Zhang, Z. Preparation and Properties of a Coated Slow-Release and Water-Retention Biuret Phosphoramide Fertilizer with Superabsorbent. *J. Agric. Food Chem.* **2011**, *59*, 322−327.

(10) Ray, S. K.; Varadachari, C.; Ghosh, K. Novel Slow-Releasing Micronutrient Fertilizers. 1. Zinc compounds. *Ind. Eng. Chem. Res* **1993**, *32*, 1218−1227.

(11) Krems-Chemie. Complete Fertilizers Containing Trace Elements, Austrian Patent 326,160, 1975.

(12) Volfkovich, S. Polymeric fertilizers. *J. Appl. Chem.* **1972**, *45*, 2479−2487.

(13) Ray, S. K.; Varadachari, C.; Ghosh, K. Novel slow-releasing micronutrient fertilizers. 1. Zinc compounds. *Ind. Eng. Chem. Res* **1993**, *32*, 1218−1227.

(14) Lyons, J. W.; Rauh, G. A., Jr.; Vandersall, H. L. Methods for Preparing Mixed Cation Polyphosphates. U.S. Patent US 3574591 A, 1971.

(15) Bandyopadhyay, S.; Bhattacharya, I.; Ghosh, K.; Varadachari, C. New slow-releasing molybdenum fertilizer. *J. Agric. Food Chem.* **2008**, *56*, 1343−1349.

(16) Geim, A. K.; Novoselov, K. S. The rise of graphene. *Nat. Mater.* **2007**, *6*, 183−191.

(17) Allen, M. J.; Tung, V. C.; Kaner, R. B. Honeycomb carbon: a review of graphene. *Chem. Rev.* **2010**, *110*, 132−145.

(18) Eda, G.; Chhowalla, M. Chemically derived graphene oxide: towards large-area thin-film electronics and optoelectronics. *Adv. Mater.* **2010**, *22*, 2392−2415.

(19) Wang, K.; Ruan, J.; Song, H.; Zhang, J.; Wo, Y.; Guo, S.; Cui, D. Biocompatibility of graphene oxide. *Nanoscale Res. Lett.* **2011**, *6*, 1−8.

(20) Perreault, F.; Fonseca de Faria, A.; Elimelech, M. Environmental applications of graphene-based nanomaterials. *Chem. Soc. Rev.* **2015**, *44*, 5861−5896.

(21) Dreyer, D. R.; Park, S.; Bielawski, C. W.; Ruoff, R. S. The chemistry of graphene oxide. *Chem. Soc. Rev.* **2010**, *39*, 228−240.

(22) Jin, L.; Yang, K.; Yao, K.; Zhang, S.; Tao, H.; Lee, S.-T.; Liu, Z.; Peng, R. Functionalized Graphene Oxide in Enzyme Engineering: A Selective Modulator for Enzyme Activity and Thermostability. *ACS Nano* **2012**, *6*, 4864−4875.

(23) Liu, Z.; Robinson, J. T.; Sun, X.; Dai, H. PEGylated Nano-Graphene Oxide for Delivery of Water Insoluble Cancer Drugs. *J. Am. Chem. Soc.* **2008**, *130*, 10876−10877.

(24) Liu, J.; Cui, L.; Losic, D. Graphene and graphene oxide as new nanocarriers for drug delivery applications. *Acta Biomater.* **2013**, *9*, 9243−9257.

(25) Pan, Y.; Sahoo, N. G.; Li, L. The application of graphene oxide in drug delivery. *Expert Opin. Drug Delivery* **2012**, *9*, 1365−1376.

(26) Shen, H.; Zhang, L.; Liu, M.; Zhang, Z. Biomedical Applications of Graphene. *Theranostics* **2012**, *2*, 283−294.

(27) Liu, Z.; Robinson, J. T.; Sun, X.; Dai, H. PEGylated Nanographene Oxide for Delivery of Water-Insoluble Cancer Drugs. *J. Am. Chem. Soc.* **2008**, *130*, 10876−10877.

(28) Ocsoy, I.; Paret, M. L.; Ocsoy, M. A.; Kunwar, S.; Chen, T.; You, M.; Tan, W. Nanotechnology in Plant Disease Management: DNA-Directed Silver Nanoparticles on Graphene Oxide as an Antibacterial against *Xanthomonas perforans*. *ACS Nano* **2013**, *7*, 8972−8980.

(29) Zhao, J.; Wang, Z.; White, J. C.; Xing, B. Graphene in the Aquatic Environment: Adsorption, Dispersion, Toxicity and Transformation. *Environ. Sci. Technol.* **2014**, *48*, 9995−10009.

(30) Zhao, G.; Li, J.; Ren, X.; Chen, C.; Wang, X. Few-Layered Graphene Oxide Nanosheets As Superior Sorbents for Heavy Metal Ion Pollution Management. *Environ. Sci. Technol.* **2011**, *45*, 10454−10462.

(31) Sitko, R.; Turek, E.; Zawisza, B.; Malicka, E.; Talik, E.; Heimann, J.; Gagor, A.; Feist, B.; Wrzalik, R. Adsorption of divalent metal ions from aqueous solutions using graphene oxide. *Dalton Trans.* **2013**, *42*, 5682−5689.

(32) Yang, S.-T.; Chang, Y.; Wang, H.; Liu, G.; Chen, S.; Wang, Y.; Liu, Y.; Cao, A. Folding/aggregation of graphene oxide and its application in Cu^{2+} removal. *J. Colloid Interface Sci.* **2010**, *351*, 122−127.

(33) Zhao, G.; Ren, X.; Gao, X.; Tan, X.; Li, J.; Chen, C.; Huang, Y.; Wang, X. Removal of Pb(ii) ions from aqueous solutions on few-layered graphene oxide nanosheets. *Dalton Trans.* **2011**, *40*, 10945−10952.

(34) Kabiri, S.; Tran, D. N. H.; Azari, S.; Losic, D. Graphene-Diatom Silica Aerogels for Efficient Removal of Mercury Ions from Water. *ACS Appl. Mater. Interfaces* **2015**, *7*, 11815−11823.

(35) Madadrang, C. J.; Kim, H. Y.; Gao, G.; Wang, N.; Zhu, J.; Feng, H.; Gorring, M.; Kasner, M. L.; Hou, S. Adsorption Behavior of EDTA-Graphene Oxide for Pb (II) Removal. *ACS Appl. Mater. Interfaces* **2012**, *4*, 1186−1193.

(36) Deng, X.; Lü, L.; Li, H.; Luo, F. The adsorption properties of Pb(II) and Cd(II) on functionalized graphene prepared by electrolysis method. *J. Hazard. Mater.* **2010**, *183*, 923−930.

(37) Zhang, X.; Yin, J.; Peng, C.; Hu, W.; Zhu, Z.; Li, W.; Fan, C.; Huang, Q. Distribution and biocompatibility studies of graphene oxide in mice after intravenous administration. *Carbon* **2011**, *49*, 986−995.

(38) Chang, Y.; Yang, S.-T.; Liu, J.-H.; Dong, E.; Wang, Y.; Cao, A.; Liu, Y.; Wang, H. In vitro toxicity evaluation of graphene oxide on A549 cells. *Toxicol. Lett.* **2011**, *200*, 201−210.

(39) Ryoo, S.-R.; Kim, Y.-K.; Kim, M.-H.; Min, D.-H. Behaviors of NIH-3T3 Fibroblasts on Graphene/Carbon Nanotubes: Proliferation, Focal Adhesion, and Gene Transfection Studies. *ACS Nano* **2010**, *4*, 6587−6598.

(40) Strayer, A.; Ocsoy, I.; Tan, W.; Jones, J. B.; Paret, M. L. Low Concentrations of a Silver-Based Nanocomposite to Manage Bacterial Spot of Tomato in the Greenhouse. *Plant Dis.* **2016**, *100*, 1460−1465.

(41) Akhavan, O.; Ghaderi, E. Toxicity of Graphene and Graphene Oxide Nanowalls Against Bacteria. *ACS Nano* **2010**, *4*, 5731−5736.

(42) Xu, W.-P.; Zhang, L.-C.; Li, J.-P.; Lu, Y.; Li, H.-H.; Ma, Y.-N.; Wang, W.-D.; Yu, S.-H. Facile synthesis of silver@graphene oxide nanocomposites and their enhanced antibacterial properties. *J. Mater. Chem.* **2011**, *21*, 4593−4597.

DOI: 10.1021/acsami.7b07890
ACS Appl. Mater. Interfaces 2017, 9, 43325−43335

(43) Akhavan, O.; Ghaderi, E. *Escherichia coli* bacteria reduce graphene oxide to bactericidal graphene in a self-limiting manner. *Carbon* **2012**, *50*, 1853−1860.
(44) Bianco, A.; Kostarelos, K.; Prato, M. Applications of carbon nanotubes in drug delivery. *Curr. Opin. Chem. Biol.* **2005**, *9*, 674−679.
(45) Lalwani, G.; Xing, W.; Sitharaman, B. Enzymatic Degradation of Oxidized and Reduced Graphene Nanoribbons by Lignin Peroxidase. *J. Mater. Chem. B* **2014**, *2*, 6354−6362.
(46) Kotchey, G. P.; Allen, B. L.; Vedala, H.; Yanamala, N.; Kapralov, A. A.; Tyurina, Y. Y.; Klein-Seetharaman, J.; Kagan, V. E.; Star, A. The Enzymatic Oxidation of Graphene Oxide. *ACS Nano* **2011**, *5*, 2098−2108.
(47) Allen, B. L.; Kichambare, P. D.; Gou, P.; Vlasova, I. I.; Kapralov, A. A.; Konduru, N.; Kagan, V. E.; Star, A. Biodegradation of Single-Walled Carbon Nanotubes through Enzymatic Catalysis. *Nano Lett.* **2008**, *8*, 3899−3903.
(48) Fang, R.; Liang, Y.; Ge, X.; Du, M.; Li, S.; Li, T.; Li, Z. Preparation and photocatalytic degradation activity of TiO2/rGO/polymer composites. *Colloid Polym. Sci.* **2015**, *293*, 1151−1157.
(49) Marcano, D. C.; Kosynkin, D. V.; Berlin, J. M.; Sinitskii, A.; Sun, Z.; Slesarev, A.; Alemany, L. B.; Lu, W.; Tour, J. M. Improved Synthesis of Graphene Oxide. *ACS Nano* **2010**, *4*, 4806−4814.
(50) Sydlik, S. A.; Jhunjhunwala, S.; Webber, M. J.; Anderson, D. G.; Langer, R. In Vivo Compatibility of Graphene Oxide with Differing Oxidation States. *ACS Nano* **2015**, *9*, 3866−3874.
(51) Albrecht, T. W. J.; Addai-Mensah, J.; Fornasiero, D. In *Effect of pH, Concentration and Temperature on Copper and Zinc Hydroxide Formation/Precipitation in Solution*, Chemeca, Australia, 2011.
(52) Zhao, G.; Wen, T.; Yang, X.; Yang, S.; Liao, J.; Hu, J.; Shao, D.; Wang, X. Preconcentration of U(vi) ions on few-layered graphene oxide nanosheets from aqueous solutions. *Dalton Trans.* **2012**, *41*, 6182−6188.
(53) Lim, S.-F.; Lee, A. Kinetic study on removal of heavy metal ions from aqueous solution by using soil. *Environ. Sci. Pollut. Res.* **2015**, *22*, 10144−10158.
(54) Li, R.; Liang, J.; Hou, Y.; Chu, Q. Enhanced corrosion performance of Zn coating by incorporating graphene oxide electrodeposited from deep eutectic solvent. *RSC Adv.* **2015**, *5*, 60698−60707.
(55) Marimuthu, M.; Veerapandian, M.; Ramasundaram, S.; Hong, S. W.; Sudhagar, P.; Nagarajan, S.; Raman, V.; Ito, E.; Kim, S.; Yun, K.; Kang, Y. S. Sodium functionalized graphene oxide coated titanium plates for improved corrosion resistance and cell viability. *Appl. Surf. Sci.* **2014**, *293*, 124−131.
(56) Larciprete, R.; Lacovig, P.; Gardonio, S.; Baraldi, A.; Lizzit, S. Atomic oxygen on graphite: Chemical characterization and thermal reduction. *J. Phys. Chem. C* **2012**, *116*, 9900−9908.
(57) Rupp, J. L. M.; Infortuna, A.; Gauckler, L. J. Microstrain and self-limited grain growth in nanocrystalline ceria ceramics. *Acta Mater.* **2006**, *54*, 1721−1730.
(58) Stankovich, S.; Dikin, D. A.; Piner, R. D.; Kohlhaas, K. A.; Kleinhammes, A.; Jia, Y.; Wu, Y.; Nguyen, S. T.; Ruoff, R. S. Synthesis of graphene-based nanosheets via chemical reduction of exfoliated graphite oxide. *Carbon* **2007**, *45*, 1558−1565.
(59) Milani, N.; McLaughlin, M. J.; Stacey, S. P.; Kirby, J. K.; Hettiarachchi, G. M.; Beak, D. G.; Cornelis, G. Dissolution Kinetics of Macronutrient Fertilizers Coated with Manufactured Zinc Oxide Nanoparticles. *J. Agric. Food Chem.* **2012**, *60*, 3991−3998.
(60) Tandy, S.; Bossart, K.; Mueller, R.; Ritschel, J.; Hauser, L.; Schulin, R.; Nowack, B. Extraction of Heavy Metals from Soils Using Biodegradable Chelating Agents. *Environ. Sci. Technol.* **2004**, *38*, 937−944.
(61) Degen, A.; Kosec, M. Effect of pH and impurities on the surface charge of zinc oxide in aqueous solution. *J. Eur. Ceram. Soc.* **2000**, *20*, 667−673.
(62) Bian, S.-W.; Mudunkotuwa, I. A.; Rupasinghe, T.; Grassian, V. H. Aggregation and Dissolution of 4 nm ZnO Nanoparticles in Aqueous Environments: Influence of pH, Ionic Strength, Size, and Adsorption of Humic Acid. *Langmuir* **2011**, *27*, 6059−6068.
(63) Sun, P.; Zhu, M.; Wang, K.; Zhong, M.; Wei, J.; Wu, D.; Xu, Z.; Zhu, H. Selective Ion Penetration of Graphene Oxide Membranes. *ACS Nano* **2013**, *7*, 428−437.
(64) Peng, W.; Li, H.; Liu, Y.; Song, S. Comparison of Pb(II) adsorption onto graphene oxide prepared from natural graphites: Diagramming the Pb(II) adsorption sites. *Appl. Surf. Sci.* **2016**, *364*, 620−627.
(65) Peng, W.; Li, H.; Liu, Y.; Song, S. A review on heavy metal ions adsorption from water by graphene oxide and its composites. *J. Mol. Liq.* **2017**, *230*, 496−504.
(66) Rulíšek, L.; Havlas, Z. Theoretical Studies of Metal Ion Selectivity. 1. DFT Calculations of Interaction Energies of Amino Acid Side Chains with Selected Transition Metal Ions (Co2+, Ni2+, Cu2+, Zn2+, Cd2+, and Hg2+). *J. Am. Chem. Soc.* **2000**, *122*, 10428−10439.
(67) Carrell, C. J.; Carrell, H. L.; Erlebacher, J.; Glusker, J. P. Structural aspects of metal ion carboxylate interactions. *J. Am. Chem. Soc.* **1988**, *110*, 8651−8656.
(68) Szepes, A.; Ulrich, J.; Farkas, Z.; Kovács, J.; Szabó-Révész, P. Freeze-casting technique in the development of solid drug delivery systems. *Chem. Eng. Process.* **2007**, *46*, 230−238.
(69) Costa, P.; Sousa Lobo, J. M. Modeling and comparison of dissolution profiles. *Eur. J. Pharm. Sci.* **2001**, *13*, 123−133.
(70) Jamnongkan, T.; Kaewpirom, S. Controlled-Release Fertilizer Based on Chitosan Hydrogel: Phosphorus Release Kinetics. *Sci. J. UBU 1* **2010**, *1*, 43−50.
(71) Yang, Y.-C.; Zhang, M.; Zheng, L.; Cheng, D.-D.; Liu, M.; Geng, Y.-Q. Controlled Release Urea Improved Nitrogen Use Efficiency, Yield, and Quality of Wheat. *Agron. J.* **2011**, *103*, 479−485.
(72) Degryse, F.; Baird, R.; McLaughlin, M. Diffusion and solubility control of fertilizer-applied zinc: chemical assessment and visualization. *Plant Soil* **2015**, *386*, 195−204.
(73) D.Harter, R. *Micronutrient Adsorption-Desorption Reactions in Soils*; SSSA Inc.: Madison, 1991.
(74) Zhao, A.-q.; Tian, X.-h.; Chen, Y.-l.; Li, S. Application of ZnSO4 or Zn-EDTA fertilizer to a calcareous soil: Zn diffusion in soil and its uptake by wheat plants. *J. Sci. Food Agric.* **2016**, *96*, 1484−1491.

DOI: 10.1021/acsami.7b07890
ACS Appl. Mater. Interfaces 2017, 9, 43325−43335

Supporting Information

Graphene Oxide: A New Carrier for Slow Release of Plant Micronutrients

*Shervin Kabiri[†], Fien Degryse [§], Diana N.H. Tran[†], Rodrigo C. da Silva [§], Mike J. McLaughlin *[§] and Dusan Losic*[†]*

[†]School of Chemical Engineering, The University of Adelaide, Adelaide, Engineering North Building, SA 5005, Australia

[§]Fertilizer Technology Research Centre, School of Agriculture, Food and Wine, The University of Adelaide, Waite Campus, PMB1, Glen Osmond, SA 5064, Australia

EXPERIMENTAL SECTION

Graphene oxide (GO) preparation. The improved and modified Hummer's method used to synthesis the GO sheets directly from the graphite flakes. [1, 2] Briefly, a mixture of sulphuric acid/phosphoric acid (H_2SO_4/H_3PO_4) (360:40 mL) added to mixed graphite and potassium permanganate (Graphite/$KMnO_4$) (3:18 g) and stirred at 50°C overnight. The mixture cooled down to room temperature and poured onto ice with hydrogen peroxide (H_2O_2) (3 mL). The synthesised golden-brown graphene oxide was centrifuged at 4600 g for 2 h after which the supernatant was removed. GO then washed in succession with 200 mL of 30 % hydrochloric acid (HCl) and twice with 200 mL of ethanol (4600 g for 2 h). The precipitants were then vacuum-dried overnight at room temperature to obtain a brown product, which was GO.

Batch adsorption and pH experiments. Batch adsorption experiments were conducted individually for Zn^{+2} and Cu^{+2} to examine the influence of contact time and pH on the metal ions adsorption on GO sheets. Experiments were performed using 250 mL conical flasks with 5 mg of adsorbent (GO) and 100 mL of Cu^{+2} or Zn^{+2} solution (20 mg L^{-1}) in Milli-Q water at room temperature and were mixed in a shaker (RATEK-digital Shaker model OM7) at 150 rpm. The influence of pH on Zn and Cu adsorption was assessed in the pH range of 3-8. The pH values of the solutions were adjusted with H_2SO_4 or NH_4 OH (0.1 ML^{-1}). The suspensions were shaken for 60 minutes and filtered through a filter paper (0.45 µm) before analysis with ICP-OES. (Spectro, Kleve, Germany).

The kinetics of sorption were tested at a fixed pH of 4.5 and 6. Solutions with a Cu or Zn concentration of 20 mg L^{-1} were equilibrated with the GO adsorbent (5 mg) for 10, 20, 30, 45, 60, 75, 90 and 120 minutes. The suspensions were filtered with 0.45 µm filter papers after the specified contact time. The amount of Cu and Zn ions q_t (mg g^{-1}) adsorbed by the adsorbent at time t, was calculated using the following equation:

$$q_t = \frac{(C_0 - C_t) * V}{M}$$

where C_0 and C_t are the initial solution concentration and the concentration at time *t*, respectively, while *V* is the volume of solution (L) and *M* is the mass of the composite used (g).

Cu and Zn loading on graphene oxide sheets. To prepare Cu-loaded GO (Cu-GO) and Zn-loaded GO (Zn-GO) fertilizers, $CuSO_4.5H_2O$ and $ZnSO_4.7H_2O$ salts were used. 1 mM of Cu and Zn ions were added to 1 L of GO solution (1 mg L^{-1}). The pH of the GO solution for the adsorption was fixed at 4.5 for Cu and at pH 6 for Zn. The suspensions were mixed on a shaker for 60 minutes for Cu loading and 120 minutes for Zn loading. The loaded GO suspensions were centrifuged for 30 minutes (4200 rpm). The precipitates at the bottom of tubes were collected and semi-dried in an oven at 50 °C overnight. The semi-dried materials were then cut into cubes with dimensions of 0.5 mm by 0.5 mm. Total and water-soluble Zn and Cu concentrations of Zn-GO and Cu-GO fertilizers were measured based on pervious work.[3]

Dissolution kinetics study of Zn-GO and Cu-GO fertilizers using column perfusion. Dissolution kinetic experiments were conducted as described in our previous work,[3]but using glass wool instead of quartz sand as porous medium. The dissolution kinetics were assessed for the Cu-GO and Zn-GO granules and also for Zn sulphate ($ZnSO_4.H_2O$) and Cu sulphate ($CuSO_4.5H_2O$) granules as reference. Granules with a total amount of Cu or Zn of 50 mg were placed in each polypropylene column (150 mm×15 mm), then filled with acid-washed glass wool followed by introducing $CaCl_2$ solution (10 mM and pH 6) from the bottom of using a peristatic pump with a constant flow rate (10 mL h^{-1}) and collecting samples by collector (SuperFracTM, Pharmacia) for 72 h for ICP-OES measurements as described in our previous work[52].

Zinc and copper diffusion visualization method. The micronutrients diffusion was monitored at 1, 7, 14, 21 and 28 days using a visualization method described by Degryse et al.[4] Petri dishes (5.5 cm diameter and 1 cm height) were filled with wetted soil (Tumby Bay, Table S1), covered with the lids, and incubated at 25°C oven. All products ($CuSO_4.5H_2O$, $ZnSO_4.H_2O$, Cu-GO and Zn-GO granules) were applied in the middle of a Petri dish at the same rate (10 mg per Petri dish) about 4 mm below the soil surface. Three replicates were applied for each formulation. The Petri dishes were then placed in a plastic bag to avoid water loss from the soil and incubated at 25°C. The micronutrients diffusion was monitored at 1, 7, 14, 21 and 28 days using calcium carbonate impregnated filter paper as reference.

Table S1. Selected physical and chemical properties of the soil used in this study for soil diffusion experiment are given in Table 3. The soil was collected from the top layer of (0-10 cm), air dried and sieved to < 2mm before use. ([a] pH in 0.01 M $CaCl_2$ (L:S 5l Kg^{-1}), [b] organic C[7], pressure calcimeter method[4], [c] CEC measured with 1 M ammonium acetate at pH 7.0, [d] particle size analysis with the pipette method[8], [e] Oxalate-extractable Al and Fe concentrations[9] and total Zn concentration determined by aqua regia digestion.

Soil (location)	Thumby Bay
Soil type	Loamy sand
pH ($CaCl_2$)[a]	5.1
OC(%)[b]	2.9
CEC ($cmol_c kg^{-1}$)[c]	10
Clay (%)[d]	13.7
Slit (%)[d]	10.3
Sand (%)[d]	43
Al_{oxal} (mg kg^{-1})[e]	505
Fe_{oxal} (mg kg^{-1})[e]	739
Zn_{tot}($mgkg^{-1}$)	17.2

Measuring soil pH and total Zn and Cu in the soil. At the end of the 28-day incubation period, the pH of the soil and $CaCl_2$-extractable and total amounts of Zn and Cu in the incubated soils were determined by ICP-OES for two concentric soil sections (0-9 mm and >9 mm from the fertilizer application point) as described by our previous works.[4, 5]

Plant study. An agricultural soil thought to be Zn- and Cu-deficient was selected for this plant-based experiment. The soil sample was collected near Lock, South Australia, and classified as Calcarosol according to the Australian Soil Classification.[6] The topsoil sample (0-10 cm) was dried in air and sieved (less than 2 mm) before the characterization (Table S2). The study had four fertilizers treatments (control-Zn, Control-Cu, $ZnSO_4$, Zn-GO, $CuSO_4$ and Cu-GO), three replicates for each formulation and 21 pots in total.

Table S2. Selected physical and chemical properties of the soil used for plant study. The soil was collected from the top layer of (0-10 cm), air dried and sieved to < 2mm before use.

Soil location	Lock, South Australia
Soil type	Sandy loam
Soil classification	Calcarosol
pH ($CaCl_2$)	8.5

OC (%)[b]	<0.1
$CaCO_3$ (%)	30
Total N (%)	0.05
Clay (%)	3.1
Silt (%)	0.4
Sand (%)	58
Ca (mg kg^{-1})	3.3
Mg (mg kg^{-1})	0.9
Na (mg kg^{-1})	0.3
K (mg kg^{-1})	0.2
NH_4	2.3

A balanced basal fertilization solution was added to the each 2.0 kg pot, providing a total nutrient dose of: 30 mg kg^{-1} P as monoammonium phosphate, 30 mg kg^{-1} K as potassium chloride, 15 mg kg^{-1} Ca as calcium nitrate, 10 mg kg^{-1} Mg as magnesium nitrate, 15 mg kg^{-1} S as ammonium sulphate, 3 mg kg^{-1} B as boric acid, 2 mg kg^{-1} Mn as manganese chloride, 1 mg kg^{-1} Mo as ammonium molybdate and 2 mg kg^{-1} Fe as ferric citrate. Furthermore, Cu (4 mg kg^{-1}) as copper sulphate was added to the –Zn control, the Zn-GO and the $ZnSO_4$ treatments and Zn (4 mg kg^{-1}) as zinc sulphate was added to the –Cu control, Cu-GO and $CuSO_4$ treatments. After soil treatment with liquid basal nutrient, 8 pre-germinated seeds of durum wheat (*Triticum durum cv.*Yallaroi) were planted at the 10-5 mm depth and the fertilizers granules ($ZnSO_4$, Zn-GO, $CuSO_4$ and Cu-GO) were applied in the middle of the pots at the depth of 10 cm at a rate of 10 mg Zn kg^{-1} or 5 mg Cu kg^{-1}.

The number of plants were reduced to four after one week while the most similar plants were kept in each pot. Polyethylene beads were used to cover the soil surface to decrease water evaporation from soil. The plants were kept for 6 weeks in a constant-environment chamber with following conditions: 12 h days with 20 °C and 12 h nights with15-20ºC. Plants were harvested at 6 weeks as described in detail elsewhere.[10] Zn and Cu uptake by plants were analysed using ICP-OES.

Characterizations and statistical analysis. The vibrational characteristics of GO and the prepared materials (Zn-GO and Cu-GO) were analysed by Raman spectroscopy (LabRAM HR Evolution, Horiba Jvon Yvon Technology, Japan) measured between 500-3500 cm^{-1}. Conditions were set up as follows: a 532 nm laser, 50x objective with a spot size of 100 µm, integration time of 10 s for 3 accumulations. Raman graphs are displayed with no data processing. X-ray diffraction (600 Miniflex, Rigaco, Japan) was used to confirm the structure of GO and to determine the phase of Zn and Cu for any evidence of precipitation of their oxides or hydroxides on graphene oxide sheets.

Fourier Transform Infrared (FTIR) spectrometer (Nicolet 6700 Thermo Fisher) was used to analyse graphene oxide sheets. Samples for atomic force microscopy (AFM) were prepared based on our previous work.[1] Briefly, GO suspensions was drop-casted onto clean silicon wafers, followed by washing with ethanol and Milli-Q water and plasma cleaning for 30 s. Imaging was taken under ambient conditions with a NTegra Solaris AFM (NT-MDT) in the semi-contact (tapping) mode of operation and using NSG10 AFM probes made of silicon nitride with a tip radius of 10 nm.

Thermal decomposition of GO and as-prepared Zn-GO and Cu-GO were performed using a thermal gravimetric analyser (TGA, Q500, TA Instruments, USA) under air atmosphere where the samples were heated to 900°C at a heating rate of 10°C min^{-1}.

X-ray photoelectron spectroscopy (XPS) characterization was performed using an AXIS Ultra-DLD. The instrument equipped with a monochromatic Alkα radiation source. Details of the instrument parameters are described in depth elsewhere.[2] Casa XPSTM software was used to process data and curve-fitting of XPS data.

Analysis of variance (ANOVA) was conducted using IBM SPSS statistical software. Multiple comparison of means were conducted using the LSD test when the ANOVA indicated significant differences. The level of significance was *P<0.05*.

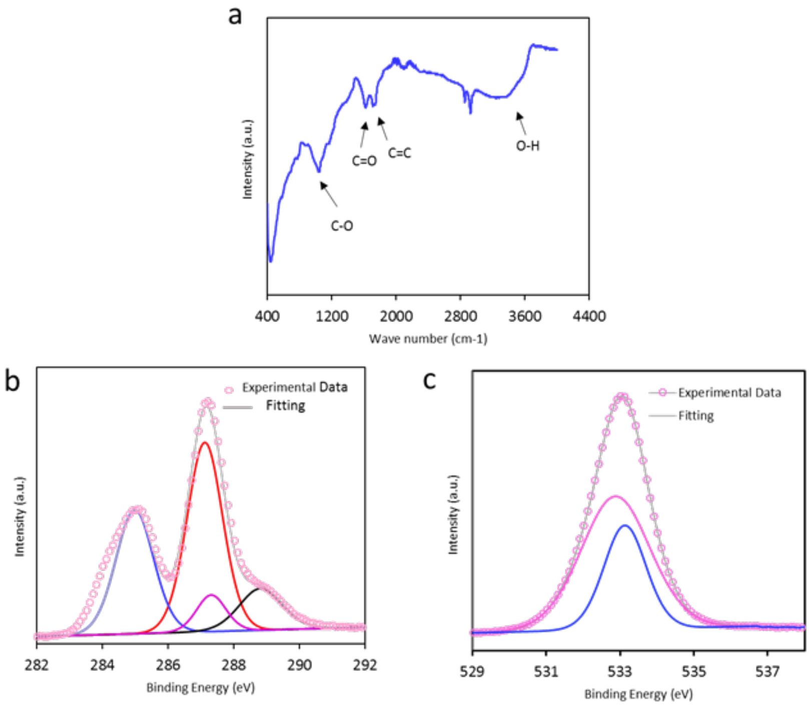

Figure S1. (a) Fourier transform infrared spectroscopy (FTIR) confirms the presence of oxygen-containing functional groups on the surface of GO. The broad band between 2600-3800 cm^{-1} results from the presence of hydroxyl groups due to the intercalated water and structural hydroxyl groups (-COOH and –COH) of GO.[11-13] The bands at 1720-1740 cm^{-1} are associated with the stretching vibration of the C=O bond, and the band at 1620 cm^{-1} can be assigned to C=C skeletal vibrations of the non-oxidized graphitic domain, 1590 cm^{-1} is related to the stretching of C=C bonds, [12, 14-17] and the bands at 1240 and 1250 cm^{-1} are associated with C-O. [1, 12, 14-17]

(b) The high resolution C1s spectra of GO obtained by X-ray photoelectron spectroscopy (XPS) revealed four peaks that corresponded to the following functional groups: carbon sp^2 (C═C, 284.9

eV), epoxy/hydroxyls (C−O, 287.1 eV), carbonyl (C═O, 287.3 eV), and carboxylates (O−C═O, 288.8 eV).

(c) The XPS spectrum of O1s was deconvoluted into two peaks. The first peak with a binding energy of 532.8 eV can be assigned to C-O. The second peak with a binding energy of 533.1 eV is associated with C=O and O=C-OH, carbonyl oxygen atoms in the carboxylic groups and esters. [13, 18, 19]

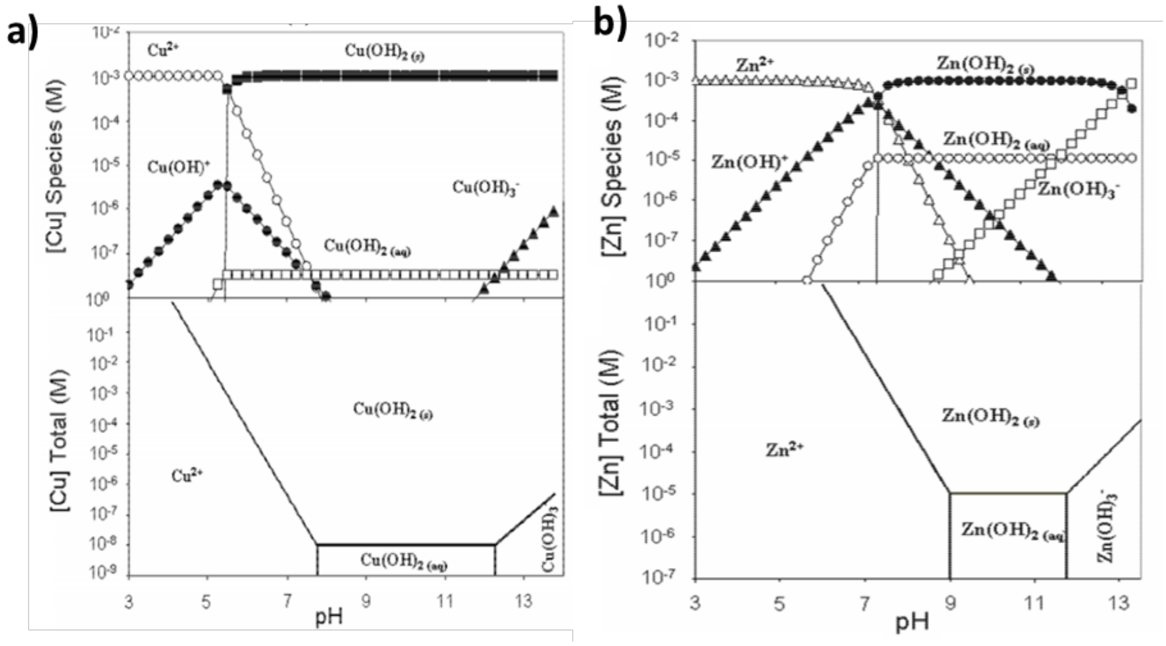

Figure S2. Thermodynamic speciation of (a) copper and (b) zinc calculated as afunction of pH (top) at a fixed (Cu and Zn) concentration of 1×10^{-3} M and (bottom) as a function of (Cu and Zn) concentration at 25°C (E_h = 0.25 V SHE).[20]

Kinetic Models (S3)

In order to investigate the controlling mechanism of sorption process such as mass transfer and chemical reaction, different theoretical models such as pseudo-first-order and pseudo-second-order kinetic were applied to the experimental data. Importantly to note that the chemical and physical features of the sorbent have large impacts on both the sorption kinetics and sorption mechanism.[21] Empirical pseudo-first-order and pseudo-second-order kinetic models can be expressed by equation (1) for reaction exponents n = 1 and 2, respectively.[22]

$$\frac{dq_t}{dt} = K_n(q_e - q_t)^n \qquad (1)$$

Here q_t (mg/g) and q_e (mg/g) represent the amount of solute sorbed per gram of sorbent at time t and at equilibrium, respectively; K_1 and K_2 are the first- and second-order kinetic rate constants, respectively. Combination of equation (1) with the boundary condition ($q_t = 0$ at $t = 0$) provides equations (2) and (3) for $n = 1$ and 2, respectively.

$$\log(q_e - q_t) = log q_e - \frac{k_1}{2.303}t \qquad (2)$$

$$\frac{t}{q_t} = \frac{1}{k_2 q_e^2} + \frac{t}{q_e} \qquad (3)$$

Table S3. Kinetic parameters of the pseudo-first order and pseudo-second order equations for Zn^{+2} and Cu^{+2} sorption on GO.

	Pseudo-first order kinetic			Pseudo-second order kinetic		
	q_e	K_1	R	q_e	K_2	R
Zn	72.1	0.03	0.725	133	0.0018	0.988
Cu	40	0.046	0.804	73	0.003	0.963

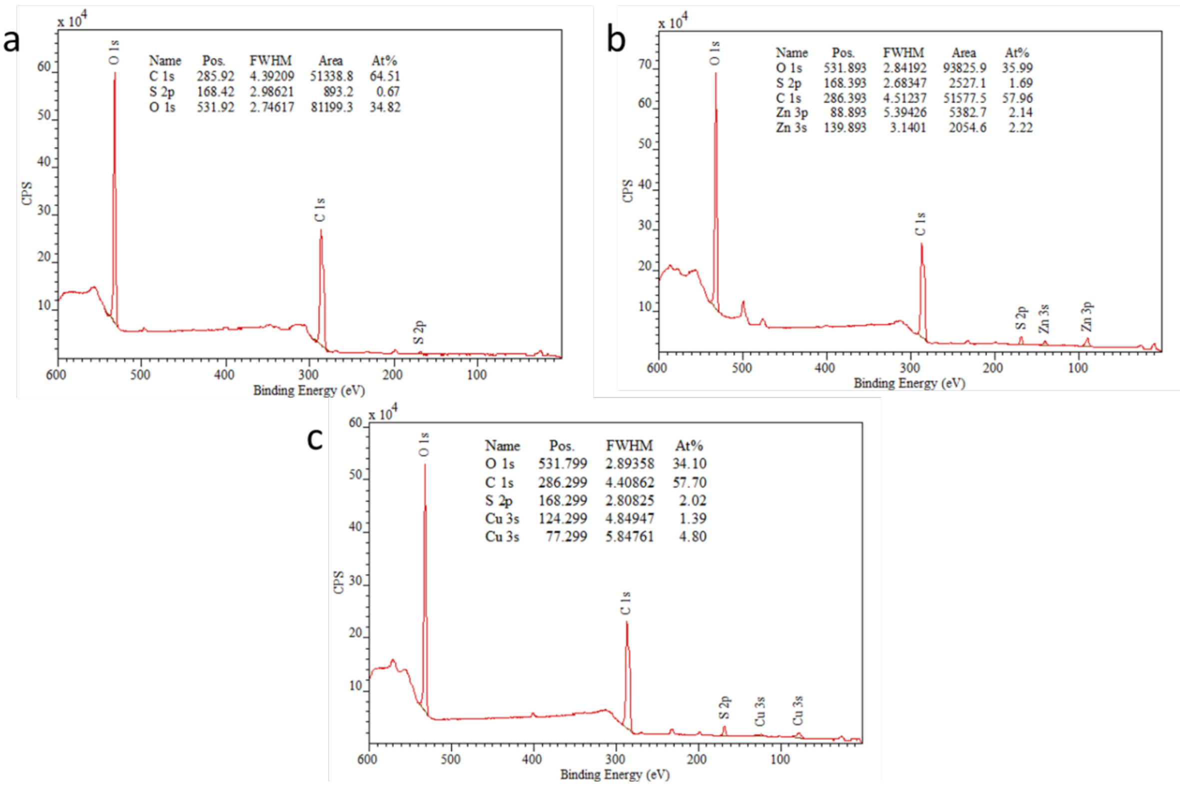

Figure S3. The survey spectra obtained from a) GO sheets, b) Zn-GO and c) Cu-GO.

Table S4. Percent elemental concentration for GO, Zn-GO and Cu-GO composites from XPS survey scans

Elements	**Position**			**Atomic composition (%)**		
	GO	Zn-GO	Cu-GO	GO	Zn-GO	Cu-GO
C 1s	285.9	286.4	286.3	64.5	57.9	57.7
O 1s	531.9	531.9	531.8	34.8	36	34.1
S 2p	168.4	168.4	168.3	0.67	1.69	2.02
Zn 3s/3p	-	139.9/88.9	-	-	4.34	-
Cu 3s	-	-	124.3/77.3	-	-	6.2

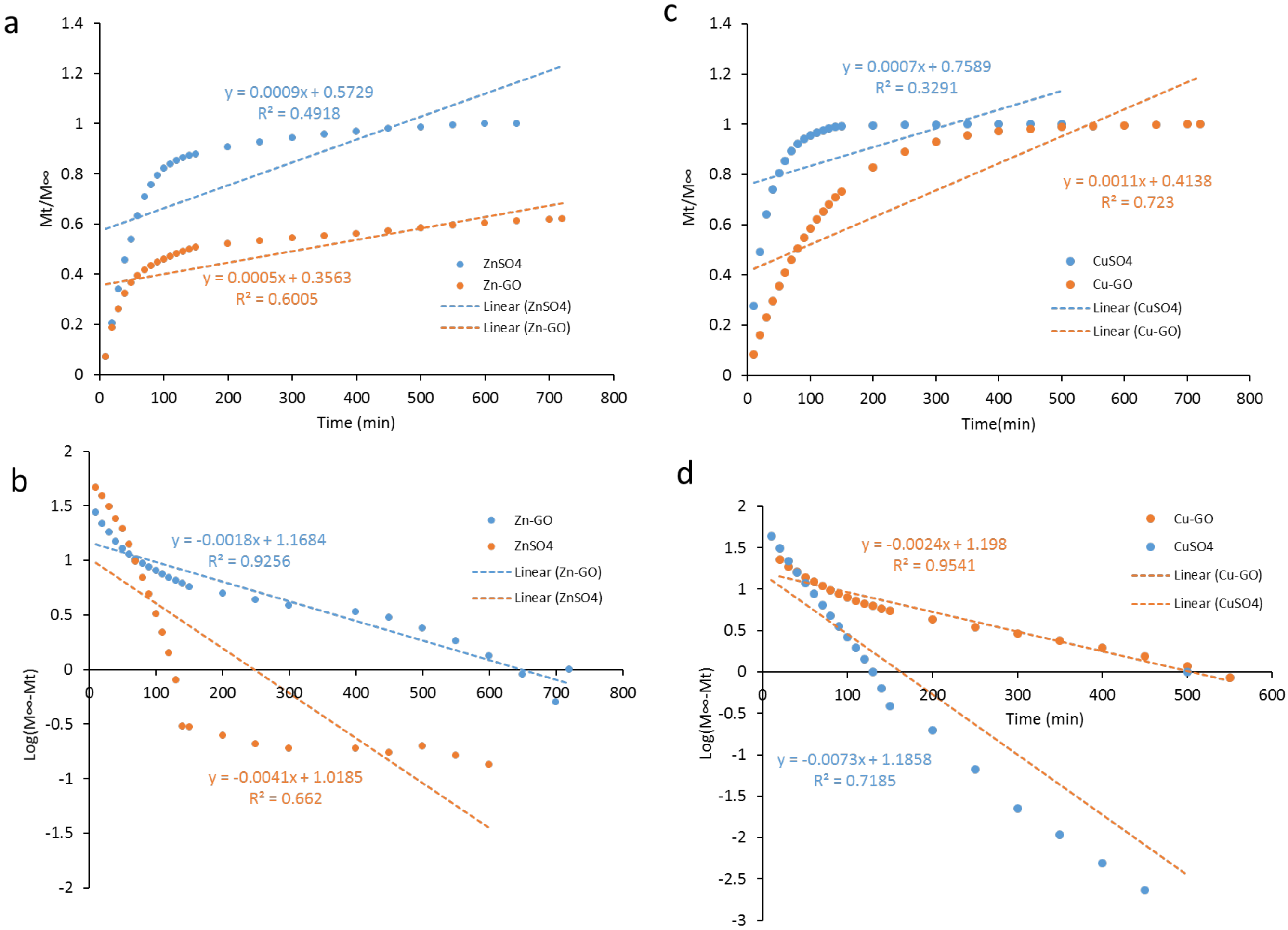

Figure S4. Mathematical release models of a) Zero-order and b) First-order models of Zn-GO, and c) Zero-order and d) First-order model of Cu-GO.

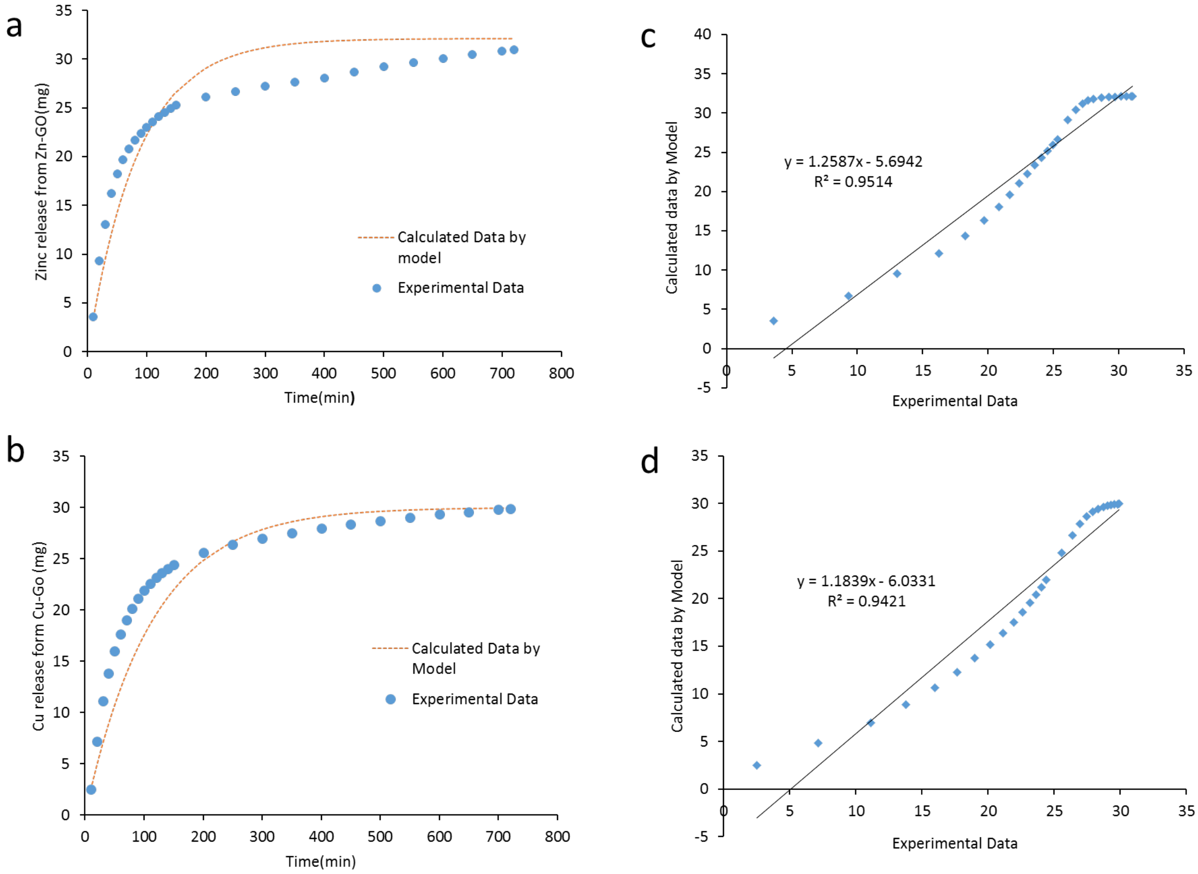

Figure S5. The cumulative release of nutrients from slow released a) Zn-GO and b) Cu-GO fertilizers as measured in experiments or as fitted with the first-order kinetic model, and the modelled versus the observed release data for c) Zn-GO and d) Cu-GO fertilizers.

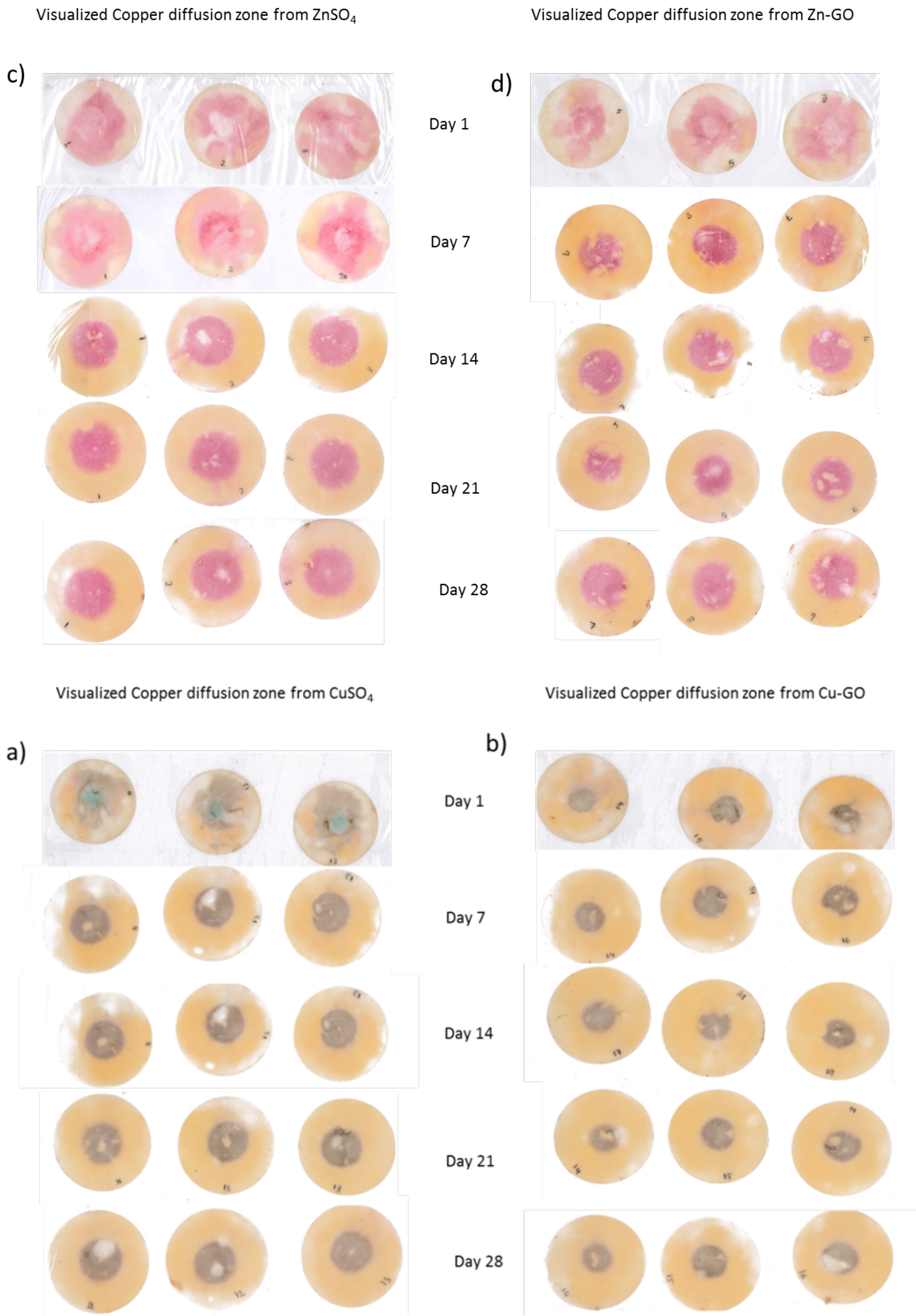

Figure S6. Visualized copper diffusion from a) $ZnSO_4$ and b) Zn-GO, and visualized zinc diffusion from c) $CuSO_4$ and d) Cu-GO at 1, 7, 14, 21 and 28 days of incubation.

References:

1. Tran, D. N. H.; Kabiri, S.; Losic, D. A green approach for the reduction of graphene oxide nanosheets using non-aromatic amino acids. *Carbon* 2014, 76, 193-202.
2. Kabiri, S.; Tran, D. N. H.; Cole, M. A.; Losic, D. Functionalized three-dimensional (3D) graphene composite for high efficiency removal of mercury. *Environmental Science: Water Research & Technology* 2016, 2, 390-402.
3. Milani, N.; McLaughlin, M. J.; Stacey, S. P.; Kirby, J. K.; Hettiarachchi, G. M.; Beak, D. G.; Cornelis, G. Dissolution kinetics of macronutrient fertilizers coated with manufactured zinc oxide nanoparticles. *Journal of Agricultural and Food Chemistry* 2012, 60, 3991-3998.
4. Degryse, F.; Baird, R.; McLaughlin, M. Diffusion and solubility control of fertilizer-applied zinc: chemical assessment and visualization. *Plant and Soil* 2015, 386, 195-204.
5. Lombi, E.; McLaughlin, M. J.; Johnston, C.; Armstrong, R. D.; Holloway, R. E. Mobility and lability of phosphorus from granular and fluid monoammonium phosphate differs in a calcareous soil. *Soil Science Society of America Journal* 2004, 68.
6. Isbell, R. f. *The Australian soil classification*. Collingwood, Victoria: CSIRO Australia: 1996; p 143.
7. Matejovic, I. Determination of carbon and nitrogen in samples of various soils by the dry combustion. *Communications in Soil Science and Plant Analysis* 1997, 28, 1499-1511.
8. Neil McKenzie, K. C., Hamish Cresswell. *Soil physical measurment and interpretation for land evaluation*. CSIRO publishing: Collingwood, 2002.
9. Rayment, G. E. *Australian laboratory handbook of soil and water chemical methods / G.E. Rayment and F.R. Higginson*. Inkata Press: Melbourne, 1992.
10. McBeath, T. M.; McLaughlin, M. J. Efficacy of zinc oxides as fertilisers. *Plant and Soil* 2014, 374, 843-855.
11. Hontoria-Lucas, C.; López-Peinado, A. J.; López-González, J. d. D.; Rojas-Cervantes, M. L.; Martín-Aranda, R. M. Study of oxygen-containing groups in a series of graphite oxides: Physical and chemical characterization. *Carbon* 1995, 33, 1585-1592.
12. Marcano, D. C.; Kosynkin, D. V.; Berlin, J. M.; Sinitskii, A.; Sun, Z.; Slesarev, A.; Alemany, L. B.; Lu, W.; Tour, J. M. Improved synthesis of graphene oxide. *ACS Nano* 2010, 4, 4806-4814.
13. Sitko, R.; Turek, E.; Zawisza, B.; Malicka, E.; Talik, E.; Heimann, J.; Gagor, A.; Feist, B.; Wrzalik, R. Adsorption of divalent metal ions from aqueous solutions using graphene oxide. *Dalton Transactions* 2013, 42, 5682-5689.
14. Acik, M.; Lee, G.; Mattevi, C.; Pirkle, A.; Wallace, R. M.; Chhowalla, M.; Cho, K.; Chabal, Y. The Role of oxygen during thermal reduction of graphene oxide studied by infrared absorption Spectroscopy. *The Journal of Physical Chemistry C* 2011, 115, 19761-19781.
15. Guo, H.-L.; Wang, X.-F.; Qian, Q.-Y.; Wang, F.-B.; Xia, X.-H. A green approach to the synthesis of graphene nanosheets. *ACS Nano* 2009, 3, 2653-2659.
16. Kabiri, S.; Tran, D. N. H.; Altalhi, T.; Losic, D. Outstanding adsorption performance of graphene–carbon nanotube aerogels for continuous oil removal. *Carbon* 2014, 80, 523-533.
17. Kabiri, S.; Tran, D. N. H.; Azari, S.; Losic, D. Graphene-diatom silica aerogels for efficient removal of mercury ions from water. *ACS Applied Materials & Interfaces* 2015, 7, 11815-11823.
18. Mattevi, C.; Eda, G.; Agnoli, S.; Miller, S.; Mkhoyan, K. A.; Celik, O.; Mastrogiovanni, D.; Granozzi, G.; Garfunkel, E.; Chhowalla, M. Evolution of electrical, chemical, and structural properties of transparent and conducting chemically derived graphene thin films. *Advanced Functional Materials* 2009, 19, 2577-2583.
19. Yang, D.; Velamakanni, A.; Bozoklu, G.; Park, S.; Stoller, M.; Piner, R. D.; Stankovich, S.; Jung, I.; Field, D. A.; Ventrice Jr, C. A.; Ruoff, R. S. Chemical analysis of graphene oxide films after heat and chemical treatments by X-ray photoelectron and micro-Raman spectroscopy. *Carbon* 2009, 47, 145-152.
20. Trent William Jay Albrecht*, J. A.-M. a. D. F. Effect of pH, concentration and temperature on copper and zinc hydroxide formation/precipitation in solution in *Chemeca*, Australia, 2011.
21. Yang, X.; Zhang, X.; Liu, Z.; Ma, Y.; Huang, Y.; Chen, Y. *J. Phys. Chem. C* 2008, 112, 17554.
22. Yu, Y.; Addai-Mensah, J.; Losic, D. Functionalized diatom silica microparticles for removal of mercury ions. *Science and Technology of Advanced Materials* 2012, 13, 015008.

Chapter 4

Suspension micronutrient fertilizers manufactured using zinc-loaded graphene oxide- are more efficient that granular forms in both banded and mixed applications

This section is included in the thesis as it appears as a manuscript submitted by **Shervin Kabiri,** Rodrigo C. da Silva,Fien Degryse, Diana N.H. Tran, Mike J. McLaughlin and Dusan Losic, "Suspension micronutrient fertilizers manufactured using zinc-loaded graphene oxide- are more efficient than granular forms in both banded and mixed applications", ***Journal of ACS,*** *Environmental Science and Technology* (2018).

Statement of Authorship

Title of Paper	Suspension micronutrient fertilizers manufactured using zinc-loaded graphene oxide- are more efficient than granular forms in both banded and mixed applications
Publication Status	☐ Published ☐ Accepted for Publication ☑ Submitted for Publication ☐ Unpublished and Unsubmitted w ork w ritten in manuscript style
Publication Details	Submitted to the journal of ACS sustainable energy and environment

Principal Author

Name of Principal Author (Candidate)	Shervin Kabiri		
Contribution to the Paper	Under the supervision of Dusan Losic, Michael McLaughlin and Diana Tran, I developed, designed and conducted the experiments, interpreted and processed the data and wrote the manuscript for submission.		
Overall percentage (%)	85		
Certification:	This paper reports on original research I conducted during the period of my Higher Degree by Research candidature and is not subject to any obligations or contractual agreements with a third party that would constrain its inclusion in this thesis. I am the primary author of this paper.		
Signature		Date	22/06/2018

Co-Author Contributions

By signing the Statement of Authorship, each author certifies that:

i. the candidate's stated contribution to the publication is accurate (as detailed above);

ii. permission is granted for the candidate in include the publication in the thesis; and

iii. the sum of all co-author contributions is equal to 100% less the candidate's stated contribution.

Name of Co-Author	Rodrigo C. da Silva		
Contribution to the Paper	I helped Shervin Kabiri (candidate) with interpreting experimental results and improving the manuscript for submission. I give consent for Shervin Kabiri to present this paper for examination towards the Doctorate of philosophy.		
Signature		Date	22/06/2018

Name of Co-Author	Fien Degryse		
Contribution to the Paper	I helped Shervin Kabiri (candidate) with interpreting experimental results and improving the manuscript for submission. I give consent for Shervin Kabiri to present this paper for examination towards the Doctorate of philosophy.		
Signature		Date	22/06/2018

Name of Co-Author	Diana N.H. Tran		
Contribution to the Paper	I acted as the secondary supervisor for Shervin Kabiri and helped her to design the experiments and improve the final drafts of the manuscript for submission. I give consent for Shervin Kabiri to present this paper for examination towards the Doctorate of philosophy.		
Signature		Date	22/06/2018

Name of Co-Author	Mike J. McLaughlin		
Contribution to the Paper	I acted as the secondary supervisor for Shervin Kabiri and aided in design and development of experiments and evaluation of manuscript for submission. I give consent for Shervin Kabiri to present this paper for examination towards the Doctorate of philosophy.		
Signature		Date	22/06/2018

Name of Co-Author	Dusan Losic		
Contribution to the Paper	I acted as the primary supervisor for Shervin Kabiri and aided in design and development of experiments and evaluation of manuscript for submission. I give consent for Shervin Kabiri to present this paper for examination towards the Doctorate of philosophy.		
Signature		Date	22/06/2018

Suspension micronutrient fertilizers manufactured using zinc-loaded graphene oxide- are more efficient that granular forms in both banded and mixed applications

*Shervin Kabiri[†], Rodrigo C. da Silva [§], Fien Degryse [§], Diana N.H. Tran[†], Mike J. McLaughlin *[§] and Dusan Losic*[†]*

[†]School of Chemical Engineering, Engineering North Building, The University of Adelaide, Adelaide, SA 5005, Australia

[§]Fertilizer Technology Research Centre, School of Agriculture, Food and Wine, The University of Adelaide, Waite Campus, PMB1, Glen Osmond, SA 5064, Australia

Abstract: A demand for doubling food production within the next 50 years necessitates the development of advanced fertilizers with better performance and less adverse effects on the environment. In this study, graphene oxide (GO) loaded with zinc (Zn), either in granular form or as a suspension was used as an alternative fertilizer to water soluble $ZnSO_4$ fertilizer in a calcareous soil. The efficiency of these new sources of Zn was compared to that of $ZnSO_4$, both for banded application or when mixed through the soil. A greenhouse experiment showed that both banded (as granular or suspension) and mixed (as suspension) treatments of Zn-loaded GO (Zn-GO) significantly increased plant dry mass and Zn uptake compared to $ZnSO_4$ (granule and solution), with suspension formulations being more effective than granular ones. Banding granular fertilizer reduced the effectiveness of $ZnSO_4$ but not of Zn-GO and banded suspension was the best treatment. It was concluded that GO-based fertilizers are a better nutrient source for increasing nutrient content in Zn-deficient calcareous soils, likely because of reduced fixation in soil due to their slow-release properties arising from specific physicochemical properties of the GO sheets and complexation of Zn with GO-based fertilizers.

Keywords: graphene oxide; slow-release; suspension; fluid; zinc fertilizer

INTRODUCTION

The world population is estimated to double by 2050 and grain production should hence double over this timeframe to fulfil global demand.[1] However, increasing agricultural output requires increased use of elements like nitrogen, phosphorus and micronutrient metal ions in the form of fertilizers, so doubling food production in a way that does not affect the environment and public health is very challenging.[2-4] Therefore, there is a need to improve fertilizer use efficiency while reducing the potential negative environmental impacts of fertilizers, by replacing current fertilizers with more efficient ones.[5, 6] Another challenge in crop production is to increase the concentrations of micronutrients, such as Zn, in staple cereal grain food crops to prevent extensive malnutrition, especially in developing countries where grain constitutes the majority of the human diet.[3, 7]

Zinc is one of the nutrients required for normal growth of plants and humans, and its deficiency is considered to be one of the most common problems regarding crop productivity and human health globally.[8] However, around 50% of soils used for cereal production contain suboptimal levels of plant-available Zn, which affects grain yield and nutritional quality, and consequently human health.[9] High soil pH and high content of calcium carbonate ($CaCO_3$) are some of the major factors responsible for low availability of Zn for plant roots, due to the various sorption and precipitation reactions of Zn in soil. [10, 11] A common practice to correct Zn deficiency of soil throughout the world is applying Zn fertilizers such as zinc sulphate ($ZnSO_4$) or zinc oxide (ZnO).[10, 12] However, only a small amount of applied Zn is taken up by crops (<5%) depending on the soil and the type and rate of fertilizer used, due to the strong adsorption of Zn onto soil surfaces.[7, 13, 14] Furthermore, Zn is a diffusion-limited nutrient in soil, so fertilizer solubility, physical form (granular, powder and fluid) and placement can affect its diffusion in soil and availability to plants.[15-18] In general, highly water-soluble Zn fertilizers such as $ZnSO_4$ perform better in highly deficient soils,[19-21] and the efficiency of less soluble sources (e.g. ZnO) depends on its placement.[17] Band-applied $ZnSO_4$ granules are superior to banded ZnO because the dissolution of granulated or powdered ZnO is restricted when banded due to increases in pH in the application zone. Mixing ZnO through soil improves its effectiveness markedly as the soil buffers pH changes more effectively (and can supply H^+ ions to aid dissolution) and provides a (sorption) sink for Zn^{2+} ions dissolved from the oxide. [17]

Fluid forms of micronutrients often diffuse further from the point of application in soil than chemically similar granular sources ,[22] and are agronomically more effective in the field.[23] Recent studies have shown an increase in grain yield and/or concentration in response to fluid Zn compared to granular form in calcareous soil. [22-24] The efficiency of the physical state of Zn fertilizers (fluid *versus* granular) on plant yield and nutrient uptake have been investigated.[18] Early research conducted by Mortvedt and Giordano [25] compared the efficiency of ZnO-based fertilizers in different physical states (granular *versus* fluid) and using different methods of applications (mixed *versus* banded) on corn in a non-calcareous soil. Their results showed that the effectiveness of the fluid forms was much higher than that of the granular forms when mixed throughout the soil, but the efficiency of the fluid sources was affected more than the granular sources by banding.[25] They suggested that the superiority of the fluid fertilizers over granular forms was related to the better distribution of Zn through the soil. Similarly, Holloway et al. [26] showed that fluid Zn outperformed a granular products in field trials.[26] However, they argued that the greater performance of fluid fertilizers compared to their granular counterparts is not related to its greater distribution in the soil, as the fluid fertilizers had very low application volumes (30-150 L/ha).[27] The greater crop response to fluid fertilizer compared to granular was suggested to be due to different chemical reactions around the point of soil:fertilizer contact, with irreversible sorption of Zn when applied in granular form.[18] Experiments conducted by Hettiarachchi et al.[22] to determine the potential available Zn from fluid or granular Zn fertilizers at different distances from the point of application showed that, irrespective of the method of application, more than 90% of fertilizer Zn was recovered close to the point of application (0-7.5 mm). However, most of the applied fluid Zn fertilizer remained in a labile form (as determined by isotopic dilution), confirming the greater availability of Zn from the fluid form.

We have previously demonstrated that granular graphene oxide (GO) is an effective carrier for micronutrients such as Zn that slows the release of this micronutrient to the soil, yet diffusion and crop uptake were similar or greater than an equivalent soluble Zn source ($ZnSO_4$).[28] This significant difference in the release pattern of the micronutrients from the GO-based carriers compared to commercial fertilizers was related to the tight coordination of the metal ions and oxygen functional groups on the GO surface, and the trapping of nutrients between stacked and folded GO sheets in the granules.[28] However, the effect of fertilizer form on the effectiveness of GO-based micronutrient fertilizers for plant growth was not examined. We hypothesise that given the strong effect of the fertilizer form on micronutrient behaviour and uptake by plants, the suspension forms of GO-based micronutrient fertilizers may be even more effective than their granulated forms. In this study, the effect of GO-fertilizer form (granular vs suspension) and placement (banded vs mixed) was evaluated on nutrient behaviour in soil and availability of Zn to wheat compared to $ZnSO_4$. To understand the mechanisms and reactions occurring during the application of these products to soils, we examined the diffusion, solubility, and potential availability of Zn from granular and fluid forms of Zn fertilizer in an alkaline calcareous soil using laboratory incubation experiments.

MATERIALS AND METHODS

Preparation of graphene-oxide based Zn fertilizers (Zn-GO)

Graphene oxide was prepared from graphite is supplied from a local mining (Uley, Eyre Peninsula, South Australia, Australia) based on the improved Hummers method. [29] Zinc-loaded GO (Zn-GO) fertilizers were prepared based on our previous work.[28] Briefly, 0.01M of Zn as $ZnSO_4$ was added to 1 L of GO solution (1 mg/mL), while the pH of the suspension was fixed at 6 and stirred for 120 min. The loaded GO with Zn was collected by centrifugation, semi-dried in an oven at 50 °C for 12 h, and then cut into small cubes (0.5 cm by 0.5 cm). Both GO and Zn-GO were characterized with Fourier transform infrared spectroscopy (FTIR), X-ray diffraction (XRD) and thermogravimetric analysis TGA (Figure S1, Supporting Information). The total Zn concentration of the granules was measured using an open vessel *aqua regia* extraction method followed by analysis with inductively coupled plasma optical emission spectrometry (ICP-OES), as described in our previous work. [30]

Water-soluble Zn concentrations of $ZnSO_4$ granules and Zn-GO granules and suspension were measured by agitating 1 g of each fertilizer in 250 mL of ultrapure deionized water for 24 h in an end-over-end shaker. The samples were then centrifuged at 2950 g and filtered before measuring Zn concentration with ICP-OES and the pH of samples was measured in the remaining supernatant. The basic information of the fertilizers is summarized in Table 1.

Soil properties

A calcareous soil was collected near Lock, South Australia. The topsoil sample (0-10 cm) was air dried and sieved to less than 2 mm. Soil pH was measured in a 1:5 soil to water suspension,[31] and soil texture was determined as described in the USDA manual on soil testing.[32] Total organic C and N were determined following Matejovic et. al.[33] Calcium carbonate content was measured according to the procedure of Peterson et. al[34] and water content at field capacity was measured using the method of Klute et. al.[35] The calcareous soil had pH 8.5, 58% sand, 0.4% slit, 3.1% clay, total C content of 3.5 g/kg, total N content of 0.05 g/kg and contained 30 g $CaCO_3$/kg.

Table 1. Total percentage of Zn in $ZnSO_4$, granules and Zn-GO granules and suspension, water soluble Zn relative to total Zn in fertilizer and pH of fertilizer after agitating in water for 24 hours.

Fertilizer	Total Zn percentage in fertilizer	Water-soluble Zn relative to total Zn in fertilizer	pH
$ZnSO_4$ granular	36.4(±0.65)	100(±0.00)	6.04 (±0.01)
Zn-GO granular	13(±0.80)	40.3 (±2.00)	3.86 (±0.07)
Zn-GO suspension	13(±0.80)	58.3(±2.60)	4.94 (±0.03)

Plant study

Durum wheat (*Triticum durum cv.* Yallaroi) was grown in the greenhouse. Plastic pots were filled with 2 kg of sieved soil samples and 50 mL of equilibrated basal fertilizer containing phosphorous (P), potassium (K), calcium (Ca), magnesium (Mg), sulphur (S), manganese (Mn), molybdenum (Mo), copper (Cu) and Iron (Fe) was supplied to each pot before placing seeds in the pots. Urea was added to soil twice, at the end of second and fourth week of plant growth in order to supply plant with nitrogen.[28] The experiment included five fertilizer treatments: (i) banded granular $ZnSO_4$ ($ZnSO_4$-G), (ii) mixed $ZnSO_4$ (in form of concentrated solution, $ZnSO_4$-S), (iii) banded granular Zn-GO (Zn-GO-G), (iv) banded Zn-GO in suspension form (Zn-GO-S), (v) mixed Zn-GO in suspension form, and three replicates were applied for each formulation. Commercial $ZnSO_4$ granules (~0.4 cm diameter) were used as a positive control treatment and an unfertilized (Zn) treatment with only the basal nutrient solutions served as a negative control treatment.

For the pots with banded application of granular fertilizers, three granules were placed in three spots 5 cm below the soil surface. For the banded application of suspension Zn-GO, 5 mL of suspension was injected in three spots. For the mixed treatments, $ZnSO_4$ dissolved in water and Zn-GO suspension dispersed homogenously in water were mixed with the soil prior to sowing. The Zn fertilizers were applied at 10 mg Zn /kg, a rate based on a preliminary response curve trial.

Following the addition of liquid basal nutrients, 8 pre-germinated seeds of durum wheat were transplanted at 10-15 mm depth below the soil surface. The plants were thinned to four seedlings per pot after one week and the soil surface was covered with 60 g of polyethylene beads to reduce moisture loss. The pots were weighed daily and watered with deionized water to field capacity. At the end of 6 weeks, plants were cut 2 cm above the soil surface and then dried in the oven at 70ºC until a constant weight was obtained. Dried plants were digested and analysed using ICP-OES for Zn concentration as previously described.[17]

Nutrient diffusion visualization method in soil

A laboratory experiment was set up similar to the work described by Degryse et.al.[8] Briefly, small-size Petri dishes (diameter of 5.5 cm and 1 cm height) were filled with soil, watered to field capacity (same soil as the plant study), covered with lids, and incubated at 25°C. The granules of $ZnSO_4$ and Zn-GO were applied as a single granule in the centre of the dish, whereas the fluid treatments were applied as 1 mL of viscous Zn-GO suspension in a similar position (the Zn-GO suspension stayed in the point of application due to its high viscosity). Three replicates were applied for each formulation. The rate of Zn was similar (10 mg per Petri dish) for all formulations. The Petri dishes were then placed in a plastic bag to avoid moisture loss from the soil and incubated at 25°C. Calcium carbonate ($CaCO_3$)-impregnated filter papers were placed on the surface of the moist soil at 1, 2, 3, 4, 5 and 6 weeks of incubation to monitor Zn diffusion in the soil. A dithizone solution was used to detect adsorbed Zn on the $CaCO_3$-impregnated filter paper and all papers were scanned and analysed using imaging software (ImageJ).

Measuring soil pH and $CaCl_2$-extractable Zn

Soil pH and $CaCl_2$-extractable Zn were measured at the end of the incubation period using a method described by Lombi et al.[36] Independent set of Petri dish was incubated for these wet chemical analyses. Briefly, small size Petri dishes were filled with moist soil (Lock) and granules of $ZnSO_4$ and Zn-GO were applied as a single granule in the centre of a Petri dish for banded application. The suspension of Zn-GO was applied in the centre of the Petri dish for fluid treatments. For mixed application, Zn-GO suspension or $ZnSO_4$ solution were mixed thoroughly with the soil. Three replicates were applied for each formulation. The rate of Zn was 10 mg per Petri dish for all formulations. The Petri dishes were then placed in a plastic bag to avoid moist loss from the soil and incubated at 25°C. After 2, 4 and 6 weeks of incubation, the soil pH and $CaCl_2$-extractable Zn were measured in two concentric soil sections (0-8 mm and >8 mm from the fertilizer application point) for banded applications. Soil samples from the inner and outer sections were homogenised after drying in the oven overnight. 10 mL of $CaCl_2$ solution (1 mM) was added to 1 g of soil from the inner section and 20 mL of $CaCl_2$ solution (1 mM) was added to 2 g of soil from the outer section. For mixed applications, pH and $CaCl_2$-extractable Zn were measured for dried and homogenised soil by adding 20 mL of $CaCl_2$ solution (1 mM) to 2 g of soil. The resulting suspensions were shaken overnight and centrifuged at 4000 rpm (2950 g) for 30 min. The concentration of Zn in the supernatant was analysed by ICP-OES and the pH of the samples was measured on the remaining supernatant.

Characterizations and statistics

Zn-GO and $ZnSO_4$ granules were incubated with the moist soil (Lock) for 2 weeks. The fertilizer granules were taken out and attached soil was carefully removed from their surface before characterization. Scanning electron microscopy (SEM) images were acquired using a field-emission scanning electron microscope (Quanta 450, FEI, USA), elemental analysis from the surface of granules was conducted using an Aztec EDX system on a SEM Quanta 450, and microscopic photos were taken with a Nikon SMZ 745T stereomicroscope. Mineralogical characterization of $ZnSO_4$ and Zn-GO granules before and after incubation in the soil was investigated using XRD (600 Miniflex, Rigaco, Japan).

Statistics

Analysis of variance (ANOVA) was performed using IBM SPSS statistical software for the plant study and the incubation experiments. Multiple comparison of means was conducted using the LSD and Tukey tests when the ANOVA indicated significant differences. The level of significance was set at $P \leq 0.05$.

RESULTS

Plant yield and Zn placement effects

The response of wheat to Zn fertilizers varied according to the form of fertilizers and, banded and mixed methods of application (Figure 1). In the mixed application, the yield was significantly higher (29%) for the Zn-GO suspension (Zn-GO-S) than for the $ZnSO_4$ solution ($ZnSO_4$-S), (Figure S2, Supporting Information). Similarly, for banded treatments, the suspension form of Zn-GO yielded 46.2% and 71.6% more than the granular form of Zn-GO and $ZnSO_4$, respectively.

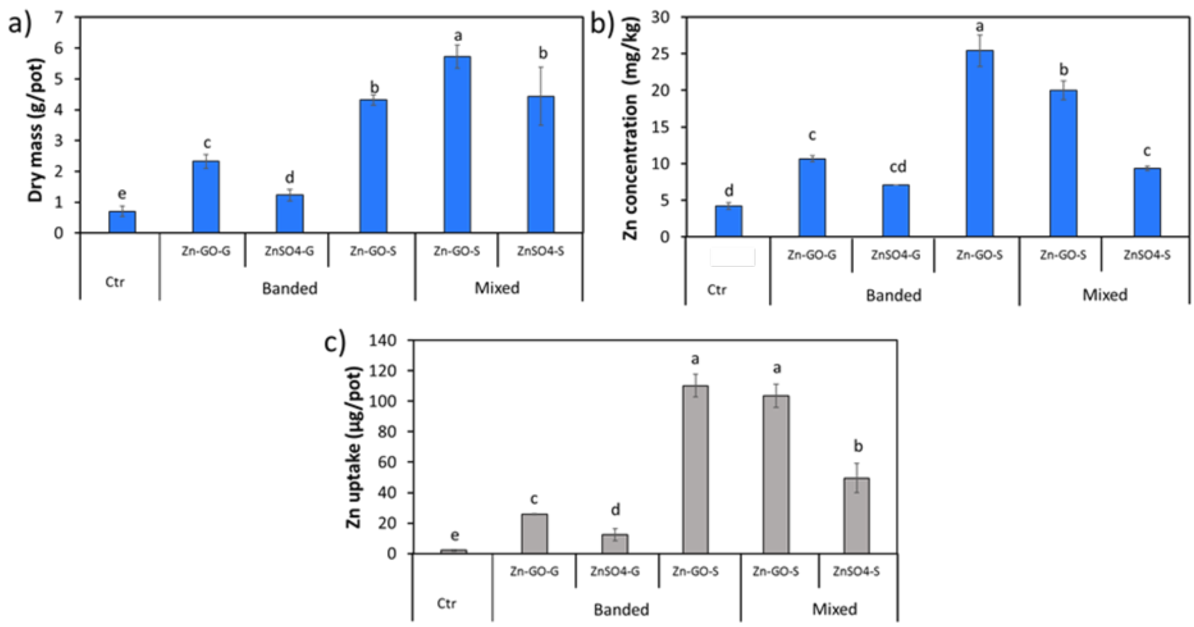

Figure 1. a) Dry mass, b) Zn concentration and c) Zn uptake for wheat plants with different Zn treatments and placement methods (banded and mixed) for a Zn rate of 10 mg/kg, (Ctr=control (no Zn), Zn-GO-G=Zn-GO granules, $ZnSO_4$-G= $ZnSO_4$ granules, Zn-GO-S=Zn-GO suspension

and $ZnSO_4$-S=$ZnSO_4$ solution (after 6 weeks). Different letters above the column indicate significant differences at a 5% significance level. Error bars indicate standard deviation of (n = 3).

The application of Zn fertilizer to the soil significantly enhanced the Zn concentration in plants with the Zn-GO suspension treatment having the highest Zn concentration in wheat plants. Zn-GO suspension whether banded or mixed (Figure 1b) performed better than mixed fluid $ZnSO_4$. However, the concentration of Zn in plants treated with granular Zn-GO and granular or fluid $ZnSO_4$ were below the critical value of 13 mg Zn/kg plant tissue.[17] Zinc uptake was increased by Zn addition for all types of fertilizers and method of applications (Figure 1c). Similar to results obtained from plant yield, the plants treated with suspension Zn-GO fertilizer (banded or mixed) had the highest Zn uptake followed by $ZnSO_4$ solution and the granular Zn-GO and $ZnSO_4$. Zn-GO suspension either banded or mixed with soil showed 77.5 and 76.5% higher Zn uptake than granular Zn-GO, showing the high effectiveness of Zn supply to plants by the Zn-GO suspension.

Diffusion and solubility of Zn from fertilizers in soil

The effective radius of Zn diffusion from the point of application is shown in Figure 2a and b. Zinc diffusion from Zn-GO suspension was significantly higher for Zn-GO suspension compared to granular fertilizers during the 6 week incubation period (Figure 2b). In the case of Zn-GO and $ZnSO_4$ granules, there was no significant difference in Zn diffusion for the first 2 weeks but the diffusion radius was significantly higher for Zn-GO-G compared to $ZnSO_4$-G from the third week of incubation onwards (Figure 2b).

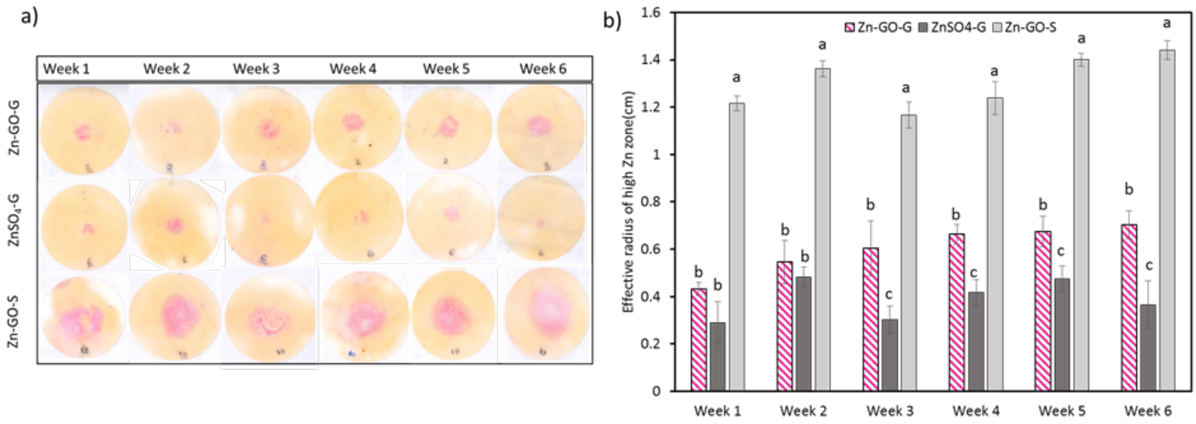

Figure 2. (a) Visualization of Zn diffusion and (b) radius of the high-Zn zone at 1, 2, 3, 4, 5 and 6 weeks after addition of Zn fertilizer in soil. Zinc was added to the soil at a rate of 10 mg Zn, as Zn-GO and $ZnSO_4$ granules (G), $ZnSO_4$ solution (S) and Zn-GO suspension (S).

The concentrations of $CaCl_2$-extractable Zn from soil incubated with Zn-GO and $ZnSO_4$ granules (banded) and Zn-GO suspension (banded) and Zn-GO suspension and $ZnSO_4$ solution (mixed) in the different soil sections are reported in Table 2. Zinc concentrations were much higher in the inner sections (< 8 mm) than in the outer sections, regardless of the source of Zn. For banded fertilizers, extracted Zn was significantly higher for the Zn-GO suspension compared to the granular formulations. In addition, concentrations of extracted Zn decreased from week 2 to week 6 for granular formulations but not for the Zn-GO suspension. Extracted Zn from granular formulations was high in the inner zone compared to the fluid formulations indicating most of the Zn remained in, or close to, the granules during the incubation. Similar results were reported by Hettiarachchi et al.[22] who showed that most of the fertilizer Zn (84.7%±4.8%) remained in Zn-enriched fertilizer granules after 5 weeks of incubation. The concentration of extracted Zn decreased from week 2 onwards when the fertilizers were mixed through soil. However, more Zn was extracted from soil treated with suspension Zn-GO compared to solution $ZnSO_4$. Zinc concentrations in the outer section (> 8 mm) were below detection limit except for banded Zn-GO suspension incubated for 2 weeks (0.25 mg/kg (±0.08)).

Table 2. Concentrations of Zn extracted by $CaCl_2$ from soil incubated with Zn-GO and $ZnSO_4$ granules (banded) and Zn-GO suspension (banded) and Zn-GO suspension and $ZnSO_4$ solution (mixed) for 2, 4 and 6 weeks in the inner zone (< 8 mm) and outer zone (> 8 mm) from the point of fertilizer application. Values are the mean of three replicates and figures in parentheses are standard deviation. Small letters refer to significant differences between formulations. (BDL means Zn concentration was below the detection limit in ICP analysis, 0.0004 mg/L).

Treatments	Fertilizer	Zn concentration extracted by $CaCl_2$ (mg/l)					
		2 weeks		4 weeks		6 weeks	
		Inner section	Outer section	Inner section	Outer section	Inner section	Outer section
Banded							
Granule	$ZnSO_4$	7.06(±0.68)^b	BDL	6.65(±0.62)^b	BDL	2.30(±0.45)^b	BDL
Granule	Zn-GO	6.24(±0.19)^b	BDL	7.42(±0.43)^b	BDL	2.38(±0.17)^b	BDL
Suspension	Zn-GO	10.05(±0.44)^a	0.25(±0.08)	9.26(±0.24)^a	BDL	10.95(±0.40)^a	BDL
Mixed							
Solution	$ZnSO_4$	1.19(±0.09)^a		0.41(±0.01)^a		0.48(±0.07)^b	
Suspension	Zn-GO	2.52(±0.71)^a		2.20(±0.10)^b		0.93(±0.24)^b	

Soil pH of the inner zone (< 8 mm) and outer zone across all fertilizers for the banded and mixed method of application are presented in Table 3. The average pH of soil for banded treatments of granular $ZnSO_4$ and Zn-GO was 0.56 and 0.53 pH units, respectively, lower than unfertilized soil (8.5 (±0.05)) by the second week of incubation. The pH difference for Zn-GO suspension was 0.65 pH unit lower than unfertilized soil. Change in soil pH near fertilizer application point could be related to the cation and H^+ exchange between fertilizer and soil or for GO-based fertilizer, due to their low pH as indicated in Table.1. The difference between pH of unfertilized soil and inner section for $ZnSO_4$ and Zn-GO granules decreased by end of incubation time but it increased for Zn-GO suspension (0.8 pH unit), pointing more acidity of suspension Zn-GO due to the ability of GO to generate acidic functional groups through to interaction with water molecules by the time.[37] There were no differences in soil pH between Zn-GO and $ZnSO_4$ treatments when these were mixed through soils due to soil buffering,[17] but pH values were still lower than in the unfertilized soil.

Table 3. Soil pH_{CaCl2} in treatments incubated with $ZnSO_4$ and Zn-GO granules or fluid which banded mixed with soil after 2, 4 and 6 weeks of incubation in the inner zone (< 8 mm) and outer zone (> 8 mm) from the point of application. (na refers to not applicable).

Treatments	Fertilizer	2 weeks pH		4 weeks pH		6 weeks pH	
		Inner section	Outer section	Inner section	Outer section	Inner section	Outer section
Banded							
Granule	$ZnSO_4$	7.93(±0.03)^{na}	8.01(±0.04)^{na}	7.91(±0.02)^{na}	8.15(±0.06)^{a}	8.14(±0.03)^{a}	8.21(±0.10)^{na}
Granule	Zn-GO	7.96(±0.15)^{na}	8.09(±0.09)^{na}	7.89(±0.09)^{na}	8.01(±0.05)^{b}	8.20(±0.06)^{a}	8.14(±0.07)^{na}
Suspension	Zn-GO	7.85(±0.11)^{na}	7.95(±0.00)^{na}	7.77(±0.09)^{na}	7.92(±0.05)^{b}	7.70(±0.04)^{b}	8.08(±0.09)^{na}
Mixed							
Solution	$ZnSO_4$	8.00(±0.12)		8.07(±0.02)		8.08(±0.07)	
Suspension	Zn-GO	7.95(±0.00)		7.95(±0.05)		8.06(±0.02)	

Characterization of granular fertilizers before and after incubation in soil

The changes in the morphology of $ZnSO_4$ and Zn-GO granules incubated in the soil were analysed using SEM. Both $ZnSO_4$ and Zn-GO granules preserved their shape after 2 weeks of incubation in soil (Figure S3, Supporting Information). SEM analysis of the surface of the incubated $ZnSO_4$ granule revealed the formation of interconnected layers of Zn precipitates (Figure 3a and b), while the surface of the original $ZnSO_4$ granule before incubation contained individual $ZnSO_4$ micro particles (Figure 3c and d). High and low resolution SEM images from Zn-GO granules after incubation for the same time did not show any precipitates or differences in the morphology of incubated granules compared to the original Zn-GO granules (Figure 3e-h).

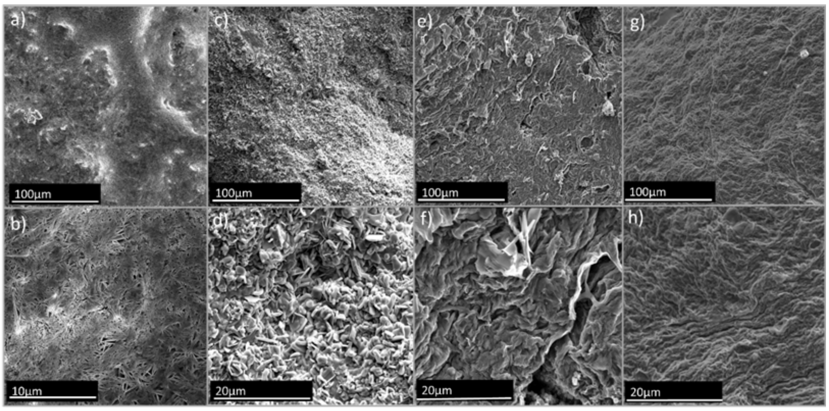

Figure 3. Low resolution and high resolution SEM images from the surface of (a and b) $ZnSO_4$ granules after incubation for two weeks in soil, (c and d) $ZnSO_4$ granules before incubation in the soil, (e and f) Zn-GO granules after incubation for two weeks in soil, and (g and h) Zn-GO granules before incubation in the soil.

Optical microscopic images of the soil cavity in which $ZnSO_4$ granules had been incubated with soil for 2 weeks (Figures 4a and b) showed the presence of a thick layer of residue on the soil surface and SEM image from the same sample showed the presence of precipitates (likely secondary) on the soil surface which was not seen in SEM images of the original soil (Figure S4, Supporting Information). In contrast, there were no secondary precipitates in the soil cavity in which a Zn-GO granule had been incubated (Figures 4c and d). Also the SEM images from this sample did not show any secondary precipitates and was morphologically similar to the SEM image of the original soil surface.

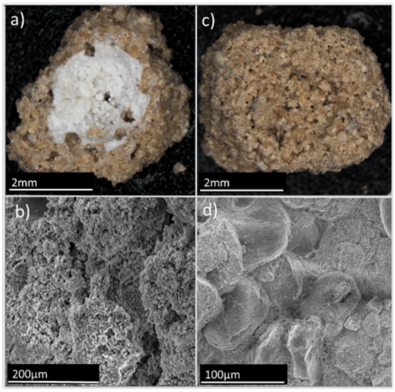

Figure 4. a) Optical microscopic cross section image of the soil after removal of a $ZnSO_4$ granule which had been incubated with soil for 2 weeks, b) SEM images of the soil surface in Figure (4a), c) optical microscopic cross sectional images of the soil after removal of a Zn-GO granule which had been incubated with soil for 2 weeks and d) SEM images of the soil in Figure (4c).

The precipitates observed in the soil around the $ZnSO_4$ granule were confirmed to be secondary in nature by XRD analysis, which showed the appearance of peaks completely different to those of $ZnSO_4$, representing a change to new secondary crystalline solid phases (Figure 5a). The XRD pattern of the $ZnSO_4$ granule before incubation was consistent with those for $ZnSO_4.H_2O$,[38,39] while after incubation most of the $ZnSO_4$ peaks disappeared and were replaced with new peaks related to ZnO, $Zn(OH)_2$, zinc hydroxyl carbonate ($Zn_x(OH)_x(CO_3)_x$) or calcium zincate ($CaZn(OH)_4.2H_2O$).[40-45] Furthermore, the changes in the XRD peaks of the $ZnSO_4$ granule after incubation in soils for two weeks was not confounded by adhering soil, as XRD peaks characteristic of the unfertilized soil were absent from the granule spectra.

The XRD spectra of Zn-GO (Figure 5b) before and after incubation were almost identical and the presence of any new peaks was mostly related to adhering soil. It was difficult to completely remove soil residues from the Zn-GO granules surface, as also can be seen from the optical microscopic images (Figure S3, Supporting Information).

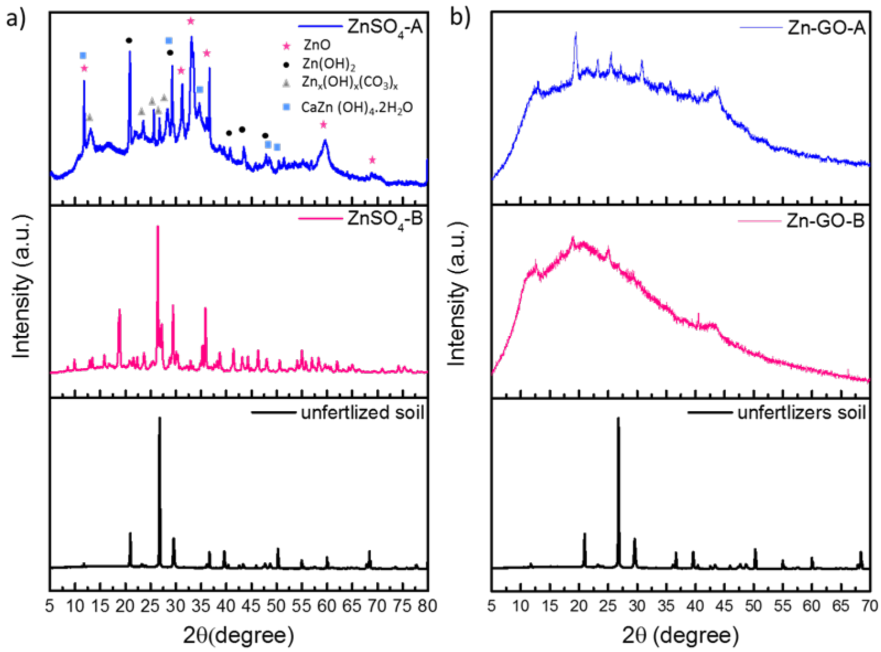

Figure 5. XRD patterns of (a) unfertilized soil, $ZnSO_4$ granules before ($ZnSO_4$-B) and after ($ZnSO_4$-A) incubation with soil and (b) unfertilized soil Zn-GO granules before (Zn-GO-B) and after (Zn-GO-B) incubation with soil and from unfertilized soil.

These results were further confirmed with EDX analysis of the surface of $ZnSO_4$ and Zn-GO granules before and after incubation in soil. According to EDX analysis (Figures 6a and b), the weight percent of oxygen (O), Zn and S were 24.3, 33.9 and 8.5, respectively for $ZnSO_4$ granules before incubation while they changed to 38.3, 9.2 and 0.4, respectively after incubation. The increase in the O percent and decreasing Zn and S percentage is representing changing of $ZnSO_4$ salts to ZnO or $Zn(OH)_2$, although the decrease of Zn and S could be related to release and diffusion of Zn and especially S during incubation as well. Furthermore, a high percentage of Ca (23%) was observed in the granule after incubation, suggesting the presence of insoluble Ca/Zn hydroxyl carbonate precipitates in the granule shell after incubation. The presence of calcium zincate ($CaZn(OH)_4.2H_2O$) crystals on soil near the $ZnSO_4$ granules was confirmed more with SEM images and EDX analysis form same spot (Figure S5, Supporting Information). For Zn-GO granules, the percent of O was almost the same before and after incubation, 37.2% and 38.2%, respectively, related to the presence of the different oxygen functional groups of GO. A decrease in Zn content from16.1% (before incubation) to 11.3% (after incubation) was likely related to the release of Zn during incubation in soil (Figure 6c and d).

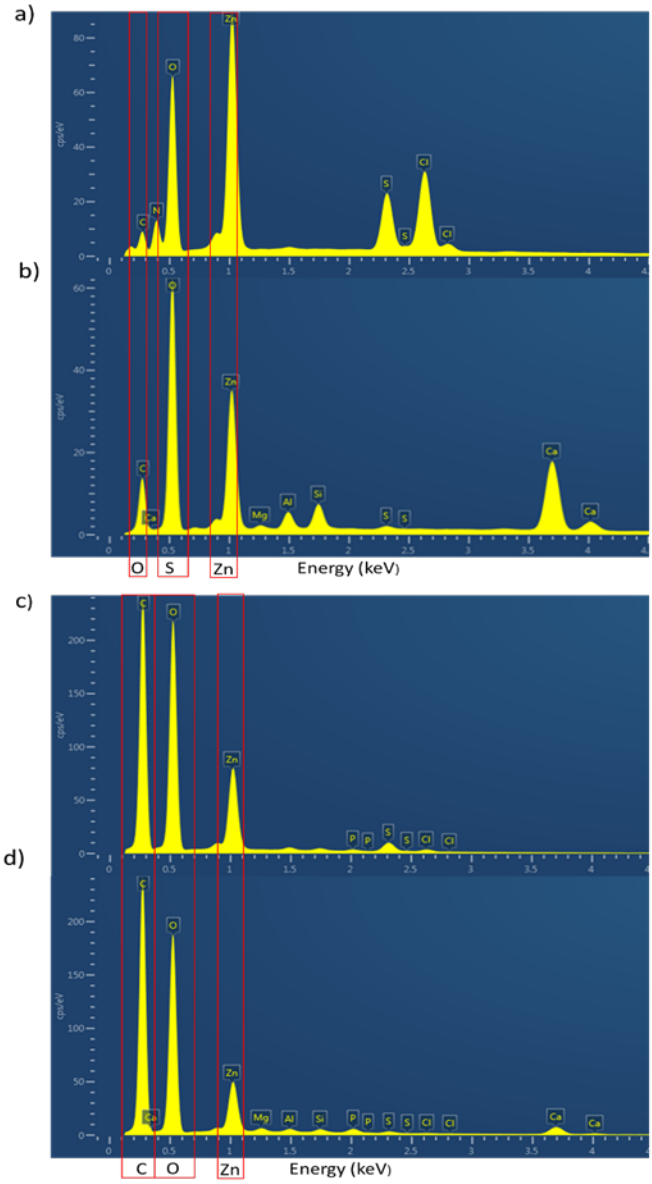

element	W%	A%
Zn	33.9	36.7
O	24.3	18.3
Cl	14.7	16
N	10.6	12.5
S	8.5	6.4
C	7.9	10

element	W%	A%
O	38.3	55.6
C	24	17.7
Ca	23	13.9
Zn	9.2	8.2
Si	2.8	2.3
Al	1.8	1.5
Mg	0.4	0.4
S		0.3

element	W%	A%
C	44.3	58.3
O	37.2	36.7
Zn	16.1	3.9
S	1.6	0.8
Cl	0.5	0.2
P	0.3	0.1

element	W%	A%
C	44.6	57.6
O	38.2	37.1
Zn	11.3	2.7
S	0.4	0.2
Ca	3.5	1.3
P	0.7	0.4
Mg	0.4	0.3
Al	0.4	0.2
Si	0.4	0.2

Figure 6. The SEM/EDX results of (a) $ZnSO_4$ granules before, (b) after incubation in the soil, (c) Zn-GO granules before and (d) after incubation in the soil with corresponded weight percentage (w%) and atomic percentage (A%) elemental analysis reported in table.

DISCUSSION

The results of this study show that the fluid form of either Zn-GO or $ZnSO_4$ fertilizers outperformed granular fertilizers regarding plant dry mass and Zn uptake in a highly calcareous soil. The greater performance of the fertilisers in fluid form can be explained by several factors, which are their physical state,[45,46] placement effects, soil chemical properties and pH.[17, 47-49] The physical state of applied Zn (granular or fluid) can influence nutrient availability in soil due to their different physical interaction with the surrounding soil.[18] When a granular fertilizer is added to soil, wetting of the granule occurs through capillary flow of water from moist soil to the porous granule.[45,46] This movement of water towards the fertilizer granule occurs in an opposite direction to the dissolved Zn diffusion which could consequently restrict or slow the diffusion of the dissolved fertilizer.[50] In an alkaline soil, this flow of water towards the granule also draws Ca and Mg (in soil solution) towards, and into the granule.[36] On the other hand, there is no mass flow of water (and solutes) from the soil towards the fertilizer application point with fluid fertilizers therefore they can diffuse faster in the soil.[50] This mechanism has been reported by Hettiarachchi et al.[50] that the diffusion of P from granular monoammonium phosphate (MAP) in calcareous soil is limited compared to fluid MAP due to the flow of water towards granules.

Another reason for the low response of wheat plants to granular Zn compared to its fluid form could have been due to limited root interception with granules since there are only three granules per pot and it is possible that some roots did not "find" the granules. Similar results were reported by others when the lack of response to granular $ZnSO_4$ granules was due to limited root interception in banded method of application compared to $ZnSO_4$ mixed through soil.[51,52] Work by Mortvedt and Giordano[25] showed that the efficiency of fluid Zn fertilizers over the granular form was greater due to the better distribution of Zn in the soil. Similarly, in a calcareous soil Soper et al.[53] reported Zn concentrations in beans were enhanced best when the volume of soil treated with $ZnSO_4$ was increased. This could also explain the enhanced performance of Zn-GO suspension over Zn-GO granules when banded in soil, due to the larger volume of soil treated by the suspension product and the greater probability of roots intercepting the suspension fertilizer despite being placed at the same depth as the granular Zn.

Besides the effect of the fertilizer physical states and their method of application, the chemical reactions between the added fertilizers and different soil components including phosphate, carbonate, aluminium and iron oxides can also influence their availability to plants.[22,49,54,55] It is generally accepted that diffusion is the principle source of Zn movement in soil,[17,19,56] and that soil pH and chemical properties influence the solubility and diffusion of Zn fertilizers in the soil.[8,22,49] Fluid fertilizers tend to have a lower nutrient concentration compared to the granular equivalent formulation when added to soil because of dilution in a larger soil volume. The lower concentrations of nutrient in fluid fertilizers lead to less precipitation with soil components. This process has been reported earlier as the mechanism that enhanced the diffusion of P from liquid fertilizers compared to granules due to low concentration of P in liquid fertilizer and less formation of P precipitates in the soil.[57] On the other hand, in the calcareous soil, there is a high chance of precipitation of Zn at the granule:soil interface due to the high concentration of Zn at the surface of the granule, which can consequently affect Zn diffusion and uptake by plants. Ghosh et al.[58] identified two reaction zones around Zn granules: a saturated zone immediately adjacent to the fertilizer granule with high concentration of Zn and an outer zone with a lower concentration of Zn. Different chemical reactions take place in these two zones where the Zn precipitates may form in the high concentration zone while adsorption reactions may occur in the low concentration zone.[58] Others have noted similar results when the movement of Zn from granular fertilizers in soil was limited compared to fluid products due to the precipitation of dissolved Zn.[22]

Many studies have shown that there is a positive correlation between the water solubility of Zn fertilizers and plant biomass and Zn uptake.[15,20,51,59] However, there was no such correlation in our study, as the plant response to highly soluble $ZnSO_4$ granules was low compared to the sparingly soluble Zn-GO. As indicated earlier in this section, diffusion is the principle mode of Zn movement in the soil and the rate of diffusion depends on the Zn solution concentration at the granule:soil interface, which is affected by the water solubility of the Zn fertilizer.[15,17,20,59] However, water solubility of fertilizer Zn in soil highly dependent on soil pH with solubility decreasing with increasing pH beyond 7.[17,22,47] In calcareous soil, the Zn^{+2} activity decreases [15,59]$Zn(OH)_2$, $ZnCO_3$ or insoluble calcium zincate , hence decreasing the availability of Zn to plants.[52,60,61] Our SEM image (Figures 3a-d) indicated the presence of a thick and interconnected surface precipitate around $ZnSO_4$ granules and in the soil adjacent to the granules after incubation in the soil for 2 weeks. It appears that precipitation of Zn in or near to $ZnSO_4$ granules could be responsible for the poor Zn diffusion in soil. In addition, the presence of XRD peaks related to insoluble Zn compounds, such as ZnO, $Zn(OH)_2$ and calcium zincate (Figure 4a) provides further evidence for secondary precipitate formation around the $ZnSO_4$ granules. Kalbasi et al.[62] identified crystalline Zn precipitates related to $Zn(OH)_2$ and zinc carbonates in the soil adjacent to banded $ZnSO_4$ granules similar to those we report here.

XRD spectra and SEM images of Zn-GO fertilizers before and after incubation in the soil (Figures 3e-h and 4b) indicate that Zn-GO fertilizers were affected less by these reactions. Our previous study showed that Zn release from Zn-GO granules was much slower than $ZnSO_4$ granules in both batch extractions, column leaching and soil environments due to the tight chemical bond between Zn and GO sheets.[28] In Zn-GO granules, Zn ions are also trapped inside the wrinkled or aggregated GO sheets, and the layered structure of stacked GO sheets in the final granule reduces the release of nutrients. Hence, Zn ions in Zn-GO granules were less affected by soil components, as indicated by the fact that no peaks related to Zn-insoluble compounds were found in the XRD patterns of these granules after incubation in soil. Furthermore, difference in the release and availability of Zn from Zn-GO and $ZnSO_4$ granules can be related to pH differences of the granules. As indicated in Table 1, Zn-GO granules had a pH of 3.84, which is 2.2 units less than the pH of the $ZnSO_4$ granules. This lower pH of the granules may have resulted in a lower pH at the soil:granule interface, resulting in less formation of precipitates as indicated in Figure 4b as well. The results of soil pH depicted in Table. 3 also show slight acidification of soil near the GO-based fertilizers. Others proposed that GO can constantly change its chemical structure due to interaction with water molecules and can gradually generate significant quantity of acidic functional groups through the interaction with water molecules,[37] which can explain the acidity of GO-based fertilizers and their greater performance in calcareous soil.

The Zn-GO suspensions performed better than fluid $ZnSO_4$ in terms of plant dry matter and Zn uptake when mixed through soil. The better performance of the Zn-GO suspension compared to fluid $ZnSO_4$ could be related to the attachment of Zn ions to GO sheets and the acidity of the GO-based fertilizer. Surface complexation between metal ions and oxygen functional groups on the surface of GO plays a dominated role in their adsorption onto GO sheets.[63,64] Furthermore, the metal ions can attach to GO sheets through the complexation with hydroxyl or carboxyl groups presented at the edges of GO sheets.[63] Therefore, the better performance of suspension Zn-GO could be related to the high stability of Zn complexation with GO sheets which diminishes the possibility of Zn being precipitated in soil around the granule, similar to chelated-zinc fertilizer.[60] It has been also confirmed that GO sheets degrade in the soil[65,66] and their prolonged exposure to water molecules can generate a significant quantity of acidic functional groups and gradually convert them into humic acid-like structures.[37] These reactions are more likely to have occurred with the suspension Zn-GO treatments as they were dispersed in soil and would have had extensive contact with water molecules and soil enzymes. Degradation of GO-based material to humic acid-like structures could enhance Zn diffusion through soil, similar to synthetic chelates, and enhance plant growth through better Zn nutrition.[67-69] The presence of humic acids and the generation of acidic groups on the GO surface could also decrease soil pH which is advantageous in calcareous soils for crop production due to benefits in terms of Zn availability.[70] The relatively high extractability of Zn for Zn-GO compared to $ZnSO_4$, when mixed through soil, may have been a result of these reactions.

The results of this study indicate that the application of graphene-based Zn fertilizers (Zn-GO) increased the plant yield in wheat more than formulations based on $ZnSO_4$. Suspensions of Zn-GO were more effective than granular Zn-GO. Compared to mixing through soil, banding of $ZnSO_4$ significantly constrained plant growth (as has been found previously), but Zn-GO suspensions were not affected by banding to the same extent. Diffusion and solubility of fertilizer Zn in soils away from the point of fertilizer application was restricted for $ZnSO_4$ compared to Zn-GO (granular or suspension). The formation of insoluble Zn precipitates around $ZnSO_4$ granules in soil and the absence of these compounds in soil around Zn-GO formulations was likely the reason for the better agronomic effectiveness of the Zn-GO products.

The excellent performance of Zn-GO fertilizers compared to $ZnSO_4$ may be related to the tight coordination of Zn ions with the GO sheets and trapping of Zn in wrinkled or aggregated GO sheets which makes Zn less affected by soil pH and interaction with soil components in addition to their acidity which keeps Zn in soluble form and prevent its precipitation. It is expected that this graphene based nutrients carrier strategy as new generation of fertilizers could be applicable to a wide range of calcareous soils and plant macro and micronutrients, as GO can be used as a loading platform for both cations and anions,[71] and it can be produced in industrial scale.[72] More studies are needed to further expand this concept for other nutrients and investigated their plant growth performances in complex soil environment.

ACKNOWLEDGEMENTS

The support from The University of Adelaide and the Schools of Chemical Engineering and Agriculture, Food and Wine and Adelaide Microscopy is acknowledged. Mike J. McLaughlin, Rodrigo C. da Silva and Fien Degryse thank The Mosaic Company for financial support. The authors would like to thank Bogumila Tomczak for assistance with the plant study and her technical support with ICP-OES analysis.

Supporting Information Description

Supporting information provides supplementary figures which includes: Selected characterization (FTIR, XRD and TGA) of graphene oxide (GO) and zinc loaded GO (Zn-GO) (Figure S1), Photo of plants treated with granular and suspension Zn-GO, and plants treated with granular and suspension $ZnSO_4$ (Figure S2), SEM image of $ZnSO_4$ and their microscopic images after incubation for 2 weeks in the soil, and SEM image of Zn-GO granule and their microscopic images after incubation for 2 weeks (Figure S3), SEM images from soil surface without any fertilizer (Figure S4) and SEM image of soil incubated with $ZnSO_4$ granule for 2 weeks and EDX analysis from different spots (Figure S5).

Funding Information

This research was supported by the Australian Research Council (ARC) funding ARC DP 150101760 and ARC IH 150100003 (Graphene Enabled Industry Transformation).
The authors declare no competing financial interest.

REFERENCES

1. Tilman, D.; Balzer, C.; Hill, J.; Befort, B. L. Global food demand and the sustainable intensification of agriculture. *Proceedings of the National Academy of Sciences* 2011, 108, 20260-20264.
2. Vitousek, P. M.; Mooney, H. A.; Lubchenco, J.; Melillo, J. M. Human domination of earth's ecosystems. *Science* 1997, 277, 494-499.
3. Tilman, D.; Cassman, K. G.; Matson, P. A.; Naylor, R.; Polasky, S. Agricultural sustainability and intensive production practices. *Nature* 2002, 418, 671-677.
4. Tilman, D.; Fargione, J.; Wolff, B.; D'Antonio, C.; Dobson, A.; Howarth, R.; Schindler, D.; Schlesinger, W. H.; Simberloff, D.; Swackhamer, D. Forecasting agriculturally driven global environmental change. *Science* 2001, 292, 281-284.
5. Mukerabigwi, J. F.; Wang, Q.; Ma, X.; Liu, M.; Lei, S.; Wei, H.; Huang, X.; Cao, Y. Urea fertilizer coated with biodegradable polymers and diatomite for slow release and water retention. *Journal of Coatings Technology and Research* 2015, 12, 1085-1094.
6. Azeem, B.; KuShaari, K.; Man, Z. B.; Basit, A.; Thanh, T. H. Review on materials & methods to produce controlled release coated urea fertilizer. *Journal of Controlled Release* 2014, 181, 11-21.
7. Zhang, Y.-Q.; Pang, L.-L.; Yan, P.; Liu, D.-Y.; Zhang, W.; Yost, R.; Zhang, F.-S.; Zou, C.-Q. Zinc fertilizer placement affects zinc content in maize plant. *Plant and Soil* 2013, 372, 81-92.
8. Degryse, F.; Baird, R.; McLaughlin, M. J. Diffusion and solubility control of fertilizer-applied zinc: chemical assessment and visualization. *Plant and Soil* 2015, 386, 195-204.
9. Cakmak, I.; Ekiz, H.; Yilmaz, A.; Torun, B.; Köleli, N.; Gültekin, I.; Alkan, A.; Eker, S. Differential response of rye, triticale, bread and durum wheats to zinc deficiency in calcareous soils. *Plant and Soil* 1997, 188, 1-10.
10. Watts-Williams, S. J.; Turney, T. W.; Patti, A. F.; Cavagnaro, T. R. Uptake of zinc and phosphorus by plants is affected by zinc fertiliser material and arbuscular mycorrhizas. *Plant and Soil* 2014, 376, 165-175.
11. Sadiq, M. Solubility and speciation of zinc in calcareous soils. *Water, Air, and Soil Pollution* 1991, 57, 411-421.
12. Nayyar, V. K.; Takkar, P. N. Evaluation of various zinc sources for rice grown on alkali soil. *Zeitschrift für Pflanzenernährung und Bodenkunde* 1980, 143, 489-493.
13. Zhao, A.; Lu, X.; Chen, Z.; Tian, X.; Yang, X. Zinc fertilization methods on zinc absorption and translocation in wheat. *Journal of Agricultural Science* 2011, 3, 28-35.
14. Cakmak, I. Enrichment of cereal grains with zinc: Agronomic or genetic biofortification? *Plant and Soil* 2008, 302, 1-17.
15. Mortvedt, J. J. Crop response to applied zinc in ammoniated phosphate fertilizers. *Journal of Agricultural and Food Chemistry* 1968, 16, 241-245.
16. Andersson, M. Prediction of plant available copper, zinc and phosphorus in arable soils : comparison of diffusive gradients in thin film (DGT) technique with soil extraction methods. Mater dessertation, Swedish University of Agricultural sciences, SLU, 2016.
17. McBeath, T. M.; McLaughlin, M. J. Efficacy of zinc oxides as fertilisers. *Plant and Soil* 2014, 374, 843-855.
18. Montalvo, D.; Degryse, F.; da Silva, R. C.; Baird, R.; McLaughlin, M. J. Chapter Five - Agronomic effectiveness of zinc sources as micronutrient fertilizer. In *Advances in Agronomy*, Sparks, D. L., Ed. Academic Press: 2016; Vol. 139, pp 215-267.
19. Mortvedt, J. J; Giordano, P.M. Extractability of zinc granulated with macronutrient fertilizers in relation to its agronomic effectiveness. *Journal of Agricultural and Food Chemistry* 1969, 17,1272-1275.
20. Amrani, M.; Westfall, D. G.; Peterson, G. A. Influence of water solubility of granular zinc fertilizers on plant uptake and growth. *Journal of Plant Nutrition* 1999, 22, 1815-1827.
21. Gangloff, W. J.; Westfall, D. G.; Peterson, G. A.; Mortvedt, J. J. Relative availability coefficients of organic and inorganic Zn fertilizers. *Journal of Plant Nutrition* 2002, 25, 259-273.
22. Hettiarachchi, G. M.; Lombi, E.; McLaughlin, M. J.; Chittleborough, D. J.; Johnston, C. Chemical behavior of fluid and granular Mn and Zn fertilisers in alkaline soils. *Soil Research* 2010, 48, 238-247.

23. Holloway, R. E.; Bertrand, I.; Frischke, A. J.; Brace, D. M.; McLaughlin, M. J.; Shepperd, W. Improving fertiliser efficiency on calcareous and alkaline soils with fluid sources of P, N and Zn. *Plant and Soil* 2001, 236, 209-219.
24. Lombi, E.; McLaughlin, M. J.; Johnston, C.; Armstrong, R. D.; Holloway, R. E. Mobility, solubility and lability of fluid and granular forms of P fertiliser in calcareous and non-calcareous soils under laboratory conditions. *Plant and Soil* 2005, 269, 25-34.
25. Mortvedt, J. J.; Giordano, P. M. Crop response to zinc oxide applied in liquid and granular fertilizers. *Journal of Agricultural and Food Chemistry* 1967, 15, 118-122.
26. Holloway, B.; Brace, D.; Ritcher, I.; McLaughlin, M.; Hettiarachchi, G.; Armstrong, R. Micronutrient availability improved with fluids. *Fluid journal* 2006, 54, 17-19.
27. Holloway, B.; McLaughlin, M.; McBeath, T.; Kelly, J. *Fluid fertilisers: A South Australian Manual.*; Fluid Fertilizer Foundation: Australia, 2008.
28. Kabiri, S.; Degryse, F.; Tran, D. N. H.; da Silva, R. C.; McLaughlin, M. J.; Losic, D. Graphene oxide: A new aarrier for slow release of plant micronutrients. *ACS Applied Materials & Interfaces* 2017, 9, 43425-43335.
29. Marcano, D. C.; Kosynkin, D. V.; Berlin, J. M.; Sinitskii, A.; Sun, Z.; Slesarev, A.; Alemany, L. B.; Lu, W.; Tour, J. M. Improved synthesis of graphene oxide. *ACS Nano* 2010, 4, 4806-4814.
30. Milani, N.; McLaughlin, M. J.; Stacey, S. P.; Kirby, J. K.; Hettiarachchi, G. M.; Beak, D. G.; Cornelis, G. Dissolution kinetics of macronutrient fertilizers coated with manufactured zinc oxide nanoparticles. *Journal of Agricultural and Food Chemistry* 2012, 60, 3991-3998.
31. Rayment, G. E. *Australian laboratory handbook of soil and water chemical methods / G.E. Rayment and F.R. Higginson*. Inkata Press: Melbourne, 1992.
32. USDA. *Particle size analyse. In 'Procedures for collecting soil samples and methods of analysis of soil survey'.* ; USDA: Washington, DC, 1982
33. Matejovic, I. Determination of carbon and nitrogen in samples of various soils by the dry combustion. *Communications in Soil Science and Plant Analysis* 1997, 28, 1499-1511.
34. Sherrod, L. A.; Dunn, G.; Peterson, G. A.; Kolberg, R. L. Inorganic carbon analysis by modified pressure-calcimeter method. *Soil Science Society of America Journal* 2002, 66, 299-305.
35. A.Klute. *Water Retentiion: laboratory Methods*. Fort Collind, Colorado, 1986.
36. Lombi, E.; McLaughlin, M. J.; Johnston, C.; Armstrong, R. D.; Holloway, R. E. Mobility and lability of phosphorus from granular and fluid monoammonium phosphate differs in a calcareous soil. *Soil Science Society of America Journal* 2004, 68, 682-689.
37. Dimiev, A. M.; Alemany, L. B.; Tour, J. M. Graphene oxide: Origin of acidity, Its instability in water, and a new dynamic structural model. *ACS Nano* 2013, 7, 576-588.
38. Li, B.; Wang, X.; Wei, Y.; Wang, H.; Hu, G. Preparation of $ZnSO_4 \cdot 7H_2O$ using filter cake enriched in calcium and magnesium from the process of zinc hydrometallurgy. *Scientific Reports* 2017, 7, 16205.
39. Lee, S.; Nam, S.; Choi, Y.; Kim, M.; Koo, J.; Chae, B.-J.; Kang, W.-S.; Cho, H.-J. Fabrication and characterizations of hot-melt extruded nanocomposites based on zinc sulfate monohydrate and soluplus. *Applied Sciences* 2017, 7, 902.
40. Adnan, A.; Kamran, A.; Young Jin, Y.; Jeongdai, J.; Kyung Hyun, C. Rapid fabrication of graphene/ZnO composite thin film. *Japanese Journal of Applied Physics* 2014, 53, 05HA01.
41. Yang, W.; Li, Q.; Gao, S.; Shang, J. K. NH^{4+} directed assembly of zinc oxide micro-tubes from nanoflakes. *Nanoscale Research Letters* 2011, 6, 491.
42. Moezzi, A.; Cortie, M.; McDonagh, A. Aqueous pathways for the formation of zinc oxide nanoparticles. *Dalton Transactions* 2011, 40, 4871-4878.
43. Ding, S.; Wang, M. Studies on synthesis and mechanism of nano-$CaZn_2(PO_4)_2$ by chemical precipitation. *Dyes and Pigments* 2008, 76, 94-96.
44. Yuan, Y. F.; Tu, J. P.; Wu, H. M.; Li, Y.; Shi, D. Q.; Zhao, X. B. Effect of ZnO nanomaterials associated with $Ca(OH)_2$ as anode material for Ni–Zn batteries. *Journal of Power Sources* 2006, 159, 357-360.
45. Lawton, K.; Vomocil, J. A. The dissolution and migration of phosphorus from granular superphosphate in some Michigan soils1. *Soil Science Society of America Journal* 1954, 18, 26-32.
46. Williams, C. Moisture uptake by surface-applied superphosphate and movement of the phosphate and sulphate into the soil. *Soil Research* 1969, 7, 307-316.

47. Bickel A, K. R. Spatial response of corn to banded zinc sulfate fertilizer in Iowa. In *Thirty-first north central extension-industry soil fertility conference*, Potash and Phosphate Institute, Des Moins, 2001; pp 144–155.
48. Stietiya, M. H.; Wang, J. J.; Roy, A. Macroscopic and extended X-ray absorption fine structure spectroscopic investigation of ligand effect on zinc adsorption to kaolinite as a function of pH. *Soil Science* 2011, 176, 464-471.
49. Brümmer, G.; Tiller, K. G.; Herms, U.; Clayton, P. M. Adsorption—desorption and/or precipitation—dissolution processes of zinc in soils. *Geoderma* 1983, 31, 337-354.
50. Hettiarachchi, G. M.; Lombi, E.; McLaughlin, M. J.; Chittleborough, D.; Self, P. Density changes around phosphorus granules and fluid bands in a calcareous soil. *Soil Science Society of America Journal* 2006, 70, 960-966.
51. Goos, R. J.; Johnson, B. E.; Thiollet, M. A comparison of the availability of three zinc sources to maize (Zea mays L.) under greenhouse conditions. *Biology and Fertility of Soils* 2000, 31, 343-347.
52. Zhao, A.-q.; Tian, X.-h.; Chen, Y.-l.; Li, S. Application of $ZnSO_4$ or Zn-EDTA fertilizer to a calcareous soil: Zn diffusion in soil and its uptake by wheat plants. *Journal of the Science of Food and Agriculture* 2016, 96, 1484-1491.
53. Soper, R. J.; Morden, G. W.; Hedayat, M. W. The effect of zinc rate and placement on yield and zinc utilization by blackbean(Phaseolus vulgaris var. Black Turtle). *Canadian Journal of Soil Science* 1989, 69, 367-372.
54. Hossner, L. R.; Blanchar, R. W. The utilization of applied zinc as affected by pH and pyrophosphate content of ammonium phosphates1. *Soil Science Society of America Journal* 1969, 33, 618-621.
55. Degryse, F.; Smolders, E.; Parker, D. R. Partitioning of metals (Cd, Co, Cu, Ni, Pb, Zn) in soils: concepts, methodologies, prediction and applications – A review. *European Journal of Soil Science* 2009, 60, 590-612.
56. Wilkinson, H. F., Loneragan, J. F. & Quirk, J. P.The movement of zinc to plant roots. . *Soil Science Society of American Proceedings* 1968, 32, 831-833.
57. McBeath. T.M, McLaughlin. M. J., Kirby J.K. Armstrong R.D. Dry soil reduces fertlizer phosphorouse and Zn diffusion but nor bioavailibility. *Alliance of Crop Soil and Environemntal Science Societies* 2011, 76, 1301-1310.
58. Gosh, AK. Chemistry and agronomic effectiveness of Zn-enriched fertiliser. PhD Thesis, University of Western Australia, Nedlands, WA, 1990.
59. Mortvedt, J. J. Crop response to level of water-soluble zinc in granular zinc fertilizers. *Fertilizer Research* 1992, 33, 249-255.
60. Rico, M. I.; Alvarez, J. M.; Mingot, J. I. Efficiency of zinc ethylenediaminetetraacetate and zinc lignosulfonate soluble and coated fertilizers for maize in calcareous soil. *Journal of Agricultural and Food Chemistry* 1996, 44, 3219-3223.
61. Martín-Ortiz, D.; Hernández-Apaolaza, L.; Gárate, A. Efficiency of a zinc lignosulfonate as Zn source for wheat (Triticum aestivum L.) and corn (Zea mays L.) under hydroponic culture conditions. *Journal of Agricultural and Food Chemistry* 2009, 57, 226-231.
62. Kalbasi, M.; Racz, G. J.; Lewen-Rudgers, L. A. Reaction products and solubility of applied zinc compounds in some manitoba soils. *Soil Science* 1978, 125, 55-64.
63. Peng, W.; Li, H.; Liu, Y.; Song, S. A review on heavy metal ions adsorption from water by graphene oxide and its composites. *Journal of Molecular Liquids* 2017, 230, 496-504.
64. Sitko, R.; Turek, E.; Zawisza, B.; Malicka, E.; Talik, E.; Heimann, J.; Gagor, A.; Feist, B.; Wrzalik, R. Adsorption of divalent metal ions from aqueous solutions using graphene oxide. *Dalton Transactions* 2013, 42, 5682-5689.
65. WeiLiang, X.; Gaurav, L.; Irene, R.; Balaji, S. Degradation of graphene by hydrogen peroxide. *Particle & Particle Systems Characterization* 2014, 31, 745-750.
66. Lalwani, G.; Xing, W.; Sitharaman, B. Enzymatic degradation of oxidized and reduced graphene nanoribbons by lignin peroxidase. *Journal of materials chemistry. B, Materials for biology and medicine* 2014, 2, 6354-6362.
67. Chen, Y.; Aviad, T. Effects of humic substances on plant growth 1. In *Humic Substances in Soil and Crop Sciences: Selected Readings*, MacCarthy, P.; Clapp, C. E.; Malcolm, R. L.; Bloom, P. R., Eds. Soil Science Society of America: Madison, WI, 1990; pp 161-186.

68. Jalali, V. K., and P.N. Takkar. Evaluation of parameters for simultaneous determination of micronutrient cations available to plants from soils. *Indian J. Agric. Sci.* 1979, 49, 5.
69. Rauthan, B. S.; Schnitzer, M. Effects of a soil fulvic acid on the growth and nutrient content of cucumber (Cucumis sativus) plants. *Plant and Soil* 1981, 63, 491-495.
70. Mitchell J, D. J., Dion HG. The effect of small additions of elemental sulphur on the availability of phosphate fertilizers. *Scientific Agriculture [Ottawa]* 1952, 32, 5.
71. Andelkovic, I. B.; Kabiri, S.; Tavakkoli, E.; Kirby, J. K.; McLaughlin, M. J.; Losic, D. Graphene oxide-Fe(III) composite containing phosphate – A novel slow release fertilizer for improved agriculture management. *Journal of Cleaner Production* 2018, 185, 97-104.
72. Zhu, Y.; Ji, H.; Cheng, H.-M.; Ruoff, R. S. Mass production and industrial applications of graphene materials. *National Science Review* 2018, 5, 90-10

Supporting information

Suspension micronutrient fertilizers manufactured using zinc-loaded graphene oxide- A highly efficient fertilizer for enhancing wheat plant yield and zinc uptake in calcareous soil

Shervin Kabiri[†], *Rodrigo C. da Silva* [§], *Fien Degryse* [§], *Diana N.H. Tran*[†], *Mike J. McLaughlin* *[§] *and Dusan Losic**[†]

[†]School of Chemical Engineering, Engineering North Building, The University of Adelaide, Adelaide, SA 5005, Australia

[§]Fertilizer Technology Research Centre, School of Agriculture, Food and Wine, The University of Adelaide, Waite Campus, PMB1, Glen Osmond, SA 5064, Australia

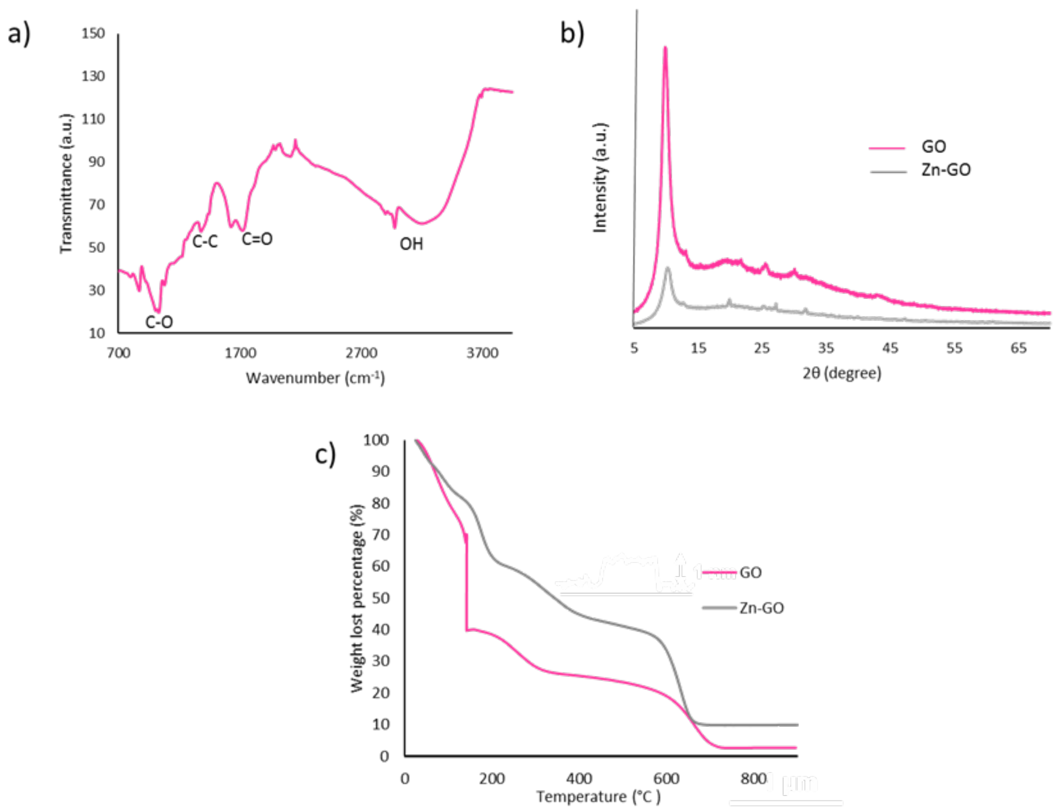

Figure S1. a) FTIR from graphene oxide (GO), b) XRD pattern of GO and zinc loaded GO (Zn-GO) and c) TGA analysis of GO and Zn-GO.

Fourier transform infrared spectroscopy (FTIR) confirms the presence of oxygen-containing functional groups on the surface of GO. The presence of Hydroxyl group (OH) was identified by a broad band between 2600-3800 cm^{-1}. The bands at 1720-1740 cm^{-1} are associated with the stretching vibration of the C=O bond, and the bands at 1240 and 1250 cm^{-1} are associated with

C-O.[1] The X-ray diffraction pattern of GO showed a peaks at $2\theta \sim 9.86°$, which is related to the (001) reflection corresponding to the graphite interlayer distance. This peak was also observed for Zn-GO, but it shifted to lower 2θ values which is evidence of the intercalation of the metal ions.[1] The thermogravimetric (TGA) of GO is showed it thermally instability. The major weight loss of GO happened at around 300 °C, which is probably due to the pyrolysis of the liable oxygen-containing functional groups. Zn-GO showed a similar trend as GO for weight lost but its thermal stability improved compared to GO. The overall weight loss of Zn-GO was less than GO which confirmed the presence of Zn and Cu in the GO structure.[1]

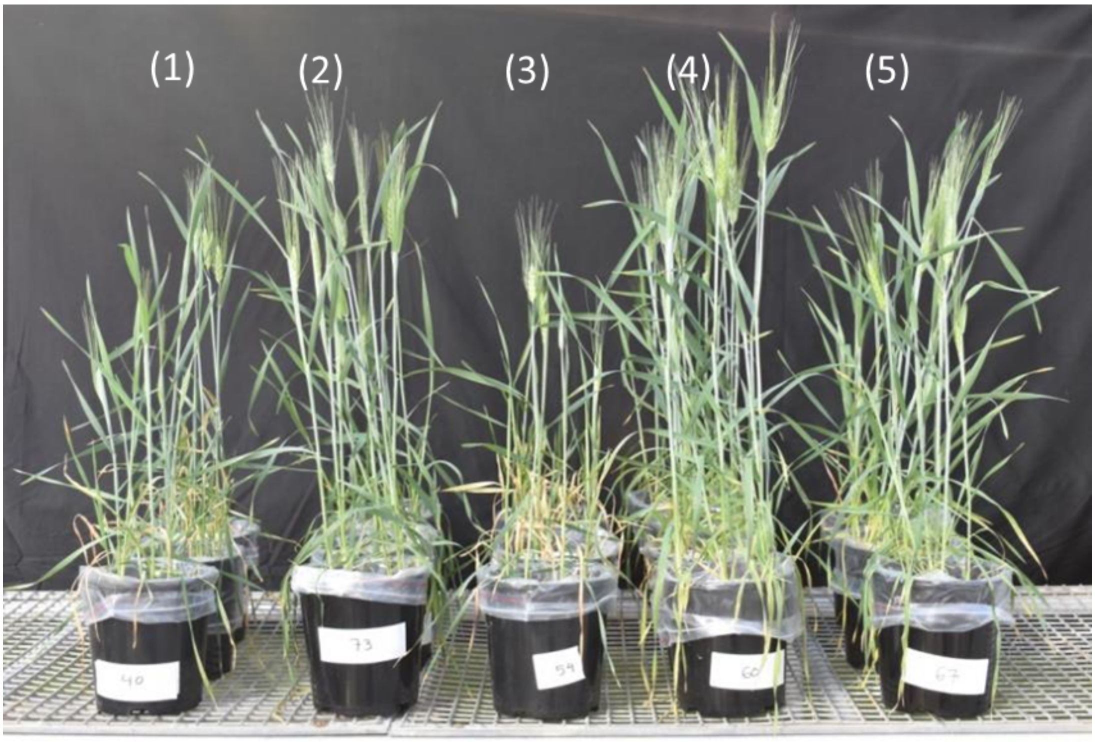

Figure S2. Photo of plants treated with (1) Zn-GO granules banded, (2) Zn-GO suspension-banded, (3) $ZnSO_4$ granules banded, (4) Zn-GO suspension mixed and (5) $ZnSO_4$ liquid mixed with soil. (Zn rate was 10 mg /kg soil).

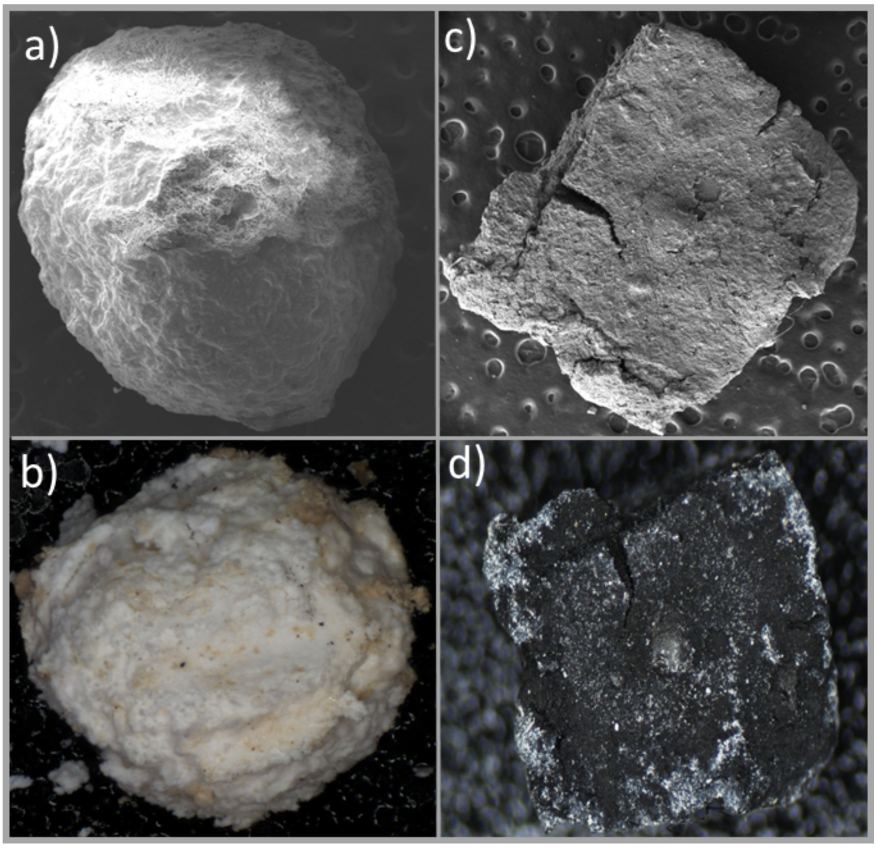

Figure S3. a) SEM image of $ZnSO_4$ granule incubated for 2 weeks in the soil, b) Microscopic image of same granule, c) SEM image of Zn-GO granule incubated for 2 weeks in the soil and d) Microscopic image of same granule.

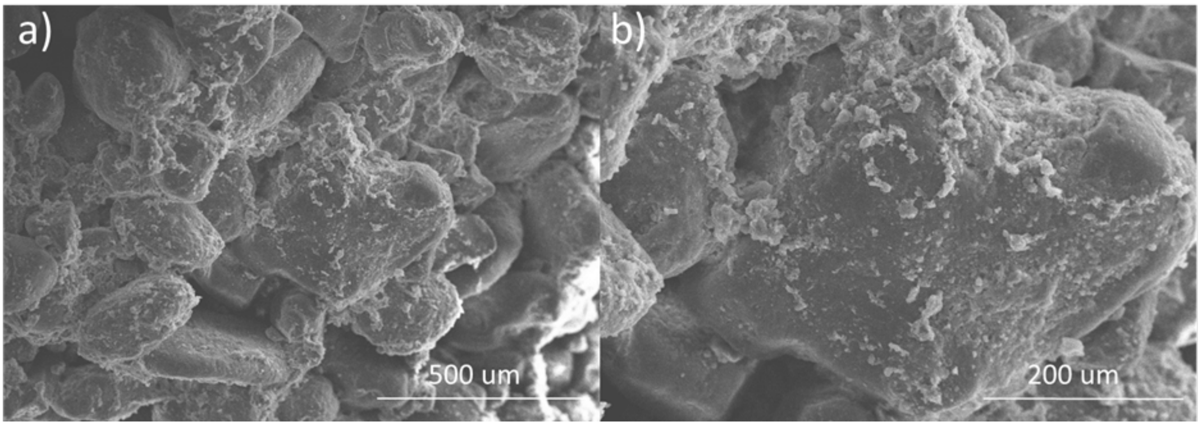

Figure S4. SEM images from soil surface without any fertilizer.

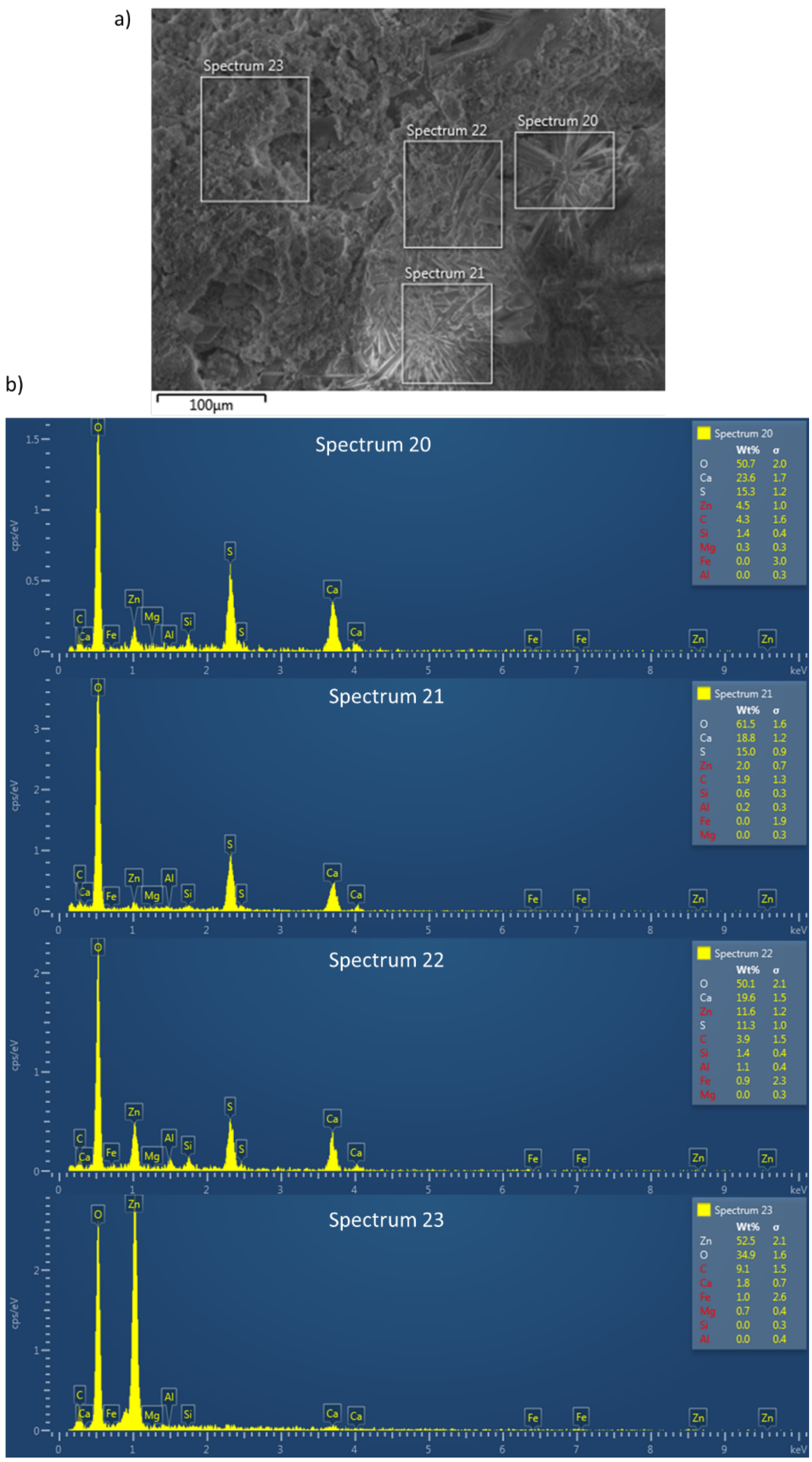

Figure S5. a) SEM image of soil incubated with $ZnSO_4$ granule for 2 weeks showing presence of some crystals after removal of granules on soil surface and b) EDX analysis from different spots with (spectrum 20, 21 and 22) and without crystals (spectrum 23).

References:

1. Kabiri, S.; Degryse, F.; Tran, D. N. H.; da Silva, R. C.; McLaughlin, M. J.; Losic, D. Graphene oxide: A new carrier for slow release of plant micronutrients. *ACS Applied Materials & Interfaces* 2017.

Chapter 5

Co-granulation of low rates of graphene and graphene oxide with macronutrient fertilizers remarkably improves their physical properties

This section is included in the thesis as it appears as a journal paper published by **Shervin Kabiri,** Roslyn Baird, Diana N.H. Ivan Andelkovic, Mike J. McLaughlin and Dusan Losic, "Co-granulation of Low Rates of Graphene and Graphene Oxide with Macronutrient Fertilizers Remarkably Improves their Physical Properties", ***Journal of ACS Sustainable Chem. Eng.*** 2018, 6, 1299-1309.

Statement of Authorship

Title of Paper	Co-granulation of Low Rates of Graphene and Graphene Oxide with Macronutrient Fertilizers Remarkably Improves their Physical Properties
Publication Status	☑ Published ☐ Accepted for Publication ☐ Submitted for Publication ☐ Unpublished and Unsubmitted work written in manuscript style
Publication Details	Journal of ACS Sustainable Chemistry and engineering

Principal Author

Name of Principal Author (Candidate)	Shervin Kabiri		
Contribution to the Paper	Under the supervision of Dusan Losic, Michael McLaughlin and Diana Tran, I developed, designed and conducted the experiments, interpreted and processed the data and wrote the manuscript for submission.		
Overall percentage (%)	85		
Certification:	This paper reports on original research I conducted during the period of my Higher Degree by Research candidature and is not subject to any obligations or contractual agreements with a third party that would constrain its inclusion in this thesis. I am the primary author of this paper.		
Signature		Date	22/06/2018

Co-Author Contributions

By signing the Statement of Authorship, each author certifies that:

i. the candidate's stated contribution to the publication is accurate (as detailed above);

ii. permission is granted for the candidate in include the publication in the thesis; and

iii. the sum of all co-author contributions is equal to 100% less the candidate's stated contribution.

Name of Co-Author	Roslyn Baird		
Contribution to the Paper	I helped Shervin Kabiri (candidate) with interpreting experimental results and improving the manuscript for submission. I give consent for Shervin Kabiri to present this paper for examination towards the Doctorate of philosophy.		
Signature		Date	22/06/2018

Name of Co-Author	Ivan Andelkovic		
Contribution to the Paper	I helped Shervin Kabiri (candidate) with interpreting experimental results and improving the manuscript for submission. I give consent for Shervin Kabiri to present this paper for examination towards the Doctorate of philosophy.		
Signature		Date	22/06/2018

Name of Co-Author	Diana N.H. Tran
Contribution to the Paper	I acted as the secondary supervisor for Shervin Kabiri and helped her to design the experiments and improve the final drafts of the manuscript for submission. I give consent for Shervin Kabiri to present this paper for examination towards the Doctorate of philosophy.
Signature		Date	22/06/2018

Name of Co-Author	Mike J. McLaughlin
Contribution to the Paper	I acted as the secondary supervisor for Shervin Kabiri and aided in design and development of experiments and evaluation of manuscript for submission. I give consent for Shervin Kabiri to present this paper for examination towards the Doctorate of philosophy.
Signature		Date	22/06/2018

Name of Co-Author	Dusan Losic
Contribution to the Paper	I acted as the primary supervisor for Shervin Kabiri and aided in design and development of experiments and evaluation of manuscript for submission. I give consent for Shervin Kabiri to present this paper for examination towards the Doctorate of philosophy.
Signature		Date	22/06/2018

ACS Sustainable Chemistry & Engineering
Research Article
Cite This: ACS Sustainable Chem. Eng. 2018, 6, 1299−1309
pubs.acs.org/journal/ascecg

Cogranulation of Low Rates of Graphene and Graphene Oxide with Macronutrient Fertilizers Remarkably Improves Their Physical Properties

Shervin Kabiri,[†,§] Roslyn Baird,[‡] Diana N. H. Tran,[†,§] Ivan Andelkovic,[†,‡] Mike J. McLaughlin,[*,‡,§] and Dusan Losic[*,†,§]

[†]School of Chemical Engineering, Engineering North Building, The University of Adelaide, Adelaide, South Australia 5005, Australia
[§]ARC Research Hub for Graphene Enabled Industry Transformation, The University of Adelaide, South Australia 5005, Australia
[‡]Fertilizer Technology Research Centre, School of Agriculture, Food and Wine, The University of Adelaide, Waite Campus, PMB1, Glen Osmond, South Australia 5064, Australia

Supporting Information

ABSTRACT: The beneficial effects of graphene (GN) and graphene oxide (GO) additives on the physical properties of monoammonium phosphate (MAP) fertilizer granules were investigated. Low doses (0.05 to 0.5% w/w) of GN and GO sheets were cogranulated with MAP and effects on the crushing strength, abrasion and impact resistance of prepared granules were evaluated. Cogranulation with 0.5% w/w GN sheets (MAP-GN) significantly enhanced the mechanical strength of MAP granules (~18 times improvement) whereas inclusion of same amounts of GO sheets (MAP-GO) improved the strength to a lesser extent (~8 times improvement). The cogranulation of GN also improved MAP granules resistance to abrasion (>70%) and impact resistance (>75%). Heating MAP-GO granules at 50 °C after granulation is shown to enhance their physical properties in comparison to MAP-GO granules dried under ambient temperatures. The advantages of GN and GO sheets compared with current additives in enhancing the physical properties of MAP granules are explained by their high specific area, superior nanofiller−matrix and adhesion/interlocking ability arising from their unique wrinkled structures and two-dimensional (2D) geometry. These results confirm the potential of GN/GO additives to enhance the physical properties of MAP granules that could be translated to other fertilizers and applied in the industry.

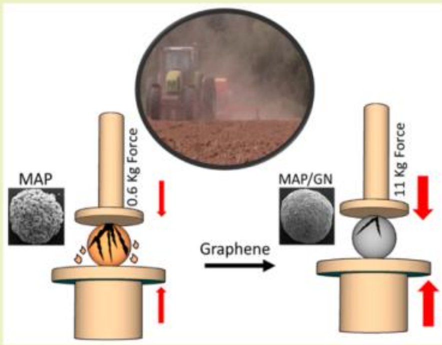

KEYWORDS: Graphene, Graphene oxide, Fertilizers, Crushing strength, Abrasion, Impact resistance, Caking tendency

INTRODUCTION

Fertilizers are common amendments to agricultural soils to refill the soil during the harvest with plant essential nutrients and improve crop yields and health for food production.[1,2] One critical parameter in selection of particulate fertilizer is its physical quality. The acceptability of the fertilizers in the market not only is determined by their nutrient content but also by their physical quality and is often the reason for selecting one fertilizer over another.[3,4] Also, granular fertilizers should have appropriate mechanical strength to resist significant fracturing and creation of excessive dust during the handling and storage process to meet market needs.[5] However, most of the fertilizers produced by different techniques such as granulation, prilling or compaction techniques are never perfectly spherical and suffer from having irregular protrusions on their surface.[4] These protrusions and jagged edges tend to weaken and break off during the routine handling of fertilizers, or transport and spreading on the farm and create substantial quantities of dust.[4,6] This airborne dust produced is undesirable due to its health and safety risks for those exposed during manufacturing of fertilizers or their application on the farm. Furthermore, the abrasion of granules and dust formation leads to negative environmental impacts and increased costs for both fertilizer producers and users due to the loss of nutrient.[4]

Another issue associated with handling of fertilizer granules is their tendency to cake during bulk storage and transportation as the initial free-flowing particles may absorb water and form a solid agglomerated coherent mass.[7−9] This can be the result of crystal bridges formed between granules as the air humidity cycles, dissolving the surfaces causing recrystallization to occur.[8] The caked particles may easily break into smaller particles producing significant amounts of dust during handling and transporting or hard agglomerates may block the spreading equipment resulting in uneven nutrient spreading when applied to the soil.[9,10]

Received: October 9, 2017
Revised: November 1, 2017
Published: November 20, 2017

DOI: 10.1021/acssuschemeng.7b03655
ACS Sustainable Chem. Eng. 2018, 6, 1299−1309

To overcome these considerable drawbacks, manufacturers use different hardening additives or coating materials to improve the physical properties of fertilizers and reduce the propensity for dust generation and caking. For example, antidusting properties have been imparted to urea fertilizers by utilizing formaldehyde or low concentrations of lignosulfonate.[10−12] However, these additives have several disadvantages: formaldehyde use presents serious health and safety issues, whereas lignosulfonate can discolour the urea product and affect acceptance in the marketplace.[10,11] Addition of gelling type clay such as attapulgite or sepiolite to the urea melt or synthetic liquor has been used to overcome the previously discussed disadvantages and to increase the hardness of urea fertilizers. However, these mineral additives are needed in higher quantity to enhance the physical quality of fertilizer and their mining sites are located in a geographical isolated area, therefore the overall cost of the final product will increase.[11] Another strategy used to harden granules is to add a binder such as melamine and its hydrolyzed products to bind fine particles of a poorly or slightly soluble source to form a hardened agglomerate or prill.[13] However, this method is restricted to nitrogen source materials with a certain size, and the granulation or prilling machinery used to make such hardened granular fertilizers are relatively expensive.[4] Calcium oxide, calcium hydroxide, cement and fly ash have also been used to improve the hardness of fertilizers, especially urea. The problem with using these materials is the reduction of available fertilizer nutrient in the final granules.[11,14]

Another approach to improve the physical properties and release performances of fertilizers is to coat fertilizer granules with different coating materials. Many materials have been considered for this purpose including molten elemental sulfur, diatomaceous earth and clay, hydrated cement, gypsum, zeolite, wax, plastic, and a combination of a biodegradable aliphatic copolyester and fatty acids to create slow-releasing urea fertilizers that also have anticaking properties.[15−18] Although these coatings decrease the rate of release of nutrients and in some cases enhance the anticaking properties of the granules, most of them incorporate foreign elements into the fertilizers, which are not compatible with the specific fertilizer and sophisticated equipment is usually needed to apply them.[4,14] In addition, coatings or materials that comprise a high percentage of the total fertilizer composition tend to dilute the available fertilizer nutrient content and increase transport and handling costs. Therefore, there is a need for new materials to address the limitations of currently used methods in terms of improved performance, multiple modes of action, very low dosages, and acceptable costs that can be used on an industrial scale.

Graphene (GN) and its oxidized form graphene oxide (GO) are new materials with unique properties such as distinctive 2D structures, high surface area, tailorable surface chemistry and have exceptional mechanical properties.[19,20] In fact, GN possesses a very high specific surface area with a theoretical value of 2630 m^2 g^{-1}, because every atom of the single-layer sheet is exposed from both sides.[21,22] Furthermore, despite being one atom thick, GN is the strongest material measured with a Young's modulus of E = 1.0 TPa and an intrinsic strength of 130 GPa in its pristine, atomically perfect form.[20] Therefore, these outstanding mechanical properties of GN have initiated considerable interest for their application as an additive to enhance the mechanical properties of softer materials and strengthen them. Most significant examples are the use of GN as nanofillers to increase the mechanical properties of different polymers due to the improved interactions of GN and the polymer matrix, resulting from the high surface area of the planar GN sheets.[23,24] Two-dimensional GN sheets are not only used as an ideal filler or reinforcing nanomaterial for polymer matrices but are also incorporated on metal matrices or ceramics to enhance the properties of metal-matrix-composites or ceramic composites.[25−27]

GO is an oxidized form and water-soluble derivative of GN, with a high specific area, ultrahigh strength, exceptional mechanical properties and flexibility.[19,28] The hydrophilic nature of GO allows for a wide variety of chemical functionalization and provides stronger interactions with host materials.[22,29] It has been reported that GO has the capability of forming composites with polymers, construction materials and ceramics, and can remarkably enhance the toughness of formed composites by controlling the microstructure of crystals in the composites.[30−32] Recent studies show that low dosages of GO (0.01−1%) could significantly enhance the performance and mechanical properties of cement composites.[30,33−36] GO can accelerate the hydration of cement due to its high surface area and also densify the cement microstructure as a filler because of the nanosize and flexibility of the GO sheets.[33,37]

Inspired by the unique properties of graphene-based materials (GBMs) and their capability to significantly improve the mechanical properties of many other composite materials with very low dosages, we proposed that these materials can be used as additives to enhance the physical properties of granular fertilizers. The aim of this work is to demonstrate that GN based additives in small quantities can significantly enhance the physical properties of commercial fertilizers and address the long-standing problems caused by their fragility and physical losses related to low crushing strength, abrasion and impact resistance. Monoammonium phosphate (MAP) was used as a model to demonstrate this concept, as it is a widely used fertilizer that is transported and handled around the globe and could be prepared in the laboratory. GN and GO materials were made from low cost natural graphite using scalable industry processes and their cogranulation into MAP granules were performed using a rotating pan and water atomization process commonly used in the fertilizers industry. The addition of both GN and GO additives were explored using different dosages (0.05 to 0.5% w/w) to investigate their effect on improving the key physical properties of MAP granules including the crushing strength, abrasion, impact resistance and caking tendency of granules and compared with MAP (no additive). Finally, to demonstrate the additional benefits of these additives on MAP granules, the release of nutrients from GN and GO treated granules was evaluated in soil.

■ EXPERIMENTAL SECTION

Synthesis of GO and GN. GO sheets were synthesized by the improved Hummer's method from graphite powders.[38] A modified hydrothermal method for the reduction of GO was used to prepare the GN sheets.[39] A GO dispersion (1 mg mL^{-1}, 500 mL) was transferred to a Teflon lined autoclave and heated at 180 °C for 2 h. The autoclave was then cooled to room temperature and the formed GN hydrogel was ultrasonicated in a H_2O/acetone (ratio 3:1) mixture. Some of the final product was freeze-dried for FTIR, Raman, XRD, TGA and SEM characterization and particle size measurement (Figure S1 and S2, Supporting Information).

Preparation of Monoammonium Phosphate (MAP) Fertilizer Granules Cogranulated with GN (MAP-GN) and GO (MAP-GO). Monoammonium phosphate granules were ground and sieved to

DOI: 10.1021/acssuschemeng.7b03655
ACS Sustainable Chem. Eng. 2018, 6, 1299−1309

obtain a powder with sizes less than 250 μm. A GN or GO paste with ~20% water was mixed with the MAP powder at dosage rates of 0.05%, 0.1%, 0.2% and 0.5% by weight. GN and GO sheets with particle sizes of ~150 and ~200 μm, respectively, were added in wet form to reduce the risk of dust exposure during formulation. The mixtures of MAP with different ratios of GN or GO were homogenized, dried and sieved through a 250 μm sieve before granulation. The MAP fertilizer mixture with GN or GO (3 g) were placed in a rotating pan and a small amount of ultrapure deionized water was sprayed onto the fertilizer using a 50 μL min^{-1} nebulizer while the drum was rotating at 12−15 rpm at an angle of 39.2°. The fertilizer powder was granulated in the rotating pan to form particles of approximately 2−4 mm in size, separated by sieving. Oversize granules were crushed and regranulated.

Granule Crushing Strength. To measure crushing strength, fertilizer samples were screened according to International Fertilizer development Centre (IFDC) method S-107 to obtain at least 25 granules with sizes between 2.80 and 2.36 mm diameter.[40] A commercial table-top Wykeham Farrance ring penetrometer (England) was used to measure the mechanical strength of the fertilizer granules. Individual granules were placed on a mounted flat surface and pressure was applied by a flat-end rod attached to the compressor tester. A gauge mounted in the compression tester measured the pressure required to fracture the granule. The load at which the granule fractured was considered as the crushing strength and a total of 25−30 parallel measurements were carried out for each formulation. The average of those measurements determined the crushing strength of the granules.

Granule Abrasion Test. Abrasion resistance of granules was measured by modifying IFDC S-116.[40] To measure the abrasion resistance of the MAP fertilizers, first the samples were screened over 2.80 and 1.00 mm sieves. A portion of the fertilizers (50 g) was accurately weighed and placed in a container. The container was placed in a Spex-mixer/Mill (8000 M Mixer/Mill) and rotated at 30 rpm for times ranging between 5 to 30 s and 5 min. The contents were removed and hand screened over a 1.0 mm screen for 5 min. The material retained on the 1.0 mm screen was then weighed and the "percentage of degradation" was calculated as follows:

$$\text{degradation\%} = 100 - 100 \times \frac{\text{wt of} - 2.80 + 1.00\text{ mm fraction recovered}}{\text{wt of} - 2.80 + 1.00\text{ mm fraction charged}} \quad (1)$$

Granule Impact Resistance. Impact resistance of granules was measured by modifying IFDC method S-118.[40] Each fertilizer formulation (200 g) was passed through a series of sieves; namely 2.80, 2.36 and 2.00 mm. The size range of granules selected for testing in this case was between 2.00 and 2.80 mm diameter, which contained 85% of the overall sample. The 100 g (±1 g) subsamples were accurately weighed and then allowed to fall 10.7 m in an 15 cm diameter enclosed pipe and impact on a metal catch plate in a catch pan at the base of the pipe. The dropped samples were collected and screened over the smallest selected sieve. The material retained on the previously selected sieve was weighed and the percentage of "shattered granules" was calculated as follows:

$$\text{shattered granules\%} = 100 - 100 \times \frac{\text{material retained on bottom sieve after test (g)}}{100\text{ g }(\pm 1)} \quad (2)$$

Caking Tendency of Fertilizer Granules. To investigate the caking tendency of the fertilizers an apparatus was made similar to the caking apparatus designed by Lafci et al.[41] The apparatus consisted of a PVC cylindrical mold and a plunger. The internal diameter of the cylindrical mold was 2 cm and its height was 7 cm. The mold can be split into two parts so that the cake formed could be removed without any breakage. To study the influence of pressure on caking, 4.0 g of MAP-0.5%GN, MAP-0.5%GO and untreated MAP formulations was placed in each caking apparatus and loads applied from 1 to 2.5 kg using weights placed on the plunger. All caking tendency experiments were conducted in a humidity chamber (Environmental Temperature and Humidity Cabinets, Envirotherm, Thermoline Scientific, Australia) with 70% humidity (near to the critical relative humidity of MAP fertilizers) at 30 °C. Samples were taken at the end of 7 days from the humidity chamber and where any cakes were formed the force needed to crush them were determined using a ring penetrometer.

Phosphorus (P) Diffusion from Fertilizer Granules. The P diffusion method of Degryse and McLaughlin was used to investigate the release of P from amended and untreated MAP granules.[42] Briefly, Petri dishes with a diameter of 5.5 and 1 cm height were filled with wetted soil and a granule of the selected products (MAP-0.05%GN, MAP-0.5%GN, MAP-0.05%GO, MAP-0.5%GO and MAP) were placed in the center of the Petri dish at the same dosage rate (~6.3 mg per Petri dish) about 4 mm below the soil surface. Three replicates were prepared for each formulation. The Petri dishes were then placed in a plastic bag with moist paper towels to avoid water loss from the soil and incubated at 25 °C. The release and diffusion of P from the granules was monitored at 1, 3, 14, 21 and 28 days.

RESULTS AND DISCUSSION

Structural and Chemical Characterization of MAP Granular Fertilizer with GN and GO Additives. Light and SEM microscopic images of prepared MAP samples (control and with GO/GN additives) showed that all samples were granulated to form round-shaped granules (Figure 1a−f).

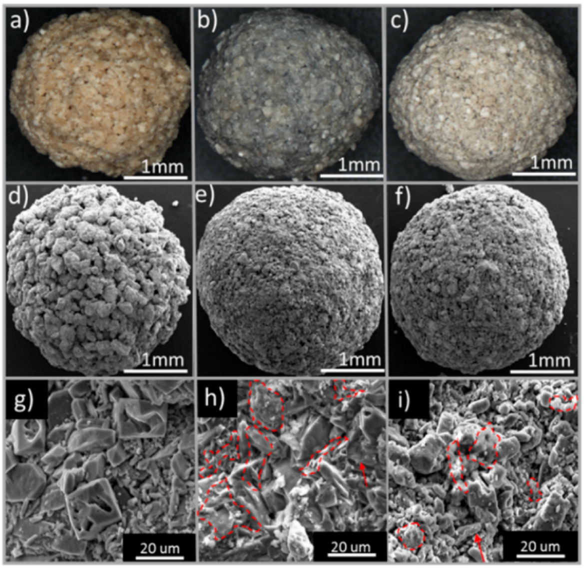

Figure 1. Microscopic images of (a) monoammonium phosphate granules (MAP) (control), MAP with (b) 0.5% graphene (GN) and (c) 0.5% graphene oxide (GO), SEM images of (d) MAP, MAP with (e) 0.5% GN and (f) 0.5% GO and high resolution SEM images of (g) MAP, MAP with (h) 0.5% GN and (i) 0.5% GO (red arrows and dot points represent the presence of GN or GO).

However, the MAP granule (control) had a rougher surface compared to the MAP-GN and MAP-GO granule surfaces (Figure 1d−f). In order to confirm the presence and distribution of GN and GO sheets in the MAP-*co*-granules, higher magnification SEM images were taken and compared with MAP (Figure 1g−i). These images show GN (or GO) sheets randomly dispersed and embedded in the MAP-GN or MAP-GO composites where some of the MAP macroparticles were wrapped by the GN or GO sheets.

DOI: 10.1021/acssuschemeng.7b03655
ACS Sustainable Chem. Eng. 2018, 6, 1299−1309

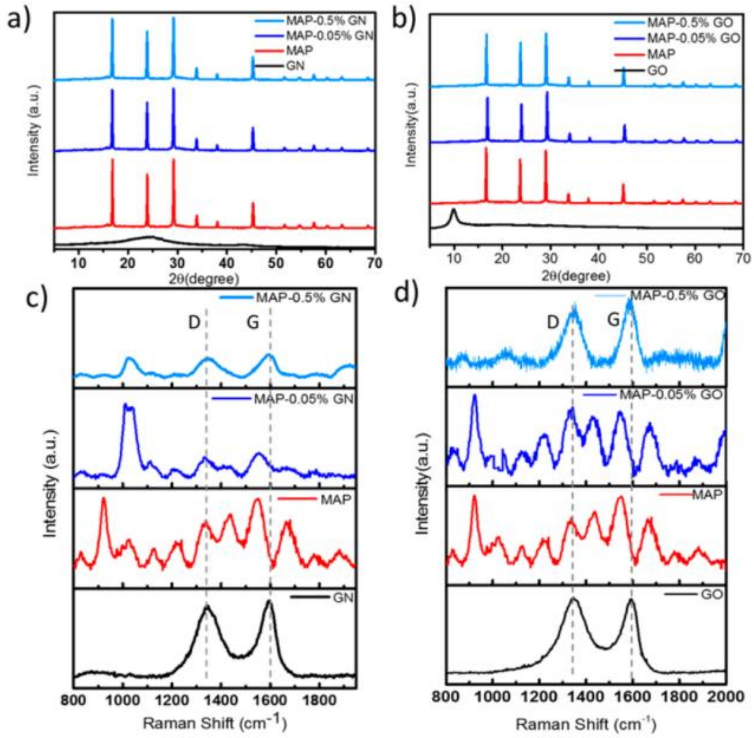

Figure 2. XRD patterns of (a) graphene (GN), monoammonium phosphate (MAP) and MAP with 0.05 and 0.5 wt % age of GN (MAP-0.05%GN and MAP-0.5%GN), (b) graphene oxide (GO), MAP and MAP with 0.05 and 0.5 wt % age of GO (MAP-0.05%GO and MAP-0.5%GO) and Raman spectra of c) GN, MAP and MAP with 0.05 and 0.5 wt % age of GN (MAP-0.05%GN and MAP-0.5%GN), and (d) GO, MAP and MAP with 0.05 and 0.5 wt % age of GO (MAP-0.05%GO and MAP-0.5%GO).

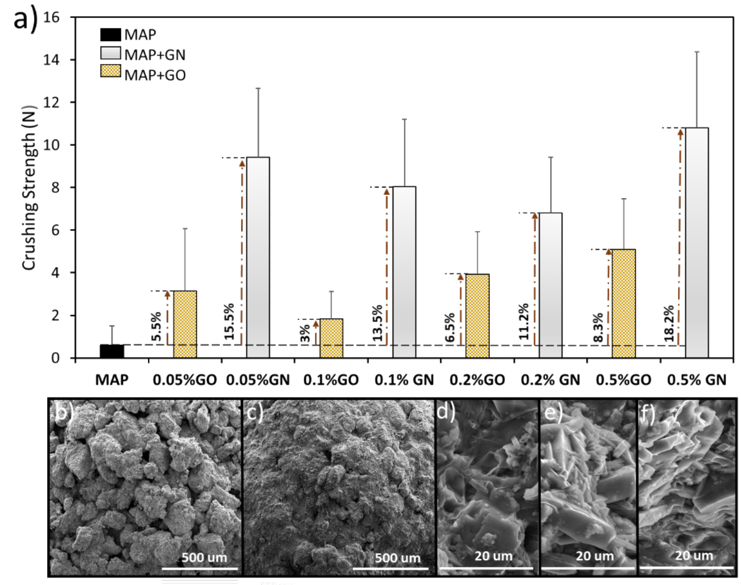

Figure 3. a) Graph showing crushing strength (newton (N)) to crush a granule of monoammonium phosphate (MAP) (control) and MAP with different concentration (0.05 to 0.5%) of graphene (GN) and graphene oxide (GO), (crushing strength and standard deviation were measured for 25 granules for each formulation, error bars represents (n = 25), Low resolution SEM images of top surface of b) MAP (control) and c) MAP-0.5%GN, high resolution SEM images of d-e) MAP-0.5%GN and f) MAP-0.5%GO.

The XRD patterns of GN and GO show typical diffraction peaks at $2\theta = 25.1°$ (d-spacing ~0.35 nm) and $2\theta = 9.9°$ (d-spacing ~0.90), respectively, compared to the XRD pattern of commercial MAP, which can be indexed to the presence of $NH_4H_2PO_4$ (JCPDS card No. 9007583) (Figure 2a,b).[38,43] Samples prepared with the lowest and highest amounts of GN

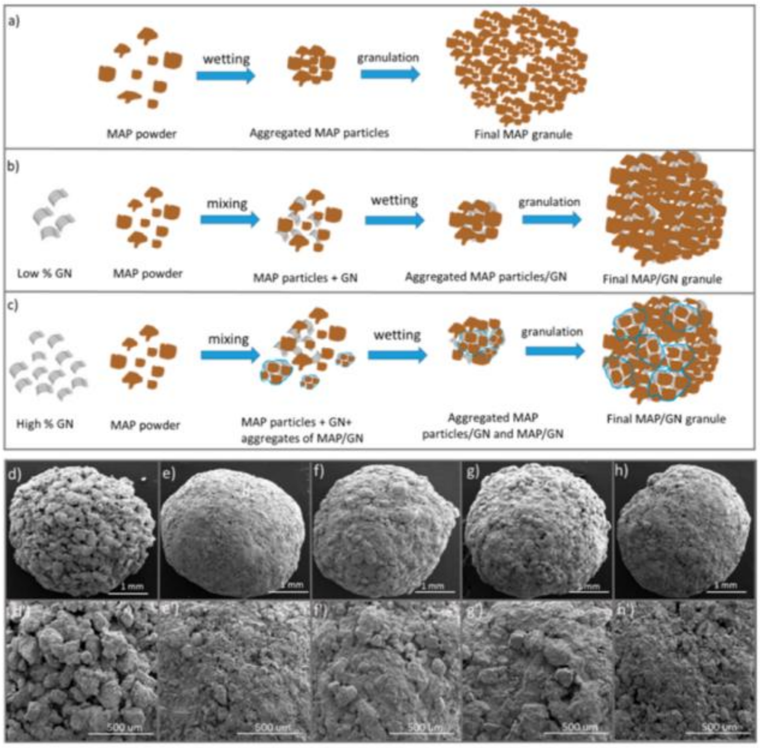

Figure 4. Schematic of cogranulation of MAP using lower and higher concentration of graphene additives: (a) Granulation of MAP showing "loose" connection of MAP particles during the granulation process resulting in rough and particulates surface morphology, (b) Granulation of MAP with lower concentration of graphene additives (0.05% GN or GO)) showing filling of the pores by GN or GO sheets and making smoother surface, (c) Granulation of MAP with graphene additives with higher concentration (>0.1%) showing formation of preaggregates during the mixing process of GN and MAP, and incorporation of aggregates in the granulation process, causing more rough surface morphology. Corresponding low and high resolution SEM images of surface of d,d′) monoammonium phosphate MAP granules prepared by low and high dosages of graphene additives (MAP), and MAP with different percentages of graphene additives (e,e′) MAP-0.05%GN, (f,f′) MAP-0.1%GN, (g,g′) MAP-0.2%GN and (h,h′) MAP-0.5%GN.

(or GO) with MAP showed XRD patterns characteristic of the commercial MAP, indicating that the presence of GN (or GO) in the mixture did not alter the structure of MAP. No diffraction peaks corresponding to either GN or GO were observed in the XDR patterns for the amended products, which is probably due to the low amounts of GN (or GO) and their diffraction intensity. However, a small decrease in the intensity of the MAP-GO composites compared to MAP could be related to the chemical reaction between MAP and GO.[44]

To confirm the presence of GN and GO in the amended MAP granules, Raman characterization was performed (Figure 2c,d). The granules showed a typical Raman spectra of GN sheets with two dominant peaks at 1346 and 1596 cm^{-1} related to the D and G bands of GN-based materials, respectively.[45] The Raman spectrum of MAP (Figure 2c) showed a high peak at 920 cm^{-1} related to the stretching vibration of the PO_4 group and a peak at 1650 cm^{-1}, which corresponds to more strongly hydrogen bonded water molecules.[46] The Raman spectrum of MAP presented in this work shows more peaks compared to the Raman spectrum of pure MAP due to the presence of some impurities such as aluminum (Al), magnesium (Mg), calcium (Ca) and sulfur (S) ions (Figure S3, Supporting Information). However, the Raman spectrum of MAP-0.05%GN showed similar peaks to the Raman spectrum of MAP, except that the intensity of the peaks were decreased and the peaks related to the D and G bands of GN were more distinct. The D and G bands of MAP-0.5%GN composite were at 1347 and 1597 cm^{-1}, respectively and were shifted compared to that of GN (used as a control) due to the charge transfer between the GN and MAP.[47] GO and its different composites with MAP followed a similar trend in Raman spectra to that of MAP-GN composites (Figure 2d). The MAP-0.5%GO composites displayed two sharp and clear peaks at 1343 (D band) and 1589 cm^{-1} (G band), similar to the peaks of GO. These results therefore confirmed the presence of GN or GO in MAP-GN and MAP-GO granules.

Physical Properties. The crushing strengths of MAP cogranulated with different weight percentages of GN and GO are presented in Figure 3a−d. It can be clearly observed that the crushing strength of MAP granules with added GN (or GO) was significantly higher (3.0 to 18.2 times) than MAP (control) and the GN incorporation produced higher crushing strengths compared to GO. The average crushing strength with 0.5 wt % GN in the MAP granule was 10.8 kg force, which was 2.8 times higher than granules with the same amount of GO. Furthermore, increase in crushing strength of granules with GN or GO showed a nonlinear concentration dependence. The average crushing strengths for GN additives showed the highest increase (10.8) using 0.5% GN and lowest increase (6.8) using 0.2% GN. The incorporation of only 0.05% GN led to a 15.5 times enhancement in the crushing strength compare to 13.5 and 11.5 times enhancement in crushing

DOI: 10.1021/acssuschemeng.7b03655
ACS Sustainable Chem. Eng. 2018, 6, 1299−1309

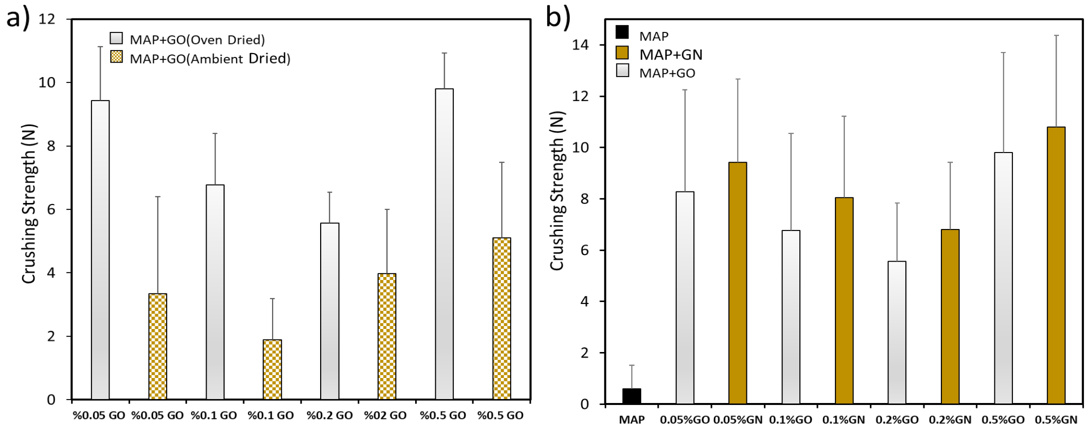

Figure 5. Comparison of crushing strength of (a) monoammonium phosphate (MAP) mixed with different weight percentage of graphene oxide (GO) (0.05, 0.1, 0.2 and 0.5%) dried at ambient temperature and in the oven (50 °C) after granulation and (b) monoammonium phosphate mixed with different weight percentage of graphene (GN) and GO (0.05, 0.1, 0.2 and 0.5%) dried in the oven after granulation (crushing strength and standard deviation were measured for 25 granules for each formulation, error bars represents (n = 25).

strength for granules with 0.1% and 0.2% GN added. For GO additives, we observed the highest increase in crushing strength (5.0) with 0.5% GO added and the lowest strength (1.8) with 0.1% added. Adding low percentages of GN/GO showed a significant improvement in MAP granules compared to commercial additives, such as Norling A (lignosulfonate). Adding 1% of Norling A only doubled the crushing strength of MAP compared to untreated MAP.[10]

We propose that the improved crushing strength of MAP granules with GN or GO additives could be attributed to the high specific surface area and the pore-filling or interlocking ability of GMBs arising from their wrinkled and 2D (planar) structures. To support this hypothesis, a series of SEM images were taken of MAP granules with GN and GO additives (Figure 3b−f). The rough surface of the MAP granule with many micropores and voids (control) (Figure 3b) was significantly different to the surface of MAP with 0.5% GN added, which was the most indicative evidence of the pore filling property of GN additives. The addition of GN caused a denser surface with less pores (or voids) and thus the mechanical behavior of the granules was improved (Figure 3c). High resolution SEM images of 0.5% MAP-GN granules revealed the presence of wrinkly GN sheets or a few layers of GN sheets between MAP macroparticles (Figure 3d,e). The same behavior and morphological characteristics were observed for MAP granules with GO using the same concentration (Figure 3f). These results are in agreement with previous studies showing that GN and GO with lower concentrations can significantly improve the physical properties of composite materials (polymers and concrete) due to pore filling and greater interactions between the GN/GO sheets and polymer/inorganic matrix resulting from the high surface area of the planar structures of sheets.[24,48]

Another reason for the improved crushing strength of GN or GO-MAP granules compared to MAP could be related to the unique mechanical properties of GBMs with a high calculated Young's modulus (E) and intrinsic strength (τ_c).[20,49,50] The results of previous studies have shown that the measured E and τ_c were higher for GN compared to GO, and the calculated E and τ_c for GO sheets depended on the water content, thickness of the samples and presence of different functional groups on the surface of GO, as well as its OH/O ratio of oxygen functional groups.[49,51−53] Therefore, the higher crushing strength of MAP-GN granules compared to MAP-GO granules can be attributed to the smaller values of E and τ_c of GO compared to GN. It is reported that the mechanical properties of GN are strongly influenced by the type and amount of its defects.[54] GN used in this study was prepared by hydrothermal reduction of GO, and therefore would inevitably be defective and thus inferior in properties to pristine monolayer GN, but still the E of the GN synthesized (0.25 TPa) was higher than that of GO (0.2 TPa).[55−57]

To explain the unexpected nonlinear concentration dependence of GN/GO additives on the crushing strength of MAP granules showing higher crushing strength values for lower inclusion rates (0.05% GN), a schematic of their granular structures based on the SEM images of prepared MAP granules with different graphene concentrations is illustrated in Figure 4. Figure 4a explains how MAP particles agglomerate together to form granules during the granulation process. SEM images of the MAP granules (Figure 4d,d′) clearly verify the proposed schematic by showing loosely agglomerated MAP particles attached together with very rough topography of granules. Adding a low percentage of GN (0.05%) to MAP particles aided the formation of denser aggregates of MAP-GN due to the pore-filling effect of GN sheets (Figure 4b). SEM images of MAP-0.05% GN (Figure 4e,e′) confirmed that the amount of pores and debris significantly decreased and MAP particles were connected tightly together due to the presence of GN showing a very smooth MAP granule surface. However, adding higher concentrations of GN (0.1%, 0.2% or 0.5%) to MAP particles during the mixing process before granulation created some initial MAP/GN aggregates due to the presence of some moisture (∼20%) in the GN paste. These preaggregated MAP/GN particles tended to bind together and to the MAP particles during the granulation process causing the final granule to have a rougher surface compared to the MAP/GN granules with 0.05% GN (Figure 4c). SEM images of the MAP-0.1% GN granules (Figure 4f,f′) showed a rougher surface with some larger aggregates compared to MAP-0.05% GN granules and

DOI: 10.1021/acssuschemeng.7b03655
ACS Sustainable Chem. Eng. 2018, 6, 1299−1309

Table 1. Comparison of the Effects of Different Materials Used as Additives or Coatings To Enhance the Crushing Strength of Fertilizer Granules[a,b,c,d,e]

fertilizer type	method of application	coating or additives	coating or additive percentage	relative increase compare to control	reference
isobutyl diurea (IBDU)[a]	coating	mixture of Norlig A[b] and urea	4.6%	1.74	4
IBDU[a]	coating	water and urea	4.7%	1.68	4
IBDU[a]	coating	UF85[c]	6.0%	4.05	4
urea	coating	poly(butylene succinate) and dimerized fatty acid	0.26%	8.09	17
urea granule[a]	additive	$Ca(OH)_2$	(0.75%)	2.52	11
urea granule	additive	CaO	(0.5%)	2.31	11
urea granule[a]	additive	cement	(0.1%)	1.9	11
urea granule	additive	fly ash	(0.5%)	1.95	11
urea granule[a]	additive	clay[d] and $Ca(OH)_2$ (10/90%)	(0.6%)	2.53	11
urea granule[a]	additive	clay[d] and cement (90/10%)	(0.5)%	1.97	11
urea granule[a]	additive	formaldehyde	0.6%	1.96	11
ammonium nitrate[a]	additive	Norlig HP[e]	0.4%	1.48	10
MAP[a]	additive	lignosulfonate	0.4%	2.14	10
diammonium phosphate(DAP)[a]	additive	Norlig HP[e]	0.6%	4.33	10
potassium nitrate	additive	modified lignosulfonate	5.0%	7	10
potassium chloride	additive	modified lignosulfonate	5.0%	5.75	10
potassium sulfate	additive	modified lignosulfonate	5.0%	9.8	10
MAP	additive	graphene	0.5%	18.20	current work
MAP	additive	graphene	0.05%	15.55	current work
MAP	additive	graphene oxide	0.5%	16.21	current work
MAP	additive	graphene oxide	0.05%	13.62	current work

[a]Refers to reporting highest amount of crushing strength among the same fertilizer with different percentages of added or coated materials as hardening agents. [b]Refers to composition of Norlig A product that is 3.8% calcium lignosulfonate. [c]Refers to composition of UF85 product that is an 85% aqueous solution of urea formaldehyde. [d]Refers to composition of clay that is a blend of diatomaceous earth and calcium bentonite. [e]Refers to composition of Norlig HP product that is reed lignin.

the number of aggregates increased in the case of MAP-0.2% GN granules (Figure 4g,g′). Although the presence of preaggregated MAP/GN particles decreased the crushing strength of MAP-0.1 and 0.2% of GN/GO granules; however, their crushing strength is higher than untreated MAP granules.

Granules of MAP treated with and without GN/GO additives were dried in the oven at 50 °C overnight to speed up their drying. Interestingly, the crushing strength of MAP-GO granules was considerably enhanced compared to MAP-GO granules dried at ambient temperature (Figure 5a). However, heating MAP or MAP-GN granules at 50 °C did not improve their crushing strength compared to the granules dried at ambient temperature. Granules were not dried at higher temperatures to avoid changes in the crystalline structure of MAP.[58] The crushing strength of all MAP-GO formulations after heating was comparable to the MAP-GN formulations with no heating (Figure 5b). These results could be explained by the conversion of GO to reduced GO (rGO) due to heating, which is a well-known process and obviously improves the performance of GO to be similar to GN. Different characterization techniques, including FTIR, TGA, Raman and XRD were used to prove this hypothesis. Compared with other additives or coatings used to enhance the crushing strength of fertilizer granules, adding a small quantity of GN or GO sheets produced a noticeable enhancement of hardness of MAP granules, as shown in Table 1.

The physical properties and mechanical performances of the prepared fertilizer granules were further investigated by measuring their abrasion resistance.[5] The abrasion resistance of the fertilizer granules reflects their resistance to the formation of dust and fine particles as a result of granule to granule, and granule to equipment contact when being handled and stored.[11,40] Therefore, the abrasion resistance of MAP granules treated with different concentrations of GN was selected for the abrasion tests due to their greater mechanical strength compared to GO formulations. Figure 6a shows the abrasion percentages for MAP granules with different GN concentrations taken at 10, 20 and 30 s from the abrasion test. Results showed that addition of GN to MAP granules significantly reduced their degradation by abrasion (>3 times) compared with untreated MAP. As expected, the degradation of the granules increased by increasing the abrasion time from 10 to 30 s. Interestingly, the abrasion of MAP-GN granules was not concentration dependence and there was a negligible difference in dust formed at very low concentration of GN (0.05%) compare to higher concentration (0.5%). This could be explained by the morphological structure and surface roughness of the granules. As mentioned previously, adding 0.05% GN decreased the amount of pores and debris on the surface of MAP-0.05GN granules due to the pore-filling effect of GN sheets. However, increasing the amount of GN from 0.05% to 0.1, 0.2 and 0.5% created a rougher surface with surface aggregates compared to the smoother surface of MAP-0.05%GN granules. Therefore, in MAP treated granules with higher concentration of GN the contacting surface between two granules, and with granules and the container increased, thus

DOI: 10.1021/acssuschemeng.7b03655
ACS Sustainable Chem. Eng. 2018, 6, 1299−1309

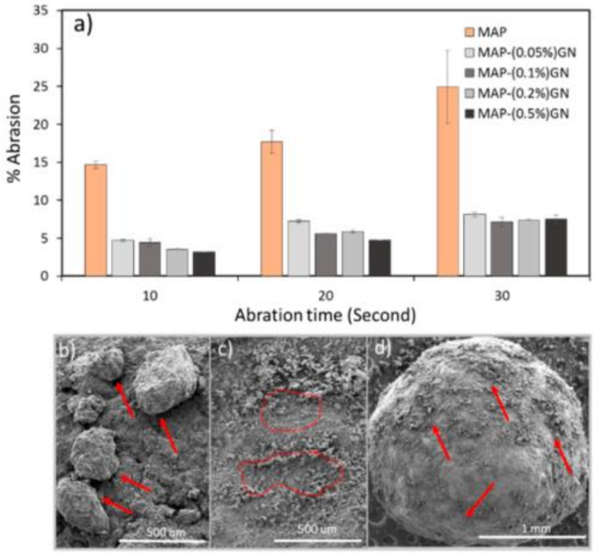

Figure 6. (a) Comparative abrasion data showing degradation of pure monoammonium phosphate (MAP) granules and MAP granules prepared with different weight percentages of graphene (0.05, 0.1, 0.2 and 0.5% GN, error bars represent standard error (n = 3)), SEM images of (b) MAP-0.5% GN before abrasion showing aggregates on granule surface and (c and d) after abrasion for 30 s showing detachments of surface fragments.

generating similar amounts of dust as 0.05% GN granules (Figure 6b). Larger aggregates on the surface of granules with high rates of added GN are more likely to separate from the granule's surface when in contact with other granules and the container during the abrasion test (Figure 6c). Furthermore, cavities developed on the surface of MAP-0.5%GN after abrasion for 30 s was related to the detachment of surface fragments (Figure 6d).

MAP-GO samples dried under ambient conditions and in the oven were tested for abrasion resistance and the effect of longer shaking time on the abrasion of granules was studied (Figure S5, Supporting Information). The results obtained from the abrasion tests showed less dust formation for oven-dried MAP-GO compared to the ambient dried MAP-GO samples. Furthermore, the abrasion of those samples with highest crushing strengths did not increase greatly with an increased shaking time of 5 min.

Testing the impact resistance of granules is important for the fertilizer industry when (i) fan-type fertilizer spreaders are used, (ii) fertilizer granules are discharged from overhead points into a bulk piles and (iii) bags of fertilizer products are dropped during handling.[40] The selected three formulations that showed higher crushing strength and low abrasion, namely MAP-GN with 0.05% and 0.5% addition rates of GN and oven-dried MAP-GO with 0.5% GO were chosen to conduct the impact resistance test. When the treated MAP granules were subjected to the impact resistance test, 18% of granules were fractured (Figure 7a). MAP granules cogranulated with GO and especially GN as hardening agents had much greater resistance with only 4.6% and <3% of granules fractured, respectively.

Finally, the effect of pressure and humidity on the caking tendency of MAP and selected MAP-GN/GO granules with the best physical properties was performed. For all three tested formulations (MAP, MAP-0.5% GN and MAP-0.5% GO), no caking was observed for the 1 kg load at the end of the incubation period. However, by changing the loading weight to 2.5 kg, some of the granules fractured and caking occurred as in the case of the MAP granules (Figure 7b,c). SEM images of the caked parts in the MAP granules (Figure 7d,e) shows two granules caked together and some broken granules. Both MAP-GN and MAP-GO granules flowed freely at the end of the incubation time with 2.5 kg weight load, but some MAP-GO granules were crushed under the applied pressure (Figure 7f–h). Therefore, adding a small quantity of GN or GO to MAP significantly increased the mechanical strength of granules, and consequently would reduce the amount of airborne dust created during the handling and transportation of fertilizer.

Soil Diffusion Experiment. As discussed previously some hardening agents or anticaking materials added to fertilizer granules can affect the release rate of nutrients, often slowing down the release.[15−17,59] Therefore, in this study, we investigated the diffusion and release of phosphorus (P) in the soil from MAP-GN based granules. Formulated granules (MAP-0.05%GN, MAP-0.5%GN, MAP-0.05%GO and MAP-0.5%GO) that achieved the greatest overall physical properties were selected for this experiment. After 1 day application of

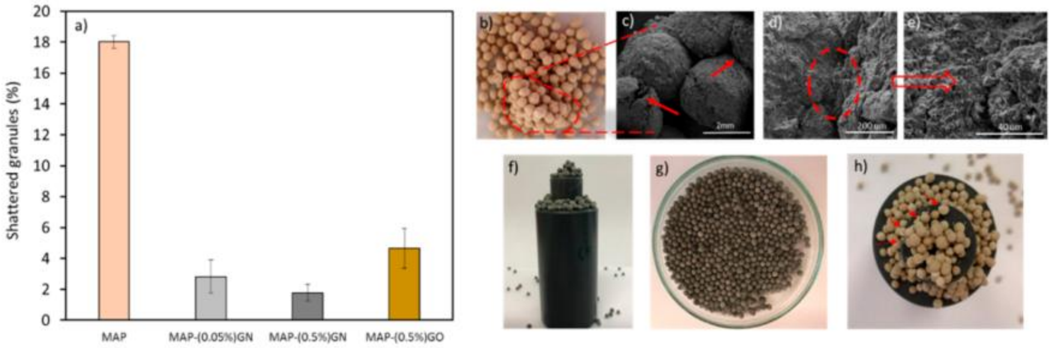

Figure 7. (a) Impact resistance of pure monoammonium phosphate (MAP) granules, MAP granules treated with 0.05% graphene oxide (GO) (MAP-0.05%GO) dried in the oven, 0.05% of graphene (GN) (MAP-0.05%GN) and 0.5% of GN (MAP-0.5%GN) (error bars represent standard error (n = 3)), (b) photograph of caked monoammonium phosphate (MAP) granules under 2.5 kg weight after incubation for 1 week at 30 °C and 80% relative humidity and (c–e) SEM images of caked MAP granules, (f,g) photographs of MAP treated with 0.5% of graphene and (h) photograph of MAP treated with 0.5% of graphene oxide (all caking test performed three times and samples were incubated for 1 week at 30 °C, 80% of humidity and under 2.5 kg of weight).

DOI: 10.1021/acssuschemeng.7b03655
ACS Sustainable Chem. Eng. 2018, 6, 1299−1309

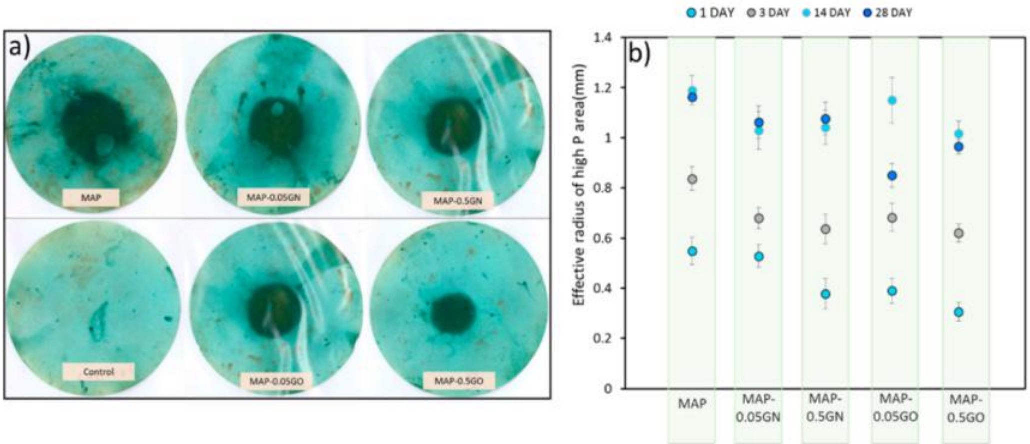

Figure 8. (a) Visualized P diffusion zones in an acid soil (Monarto, Supporting Information Table S1) from monoammonium phosphate (MAP), MAP with 0.05% graphene oxide (GO) (MAP-0.05%GO), MAP-0.5%GO, MAP with 0.05% graphene (GN) (MAP-0.05%GN) and MAP-0.5%GN. All fertilizers supplied ~6.3 mg of phosphorus (P) added to soil in the center of a Petri dish and incubated for 28 days, and (b) radius of the high-P (derived as $\sqrt{A/\pi}$ with A the area of the P diffusion zone) at 1, 3, 14, 21 and 28 days after the addition of MAP, MAP-0.05%GO, MAP-0.5%GO, MAP-0.05%GN and MAP-0.5%GN granules (error bars represent standard error (n = 3)).

untreated MAP with the GN/GO based treated fertilizers into the moist soil, the movement of P out of the granules and into the soil (represented by the dark green zone) from all treated MAP granules was less compared to the control MAP (Figure 8a). As can be seen from Figure 8b, the diffusion of P when added with MAP-0.5%GN/GO was slightly lower compared to the soils with MAP-0.05%GN/GO. Furthermore, there was less release and diffusion of P from MAP-0.5%GO compared to MAP-0.5%GN at all incubation periods, which may be due to the chemical reaction between GO and MAP. The results from the soil diffusion test confirm that the GBMs not only increase the physical properties of MAP granules but also slightly delay the release of P.

Although the unique physio-chemical properties of GBMs have made them a favorable material for many new technologies, safety issues associated with their production, application and fate in the environment must be addressed to critically consider any future development.[60] There are a number of studies conducted to evaluate the in *vitro* and in *vivo* toxicological effects of GBMs and their interactions with different living organisms such as mammalian cells, microbes and animal models. Though most of these studies showed the biocompatibility of GBMs, some studies have indicated potential risks and health hazards.[61,62] The toxic effects of GBMs, as for all other materials, are modular and can change depending on many parameters including the concentration, morphology, particle size and contact time, hydrophobicity, and surface functionalization.[62] Therefore, it is difficult to generalize GBMs toxicity risks as these are reliant on their particular applications and require specific evaluation performed by safety organizations and standards.[63]

Another potential concern about application of GBMs in agriculture is their fate and accumulation in soils, sediments or waters. However, several recent studies have shown the biodegradation of GBMs in the presence of hydrogen peroxide (H_2O_2), horseradish peroxidase, lignin peroxidase and enzyme release by white rot fungi.[64−66] Therefore, it is anticipated that both GN and GO undergo effective biodegradation in the environment as H_2O_2 could be found naturally in rain and surface water, and fungi distributed in soil world widely.[64,66]

■ CONCLUSIONS

In this work, we demonstrated for the first time that GN and GO can be used as additives in fertilizer granules to significantly improve their physical properties such as crushing strength, abrasion and impact resistance. MAP was used as a model fertilizer and GN and GO were added in the range 0.05 wt % to 0.5 wt % using a laboratory granulation process, smaller but similar to that used by fertilizer manufacturers. SEM characterization of MAP-GN and MAP-GO formulations confirmed that GN/GO sheets were randomly dispersed and embedded in the MAP cogranules improving their compactness and filled the voids between the particles. Crushing strength tests revealed that small amounts of GN (or GO) in MAP fertilizer granules remarkably increased (18.2 times for MAP-GN and 16.2 times for MAP-GO) the granule strength compared with untreated MAP. Furthermore, MAP granules containing 0.5% GN or GO abraded ~3.3 and 5 times less of the surface and produced lower dust and fines, and the mechanical tests performed showed significant impact resistance with less shattered granules (4 to 10 times) compared to control MAP. MAP-GN and GO granules also showed less or no caking when exposed to pressure and humidity. These results confirm the potential use of GN and GO as hardening agents, and antidusting and anticaking additives in the fertilizer industry. Soil experiments with MAP-GN or MAP-GO granules showed a slightly slower release of P that provides an additional benefit for these additives. The granulation of GN and GO additives with fertilizer is very simple and is based on existing fertilizer granulation processes used for fertilizer manufacturing hence it could be rapidly adapted for industry applications.

■ ASSOCIATED CONTENT

Supporting Information

The Supporting Information is available free of charge on the ACS Publications website at DOI: 10.1021/acssuschemeng.7b03655.

Material, characterization, XRD, Raman, TGA and FTIR peaks of GO and GN; SEM images and particle size measurement of GN and GO sheets; SEM-EDAX of untreated MAP; FTIR, TGA, Raman and XRD characterization of oven-dried and ambient dried MAP-GO granules and photos of MAP-GO ambient and oven-dried; degradation of MAP-GO formulations; selected physical and chemical properties of the soil used in the soil diffusion study (PDF)

AUTHOR INFORMATION

Corresponding Authors

*M. J. McLaughlin. E-mail: michael.mclaughlin@adelaide.edu.au.

*D. Losic. E-mail: dusan.losic@adelaide.edu.au.

ORCID

Diana N. H. Tran: 0000-0002-4023-3373

Dusan Losic: 0000-0002-1930-072X

Notes

The authors declare no competing financial interest.

ACKNOWLEDGMENTS

The authors express their appreciation for the financial support of this study by the Australian Research Council Discovery Project DP1501001760 and Project IH 150100003. Mike J. McLaughlin and Roslyn Baird acknowledge the support of The Mosaic Company LLC. The authors thank Colin Rivers for assistance with cogranulation of fertilizers.

REFERENCES

(1) Azeem, B.; KuShaari, K.; Man, Z. B.; Basit, A.; Thanh, T. H. Review on materials & methods to produce controlled release coated urea fertilizer. *J. Controlled Release* **2014**, *181*, 11−21.

(2) Shaviv, A. Advances in controlled-release fertilizers. *Adv. Agron.* **2001**, *71*, 1−49.

(3) Palaios, J. J.; Fernández-Rossier, J. Prediction of hidden multiferroic order in graphene zigzag ribbons. *Phys. Rev. B: Condens. Matter Mater. Phys.* **2008**, *77*, 195428.

(4) Rehberg, B. E.; Hall, W. L. Fertilizer compositions and method of making such compositions. U.S. Patent US 5238480 A, 1993.

(5) Matejovic, I. Determination of carbon and nitrogen in samples of various soils by the dry combustion. *Commun. Soil Sci. Plant Anal.* **1997**, *28*, 1499−1511.

(6) Hignett, T. P. Physical and Chemical Properties of Fertilizers and Methods for their Determination. In *Fertilizer Manual*, Hignett, T. P., Ed. Springer: Dordrecht, The Netherlands, 1985; pp 284−316.

(7) Albadarin, A. B.; Lewis, T. D.; Walker, G. M. Granulated polyhalite fertilizer caking propensity. *Powder Technol.* **2017**, *308*, 193−199.

(8) Bröckel, U.; Wahl, M.; Kirsch, R.; Feise, H. J. Formation and Growth of Crystal Bridges in Bulk Solids. *Chem. Eng. Technol.* **2006**, *29*, 691−695.

(9) Rutland, D. W. Fertilizer caking: Mechanisms, influential factors, and methods of prevention. *Fert. Res.* **1991**, *30*, 99−114.

(10) Detroit, W. J. Lignosulfonate treated fertilizer particles. U.S. Patent US 4846871 A, 1989.

(11) Aylen, P. B.; Blyth, J. C. Particulate urea with finely divided inorganic material incorporated for hardness nonfriability and anti-caking. U.S.Patent US 5782951 A, 1998.

(12) Mark Stephen, R.; Tommy, C. D. Binding Agents Effect on Physical and Chemical Attributes of Nitrogen-Fortified Poultry Litter and Biosolids Granules. *Trans. ASABE* **2013**, *56* (5), 1695−1702.

(13) Allan, G. G.; Freepons, D. E.; Crews, G. M. Fertilizer compositions, processes of making them and processes of using them. U.S Patent US 4560400 A, 1985.

(14) Blouin, G. M. Production of high-strength, storage-stable particulate urea. U.S. Patent 4587358, 1986.

(15) Fleming, P. S. Sulfur encapsulation of fertilizers to provide controlled dissolution rates. U.S. Patent US 3576613 A, 1971.

(16) Heumann, H.; Hahn, H.; Hilt, W.; Liebing, H.; Schweppe, M. Method of preparing fertilizers with retarded nutrient release. U.S. Patent US 4142885 A, 1979.

(17) Lubkowski, K.; Smorowska, A.; Grzmil, B.; Kozłowska, A. Controlled-Release Fertilizer Prepared Using a Biodegradable Aliphatic Copolyester of Poly(butylene succinate) and Dimerized Fatty Acid. *J. Agric. Food Chem.* **2015**, *63*, 2597−2605.

(18) Mohd Ibrahim, K. R.; Eghbali Babadi, F.; Yunus, R. . Comparative performance of different urea coating materials for slow release. *Particuology* **2014**, *17*, 165−172.

(19) Zhu, Y.; Murali, S.; Cai, W.; Li, X.; Suk, J. W.; Potts, J. R.; Ruoff, R. S. Graphene and graphene oxide: Synthesis, properties, and applications. *Adv. Mater.* **2010**, *22*, 3906−3924.

(20) Lee, C.; Wei, X.; Kysar, J. W.; Hone, J. Measurement of the Elastic Properties and Intrinsic Strength of Monolayer Graphene. *Science* **2008**, *321*, 385−388.

(21) Sanchez, V. C.; Jachak, A.; Hurt, R. H.; Kane, A. B. Biological Interactions of Graphene-Family Nanomaterials: An Interdisciplinary Review. *Chem. Res. Toxicol.* **2012**, *25*, 15−34.

(22) Compton, O. C.; Nguyen, S. T. Graphene Oxide, Highly Reduced Graphene Oxide, and Graphene: Versatile Building Blocks for Carbon-Based Materials. *Small* **2010**, *6*, 711−723.

(23) Potts, J. R.; Dreyer, D. R.; Bielawski, C. W.; Ruoff, R. S. Graphene-based polymer nanocomposites. *Polymer* **2011**, *52*, 5−25.

(24) Rafiee, M. A.; Rafiee, J.; Wang, Z.; Song, H.; Yu, Z.-Z.; Koratkar, N. Enhanced Mechanical Properties of Nanocomposites at Low Graphene Content. *ACS Nano* **2009**, *3*, 3884−3890.

(25) Hwang, J.; Yoon, T.; Jin, S. H.; Lee, J.; Kim, T.-S.; Hong, S. H.; Jeon, S. Enhanced Mechanical Properties of Graphene/Copper Nanocomposites Using a Molecular-Level Mixing Process. *Adv. Mater.* **2013**, *25*, 6724−6729.

(26) Li, M.-X.; Xie, J.; Li, Y.-D.; Xu, H.-H. Reduced graphene oxide dispersed in copper matrix composites: Facile preparation and enhanced mechanical properties. *Phys. Status Solidi A* **2015**, *212*, 2154−2161.

(27) Walker, L. S.; Marotto, V. R.; Rafiee, M. A.; Koratkar, N.; Corral, E. L. Toughening in Graphene Ceramic Composites. *ACS Nano* **2011**, *5*, 3182−3190.

(28) Kuila, T.; Bose, S.; Hong, C. E.; Uddin, M. E.; Khanra, P.; Kim, N. H.; Lee, J. H. Preparation of functionalized graphene/linear low density polyethylene composites by a solution mixing method. *Carbon* **2011**, *49*, 1033−1037.

(29) Dreyer, D. R.; Park, S.; Bielawski, C. W.; Ruoff, R. S. The chemistry of graphene oxide. *Chem. Soc. Rev.* **2010**, *39*, 228−240.

(30) Lv, S.; Ma, Y.; Qiu, C.; Sun, T.; Liu, J.; Zhou, Q. Effect of graphene oxide nanosheets of microstructure and mechanical properties of cement composites. *Constr. Build. Mater.* **2013**, *49*, 121−127.

(31) Zhang, X.; An, Y.; Han, J.; Han, W.; Zhao, G.; Jin, X. Graphene nanosheet reinforced ZrB2-SiC ceramic composite by thermal reduction of graphene oxide. *RSC Adv.* **2015**, *5*, 47060−47065.

(32) Lou, Y.; Liu, G.; Liu, S.; Shen, J.; Jin, W. A facile way to prepare ceramic-supported graphene oxide composite membrane via silane-graft modification. *Appl. Surf. Sci.* **2014**, *307*, 631−637.

(33) Chuah, S.; Pan, Z.; Sanjayan, J. G.; Wang, C. M.; Duan, W. H. Nano reinforced cement and concrete composites and new perspective from graphene oxide. *Constr. Build. Mater.* **2014**, *73*, 113−124.

(34) Sharma, S.; Kothiyal, N. C. Influence of graphene oxide as dispersed phase in cement mortar matrix in defining the crystal patterns of cement hydrates and its effect on mechanical, micro-structural and crystallization properties. *RSC Adv.* **2015**, *5*, 52642−52657.

(35) Wang, B.; Jiang, R.; Wu, Z. Investigation of the Mechanical Properties and Microstructure of Graphene Nanoplatelet-Cement Composite. *Nanomaterials* **2016**, *6*, 200.

(36) Qin, H.; Wei, W.; Hang Hu, Y. Synergistic effect of graphene-oxide-doping and microwave-curing on mechanical strength of cement. *J. Phys. Chem. Solids* **2017**, *103*, 67−72.

DOI: 10.1021/acssuschemeng.7b03655
ACS Sustainable Chem. Eng. 2018, 6, 1299−1309

(37) Pan, Z.; He, L.; Qiu, L.; Korayem, A. H.; Li, G.; Zhu, J. W.; Collins, F.; Li, D.; Duan, W. H.; Wang, M. C. Mechanical properties and microstructure of a graphene oxide−cement composite. *Cem. Concr. Compos.* **2015**, *58*, 140−147.

(38) Marcano, D. C.; Kosynkin, D. V.; Berlin, J. M.; Sinitskii, A.; Sun, Z.; Slesarev, A.; Alemany, L. B.; Lu, W.; Tour, J. M. Improved Synthesis of Graphene Oxide. *ACS Nano* **2010**, *4*, 4806−4814.

(39) Zhou, Y.; Bao, Q.; Tang, L. A. L.; Zhong, Y.; Loh, K. P. Hydrothermal Dehydration for the "Green" Reduction of Exfoliated Graphene Oxide to Graphene and Demonstration of Tunable Optical Limiting Properties. *Chem. Mater.* **2009**, *21*, 2950−2956.

(40) *Fertilizer manual/editors, United Nations Industrial Development Organization (UNIDO) and International Fertilizer Development Center (IFDC)*; Kluwer Academic Publishers: Sold and distributed by IFDC: Dordrecht, The Netherlands; Muscle Shoals, AL, 1998.

(41) Lafci, A.; Gürüz, K.; Yücel, H. Investigation of factors affecting caking tendency of calcium ammonium nitrate fertilizer and coating experiments. *Fert. Res.* **1988**, *18*, 63−70.

(42) Degryse, F.; McLaughlin, M. J. Phosphorus Diffusion from Fertilizer: Visualization, Chemical Measurements, and Modeling. *Soil Sci. Soc. Am. J.* **2014**, *78*, 832−842.

(43) Moon, I. K.; Lee, J.; Ruoff, R. S.; Lee, H. Reduced graphene oxide by chemical graphitization. *Nat. Commun.* **2010**, *1* (6), 73.

(44) Salavagione, H. J.; Martinez, G.; Gomez, M. A. Synthesis of poly(vinyl alcohol)/reduced graphite oxide nanocomposites with improved thermal and electrical properties. *J. Mater. Chem.* **2009**, *19*, 5027−5032.

(45) Tran, D. N. H.; Kabiri, S.; Losic, D. A green approach for the reduction of graphene oxide nanosheets using non-aromatic amino acids. *Carbon* **2014**, *76*, 193−202.

(46) Frost, R. L.; Scholz, R.; López, A.; Xi, Y. A vibrational spectroscopic study of the phosphate mineral whiteite CaMn+ +Mg2Al2(PO4)4(OH)2·8(H2O). *Spectrochim. Acta, Part A* **2014**, *124*, 243−248.

(47) Kabiri, S.; Tran, D. N. H.; Cole, M. A.; Losic, D. Functionalized three-dimensional (3D) graphene composite for high efficiency removal of mercury. *Environ. Sci.: Water Res. Technol.* **2016**, *2*, 390−402.

(48) Lu, Z.; Hou, D.; Meng, L.; Sun, G.; Lu, C.; Li, Z. Mechanism of cement paste reinforced by graphene oxide/carbon nanotubes composites with enhanced mechanical properties. *RSC Adv.* **2015**, *5*, 100598−100605.

(49) Liu, L.; Zhang, J.; Zhao, J.; Liu, F. Mechanical properties of graphene oxides. *Nanoscale* **2012**, *4*, 5910−5916.

(50) Chen, C.; Rosenblatt, S.; Bolotin, K. I.; Kalb, W.; Kim, P.; Kymissis, I.; Stormer, H. L.; Heinz, T. F.; Hone, J. Performance of monolayer graphene nanomechanical resonators with electrical readout. *Nat. Nanotechnol.* **2009**, *4*, 861−867.

(51) Dikin, D. A.; Stankovich, S.; Zimney, E. J.; Piner, R. D.; Dommett, G. H. B.; Evmenenko, G.; Nguyen, S. T.; Ruoff, R. S. Preparation and characterization of graphene oxide paper. *Nature* **2007**, *448*, 457−460.

(52) Chen, H.; Müller, M. B.; Gilmore, K. J.; Wallace, G. G.; Li, D. Mechanically Strong, Electrically Conductive, and Biocompatible Graphene Paper. *Adv. Mater.* **2008**, *20*, 3557−3561.

(53) Chen, C.; Yang, Q.-H.; Yang, Y.; Lv, W.; Wen, Y.; Hou, P.-X.; Wang, M.; Cheng, H.-M. Self-Assembled Free-Standing Graphite Oxide Membrane. *Adv. Mater.* **2009**, *21*, 3007−3011.

(54) Zandiatashbar, A.; Lee, G.-H.; An, S. J.; Lee, S.; Mathew, N.; Terrones, M.; Hayashi, T.; Picu, C. R.; Hone, J.; Koratkar, N. Effect of defects on the intrinsic strength and stiffness of graphene. *Nat. Commun.* **2014**, *5*, 3186.

(55) Suk, J. W.; Piner, R. D.; An, J.; Ruoff, R. S. Mechanical Properties of Monolayer Graphene Oxide. *ACS Nano* **2010**, *4*, 6557−6564.

(56) Park, S.; Ruoff, R. S. Chemical methods for the production of graphenes. *Nat. Nanotechnol.* **2009**, *4*, 217−224.

(57) Perreault, F.; Fonseca de Faria, A.; Elimelech, M. Environmental applications of graphene-based nanomaterials. *Chem. Soc. Rev.* **2015**, *44*, 5861−5896.

(58) Hikita, T.; Chubachi, Y.; Ikeda, T. X-Ray Study of the Phase Transition in K2Mn2(SO4)3. *J. Phys. Soc. Jpn.* **1978**, *44*, 525−528.

(59) Wittenbrook, L. S.; Scheiderer, E. L. Coated controlled-release product. U.S. Patent US 4082533 A, 1978.

(60) Ferrari, A. C.; Bonaccorso, F.; Fal'ko, V.; Novoselov, K. S.; Roche, S.; Boggild, P.; Borini, S.; Koppens, F. H. L.; Palermo, V.; Pugno, N.; Garrido, J. A.; Sordan, R.; Bianco, A.; Ballerini, L.; Prato, M.; Lidorikis, E.; Kivioja, J.; Marinelli, C.; Ryhanen, T.; Morpurgo, A.; Coleman, J. N.; Nicolosi, V.; Colombo, L.; Fert, A.; Garcia-Hernandez, M.; Bachtold, A.; Schneider, G. F.; Guinea, F.; Dekker, C.; Barbone, M.; Sun, Z.; Galiotis, C.; Grigorenko, A. N.; Konstantatos, G.; Kis, A.; Katsnelson, M.; Vandersypen, L.; Loiseau, A.; Morandi, V.; Neumaier, D.; Treossi, E.; Pellegrini, V.; Polini, M.; Tredicucci, A.; Williams, G. M.; Hee Hong, B.; Ahn, J.-H.; Min Kim, J.; Zirath, H.; van Wees, B. J.; van der Zant, H.; Occhipinti, L.; Di Matteo, A.; Kinloch, I. A.; Seyller, T.; Quesnel, E.; Feng, X.; Teo, K.; Rupesinghe, N.; Hakonen, P.; Neil, S. R. T.; Tannock, Q.; Lofwander, T.; Kinaret, J. Science and technology roadmap for graphene, related two-dimensional crystals, and hybrid systems. *Nanoscale* **2015**, *7*, 4598−4810.

(61) Montagner, A.; Bosi, S.; Tenori, E.; Bidussi, M.; Alshatwi, A. A.; Tretiach, M.; Prato, M.; Syrgiannis, Z. Ecotoxicological effects of graphene-based materials. *2D Mater.* **2017**, *4*, 012001.

(62) Lalwani, G.; D'Agati, M.; Khan, A. M.; Sitharaman, B. Toxicology of graphene-based nanomaterials. *Adv. Drug Delivery Rev.* **2016**, *105*, 109−144.

(63) Bianco, A. Graphene: Safe or Toxic? The Two Faces of the Medal. *Angew. Chem., Int. Ed.* **2013**, *52*, 4986−4997.

(64) Lalwani, G.; Xing, W.; Sitharaman, B. Enzymatic Degradation of Oxidized and Reduced Graphene Nanoribbons by Lignin Peroxidase. *J. Mater. Chem. B* **2014**, *2*, 6354−6362.

(65) Kotchey, G. P.; Zhao, Y.; Kagan, V. E.; Star, A. Peroxidase-mediated biodegradation of carbon nanotubes in vitro and in vivo. *Adv. Drug Delivery Rev.* **2013**, *65*, 1921.

(66) Xing, W.; Lalwani, G.; Rusakova, I.; Sitharaman, B. Degradation of Graphene by Hydrogen Peroxide. *Part. Part. Syst. Char.* **2014**, *31*, 745−750.

DOI: 10.1021/acssuschemeng.7b03655
ACS Sustainable Chem. Eng. 2018, 6, 1299−1309

Supporting information

Co-granulation of low rates of graphene and graphene oxide with macronutrient fertilizers remarkably improves their physical properties

*Shervin Kabiri[1], Roslyn Baird[2], Diana N.H. Tran[1], Ivan Andelkovic[2], Mike J. McLaughlin *[2] and Dusan Losic*[1]*

[1]School of Chemical Engineering, Engineering North Building, The University of Adelaide, Adelaide, SA 5005, Australia

[2]Fertilizer Technology Research Centre, School of Agriculture, Food and Wine, The University of Adelaide, Waite Campus, PMB1, Glen Osmond, SA 5064, Australia

Total number of pages of supporting information: 11

Total number of supporting figures: 5

Total number of supporting tables: 1

Materials. Natural graphite rocks (Uley, Eyre Peninsula, South Australia, Australia) was supplied from a local mining site. Monoammonuim phosphate (MAP) was provided by The Mosaic Company LLC (Minnesota, USA). Potassium permanganate (KMnO4, Sigma-Aldrich), 98% sulfuric acid (H_2SO_4, Chem-Supply), phosphoric acid (H_3PO_4, Chem-Supply), 30% hydrogen peroxide (H_2O_2, Chem-Supply) and 35% hydrochloric acid (HCl, Chem-Supply) were used directly without further processing. High-purity milli-Q water (18.2 MΩ·cm at 25 °C, pH of 5.6) was used throughout the study, unless otherwise stated.

Characterization. The MAP-GN and MAP-GO fertilizers were analysed by scanning electron microscopy (FE-SEM, Quanta 450, FEI, USA) combined with an integrated energy-dispersive X-Ray analysis (EDAX) Genesis EDX spectrometer system for morphological and elemental composition analysis. Mineralogical characterization of the final product was investigated using X-ray diffraction (600 Miniflex, Rigaco, Japan). Fourier transform infrared (FTIR) spectroscopy (Nicolet 6700 Thermo Fisher) in transmittance mode and range 500-4000 cm^{-1} was used to identify the functional groups of GO and the effect of MAP on GO sheets during granulation and oven drying. The vibrational characteristics of GN, GO, MAP, MAP-GN and MAP-GO were analysed by Raman spectroscopy (LabRAM HR Evolution, Horiba Jvon Yvon Technology, Japan) using a 532 nm laser. Thermal decomposition of GO, MAP-GO (died in ambient and) MAP-GO (dried in the oven) were performed using a thermal gravimetric analyser (TGA, Q500, TA Instruments, USA) under air atmosphere where the samples were heated to 900°C at a heating rate of 10 °C min^{-1}. The size distribution of both GN and GO was determined using the Mastersizer X(Malvern Instruments, U.K.).

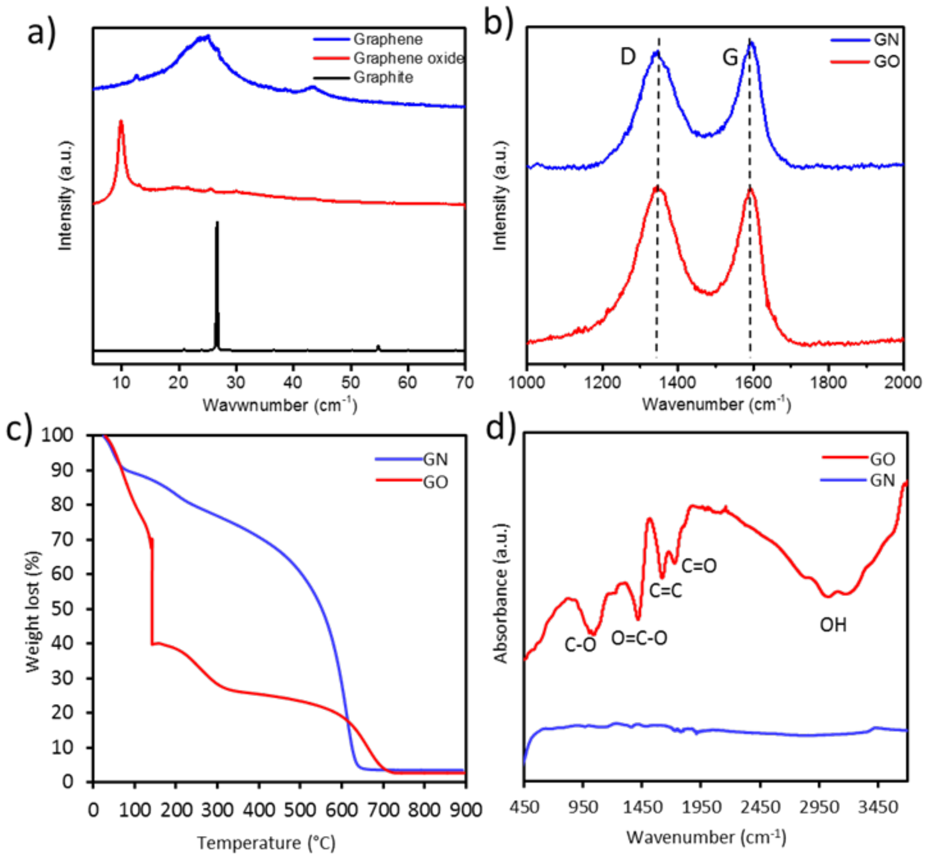

Figure S1. a) XRD, b)Raman, c)TGA and d)FTIR characterization of graphene oxide (GO) and thermally reduced graphene (GN).

The XRD pattern of pristine graphite (Figure a) shows diffraction peak at ~2θ= 26° corresponding to the diffraction patterns of graphite. The sharp peak at 26° disappears at XRD pattern of GO and a new peaks form at 2θ= 9.9° with lower intensity compare to the graphitic peak. These changes are related to the heterogeneous nature of the oxidized graphite compromised of both sp^2 domains from graphite and sp^3 domains from oxidized graphite. When graphene oxide reduced to graphene by hydrothermal reduction the intensity of peak at ~2θ= 26°becomes higher and the peaks due to graphene oxide disappear. However, the peak formed at ~2θ= 26° for reduced graphene oxide is broader compare to graphite which could be related to the presence of some oxygen functional groups on the reduced graphene oxide sheets. The XRD results of graphite, GO and reduced graphene oxide samples are in good agreement with published reports available in the literatures.[1-3]

Raman spectroscopy is a very useful method to characterize the reduction of GO (Figure b). For all carbonaceous materials, both D and G bands are the predominant features in the Raman spectra; they are represented at around 1343 and 1589 cm^{-1}, 1346 and 1596 cm^{-1}, respectively for GO and GN. The G bands corresponds to the first-order scattering of the E_{2g} mode at the Brillouin zone, indicating the graphitic structure. The decrease in the intensity of the D to G band on GN also represents quantity ratio of sp^3 hybridized carbon and sp^2 hybridized carbon, the decrease in the intensity of D to G band means the increase of sp^2 hybridized and decrease of sp^3 hybridized in GN and reduction of graphene oxide. [4-7]

Furthermore, TGA analysis conducted to characterize GO and GN. As shown in (Figure c) GO is thermally unstable and starts to loss mass upon heating and the major weigh loss happens at ~200°C due to the pyrolysis of the oxygen functional groups on the surface of GO. The thermal decomposition of GO is accompanied by a vigorous release of gas, large volume expansion and a large mass lose. On the other hand, the removal of the oxygen functional groups during the thermal reduction of GO results in the thermal stability of the GN. Apart from a slight mass loss below 100°Cdue to the loss of adsorbed water, no significant mass loss is detected when GN is heated up 600°C. [8]

The FTIR spectra of GO (Figure d) presents the following absorbance bands, O–H stretching vibrations (3410 cm^{-1}), aromatic C=C (1620 cm^{-1}), epoxy and alkoxy/alkoxide C-O (1050 and 1220cm^{-1}), C=O stretching of the COOH (1730 cm^{-1}) and carboxy C-O (1420 cm^{-1}). However, all those peaks dispread in the FTIR spectra of GN due to the reduction of GN during the thermal treatment. [3, 7]

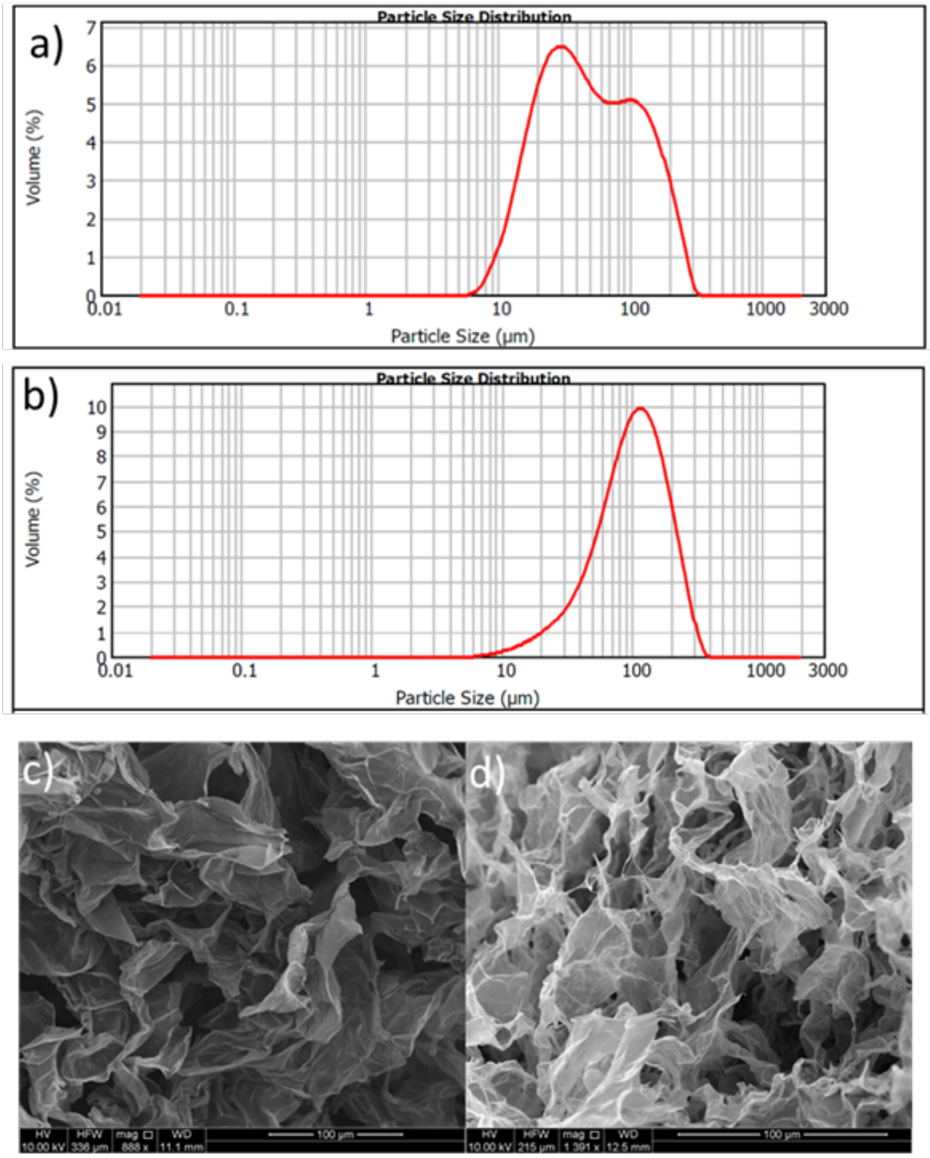

Figure S2. Particle size of a) graphene, b) graphene oxide, SEM images of freeze dried c) graphene and d) graphene oxide.

Figure a shows the particle size of GN sheets ~158 µm while the particle size of GO sheets are ~206µm. SEM images of freeze dried GN and GO sheets confirmed micron size of our particles.

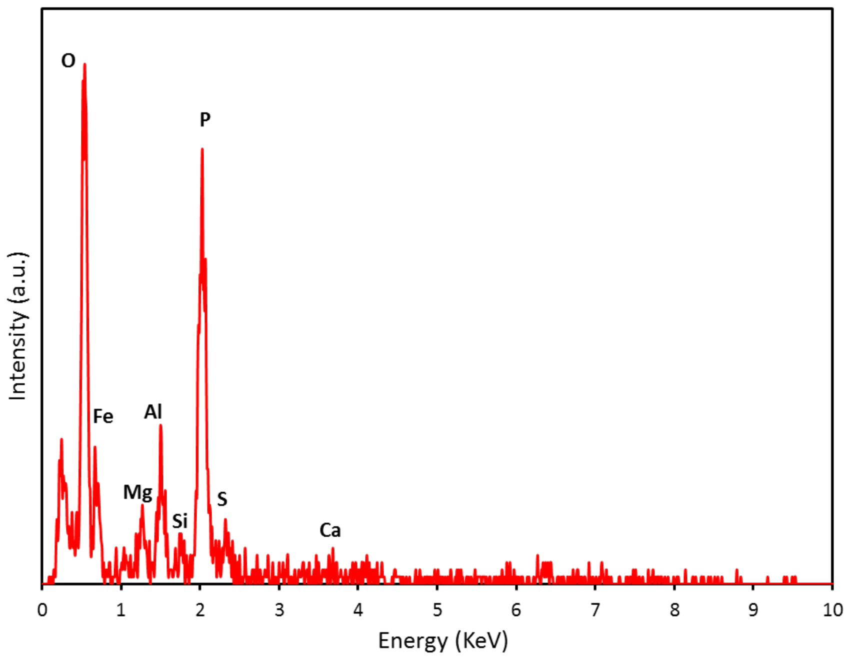

Figure S3. SEM-EDAX analysis of Monoammonium phosphate (MAP).

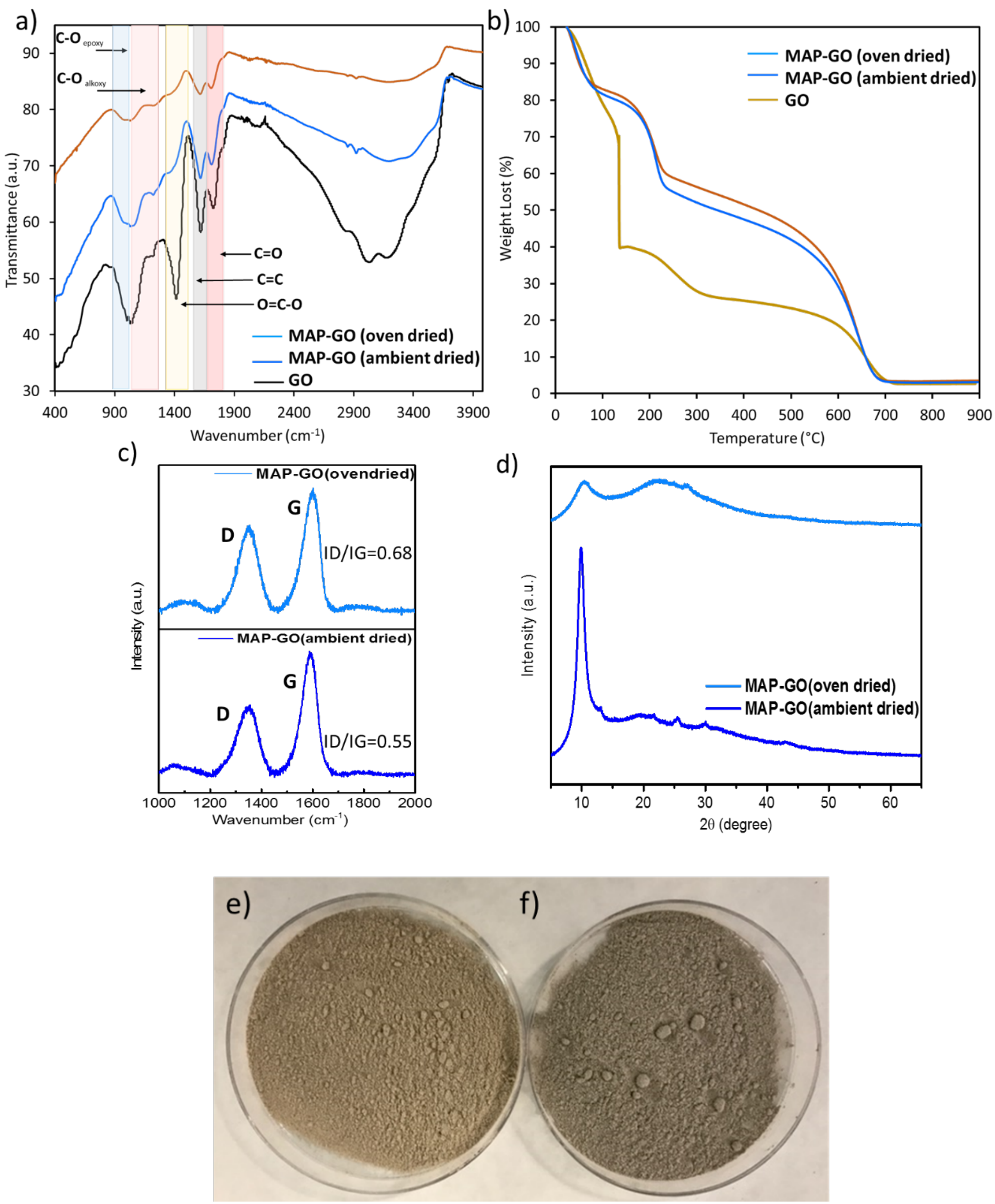

Figure S4. a) FTIR plots of graphene oxide (GO), GO extracted after washing of monoammonium phosphate (MAP-GO samples), b) TGA curves of pure GO, and GO from MAP-GO dried at ambient temperatures and in the oven, c) Raman spectra, d) XRD patterns of graphene oxide (GO) extracted from MAP-GO samples (dried under ambient conditions and in the oven) and photos of e) monoammonium phosphate-graphene oxide dried in ambient and f) dried in the oven at 50°C.

MAP-GO granules dried in the oven and at ambient conditions were washed with acid and water to remove the MAP matrix from the GO sheets before collecting FTIR spectra (Figure a). For GO, the characteristic peaks appear for O–H stretching vibrations (3410 cm^{-1}), aromatic C=C (1620 cm^{-1}), epoxy and alkoxy/alkoxide C-O (1050 and 1220cm^{-1}), C=O stretching of the COOH (1730 cm^{-1}) and carboxyl C-O (1420 cm^{-1}).[9, 10] FTIR for GO from both oven and ambient dried MAP-GO granules decreased the intensity of the oxygen functional group peaks, which was more significant in the case of the oven dried MAP-GO granules. The peaks related to the alkoxy/alkoxide C-O and O-H stretching were very weak in the case of the oven dried MAP-GO granules compared to pure GO. The results from the FTIR data and colour changes in the appearance of the oven dried MAP-GO granules from light brown to dark brown (e and f) confirmed the reduction of GO, which consequently increased the hardness of the oven dried MAP-GO granules compared to those dried under ambient conditions due to the increased mechanical strength of reduced GO.[11, 12]

TGA analysis of pure GO and GO from the ambient/oven dried MAP-GO was conducted to further investigate the effect of heating on the physical property of MAP-GO. The mass losses for all formulations below 100°C can be ascribed to the loss of water adsorbed on the interlayer spaces of GO sheets in each sample (Figure 6). Above 100°C, pure GO and GO from ambient/oven dried MAP-GO showed two degradation steps. The first degradation step initiated at 120°C for pure GO and at 175°C for GO from ambient/oven dried MAP-GO, due to the loss of hydroxyl and epoxy functional groups.[13-15] Interestingly, in the first step of the thermal decomposition process GO samples separated from ambient/oven dried MAP-GO lost only 45% and 40% of their weight, respectively, compared to 75% for pure GO. The decomposition step involves the pyrolysis of carboxylic functional group and burning of aromatic carbons.[12] Almost all samples showed the same amount of weight loss at the end of the measurement, but GO from both the ambient and oven dried MAP-GO samples was thermally more stable below 600°C compared to pure GO due to the partial removal of oxygen functional groups.[14] In addition, GO from the oven dried MAP-GO sample was slightly more stable below 600°C compared to the ambient dried sample indicating greater reduction of the sample.

The Raman spectra of GO extracted from the co-granulated products before and after drying showed a slight increase in the intensity ratio of the D band to the G band (I_D/I_G), from 0.55 to 0.68 due to drying, indicating the formation of more sp^2 regions in the dried samples (Figure c).[16] Furthermore, the XRD pattern of GO extracted after washing of ambient dried MAP-GO samples showed a peak at $2\theta=9.9°$ representing the crystallinity of the GO structure as discussed previously (Figure d). However, the XRD pattern of the GO from the oven dried MAP-GO sample shows that the intensity peak at $2\theta=9.9°$ has decreased and a new broad peak has appeared at $\sim 2\theta=24°$. The presence of this broad peak could be related to the presence of more graphitic crystallinity and a mild reduction of GO during the drying in the oven.[1, 17]

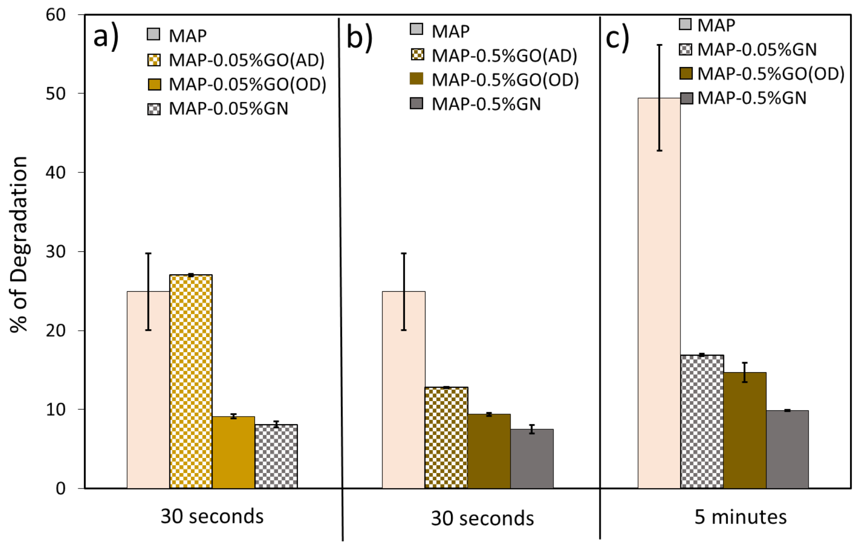

Figure S5. Degradation of a) pure monoammonium phosphate (MAP) granules, MAP granules treated with 0.05% graphene oxide (MAP-0.05%GO) dried in the ambient and oven, and 0.05% of graphene (MAP-0.05%GN) for 30 seconds, b) MAP granules, MAP-0.5%GN dried in the ambient and oven after granulation, and MAP-0.5%GN for 30 seconds and c) MAP, 0.5% of MAP-0.5%GO dried in the oven after granulation, MAP-0.05%GN and MAP-0.5%GN for 5 minutes.

MAP-GO samples dried in the ambient condition and oven were analysed for abrasion and those formulation with highest and lowest amount of GO (0.05% and 0.5%) were used for test and results were compared with MAP-GN and pure MAP samples. The results depicted in Figure S4(a &b) show that the MAP-GO granules dried in ambient with 0.05% GO created more fine particles compared to the oven dried MAP-GO and MAP-GN granules with similar amounts of the graphene-based materials when abraded for 30 seconds. Surprisingly, MAP-0.05%GO dried outside abraded more than pure MAP showing it was ineffective for use in MAP granules. However, increasing the amount of GO from 0.05% to 0.5% decreased the amount of dust produced during the abrasion test from the outside dried MAP-GO granules from 27.1% to 12.7%. MAP-GN granules containing either 0.05% or 0.5% of GN created slightly less dust compare to the oven dried MAP-GO with the same dosage rates. To study the effect of longer shaking time on the abrasion of granules, three formulations which represented higher crushing strength and less degradation at 30 seconds were chosen and abraded for 5 minutes. The results illustrated in Figure S4c show that 50 % of the MAP was abraded as fine particles during the abrasion test for 5 minutes while around 15% of the MAP-0.05%GN and oven dried MAP-0.5%GO granules were abraded as fines, and less than 10% of MAP-0.5%GN turned to fine particles. The results obtained from the abrasion test showed the effectiveness of graphene based materials specifically graphene on diminishing dust formation during the handling of MAP fertilizers.

Table S1. Selected physical and chemical properties of the soil used in this study. The soil was collected from the top layer of (0-10 cm), air dried and sieved to < 2mm before use. ([a] pH in 0.01 M $CaCl_2$ (L:S 5l Kg^{-1}), [b] organic C, pressure calcimeter method ,[d] CEC measured with 1 M ammonium acetate at pH 7.0 , [e] particle size analysis with the pipette method, [f] Oxalate-extractable Mn and Fe concentrations [18] and Total Zn concentration determined by aqua regia digestion).

Soil (location)	Monarto
pH (H_2O)	7.9
pH($CaCl_2$)[a]	7.0
OC(%)[b]	1.0
CaCO3(%)[c]	<0.2
CEC(cmolekg^{-1})[d]	8.2
Clay(%)[e]	8.2
Slit(%)[e]	68.5
Sand(%)[e]	7.12
Mn_{oxal}(mgkg^{-1})[f]	69.7
Fe_{oxal}(mgkg^{-1})[f]	325
Zn_{tot} (mgkg^{-1})[g]	0.6

REFERENCES

1. Jeong, H. K.; Jin, M. H.; So, K. P.; Lim, S. C.; Lee, Y. H. Tailoring the characteristics of graphite oxides by different oxidation times. *Journal of Physics D: Applied Physics* 2009, 42, 065418.
2. Wang, G.; Sun, X.; Liu, C.; Lian, J. Tailoring oxidation degrees of graphene oxide by simple chemical reactions. *Applied Physics Letters* 2011, 99, 053114.
3. Marcano, D. C.; Kosynkin, D. V.; Berlin, J. M.; Sinitskii, A.; Sun, Z.; Slesarev, A.; Alemany, L. B.; Lu, W.; Tour, J. M. Improved synthesis of graphene oxide. *ACS Nano* 2010, 4, 4806-4814.
4. Mei, X.; Meng, X.; Wu, F. Hydrothermal method for the production of reduced graphene oxide. *Physica E: Low-dimensional Systems and Nanostructures* 2015, 68, 81-86.
5. Kabiri, S.; Tran, D. N. H.; Cole, M. A.; Losic, D. Functionalized three-dimensional (3D) graphene composite for high efficiency removal of mercury. *Environmental Science: Water Research & Technology* 2016, 2, 390-402.
6. Tran, D. N. H.; Kabiri, S.; Wang, L.; Losic, D. Engineered graphene-nanoparticle aerogel composites for efficient removal of phosphate from water. *Journal of Materials Chemistry A* 2015, 3, 6844-6852.
7. Kabiri, S.; Tran, D. N. H.; Azari, S.; Losic, D. Graphene-Diatom silica aerogels for efficient removal of mercury ions from water. *ACS Applied Materials & Interfaces* 2015, 7, 11815-11823.
8. Stankovich, S.; Dikin, D. A.; Piner, R. D.; Kohlhaas, K. A.; Kleinhammes, A.; Jia, Y.; Wu, Y.; Nguyen, S. T.; Ruoff, R. S. Synthesis of graphene-based nanosheets via chemical reduction of exfoliated graphite oxide. *Carbon* 2007, 45, 1558-1565.
9. Kabiri, S.; Tran, D. N. H.; Altalhi, T.; Losic, D. Outstanding adsorption performance of graphene–carbon nanotube aerogels for continuous oil removal. *Carbon* 2014, 80, 523-533.
10. Park, S.; Lee, K.-S.; Bozoklu, G.; Cai, W.; Nguyen, S. T.; Ruoff, R. S. Graphene oxide papers modified by divalent ions—Enhancing mechanical properties via chemical cross-linking. *ACS Nano* 2008, 2, 572-578.
11. Khan, M.; Al-Marri, A. H.; Khan, M.; Shaik, M. R.; Mohri, N.; Adil, S. F.; Kuniyil, M.; Alkhathlan, H. Z.; Al-Warthan, A.; Tremel, W.; Tahir, M. N.; Siddiqui, M. R. H. Green approach for the effective reduction of graphene oxide using salvadora persica L. root (Miswak) extract. *Nanoscale Research Letters* 2015, 10, 281.
12. Jana, M.; Saha, S.; Khanra, P.; Murmu, N. C.; Srivastava, S. K.; Kuila, T.; Lee, J. H. Bio-reduction of graphene oxide using drained water from soaked mung beans (Phaseolus aureus L.) and its application as energy storage electrode material. *Materials Science and Engineering: B* 2014, 186, 33-40.
13. Kuila, T.; Bose, S.; Khanra, P.; Mishra, A. K.; Kim, N. H.; Lee, J. H. A green approach for the reduction of graphene oxide by wild carrot root. *Carbon* 2012, 50, 914-921.
14. Liu, H.; Kuila, T.; Kim, N. H.; Ku, B.-C.; Lee, J. H. In situ synthesis of the reduced graphene oxide-polyethyleneimine composite and its gas barrier properties. *Journal of Materials Chemistry A* 2013, 1, 3739-3746.
15. Khanra, P.; Kuila, T.; Kim, N. H.; Bae, S. H.; Yu, D. S.; Lee, J. H. Simultaneous bio-functionalization and reduction of graphene oxide by baker's yeast. *Chemical Engineering Journal* 2012, 183, 526-533.
16. Ferrari, A. C.; Robertson, J. Interpretation of Raman spectra of disordered and amorphous carbon. *Physical Review B* 2000, 61, 14095-14107.
17. Krishnamoorthy, K.; Veerapandian, M.; Yun, K.; Kim, S. J. The chemical and structural analysis of graphene oxide with different degrees of oxidation. *Carbon* 2013, 53, 38-49.
18. Rayment, G. E. *Australian laboratory handbook of soil and water chemical methods / G.E. Rayment and F.R. Higginson*. Inkata Press: Melbourne, 1992.

Chapter 6

Revealing the dependence of concentration and physicochemical properties of graphene on the crushing strength of co-granulated fertilizers

This section is included in the thesis as it appears as a manuscript ready to be submitted by **Shervin Kabiri,** Diana N.H. Tran, Roslyn Baird, Mike J. McLaughlin and Dusan Losic, "Revealing the dependence of concentration and physicochemical properties of graphene on the crushing strength of co-granulated fertilizers", ***Journal of Carbon***, (2018).

Statement of Authorship

Title of Paper	Revealing the dependence of concentration and physicochemical properties of graphene on the crushing strength of co-granulated fertilizers	
Publication Status	☐ Published ☑ Submitted for Publication	☐ Accepted for Publication ☐ Unpublished and Unsubmitted w ork w ritten in manuscript style
Publication Details	carbon	

Principal Author

Name of Principal Author (Candidate)	Shervin Kabiri		
Contribution to the Paper	Under the supervision of Dusan Losic, Michael McLaughlin and Diana Tran, I developed, designed and conducted the experiments, interpreted and processed the data and wrote the manuscript for submission.		
Overall percentage (%)	85		
Certification:	This paper reports on original research I conducted during the period of my Higher Degree by Research candidature and is not subject to any obligations or contractual agreements with a third party that would constrain its inclusion in this thesis. I am the primary author of this paper.		
Signature		Date	22/06/2018

Co-Author Contributions

By signing the Statement of Authorship, each author certifies that:

i. the candidate's stated contribution to the publication is accurate (as detailed above);

ii. permission is granted for the candidate in include the publication in the thesis; and

iii. the sum of all co-author contributions is equal to 100% less the candidate's stated contribution.

Name of Co-Author	Roslyn Baird		
Contribution to the Paper	I helped Shervin Kabiri (candidate) with interpreting experimental results and improving the manuscript for submission. I give consent for Shervin Kabiri to present this paper for examination towards the Doctorate of philosophy.		
Signature		Date	22/06/2018

Name of Co-Author	Diana N.H. Tran		
Contribution to the Paper	I acted as the secondary supervisor for Shervin Kabiri and helped her to design the experiments and improve the final drafts of the manuscript for submission. I give consent for Shervin Kabiri to present this paper for examination towards the Doctorate of philosophy.		
Signature		Date	22/06/2018

Name of Co-Author	Mike J. McLaughlin		
Contribution to the Paper	I acted as the secondary supervisor for Shervin Kabiri and aided in design and development of experiments and evaluation of manuscript for submission. I give consent for Shervin Kabiri to present this paper for examination towards the Doctorate of philosophy.		
Signature		Date	22/06/2018

Name of Co-Author	Dusan Losic		
Contribution to the Paper	I acted as the primary supervisor for Shervin Kabiri and aided in design and development of experiments and evaluation of manuscript for submission. I give consent for Shervin Kabiri to present this paper for examination towards the Doctorate of philosophy.		
Signature		Date	22/06/2018

Revealing the dependence of concentration and physicochemical properties of graphene on the crushing strength of co-granulated fertilizers

Shervin Kabiri [ǂ], *Diana N.H. Tran* [ǂ], *Roslyn Baird* [‡], *Mike J. McLaughlin** [‡] *and Dusan Losic** [ǂ]

[ǂ] School of Chemical Engineering, Engineering North Building, The University of Adelaide, Adelaide, SA 5005, Australia

[‡] Fertilizer Technology Research Centre, School of Agriculture, Food and Wine, The University of Adelaide, Waite Campus, PMB1, Glen Osmond, SA 5064, Australia

Keywords: Graphene, Fertilizers, Crushing strength, Reinforcement.

ABSTRACT

Graphene has the potential to act as a high-performance reinforcement for different composites. This paper provides a comprehensive study of the influence of graphene (GN) concentration (0.05 to 1% w/w) on the crushing strength of two fertilizer granules, monoammonium phosphate (MAP) and diammonium phosphate (DAP) with different initial hardness. The effect of different physicochemical properties of GN, such as method of preparation, particle size, specific surface area (SSA) and surface functionalization on the crushing strength of the fertilizer granules was investigated. The results show differences in concentration dependence, with the optimum concentration of 0.5% GN for MAP and 0.05% for DAP increasing the crushing strength of MAP and DAP granules by 1680 % and 67.3%, respectively, but beyond this concentration the crushing strength decreased. Results also showed that the crushing strength of granules depend on the method of GN production and their SSA, while GN samples with a high degree of reduction and SSA were more effective than others. Furthermore, GN samples functionalized with iron nanoparticles (NPs) enhanced the physical properties of co-granulated fertilizers due to the synergistic effects of iron NPs and two dimensional (2D) GN sheets. These results show the advantages of GN in enhancing the physical properties of both MAP and DAP granules due to the high mechanical strength of GN sheets and their high SSA. However, differences in the degree of reduction of GN, the SSA and the hardness of initial fertilizer can influence the crushing strength of the final product.

INTRODUCTION

The ever-increasing World population, in addition to soil degradation and climate change are having unfavourable effects on food security as well as food nutritional quality and availability.[1, 2] Global demand for food production is anticipated to increase by 53% more than current output by 2050 to satisfy the world demand, but the land used for agriculture has dropped from 0.36 ha to 0.2 ha per person in last 50 years.[1, 3] Additionally, rapid global warming due to the consumption of hydrocarbon fuels and parallel green gas emission are driving force in the replacement of those fuels with renewable sources such as biofuels.[4] This will complicate the future demand on agriculture due to the providing of feedstock for a potentially huge biofuels market while there is a need to enhance the crop production for growing population.[5] Therefore, crops yield per unit area needs to be increased by applying more fertilizer because of their important role in nutrient delivery and enhancing crop yield.[1] The amount of nitrogen, phosphorous and potash fertilizers were required in 2014 were, 110.9, 41.9 and 31.9 millions of tonnes, respectively. It is expected that this demand enhances by 6.5% for nitrogen, 8.7% for phosphorous and 10.5% for potash fertilizers by 2019.[6] Therefore, more fertilizer will be needed to transport globally which raise the challenges of maintaining their quality. One of the greatest challenges of fertilizer manufactures and farmers is dust formation of fertilizers during their handling and transportation, as fertilizer with less mechanical strength tend to break and form dust which can pose safety, health, environment and economic problems.[7]

Solid fertilizers are produced to a particle size distribution suitable for farm spreading and need to be robust for handling without degrading to produce dust. Fertiliser granules are manufactured in most cases by granulation methods or compaction of finer particles and granules being more spherical are suitable for handling.[8] Fertilizer granules are also required to have sufficient mechanical hardness to withstand normal handling without fracture. Hardness can be characterized in three different ways by measuring the granules: (i) crushing strength; (ii) resistance to abrasion; and (iii) impact resistance. A good resistance to one type of these mechanical actions is a reasonable indication of the overall mechanical strength of the granule.[9] Different attempts have been made to control or reduce dust formation of fertilizer during their handling or storage such as spraying mineral oils, wax or petroleum residues onto the fertilizer.[10] Another proposed method to control dust included mixing a solution containing binding materials such as carbohydrates, polymers, surfactants, molasses, gypsum, saccharides, starch, glycerine and even water with fertilizer.[11] Within the time, material such as mineral oil tend to volatilize or infuse into the fertilizers and lose their effectiveness, while wax and petroleum products were difficult to handle and required specific heating equipment.[10] Binding materials also tend to lose their binding property when they dried, thereby becoming ineffective as long term dust control agents.[11] Adding hardening agent to fertilizer prior to granulation is another method to make final product hard and enhance the physical properties of granules.[12]

Hardening or reinforcement materials play a significant role in determining and improving the mechanical performance of different composites. Many researchers have tried to improve the mechanical properties of different composite materials, such as polymers, cement, fertilizer granules and metal alloys using varying material like silica, clays, glass fibre and calcium carbonate particles.[13-17] However, these micron-sized materials require high loading to enhance the mechanical properties of the final products, which leads to heavier composites, especially in the case of polymers. Furthermore, the lack of interfacial interaction between the reinforcements and initial materials is another drawback of traditional reinforcements, which results in failure of the final product due to weak interfacial adhesion.[13] Recently many studies have focused on newly produced nanomaterials, especially carbon nanotubes (CNTs), graphene (GN) and graphene oxide (GO) sheets, as reinforcement materials for different composites.[18-21] Although CNTs are considered excellent reinforcement materials due to their unique properties such as high aspect ratio, high tensile strength, high conductivity etc., they suffer from agglomeration and insufficient dispersion in the matrix due to their surface chemistry. Furthermore, the equipment used to synthesise CNTs is expensive to operate.[15, 19]

Many researchers have focused on GN for use in different areas since the attribution of a Nobel Prize to two pioneering scientists in 2010.[22-24] One of the many applications of GN includes its use as a reinforcement material due to its outstanding properties. Indeed, GN is the toughest material ever measured with a Young's modulus of 1 TPa and yield strength of 130 GPa.[24, 25] In addition, two-dimensional (2D) GN sheets are flexible with a very high theoretical specific surface area (2630 m^2/g), which makes them favourable to be used as a replacement for other reinforcement materials.[18, 25, 26] In recent years, several studies have proposed the use of GN and its oxidized form graphene oxide (GO) for enhancing the mechanical properties of cementitious materials, polymers, fertilizer granules, alloys and metalloids, and new composites have been designed for specific applications.[14, 16, 17, 20, 26-28] Although, the improvement of mechanical properties of different GN-reinforced products is due to the high Young's modulus of GN, high intrinsic strength and high surface area, several other parameters can affect the mechanical properties of the final composites. Graphene concentration and physicochemical properties in addition to the chemical interaction of GN-based materials with the matrix can influence the mechanical properties of composites to which the GN is added.[28]

The effect of GN concentration on the mechanical properties of cementitious materials has investigated by Gholampur et al. who showed that there was an optimal GO concentration (i.e. 0.1%) to enhance the tensile and compressive strength of GO-cement composites.[14] They also showed that increasing the GO content beyond the optimal point led to negative effects as observed by the appearance of many micro-cracks, due to restacking and aggregation of GO sheets. Similar investigations were also carried out by Shengua et al. where the tensile, flexural and compressive strengths measured for cement composites containing various amounts of GO.[29] Their results indicated that the tensile and flexural strength increased with GO concentration up to 0.03% and decreased slightly for additions thereafter.[29] A number of studies showed that by increasing the amount of CNT beyond the critical content, the mechanical properties of some polymers decreased and sometimes these properties were less than the original matrix material.[30-33] Chen et al. studied the properties of polycarbonate/CNT nanocomposites prepared by a large-scale extruder at various concentrations of CNTs added to the matrix. They observed a 4.5% increase in tensile strength for composites containing 1 wt% CNT (compared to control) and above this concentration the tensile strength significantly decreased.[31] It was suggested that either the decrease in the fluidity of the composite, or the unpredicted shortening of CNTs during extrusion weaken the effects of CNTs as a reinforcing agent.

The mechanical strength of GN sheets is dependent on their method of preparation, number of layers, aggregation and defects of GN sheets in addition to degree of reduction (deoxygenation degree and restoring graphitic structure). Therefore, the mechanical strength of GN sheets can play a major role in the mechanical properties of the final materials which GN is added, as defect-free single sheet of GN inherits the highest amount of Young's modulus and strength.[24, 28] For example, GN-polymer composite contained GN sheets prepared by reduction of GO had medium quality compared to those composites contained pristine GN.[28] Several studies have revealed the importance of surface functionalization of GN/GO sheets on improving the mechanical properties of final composites as the chemical interaction of the reinforcement and initial materials are enhanced, especially in the case of polymers.[26, 28] Ye et al. prepared two sets of polyvinyl alcohol (PVA) composites with GN and aryl diazonuim functionalized GN. Their results showed better mechanical performance of final polymer composite with functionalized GN compared to GN due to the chemical interaction of reinforcement and PVA.[34] Amino-functionalized GN sheets have also significantly improved the mechanical properties of epoxy resins due to strong covalent bonding of amino groups and resin.[35, 36] Kim et al. reported an enhancement in the average tensile strength and Young's modulus of 30% and 40%, respectively, for epoxy resin by adding 4-aminobenzoyl-functionalized GN platelets.[37]

Inspired by the unique properties of GN and its capability to significantly improve the mechanical properties of many other composite materials, our previous study demonstrated that both GO and GN were able to enhance the physical properties of granular phosphate fertilizers.[17] In this present study, a systematic investigation is presented, with the aim to better understand the fundamental aspects of the influence of GN additives on improving the mechanical properties of fertilizers. Two types of phosphorus-based fertilizer granules with different initial hardness were used to find the critical GN concentration in which the crushing strength of granules decreased. MAP-GN and DAP-GN composites were prepared using different rates of GN (i.e. 0-1% by weight of fertilizer) and their physical, structural, chemical, and mechanical properties were comprehensively characterized. The effect of physicochemical properties of GN sheets made using different methods on the crushing strength of MAP and DAP granules were also investigated. Moreover, GN decorated with iron nanoparticles (NPs) was used as another hardening agent to investigate the influence and chemical interaction of iron NPs on the crushing strength of granules.

EXPERIMENTAL SECTION

Synthesis of graphene oxide (GO) and hydrothermally reduced graphene oxide (GN $_{HT}$). GO sheets were synthesised by the improved Hummer's method from graphite powders.[38] A modified hydrothermal method for the reduction of GO was used to prepare the GN sheets similar to our previous work.[39] Briefly, a GO dispersion (1 mg mL^{-1}, 250 ml) was transferred to a Teflon-lined autoclave and heated at 180°C for 3 h. The autoclave was then cooled to room temperature and the formed GN hydrogel was ultrasonicated in a H_2O/acetone (ratio 3:1) mixture.

Synthesis of chemically reduced graphene oxide (GN_{NH} and GN_{VC}). Chemically reduced graphene oxide samples were prepared using hydrazine (N_2H_4) or L-ascorbic acid (vitamin C) following Park et al. and Fernandez et al., respectively.[40, 41] Briefly, GO solution reduced by hydrazine monohydrate (1 μL for every 3 mg of GO) was prepared under continuous stirring conditions at 80°C for 3 h. Graphene obtained using vitamin C (VC) as the reducing agent was made by adding 0.2 mM VC to 500 ml of GO dispersion with concentration of 2 mg mL^{-1}. The mixture then stirred at 95 ^{0} C for 3 h. Reduced GO was then collected by centrifuging of the black solution. Both GN samples reduced with chemicals were washed 3 times to remove any impurity from N_2H_4 or VC. GN made by both methods was dried in the freeze-dryer for further characterization.

Synthesis of graphene-αFeOOH (GN_{FeOOH}). Graphene with αFeOOH nanoparticles was prepared by slightly modifying our previous work.[42] In a typical procedure, 200 mg of GO was dispersed in 100 mL of milli-Q water. Then, 2.5g of $FeSO_4.7H_2O$ added and the mixture kept at 80°C for 8h. The prepared GN_{FeOOH} was collected with filter paper and washed to remove unreacted $FeSO_4.7H_2O$, and some was GN_{FeOOH} freeze-dried for further characterization. As prepared GN_{FeOOH} ultrasonicated in a H_2O/acetone (ratio 3:1) mixture was mixed with MAP and DAP with different weight percentages and granulated.

Synthesis of αFeOOH nanoparticles nanoparticle: αFeOOH nanoparticles were synthesised based on following procedure.[43] Briefly, 1.5 mmol of $Fe(NO_3)_3{\cdot}9H_2O$ was dissolved in 20 mL of deionized water. Then, a concentrated NaOH solution was added dropwise to $Fe(NO_3)_3$ solution to adjust the pH of solution at 10. The aqueous solution was then transferred into a 100 mL Teflonlined autoclave, followed by the hydrothermal reaction at 100 ^{0} C for 3 h. The precipitate at the bottom of Teflonlined autoclave were washed several times with deionized water and then particles were dried for further use and X-ray diffraction analysis (Figure S1, Supporting Information).

Preparation of monoammonium phosphate with GN (MAP-GN) and diammonium phosphate GN (DAP-GN) fertilizer granules. MAP-GN and DAP-GN granules were prepared as described in our previous work.[17] Briefly, MAP and DAP fertilizer granules without de-dust coating (received from Mosaic) were ground and sieved to obtain a powder with particle sizes less than 250 μm. GN_{HT} paste with ~20% water was mixed with the MAP or DAP powder at rates of 0.05%, 0.2%, 0.5% and 1% by weight. The mixtures were homogenized, dried at 45°C and sieved through a 250 μm sieve before granulation. A small amount of ultrapure deionised water was sprayed onto 3 g of (MAP-GN or DAP-GN) mixed powder placed in the rotating pan using a 50 μL min^{-1} nebulizer while the drum rotating at 12-

15 rpm. The fertilizer powder was granulated in the rotating pan to form particles of approx. 2-4 mm in size.

GN_{NH}, GN_{VC}, GN_{FeOOH} and αFeOOH nanoparticles were mixed with MAP and DAP powder using the same rates of addition and preparation process.

Granule crushing strength. To measure the crushing strength of MAP-GN and DAP-GN fertilizers with different ratios of GN, 25 granules within the size fraction -2.80 and +2.36 mm were chosen according to IFDC S-107.[44] The mechanical or crushing strength of individual granules were measured using a commercial table-top Wykeham Farrance ring penetrometer (England), where each granule was placed on a mounted flat surface and pressure applied by a flat-end rod attached to the compression tester. The pressure required to fracture the granule was measured by a gauge mounted in the compression tester. The load at which 25 granules of each formulation fractured was averaged and compared with the mechanical properties of MAP or DAP granules.

RESULTS AND DISCUSSION

Physical and chemical characterization of MAP-GN and DAP-GN prepared with different wt% of graphene

The morphology of the prepared DAP-GN and MAP-GN granules with hydrothermally reduced (GN_{HT}) contents of 0%, 0.05%, 0.2%, 0.5% and 1% are presented in Figure 1a-j. All granulated samples showed a round shape with different degrees of roughness. The topography of DAP samples did not change by increasing the amount of GN_{HT} up to 0.2% compared to the control (DAP with no GN_{HT} additives) (Figure 1a-c). However, by increasing the amount of GN_{HT} to 0.5% and 1% many voids were detected and DAP/GN aggregates were loosely connected together (Fig. 1d and e). For MAP granules, a very different trend was observed, the surface of the granule with 0.05% GN_{HT} was smoother than the granule with 0.2% GN_{HT}; and by enhancing the content of GN_{HT} to 0.5% granules showed reduced surface roughness. The EDX analysis results of the DAP-GN and MAP-GN samples (Figures 1k-n) show the changes of elemental carbon (C) composition on the granule surface for different GN_{HT} incorporation rates. Plain DAP and MAP did not contain C and the amount of C due to the presence of GN_{HT} was increased by enhancing the content of GN_{HT} in the samples. The amount of C was not detectable in both DAP- and MAP-0.05% GN_{HT} due to the low GN_{HT} addition rate.

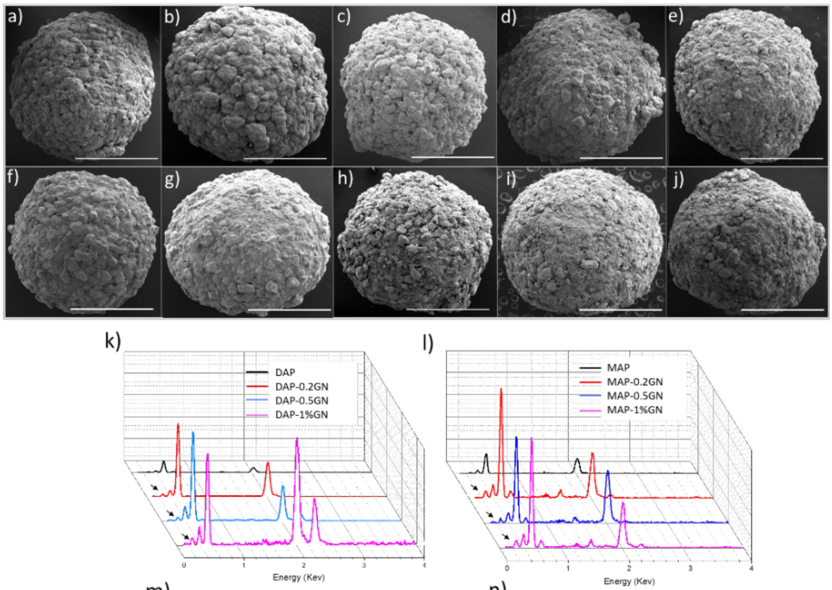

m)

Formulation	Carbon	
	W t%	At%
DAP	0	0
DAP-0.2%GN	2.5	3.8
DAP-0.5%GN	3.2	4.7
DAP-1%GN	7.0	12.6

n)

Formulation	Carbon	
	W t%	At%
MAP	0	0
MAP-0.2%GN	2.9	4.5
MAP-0.5%GN	5.7	8.8
MAP-1%GN	7.6	11.2

Figure 1. SEM images of a) Diammonium phosphate (DAP) (control), DAP with b-e) 0.05, 0.2, 0.5 and 1% GN_{HT}, and f) Mono ammonium phosphate granules (MAP) (control), MAP with g-j) 0.05, 0.2, 0.5 and 1% GN_{HT}, (all scale bars represent 2 mm) and EDX analysis of k) and m) the DAP-GN, and i) and n) the MAP-GN samples with different concentration of GN_{HT} (arrows representing C peaks in all EDX graphs).

The presence of GN_{HT} in both DAP-GN and MAP-GN samples was confirmed by thermogravimetric (TGA) analysis (Figures 2a and b). Thermal decomposition, related to the loss of ammonia and water for both DAP and MAP, took place in several stages and involved a polycondensation process, which led to the formation of different polymers.[45-47] Ammonia release took place above 100 °C due to thermal dissociation of DAP/MAP. Water liberation occurred around 170 °C, while the maximum quantity of water liberation was in the range of 220-350 °C.[45] DAP showed higher weight loss before 200 °C due to the presence of more ammonia molecules in its structure compared to MAP, and both products showed an intensive weight lost at around 600 °C due to decomposition of polycondensation products.[45] Hydrothermally reduced GN showed around 60% weight loss at ~350 °C due to the presence of some oxygen functional groups and the release of CO and CO_2 gases.[48] Another weight loss for GN_{HT} was observed between 550 and 700 °C which corresponds to the breakdown of carbon skeletons by combustion and decomposition.[49] All GN_{HT}-amended samples followed a similar trend as the controls (DAP and MAP). However, amended samples showed higher weight loss compared to control samples starting from 550 °C depending on the percentage of added GN_{HT}, and the highest overall weight loss occurred for GN_{HT}. For both DAP and MAP samples containing GN_{HT}, samples containing 1% GN_{HT} had a higher weight loss compared to other formulations.

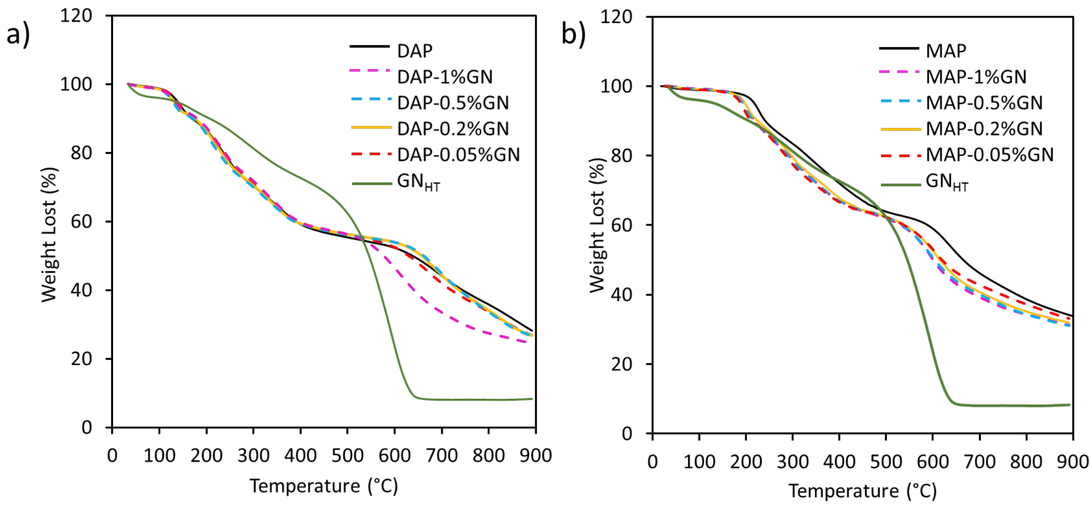

Figure 2. Thermal decomposition of a) diammonium phosphate (DAP), hydrothermally reduced graphene (GN_{HT}) and DAP amended with 0.05, 0.2, 0.5 and 1% GN_{HT} and b) monoammonium phosphate (MAP), GN_{HT} and MAP amended with 0.05, 0.2, 0.5 and 1% of GN_{HT}.

The XRD patterns of GN_{HT} showed typical diffraction peaks at $2\theta = 25.1°$ and the patterns of DAP and MAP were well matched with the XRD peaks of their commercial products (Figure S2, Supporting Information).[17, 50, 51] However, no diffraction peaks corresponding to GN_{HT} were observed in the XRD patterns of the amended products due to the low diffraction intensity of GN_{HT}. The results show that the presence of GN did not alter the crystalline structure of DAP and MAP in amended samples.

Effect of graphene concentration on crushing strength of MAP and DAP

The results of the crushing strength tests of MAP-GN and DAP-GN composites with different GN_{HT} contents are summarized in Figures 3a and b, respectively. Without GN_{HT} inclusion, DAP had a much higher crushing strength than MAP. The inclusion of GN_{HT} in MAP results in an increase in the crushing strength of amended granules, which is in agreement with our previous study.[17] The increase in crushing strength was not consistently related to the dosage of added GN_{HT}. Lower strength of MAP-GN_{HT} 0.2% granules was attributed to loose attachment of MAP-GN_{HT} aggregates bound together and their rough topography similar to our previous findings.[17] Inclusion of 0.05% GN_{HT} improved the crushing strength of DAP granules compared to control granules (DAP without GN_{HT}). However, further increasing the inclusion of GN_{HT} to 0.2 and 0.5% resulted in a decrease in the crushing strength of DAP. The crushing strength of DAP-1% GN_{HT} decreased sharply compared to other formulations and was even less than control samples (DAP without GN_{HT}).

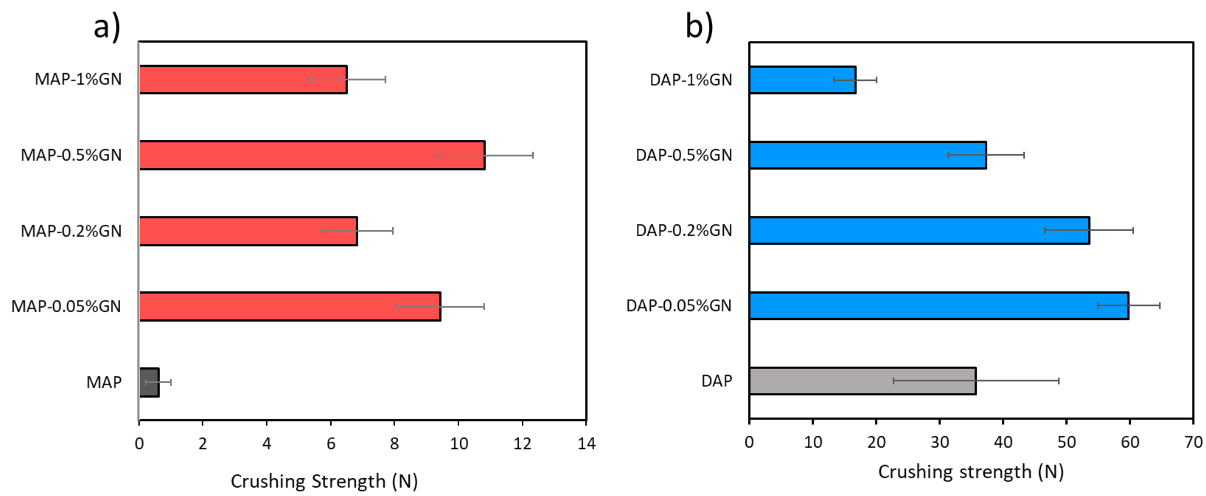

Figure 3. a) Graph showing crushing strength (Newton (N)) to crush, a) granules of mono ammonium phosphate (MAP) (control) and MAP with different concentration (0.05 to 1%) of GN_{HT} and b) granules of diammonium phosphate (DAP) (control) and DAP with different concentration (0.05 to 1%) of GN_{HT}.

Different levels of improvement in the crushing strength of MAP and DAP with inclusion of GN_{HT} could be related to their chemical, physical and crystalline structures. DAP micro particles with monolithic crystalline structures tend to aggregate and bond together strongly due to their higher solubility in water (~70 g.100 mL^{-1}) compared to MAP particles with their tetragonal crystalline structure and lower solubility in water (~40 g.100 mL^{-1}), thus the control DAP is very strong and has an interconnected structure, which needs a higher force to be crushed.[50, 52] Hence, addition of GN_{HT} sheets does not increase the relative crushing strength of amended DAP samples as much as MAP. Similar results has been reported in GN/polymer composites, where the stiffness and strength of the matrix with lower tensile modulus (such as elastomers) showed a higher percentage increase by inclusion of GN, while it was difficult to observe the same increased values for these parameters in a rigid matrix.[28] Interestingly, the modulus of GN is higher when the matrix is rigid and a small amount of reinforcement can enhance the crushing strength of the matrix as was observed for the DAP granules.[28]

The mechanism of graphene dosage on mechanical properties of fertilizers

The overall improvement in the crushing strength of MAP/DAP amended with GN_{HT} is attributed to the unique physicochemical properties of graphene-based materials including their high mechanical strength, high SSA and the pore-filling ability related to its wrinkled and 2D (planar) structure. However, several studies observed the dependence of concentration and optimal dosage on the mechanical properties of the final composite amended with GN-based materials, similar to our results.[14, 29] Gholampour et al. reported a decrease in the tensile strength of GO-cement composites when the concentration of added GO increased in the cement beyond a certain level.[14] Similarly, the mechanical properties of CNT-polymer composites decreased by increasing CNT content beyond the critical content of 3%. The aggregation of GN/CNT in the matrix or their poor dispersion was reported as the reason for the reduction in mechanical properties of both the cement and polymer composites.[19, 31] Therefore, the decrease in crushing strength of granules beyond the optimum point could be related to the aggregation of GN sheets or ‘barrier property' of GN sheets as the method of granule preparation is totally different for GN-cement/polymer composites.

As indicated in the schematic below (Figure 4), the formation of granules requires wetting the powdered particles and subsequent solid bridges between them during the granulation process. Water droplets slightly dissolve MAP or DAP powders leading to their bonding (liquid bridge) due to the adhesion and cohesion forces in the immobile liquid film between the individual primary particles. Subsequently, solid bridges form between the particles after solvent evaporation and more aggregated solid particles bind together due to the attractive force between the solid particles.[53] In MAP and DAP powders containing GN_{HT} higher than the optimum value (Figures 4e, f, g and h), the liquid and subsequent solid bridges cannot form as much as those samples containing GN_{HT} at the optimum concentration (Figures 4 a-d). This is likely due to partial or complete wrapping of MAP/DAP particles with GN_{HT} sheets, which act as barrier preventing the formation of liquid bridges. Furthermore, due to the hydrophobic nature of GN_{HT} sheets, they repel water and these MAP/DAP micro particles with GN_{HT} sheets on their surfaces are less likely to create liquid bridges and agglomerate to each other, hence are loosely bonded and have less crushing strength.

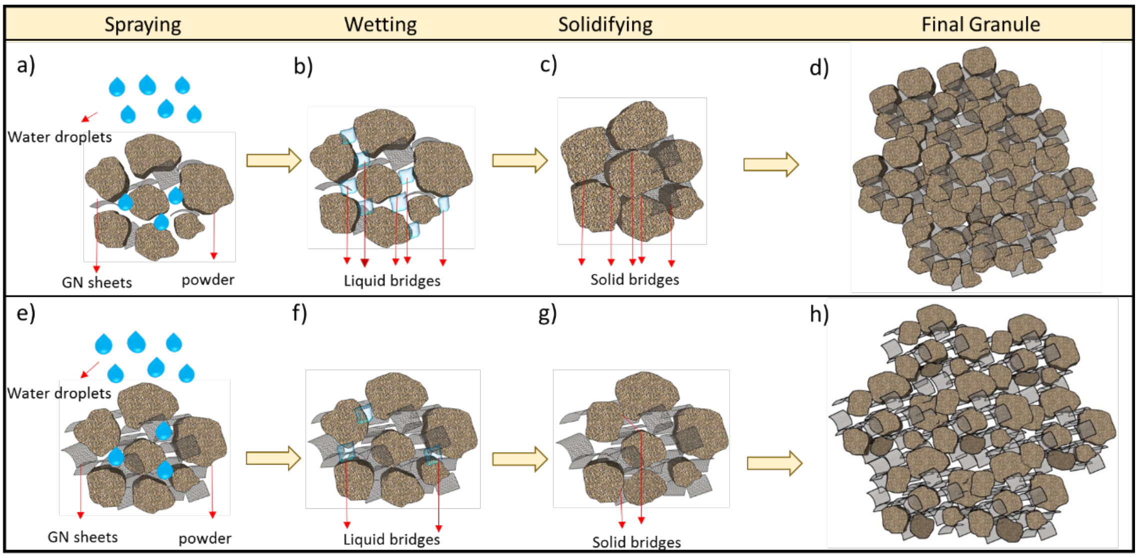

Figure 4. Schematic of co-granulation of DAP/MAP using lower (than optimum) concentration of GN a) spraying water droplets on DAP/MAP b) formation of liquid bridge between DAP/MAP micro particles, c) agglomeration of DAP/MAP micro-particles due to the formation of solid bridge between DAP/MAP micro particles after evaporation of liquid, d) formation of final granules with compacted DAP/MAP aggregates while GN sheets acting as a pore filling materials, using high (than optimum) concentration of GN e) spraying water droplets on DAP/MAP, f) formation of less liquid bridges between DAP/MAP micro-particles due to the presence of high concentration of GN sheets with hydrophobic properties, g) DAP/MAP micro particles aggregated loosely to each other due to the formation of less solid bridges as GN sheets act barriers and h) formation of final granules with loosely bonded DAP/MAP aggregates compared with granules having lower amounts of GN.

As mentioned earlier, the re-stacking of GN_{HT} sheets leading to their poor dispersion in the DAP/MAP powder matrix due to high concentrations of GN_{HT}, could be another reason for lowering the crushing strength of MAP-1%GN_{HT} or DAP-1%GN_{HT}.The aggregation of GN is commonly noted as the key limitation for improvement in mechanical performance of composites amended with high concentrations of GN.[14, 54, 55] Poor dispersion and aggregation were found to give lower load transfer to the reinforcement materials, which resulted in low mechanical properties in polymer composites.[19, 21] Both suggested mechanisms were further confirmed with high magnification SEM images (Figures 5a-d) of the surface of MAP-1%GN or DAP-1%GN granules. As indicated in Figure 5a and b, while some GN_{HT} sheets wrapped the surface of MAP microparticles, GN_{HT} aggregates were also presented in other areas on the particles (Area A, Figure 5a). EDX analysis of Area A (Figure 5a) showed high concentration of GN (31 wt %) indicating the presence of aggregated GN_{HT} sheets (Figure S3, Supporting Information). Individual MAP microparticles were also covered with GN_{HT} sheets and preserved their crystalline shape very well after granulation in MAP-1% GN_{HT}, which indicates that their structure was less affected by water molecules during granulation due to the presence of high amounts of GN sheets compared to MAP-0.5%GN (Figure S4, Supporting Information). Single or aggregated GN sheets were not detected by high magnification SEM images of DAP-1%GN_{HT} samples, however some parallel and stacked structures were observed which could be related to the presence of re-stacked GN_{HT} sheets (Figure 6c and d). These structures were not seen in the high magnification SEM images of DAP-GN_{HT} granules containing less than 1% GN (Figure S5, Supporting Information).

Raman spectra of both DAP/MAP-GN samples containing less than 0.5% GN_{HT} were the same as their controls, while in samples containing more than 0.5% GN_{HT}, two characteristic peaks of GN were distinct (Figure S6, Supporting Information). These two peaks in DAP/MAP-1% GN_{HT} were very sharp and smooth compared to DAP/MAP-0.5% GN_{HT} showing partial or complete coverage of the DAP/MAP macro particle with GN sheets and aggregation of GN sheets. These results confirmed our two aforementioned hypotheses for decreasing crushing strength of samples amended with highest content of GN_{HT}. The aggregation and wrapping property of GN_{HT} sheets were also confirmed by energy dispersive X-ray spectroscopy (EDX) mapping, as illustrated in Figure 5F. For the main elements of P, O and N, the maps clearly indicates that these elements are homogenously distributed on the MAP granules while elemental carbon's distribution was less than other elements and some aggregates were observed as indicated in Figure 5e.

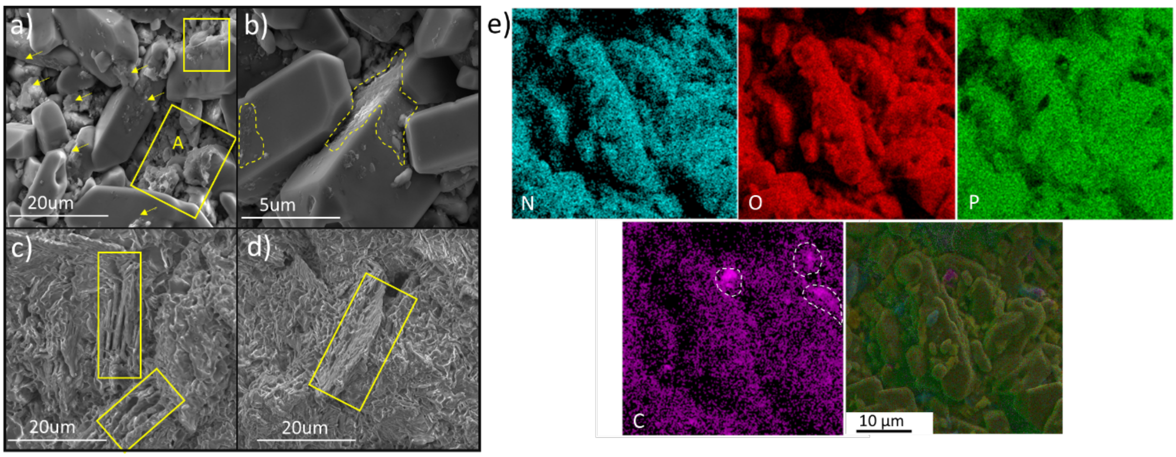

Figure 5. Low magnification SEM images a) and b) of MAP-1%GN granules showing high content of GN_{HT} covered particle surface, c) and d) DAP-1%GN, and e) elemental map of Nitrogen (N), oxygen (O), phosphorous (P) and Carbon (C) of the MAP-1%GN granule.

Crushing strength of co-granulated MAP and DAP with GN made by different methods

Chemically reduced GN with hydrazine was co-granulated with MAP/DAP to see how different physicochemical properties of GN, due to its method of preparation, can affect the crushing strength of MAP/DAP-GN granules. Although reduced GN with hydrazine restores the graphitic structure and relevant properties of pristine GN, the use of such highly toxic reagents in a large-scale is not desirable. Different studies showed that vitamin C is not only a non-hazardous reagent, but that it also has reducing characteristics and can compete with the widely used hydrazine in deoxygenating GO.[41] Therefore, two concentrations of (0.05% and 0.05%) GN reduced with hydrazine (GN_{NH}) and vitamin C (GN_{VC}) were co-granulated with MAP and DAP to compare their effectiveness on the crushing strength of fertilizers and to observe whether GN_{NH} could be replaced with GN_{VC} in a large-scale production for application in the fertilizer industry. Furthermore, the crushing strength of MAP/DAP amended with 0.05 and 0.5% of GN with iron NPs (GN_{FeOOH}) was measured to demonstrate the synergistic effect of iron NPs and GN sheets and their chemical interaction with MAP/DAP particles on the crushing strength of granules. The combined addition of iron NPs and GN sheets is expected to further enhance the crushing strength of MAP/DAP by reacting iron NPs and phosphate. SEM images of both MAP and DAP granules co-granulated with 0.5% of GN_{HT}, GN_{NH}, GN_{VC} or GN_{FeOOH} are represented in Figure 6(a-h). The morphology of MAP and DAP granulated with different types of GN (chemically reduced, hydrothermally reduced, chemically reduced containing iron NPs) looked the same with no difference in their topography which indicated that by applying different types of GN the physical appearance of granules affected at the same way.

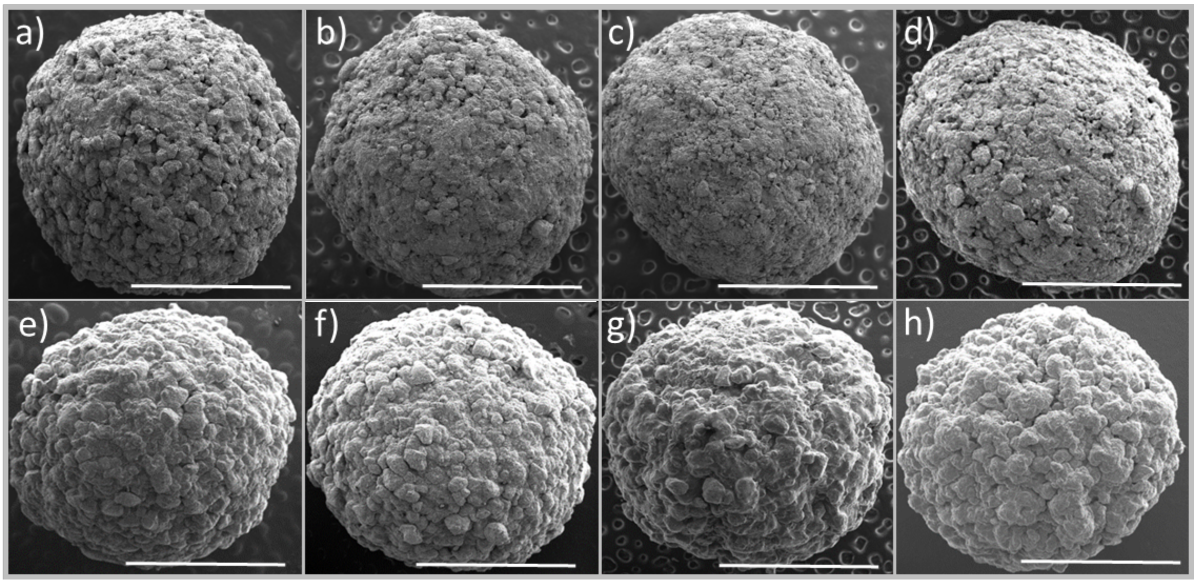

Figure 6. High magnification SEM images of MAP amended with 0.5% of a)GN_{HT}, b)GN_{NH}, c)GN_{VC} and GN_{FeOOH} and DAP amended with 0.5% of a)GN_{HT}, b)GN_{NH}, c)GN_{VC} and GN_{FeOOH} , (all scale bars represent 2 mm).

The results of the crushing strength tests of MAP and DAP granules amended with two weight percentages of GN_{HT}, GN_{NH}, GN_{VC} and GN_{FeOOH} are summarized in Figures 7a and b. The inclusion of low (0.05%) and high (0.5%) concentration of GN made by all methods increased the crushing strength of MAP granules compared to the control. However, MAP granules amended with chemically reduced GN (GN_{VC} and GN_{NH}) had higher crushing strengths compared to those amended with GN_{HT} for both dosages of 0.05 and 0.5%. MAP granules containing GN_{FeOOH} as a hardening agent had better crushing strength compared to those treated with GN_{HT} at the 0.5% rate, despite having 40% less GN compared to other formulations. The crushing strength of MAP granules amended with high (0.5%) dosage of either GN_{NH}, GN_{VC} or GN_{FeOOH} was up to 1.5 times higher than those with low dosage (0.05 %), while this difference was negligible for MAP amended with 0.05 and 0.5% GN_{HT}. Interestingly, all of the chemically reduced GN additives increased the crushing strength of MAP either equally or greater than other forms of GN as indicated in Table 1. Some DAP composites showed an enhancement in crushing strength, namely GN_{NH} and GN_{HT} and their greater hardness response was found with the lower GN dosage compared to the high dosage.

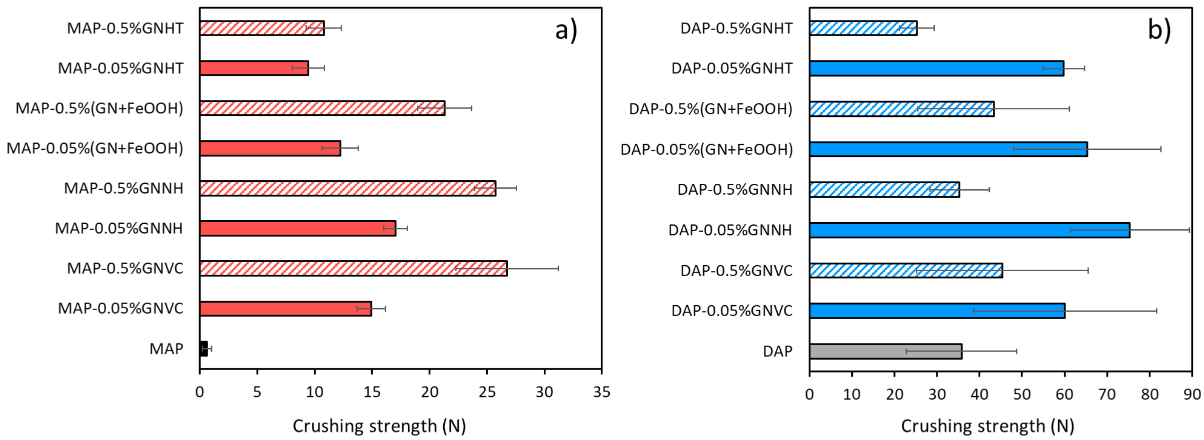

Figure 7. Crushing strength (Newton (N)) for a) granules of mono ammonium phosphate (MAP) and MAP amended with different forms of GN at concentrations of 0.05 and 0.5% and b) granules of diammonium phosphate (DAP) and DAP amended with different forms of GN at two concentrations of 0.05 and 0.5%.

Table 1. Comparison of the effects of GN made with different methods when used as additives to enhance the crushing strength of MAP and DAP fertilizer granules.

Fertilizer type	Type of GN used	Additive percentage	Percent increase in crushing strength
MAP	GN_{HT}	0.05%	1451% (±201)
MAP	GN_{HT}	0.5%	1679% (±735)
MAP	GN_{VC}	0.05%	2470%(±170)
MAP	GN_{VC}	0.5%	4185%(±301)
MAP	GN_{NH}	0.05%	2547%(±158)
MAP	GN_{NH}	0.5%	4141%(±192)
MAP	GN decorated with αFeOOH NPs	0.05% (total GN + αFeOOH)	1910%(±258)
MAP	GN decorated with αFeOOH NPs	0.5% (total GN + αFeOOH)	3406%(±384)
DAP	GN_{HT}	0.05%	67%(±17)
DAP	GN_{HT}	0.5%	-[a]
DAP	GN_{VC}	0.05%	102%(±5)
DAP	GN_{VC}	0.5%	26%(±8)
DAP	GN_{NH}	0.05%	82%(±12)
DAP	GN_{NH}	0.5%	-[a]
DAP	GN decorated with αFeOOH NPs	0.05% (total GN + αFeOOH)	82%(±13)
DAP	GN decorated with αFeOOH NPs	0.5% (total GN + αFeOOH)	21%(±4)

[a] refers to less than 1%

The physicochemical properties of GN which is related to its preparation method, and the interaction and orientation of them in the matrix, can affect the mechanical properties of composites amended with GN.[28] Therefore, to investigate whether the difference in crushing strength of MAP and DAP is related to the properties of GN reduced with different methods (or chemicals), TGA and Raman analysis were conducted on the GN additives. TGA results (Fig. 8a) for all samples showed a mass loss between 200 to 400 °C, which was attributed to the decomposition of some residual oxygen-containing groups that were not fully removed during the reduction process of GO.[56] However, GN_{HT} showed higher weight loss in this temperature range, which is attributed to more oxygen functional groups remaining in its structure. GN_{NH} and GN_{VC} had similar TGA trends showing the same degree of reduction and less weight loss in the range of 200-400 °C, indicating fewer oxygen functional groups and greater reduction compared to GN_{HT}. The thermal stability of GN decorated with αFeOOH nanoparticles was greater than the other GN reduction methods, which could be attributed to the restoration of the carbon network during the reaction with iron nanoparticles.[57] Furthermore, due to the presence of 40 % iron NPs, its weight loss was less than other forms of GN.

The Raman spectroscopy results of all forms of GN represented a typical spectrum for GN-based materials with two distinct peaks, the in-phase vibration of the graphite lattice (G-band) and the disorder band caused by the graphite edges (D-band) (Fig. 8b). The G-band arises from in-plane vibrations of sp^2-carbon atoms while the D-band arises from the defective carbon structure and the intensity ratio of the G-band to the D-band (i.e., I_G/I_D) reflects the relative amount of sp^2-hybridized carbon atoms on the surface GN. Therefore, changes in the relative amount of sp^2-hybridized carbon atoms in the sample can be estimated by determining the I_G/I_D ratio. The I_G/I_D ratio followed $GN_{NH} > GN_{VC} > GN_{FeOOH} > GN_{HT}$ order which shows less reduction of GN_{HT} compared to other forms of GN. Therefore, the improvement in the crushing strength of granules amended with GN_{NH} and GN_{VC} compared to GN_{HT} could be related to their increased reduction and restoration of the graphitic structure.

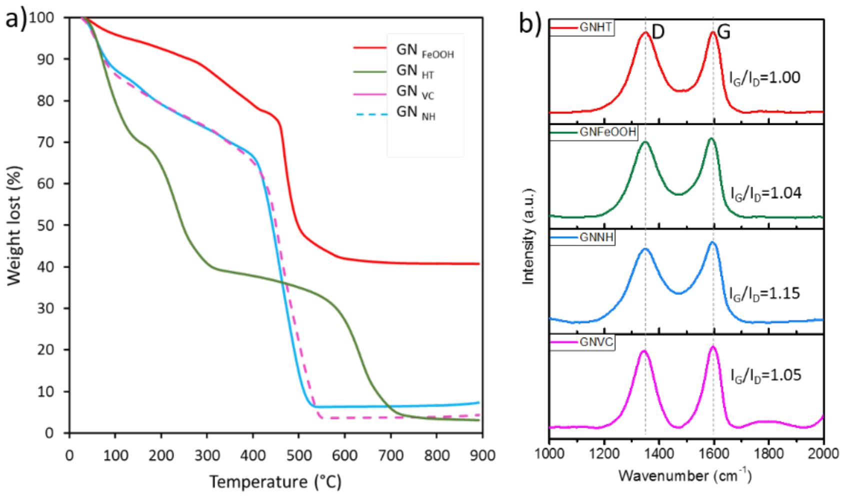

Figure 8. a) Thermal decomposition of hydrothermally reduced graphene (GN_{HT}), graphene reduced by hydrazine (GN_{NH}), GN reduced by vitamin C (GN_{VC}) and GN decorated with αFeOOH nanoparticles (GN_{FeOOH}), and b) Raman spectra of GN_{HT}, GN_{NH}, GN_{VC} and GN_{FeOOH}.

In addition to the physicochemical properties of GN, the differences in the crushing strength of MAP granules produced with different types of GN (GN_{HT}, GN_{NH} and GN_{VC}) could also be related to their SSA. Specific surface area measured for GN made by the different methods was 672, 777 and 935 g m^{-2} for $GN_{HT,}$ GN_{NH} and GN_{VC}, respectively. Both GN_{NH} and GN_{VC} had a higher SSA than GN_{HT} resulting in an enhancement of the crushing strength of the final composites. Although, the initial geometry of the GO sheets used to synthesise all GN materials was identical, the particle size analysis results showed GN_{HT} was almost three times larger than GN_{NH} and GN_{VC}, due to the aggregation of GN sheets during the reduction process, which was performed under high temperature and pressure (Figure S7, Supporting Information). Therefore, it is expected that GN_{HT} samples with larger size and aggregated sheets show lower SSA compared to GN_{NH} and GN_{VC}. Similar results have been reported by others where the capability of GN to enhance the mechanical properties of different alloys and polymers is correlated to its high specific surface area, therefore, it is expected that GN with higher specific area will enhance the crushing strength of both MAP and DAP granules.[19, 21, 28, 58]

In the case of GN_{FeOOH}, the enhanced crushing strength of granules could be related the effect of both GN sheets and αFeOOH nanoparticles. To confirm the effect of αFeOOH nanoparticles on crushing strength of granules, αFeOOH nanoparticles synthesised and congratulated with MAP and their crushing strength were measured. The crushing strength of MAP amended 0.2% of nanoparticles (the percentage of nanoparticles was 0.2 and GN 0.3% in MAP amended with 0.5% GN_{FeOOH}) was 8.6 (±1.3) Newton, 14 times higher than crushing strength of MAP (control) pointing the effect of αFeOOH nanoparticles on enhancement of crushing strength of MAP granules. Although the percentage of GN added to MAP/DAP was lower than other formulations, the crushing strength of the final composite enhanced due to the presence of nanoparticles and /or chemical binding of αFeOOH nanoparticles with PO_4^{-2} present in the MAP/DAP structure. For example, it has been shown that GN aerogels decorated with αFeOOH nanoparticles have high affinity for adsorption and removal of phosphorous (P) from water, indicating a strong affinity of Fe ions to P.[42]

CONCLUSIONS

The optimal percentage of inclusion of GN in the fertilizers was 0.5% for MAP and 0.05% for DAP leading to a 1680% and 67.3% enhancement in the crushing strength, respectively. Crushing strength tests also revealed that the enhancement of crushing strength depends on the strength of the initial fertilizer. Granules of MAP, with a softer structure, were improved more by the GN addition compared to DAP granules, which have an inherently harder structure. We have also discovered that there is a critical GN concentration for strength improvement, above which crushing strength decreases due to the (water) barrier properties and aggregation of GN sheets.

Results also showed that the crushing strength of granules depend on the method of GN production, while GN samples deoxygenate more were more effective than others due to recovering graphitic structure and higher SSA. Also, our results revealed that GN with Fe nanoparticles can enhance the crushing strength of fertilizer granules due to the chemical interaction of iron nanoparticles and synergic effects of NP and micron-size GN sheets despite the low SSA of GN_{FeOOH} compared to other types of GN. These results show the advantages of GN in enhancing the physical properties of both MAP and DAP granules due to the high mechanical strength of GN sheets and their high SSA.

ACKNOWLEDGMENTS

The authors wish to express their appreciation for the financial support of this study by the Australian Research Council Discovery Project DP1501001760 and Project IH 150100003. Mike J. McLaughlin and Roslyn Baird acknowledge the support of The Mosaic Company LLC. The authors would like to thank Colin Rivers for assistance with co-granulation of fertilizers.

REFERENCES

[1] Albadarin AB, Lewis TD, Walker GM. Granulated polyhalite fertilizer caking propensity. Powder Technology. 2017;308:193-9.
[2] Baltrusaitis J, Sviklas AM, Galeckiene J. Liquid and solid compound granulated diurea sulfate-based fertilizers for sustainable sulfurs source. ACS Sustainable Chemistry & Engineering. 2014;2(10):2477-87.
[3] Schroeder JI, Delhaize E, Frommer WB, Guerinot ML, Harrison MJ, Herrera-Estrella L, et al. Using membrane transporters to improve crops for sustainable food production. Nature. 2013;497:60.
[4] Gelfand I, Sahajpal R, Zhang X, Izaurralde RC, Gross KL, Robertson GP. Sustainable bioenergy production from marginal lands in the US Midwest. Nature. 2013;493:514.
[5] Stewart WM, Roberts TL. Food security and the role of fertilizer in supporting it. Procedia Engineering. 2012;46:76-82.
[6] FAO. World fertilizer trends and outlook to 2019, Food and Agriculture Organization of United Nations. pp 66; 2016.
[7] Stacy Spence, Haven W. Anti-caking and dust control coating compositions containing liquid-dispersed metallic salts of fatty acids and methods of using same. 2006, U.S.patent US 2006/0040049 A1.
[8] Rodrigues LM, Pires RF, de Souza DL. Study of granulated gypsum hardness coming from the granulation process in rotating disk. Materials Science Forum. 2017;899:160-6.
[9] Walker GM, Magee TRA, Holland CR, Ahmad MN, Fox N, Moffatt NA. Compression testing of granular NPK fertilizers. Nutrient Cycling in Agroecosystems. 1997;48(3):231-4.
[10] Helio Haruo Ushijima, Silvia Rcd. Concentrated sugar additives as anti-dusting agent. 2014, U.S. patent US20140345342A1.
[11] Kucera P, Sawyer WG. Fertilizer composition incorporating fibrous material for enhanced particle integrity. 2015,U.S. patent US20120285211A1.
[12] Rehberg BE, Haven W, Hall WL. Fertlizer composition and method of making such composites. 1993, U.S. patentUS005238480A.

[13] Bhattacharya M. Polymer nanocomposites-A comparison between carbon nanotubes graphene, and clay as nanofillers. Materials. 2016;9(4):262.
[14] Gholampour A, Kiamahalleh MV, Tran DH, Ozbakkaloglu T, Losic D. Revealing the dependence of the physiochemical and mechanical properties of cement composites on graphene oxide concentration. RSC Advances. 2017;7(87):55148-56.
[15] Sharma S, Kothiyal NC. Comparative effects of pristine and ball-milled graphene oxide on physico-chemical characteristics of cement mortar nanocomposites. Construction and Building Materials. 2016;115:256-68.
[16] Li Z, Guo Q, Li Z, Fan G, Xiong D-B, Su Y, et al. Enhanced mechanical properties of graphene (reduced graphene oxide)/aluminum composites with a bioinspired nanolaminated structure. Nano Letters. 2015;15(12):8077-83.
[17] Kabiri S, Baird R, Tran DNH, Andelkovic I, McLaughlin MJ, Losic D. Cogranulation of low rates of graphene and graphene oxide with macronutrient fertilizers remarkably improves their physical properties. ACS Sustainable Chemistry & Engineering. 2018;6(1):1299-309.
[18] Chuah S, Pan Z, Sanjayan JG, Wang CM, Duan WH. Nano reinforced cement and concrete composites and new perspective from graphene oxide. Construction and Building Materials. 2014;73:113-24.
[19] Mittal G, Dhand V, Rhee KY, Park S-J, Lee WR. A review on carbon nanotubes and graphene as fillers in reinforced polymer nanocomposites. Journal of Industrial and Engineering Chemistry. 2015;21:11-25.
[20] Hwang J, Yoon T, Jin SH, Lee J, Kim T-S, Hong SH, et al. Enhanced mechanical properties of graphene/copper nanocomposites using a molecular-level mixing process. Advanced Materials. 2013;25(46):6724-9.
[21] Rashad M, Pan F, Tang A, Lu Y, Asif M, Hussain S, et al. Effect of graphene nanoplatelets (GNPs) addition on strength and ductility of magnesium-titanium alloys. Journal of Magnesium and Alloys. 2013;1(3):242-8.
[22] Geim AK, Novoselov KS. The rise of graphene. Nature Materials. 2007;6:183.
[23] Zhu Y, Murali S, Cai W, Li X, Suk JW, Potts JR, et al. Graphene and graphene oxide: synthesis, properties, and applications. Advanced Materials. 2010;22(46):3906-3924.
[24] Lee C, Wei X, Kysar JW, Hone J. Measurement of the elastic properties and intrinsic strength of monolayer graphene. Science. 2008;321(5887):385-8.
[25] Kim H, Abdala AA, Macosko CW. Graphene/Polymer nanocomposites. Macromolecules. 2010;43(16):6515-30.
[26] Pazat A, Barrès C, Bruno F, Janin C, Beyou E. Preparation and properties of elastomer composites containing "Graphene"-based fillers: A review. Polymer Reviews. 2017:1-41.
[27] Gholampour A, Valizadeh Kiamahalleh M, Tran DNH, Ozbakkaloglu T, Losic D. From graphene oxide to reduced graphene oxide: Impact on the physiochemical and mechanical properties of graphene–cement composites. ACS Applied Materials & Interfaces. 2017;9(49):43275-86.
[28] Papageorgiou DG, Kinloch IA, Young RJ. Mechanical properties of graphene and graphene-based nanocomposites. Progress in Materials Science. 2017;90:75-127.
[29] Lv S, Ma Y, Qiu C, Sun T, Liu J, Zhou Q. Effect of graphene oxide nanosheets of microstructure and mechanical properties of cement composites. Construction and Building Materials. 2013;49:121-7.
[30] Cooper CA, Ravich D, Lips D, Mayer J, Wagner HD. Distribution and alignment of carbon nanotubes and nanofibrils in a polymer matrix. Composites Science and Technology. 2002;62(7-8):1105-12.

[31] Chen L, Pang XJ, Yu ZL. Study on polycarbonate/multi-walled carbon nanotubes composite produced by melt processing. Materials Science and Engineering A. 2007;457(1-2):287-91.
[32] Kosmidou TV, Vatalis AS, Delides CG, Logakis E, Pissis P, Papanicolaou GC. Structural, mechanical and electrical characterization of epoxy-amine/carbon black nanonocomposites. Express Polymer Letters. 2008;2(5):364-72.
[33] Ma PC, Kim JK, Tang BZ. Effects of silane functionalization on the properties of carbon nanotube/epoxy nanocomposites. Composites Science and Technology. 2007;67(14):2965-72.
[34] Yu DS, Kuila T, Kim NH, Lee JH. Enhanced properties of aryl diazonium salt-functionalized graphene/poly(vinyl alcohol) composites. Chemical Engineering Journal. 2014;245:311-22.
[35] Liu W, Koh KL, Lu J, Yang L, Phua S, Kong J, et al. Simultaneous catalyzing and reinforcing effects of imidazole-functionalized graphene in anhydride-cured epoxies. Journal of Materials Chemistry. 2012;22(35):18395-402.
[36] Chong HM, Hinder SJ, Taylor AC. Graphene nanoplatelet-modified epoxy: effect of aspect ratio and surface functionality on mechanical properties and toughening mechanisms. Journal of Materials Science. 2016;51(19):8764-90.
[37] Kim K-S, Jeon I-Y, Ahn S-N, Kwon Y-D, Baek J-B. Edge-functionalized graphene-like platelets as a co-curing agent and a nanoscale additive to epoxy resin. Journal of Materials Chemistry. 2011;21(20):7337-42.
[38] Marcano DC, Kosynkin DV, Berlin JM, Sinitskii A, Sun Z, Slesarev A, et al. Improved synthesis of graphene oxide. ACS Nano. 2010;4(8):4806-14.
[39] Zhou Y, Bao Q, Tang LAL, Zhong Y, Loh KP. Hydrothermal dehydration for the "Green" reduction of exfoliated graphene oxide to graphene and demonstration of tunable optical limiting properties. Chemistry of Materials. 2009;21(13):2950-6.
[40] Park S, An J, Potts JR, Velamakanni A, Murali S, Ruoff RS. Hydrazine-reduction of graphite- and graphene oxide. Carbon. 2011;49(9):3019-23.
[41] Fernández-Merino MJ, Guardia L, Paredes JI, Villar-Rodil S, Solís-Fernández P, Martínez-Alonso A, et al. Vitamin C is an ideal substitute for hydrazine in the reduction of graphene oxide suspensions. The Journal of Physical Chemistry C. 2010;114(14):6426-32.
[42] Tran DNH, Kabiri S, Wang L, Losic D. Engineered graphene-nanoparticle aerogel composites for efficient removal of phosphate from water. Journal of Materials Chemistry A. 2015;3(13):6844-52.
[43] Amani-Ghadim AR, Alizadeh S, Khodam F, Rezvani Z. Synthesis of rod-like α-FeOOH nanoparticles and its photocatalytic activity in degradation of an azo dye: Empirical kinetic model development. Journal of Molecular Catalysis A: Chemical. 2015;408:60-8.
[44] Fertilizer manual/editors, United Nations Industrial Development Organization (UNIDO) and International Fertilizer Development Center (IFDC). Dordrecht, The Netherlands; Muscle Shoals, AL: Kluwer Academic Publishers; 1998.
[45] Pérez J, Pérez E, del Vas B, García L, Serrano JL. Analysis of $(NH_4)_2SO_4/(NH_4)H_2PO_4$ mixtures by thermogravimetry and X-ray diffraction. Thermochimica Acta. 2006;443(2):231-4.
[46] Marcilla A, Beltran MI, Gómez-Siurana A, Martinez-Castellanos I, Berenguer D, Pastor V, et al. TGA/FTIR study of the pyrolysis of diammonium hydrogen phosphate–tobacco mixtures. Journal of Analytical and Applied Pyrolysis. 2015;112:48-55.
[47] Statheropoulos M, Kyriakou SA. Quantitative thermogravimetric-mass spectrometric analysis for monitoring the effects of fire retardants on cellulose pyrolysis. Analytica Chimica Acta. 2000;409(1-2):203-14.

[48] Dave K, Park KH, Dhayal M. Two-step process for programmable removal of oxygen functionalities of graphene oxide: functional, structural and electrical characteristics. RSC Advances. 2015;5(116):95657-65.
[49] Liu S, Peng W, Sun H, Wang S. Physical and chemical activation of reduced graphene oxide for enhanced adsorption and catalytic oxidation. Nanoscale. 2014;6(2):766-71.
[50] Dong D, Choi OK, Lee K, Hong Y, Lee JW. Alternative route for the recovery of nitrogen as ammonium phosphate crystals from high strength waste streams. Journal of Material Cycles and Waste Management. 2018;20(1):578-84.
[51] Gargouri M, Chtara C, Charrock P, Nzihou A, El Feki H. Synthesis and physicochemical characterization of pure diammonium phosphate from industrial fertilizer. Industrial & Engineering Chemistry Research. 2011;50(11):6580-4.
[52] Sepehri-Nik E. FCI: Fertilizer Technical Data Book: FCI Chemical Engineers; 1995.
[53] Lister BEaJ. The science and engineering of granulation first edition: Springer metherlands; 2004.
[54] Pan Z, He L, Qiu L, Korayem AH, Li G, Zhu JW, et al. Mechanical properties and microstructure of a graphene oxide–cement composite. Cement and Concrete Composites. 2015;58:140-7.
[55] Lu C, Lu Z, Li Z, Leung CKY. Effect of graphene oxide on the mechanical behavior of strain hardening cementitious composites. Construction and Building Materials. 2016;120:457-64.
[56] Chen H, Müller MB, Gilmore KJ, Wallace GG, Li D. Mechanically strong, electrically conductive, and biocompatible graphene paper. Advanced Materials. 2008;20(18):3557-61.
[57] Ok-Kyung P, Yong-Mun C, Jun Yeon H, Cheol-Min Y, Tea-Wook K, Nam-Ho Y, et al. Defect healing of reduced graphene oxide via intramolecular cross-dehydrogenative coupling. Nanotechnology. 2013;24(18):185604.
[58] Zhao X, Zhang Q, Chen D, Lu P. Enhanced mechanical properties of graphene-based Poly(vinyl alcohol) composites. Macromolecules. 2010;43(5):2357-63.

Supporting information

Revealing the dependence of crushing strength of co-granulated fertilizer with graphene on physio chemical properties and concentration of graphene

Shervin Kabiri [ǂ], *Diana N.H. Tran*[ǂ], *Roslyn Baird*[‡], *Mike J. McLaughlin**[‡] *and Dusan Losic** [ǂ]

[ǂ] School of Chemical Engineering, Engineering North Building, The University of Adelaide, Adelaide, SA 5005, Australia

[‡] Fertilizer Technology Research Centre, School of Agriculture, Food and Wine, The University of Adelaide, Waite Campus, PMB1, Glen Osmond, SA 5064, Australia

Materials. Natural graphite flakes (Uley, Eyre Peninsula, South Australia, Australia) was supplied from a local mining site. Monoammonuim phosphate (MAP) and di ammonium phosphate (DAP) were provided by The Mosaic Company LLC (Minnesota, USA). Potassium permanganate ($KMnO_4$, Sigma-Aldrich), 98% sulfuric acid (H_2SO_4, Chem-Supply), phosphoric acid (H_3PO_4, Chem-Supply), 30% hydrogen peroxide (H_2O_2, Chem-Supply), 35% hydrochloric acid (HCl, Chem-Supply), 65% hydrazine (N_2H_4, Sigma-Aldrich), L-ascorbic acid (vitamin C, Sigma-Aldrich) and ferric nitrate ($Fe(NO_3)_3.9H_2O$, Sigma-Aldrich) were used directly without further processing. High-purity milli-Q water (18.2 MΩ·cm at 25 °C, pH of 5.6) was used throughout the study, unless otherwise stated.

Characterization. The MAP-GN and DAP-GN fertilizers were analysed by scanning electron microscopy (FE-SEM, Quanta 450, FEI, USA) combined with an integrated energy-dispersive X-Ray analysis (EDAX) Aztec system for morphological and elemental composition analysis. Mineralogical characterization of the final product was investigated using X-ray diffraction (600 Miniflex, Rigaco, Japan). The vibrational characteristics of GN, GO, MAP, DAP, MAP-GN and DAP-GN were analysed by Raman spectroscopy (LabRAM HR Evolution, Horiba Jvon Yvon Technology, Japan) using a 532 nm laser. Thermal decomposition of GN (made with different methods), MAP-GN (with different dosage of GN), DAP-GN (with different dosage of GN) were performed using a thermal gravimetric analyser (TGA, Q500, TA Instruments, USA) under air atmosphere where the samples were heated to 900 °C at a heating rate of 10 °C min^{-1}. The specific surface area of the all GN samples were measured using methylene blue similar to our previous work.[1] The size distribution of both GN and GO was determined using the Mastersizer X (Malvern Instruments, U.K.).

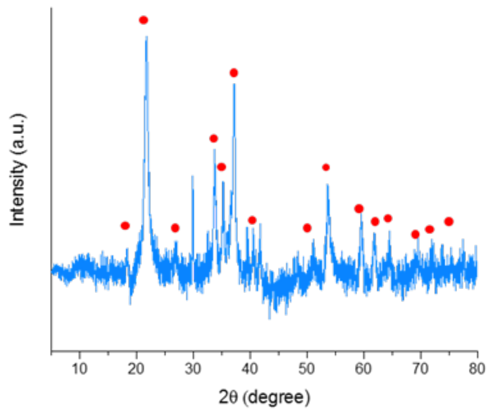

Figure S1. The XRD pattern of as synthesised αFeOOH nanoparticles (NPs) and dot points represented the XRD pattern of pure goethite (JCPDS file:00-029-713).

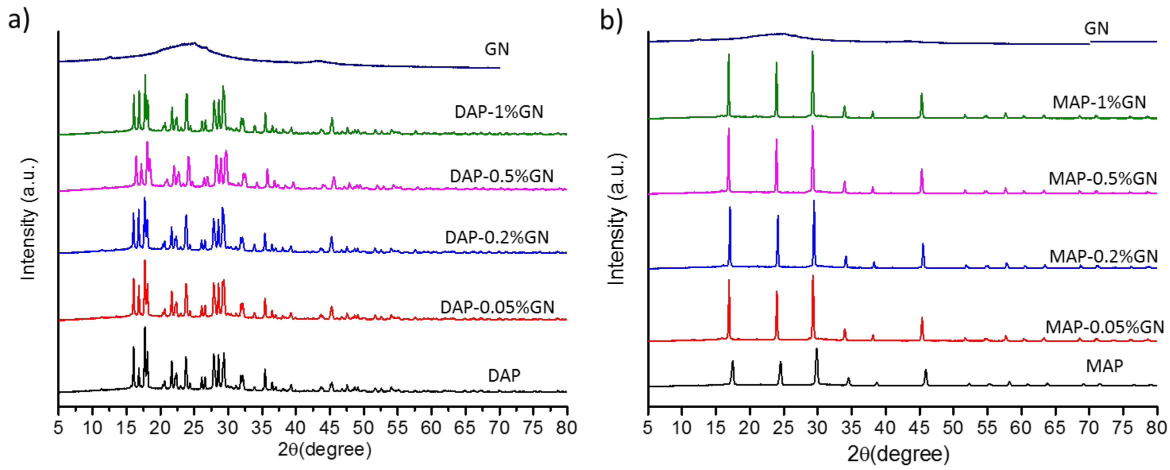

Figure S2. XRD patterns of a) diammonium phosphate (DAP), hydrothermally reduced graphene (GN_{HT}) and DAP amended with 0.05, 0.2, 0.5 and 1% of GN and b) monoammonium phosphate (MAP), hydrothermally reduced graphene (GN_{HT}) and MAP amended with 0.05, 0.2, 0.5 and 1% of GN_{HT}.

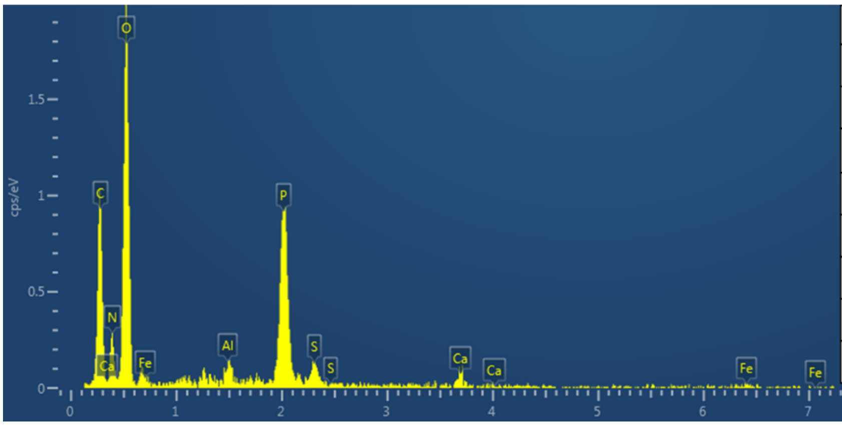

Element	Wt %	At %
O	32.8	41.3
C	31	32.9
P	13.9	14.8
N	12.9	7.2
Fe	3.2	1.2
Ca	3.1	0.9
S	1.9	0.9
Al	1.2	0.7

Figure S3. EDX analysis of high GN_{HT} area in MAP-1%GN granules (Area A of Figure 5a)

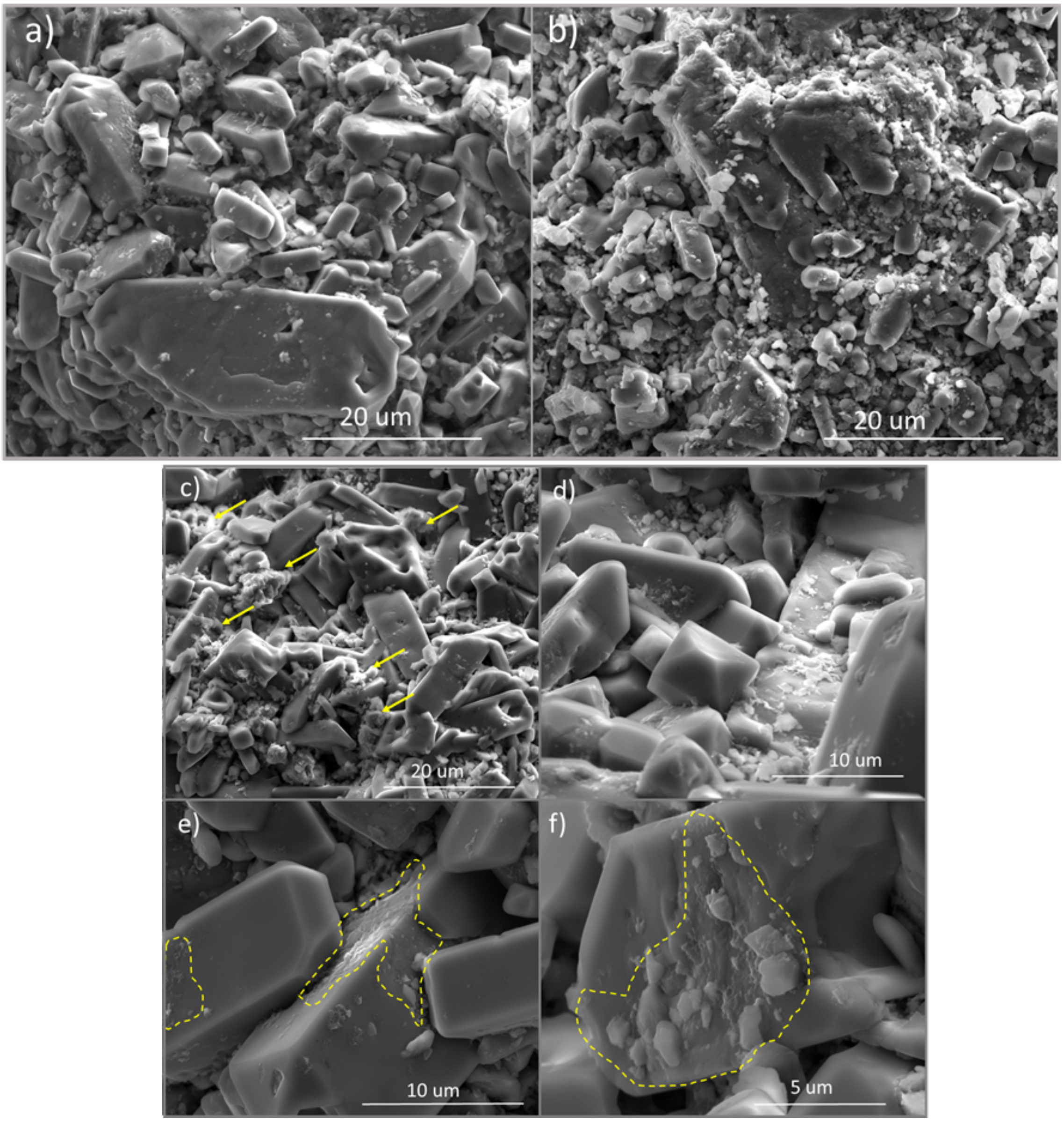

Figure S4. SEM images of MAP with a) 1%GN showing MAP microparticles preserved their tetragonal structure, b) 0.5% GN showing irregular shaped MAP microparticles and, c) 1% GN showing presence of high amount of GN aggregates between MAP microparticles, and d, e and f) 1% GN showing coverage of MAP microparticles with GN Sheets.

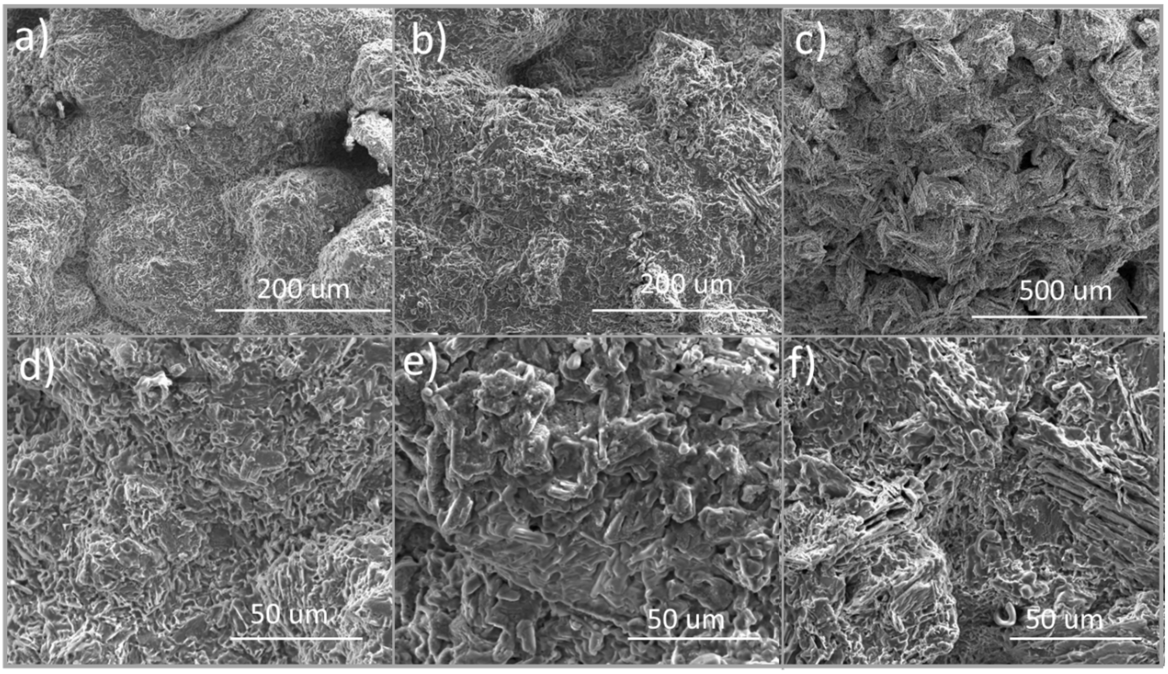

Figure S5. High and low magnification SEM images of DAP amended with a and d) 0.2%GN, b and e) 0.5%GN and, c and f) 1%GN.

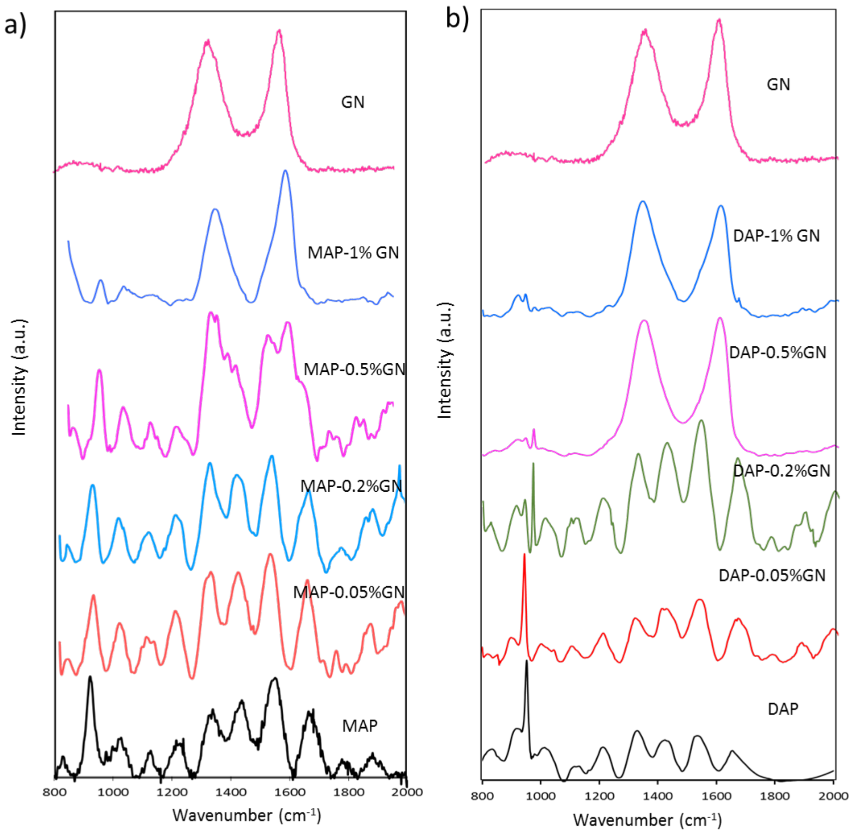

Figure S6. Raman spectra of a) MAP, GN and MAP amended with different percentage of GN (0.05%-1%) and b) DAP, GN and DAP amended with different percentage of GN (0.05%-1%).

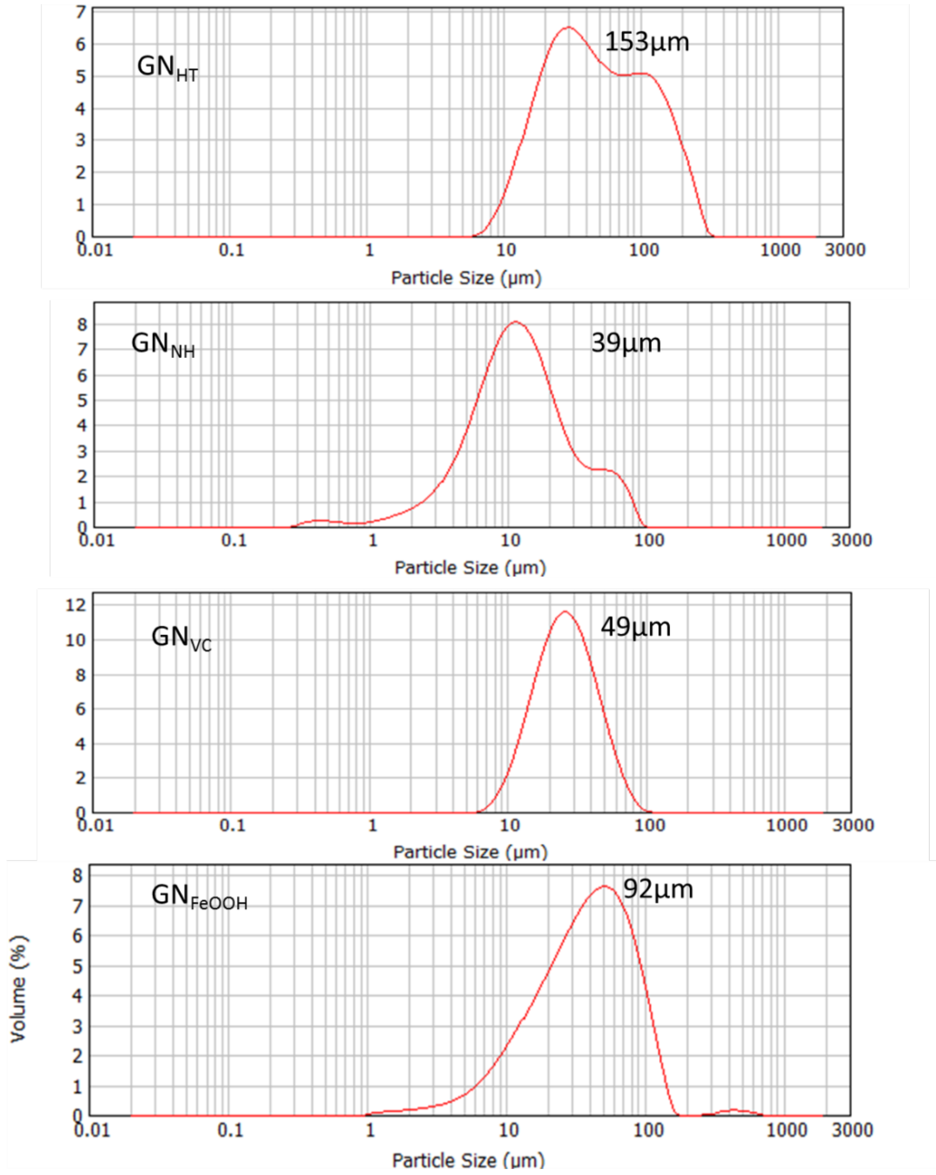

Figure S7. Particle size of hydrothermally reduced GN (GN$_{HT}$), GN reduced by hydrazine (GN$_{NH}$), GN reduced by vitamin C (GN$_{VC}$) and GN decorated with αFeOOH NPs (GN$_{FeOOH}$).

References:

1. Kabiri, S.; Tran, D. N. H.; Altalhi, T.; Losic, D., Outstanding adsorption performance of graphene–carbon nanotube aerogels for continuous oil removal. *Carbon* **2014,** *80*, 523-533.

Chapter 7

Conclusion and recommendations for future work

7.1 Conclusions

The chapter overviews the contribution of the whole thesis to apply graphene (GN) and its derivatives to address specific problems in the agriculture and improve the performance of fertilizers and provide solution to the constantly rising world environmental, and economic concerns due to the application of conventional fertilizers. This thesis is devoted to develop new concepts for delivery of plant nutrients using graphene oxide (GO) for the first time. Based on the recent progress in this field, a series of new objectives were set with a purpose to enforce the application of GO as a platform for carrying plant's nutrient to slow down the nutrient release in the soil and enhance plant nutrient uptake. Furthermore, this thesis introduced GN-based materials as a hardening agents to enhance the mechanical properties of existed fertilizers. Based on the research results and outcomes from this thesis, the following conclusions can be drawn:

Chapter 2: The fundamental properties of GN-based materials and their applications in agriculture that are published in recent years were comprehensively reviewed to identify key drivers, and the most promising developments and limitations in this emerging field. Some key conclusions from this review are highlighted.

- The main properties of GN-based materials relevant to their applications in different sections of agriculture ranging from nutrients and pesticides delivery, gene delivery, biosensors, protective coatings and hardening materials have been comprehensively reviewed in order to assess their possibilities and limitations to be translated for real applications in agriculture. The current application of GN-based materials in agriculture are still in the research and development stage but there are strong possibilities to be commercialized in particular for fertilizer (micro- and macro-nutrient) delivery for balanced and sustained nutrient and pesticide delivery, hardening materials to enhance fertilizer physical properties as well as a barrier coating to slow nutrient release from existed fertilizers.

- The mass production of GN-based materials, their supply to market at large quantities and related problems has also been reviewed and presented.
- This chapter also introduced some new possible applications of GN-based materials in different areas of agriculture science which have not yet been explored, but there are high demands for these applications.

Chapter 3: A new concept using GN-based materials for nutrients delivery is introduced for the first time showing their enormous potential in this field. Specifically, a new carrier platform based on GO sheets was developed that can provide a high loading capacity of plant micronutrients with a slow and sustained release property. Some specific findings are highlighted below:

- Two micronutrients of zinc (Zn) and copper (Cu) were successfully loaded on GO sheets and hence formulated the GO-based micronutrient fertilizer for the first time. The micronutrient fertilizers (Zn-GO and Cu-GO) prepared in the form of solid pellets had a high nutrient loading capacity (more than 10%) related to the high surface area of GO and high density of oxygen binding sites on the surface and edge of GO.
- The GO-based carriers have shown a biphasic nutrient release characteristics with an ability to supply micronutrients in both fast-release (ca 40% for 5 h) and slow sustained release. This release pattern was highly desirable and advantageous for the crops where seedling establishment needs high nutrient loadings, and at later stages of crops' growth a slower and sustained release of micronutrients is needed.
- The significant loading capacity of Zn and Cu on GO and desirable release performances of GO-based carriers makes them a favourable material for loading any

nutrients (macro, micro and their combinations), and therefore could be used as generic carriers for creating a new generation of advanced slow release fertilizers.

Chapter 4: The application of graphene-based Zn fertilizers (Zn-GO) versus commercial Zinc sulphate ($ZnSO_4$) fertilizer in plant yield and nutrient uptake was investigated by using different forms of both fertilizers (granular versus suspension). Different methods of fertilizer application (banded versus mixing) was also examined in this study. Some specific performances are highlighted below:

- Suspension form of either Zn-GO or $ZnSO_4$ was better source of Zn compared to their granular form.
- Zn-GO fertilizer increased the plant yield in wheat more than the commercial formulation based on $ZnSO_4$ in both granular and suspension forms and methods of applications (banded and mixed) while Zn-GO suspension was more effective than granular Zn-GO.
- Compared to mixing through the soil, banding of $ZnSO_4$ significantly constrained the plant's growth, but Zn-GO suspensions were not affected by banding to the same extent.
- Diffusion and solubility of fertilizer Zn in soils away from the point of fertilizer application was restricted for $ZnSO_4$ compared to Zn-GO (granular or suspension) due to the formation of insoluble Zn precipitates around $ZnSO_4$ granules in soil.
- Graphene oxide-based fertilizers were a greater nutrient source for increasing nutrient content in Zn-deficient calcareous soils, likely because of the reduced fixation in soil due to their slow-release properties arising from specific physicochemical properties of the GO sheets and complexation of Zn with GO sheets, in addition to the acidity of GO-based fertilizers.

- The greater performance of GO-based fertilizers on enhancing plant mass and nutrient uptake make theses fertilizers a favourable candidate to be used as Zn nutrient in Zn deficient soil.

Chapter 5: The beneficial effects of GN and GO additives on enhancement of physical properties of monoammonium phosphate (MAP) fertiliser granules such as crushing strength, abrasion and impact resistance were demonstrated. Some specific discoveries are highlighted below:

- Co-granulation of 0.5% w/w GN sheets with MAP significantly enhanced the crushing strength of MAP granules (~18 times improvement) while inclusion of same amounts of GO sheets improved the strength to a lesser extent (~8 times improvement). The co-granulation of GN also improved MAP granules resistance to abrasion (>70 %) and impact resistance (>75 %).
- Heating MAP-GO granules at 50°C after granulation was shown to enhance their physical properties in comparison to MAP-GO granules dried under ambient temperatures.
- Granules of MAP-GN/GO also showed less or no caking when exposed to pressure and humidity.
- Soil experiments with MAP-GN or MAP-GO granules showed a slightly slower release of phosphorous in soil compared to unamended MAP granules that provides an additional benefit for these hardening materials.
- The advantages of GN and GO sheets compared to current additives as enhancer of the physical properties of MAP granules were explained by their high specific area, superior nanofiller-matrix and adhesion/interlocking ability arising from their unique wrinkled structures and two-dimensional (2D) geometry.

- These results confirmed the potential application of GN/GO additives to enhance the physical properties of MAP granules that could be translated to other fertilizers and applied in the industry.

Chapter 6: A comprehensive study of the influence of GN concentration (0.05 to 1% w/w) on the crushing strength of two fertilizer granules, monoammonium phosphate (MAP) and diammonium phosphate (DAP) with different initial hardness were investigated. Furthermore, the effect of GN method of preparation, particle size, specific surface area (SSA) and surface functionalization on the crushing strength of the fertilizer granules was explored. Some specific findings are summarized below:

- The enhancement in the crushing strength of MAP and DAP fertilizers was dependent on the concentration of added GN, with the optimum concentration of 0.5% GN for MAP and 0.05% for DAP which increased the crushing strength of MAP and DAP granules by 1680 % and 67.3%, respectively, and beyond this concentration the crushing strength of MAP and DAP decreased.
- The enhancement in the crushing strength of amended granules with GN was also related to the initial hardness of the granules.
- This study also showed that the crushing strength of granules depended on the method of GN production (degree of deoxygenation) and their SSA, while GN samples with a high degree of reduction and SSA were more effective than others.

Owing to the unique physicochemical properties of GN-based materials, their use in the fertilizer industry as a platform for carrying plant micro-nutrient and as a hardening agent to enhance the physical properties of fertilizer granules were explored in this thesis. Herein, the dissertation with a sets of objectives showed valuable development in application of GN-based materials in agriculture which created intellectual property with one patent application.

7.2. Future directions and recommendations

As demonstrated from the presented research outputs included in this thesis, GN-based materials have considerable potential for application as fertilizers in agriculture. Although all the aims of this thesis listed in Chapter 1 have been addressed, there are still some challenges and more exciting areas discovered by this work that require further attention.

- Multinutrient delivery systems: One of the new concept anticipated from this thesis is to explore the possibility of using GN-based materials for delivery of broad range cationic micro- or macro-nutrients such as magnesium, manganese, potassium, calcium and iron and their mixtures should be investigated. Furthermore, functionalized GO or GN with a positive surface charge could be applied as a platform to carry plant anionic micro- or macro-nutrients such as nitrogen, phosphorous and boron. Graphene and its derivatives could act as a multinutrient delivery platform by combining GN/GO loaded with individual nutrients.
- Multipurpose delivery systems: Based on the previous concept on designing a multi nutrient delivery system the next step that should be explored is a multipurpose delivery system. Graphene and its derivatives could be developed to act as a simultaneous carrier of fertilizers and pesticides, herbicides or fungicides, which could provide sustained release of nutrient and active ingredient for plant protection.
- Optimizing the loading condition of micro- or macro-nutrient on GN-based materials can increase their loading capacity. This approach can decrease the cost of the final products as GN-based materials are currently expensive.
- Investigation of the potential toxicity of GN-based fertilisers to soil microbial populations and their persistence or degradation in soil.
- To explore the effect of GN-based materials on enhancing the physical properties of other fertilizers e.g. urea, muriate of potash, ammonium nitrate, etc. Furthermore, to

apply GN-based materials as a hardening agent to other techniques of fertilizer production such as compaction and prilling.

- Environmental risks: More work should be allocated to explore a potential risk of long term effect of GN-based materials on the environment especially soil microorganisms.

In summary, the world's population is increasing at a high rate and will reach 9.8 million by 2050, which will result in a great need to produce sufficient food for this growing population. Scientists are trying to find new ways to address this rising global demand for food without stressing on natural resources. Therefore, the development and use of GN-based fertilizers can be a promising strategy to enhance plant growth, and its development and productivity due to the multifunctional application of these materials in agriculture science.

Although preparation of GN-based materials as slow-release carriers is currently more costly than manufacturing costs for common fertilizers, it is clear that these materials can not only synchronize the release of nutrients with crop demand, they can also prevent undesirable nutrient losses from soil and enhance the physical properties of common fertilizers. As GN-based materials become cheaper, the opportunity for their use in fertilizers will increase.